UNIVERSITÉ DE STRASBOURG

ÉCOLE DOCTORALE DES SCIENCES DE LA VIE ET DE LA SANTÉ
Architecture et Réactivité de l'ARN – UPR 9002 du CNRS

et / und

UNIVERSITÄT LEIPZIG

FAKULTÄT FÜR BIOWISSENSCHAFTEN, PHARMAZIE UND PSYCHOLOGIE

THÈSE / DISSERTATION

présentée par / vorgelegt von

Tina MÜLLER (ép. JÜHLING)

soutenue le / verteidigt am **14.12.2016**

pour obtenir le grade de **Docteur de l'université de Strasbourg (Dr.)**
zur Erlangung des akademischen Grades **Doctor rerum naturalium (Dr. rer. nat.)**

Discipline/Spécialité : Aspects moléculaires et cellulaires de la biologie
im Fachgebiet : Biochemie

ARNt « manchots »
structure, fonctionnalité et évolution

THÈSE co-dirigée par:
  Prof. FLORENTZ Catherine   Professeur, IBMC, Université de Strasbourg
  Prof. MÖRL Mario   Professeur, Institut de Biochimie, Université de Leipzig

RAPPORTEURS :
  Prof. LAYER Gunhild   Professeur, Institut de Biochimie, Université de Leipzig
  Prof. CHIHADE Joseph   Professeur, Department of Chemistry, Carleton College

---

AUTRES MEMBRES DU JURY :
  Prof. GIEGÉ Philippe   Directeur de recherche, IBMP, Université de Strasbourg

Structure, function and evolution of armless mitochondrial tRNAs

Der Fakultät für Biowissenschaften, Pharmazie und Psychologie
der Universität Leipzig

und / et

École Doctorale des Sciences de la Vie et de la Santé
Architecture et Réactivité de l'ARN – UPR 9002 du CNRS
Université de Strasbourg

eingereichte

D I S S E R T A T I O N / *T H È S E*

zur Erlangung des akademischen Grades / pour obtenir le grade de

DOCTOR RERUM NATURALIUM (Dr. rer. nat.)

und / *et*

DOCTEUR DE L'UNIVERSITÉ DE STRASBOURG (Dr.)

im Fachgebiet / *Discipline-Specialité*
Biochemie / *Aspects Moléculaire et Cellulaires de la Biologie*

vorgelegt von / présentée par Frau *Master of Science*

Tina Jühling (geb. Müller)

Geboren am / *née le* 25.07.1988 in Haldensleben

Leipzig, den 10.10.2016

Le présent travail a été réalisé du 01/10/2013 au 30/04/2015 dans le groupe de Prof. Dr. Mario Mörl à l'Institut de biochimie, Faculté de Biosciences, pharmacie et de psychologie, Université de Leipzig, et du 01/05/2015 au 31/12/2016, dans le groupe de Prof. Dr. Catherine Florentz à l'IBMC/CNRS UPR9002 de l'Université de Strasbourg.

Die vorliegende Arbeit wurde vom 01.10.2013 bis zum 30.04.2015 in der Arbeitsgruppe von Prof. Dr. Mario Mörl am Institut für Biochemie der Fakultät für Biowissenschaften, Pharmazie und Psychologie der Universität Leipzig, sowie vom 01.05.2015 bis zum 31.12.2016 in der Arbeitsgruppe von Prof. Dr. Catherine Florentz am IBMC/CNRS UPR9002 der Universität Strasbourg angefertigt.

Nothing in life is to be feared, it is only to be understood.
Marie Curie (7 November 1867 – 4 July 1934)

Acknowledgments

It is a great pleasure for me to thank all those who have directly or indirectly contributed to this work during the last three years.

First of all, I want to thank the jury members **Prof. Gunhild Layer** (Institut für Biochmie, Universität Leipzig), **Prof. Joseph Chihade** (Carleton College, Northfield, Minnesota), and **Prof. Philippe Giegé** (IBMP, Université de Strasbourg), for their interest in my work and its evaluation.

Foremost, I want to express my sincere gratitude to my two thesis directors **Prof. Catherine Florentz** and **Prof. Mario Mörl** for sharing the responsibility of my joint PhD project. I am very grateful for your trust and support over the past three years. I would like to thank you, Catherine, for the opportunity to join your group again, five years after I finished my Bachelor thesis in your team. Then as now, I spent a wonderful time in your group and had benefit a lot from your immense knowledge and guidance during my research and writing of this thesis. I also want to thank you, Mario, for the heartily admission in your team during my time in Leipzig. I appreciated very much the continuous support during the course of my PhD study as well as your patience, motivation, and enthusiasm for my project.

I want to express my deepest gratitude to my advisor **Dr. Joern Pütz**, for his great support during my several stays at Strasbourg that started already during the French-German Bachelor program. Thanks to you, I spent a wonderful time as an Erasmus student in Strasbourg, and discovered the interesting world of tRNAs during my internship and Bachelor thesis. I thank you for all the help and support that you spent to establish this "Cotutelle de thèse". I am very grateful that you always had an open ear for my little and big problems. Your comforting and encouraging words motivated me a lot. Thank you for all!

Bibliographic references and abstract

Transfer RNAs (tRNAs) are important adapter molecules linking the genetic information of messenger RNAs (mRNA) with the primary amino acid sequence of proteins. In all kingdoms of life, these small RNA transcripts have a typical cloverleaf-like secondary structure, consisting of an acceptor stem, a D-arm, an anticodon arm, a variable loop, and a T-arm. The 3′ terminus ends with the CCA sequence, which is often post-transcriptionally added by CCA-adding enzymes. The CCA-tail is an important prerequisite for the attachment of the correct amino acid by aminoacyl-tRNA synthetases (aaRS). Mitochondrial (mt) tRNAs show a high derivation from this canonical tRNA structure with reduced D- or T-arms, or even completely lack one of these elements. An extreme case of structural truncations can be observed in mitochondria of Enoplea. Here, mitochondrial tRNAs of half of the size of their cytosolic counterparts are present, representing the smallest tRNAs identified so far. It could already be shown that several of these miniaturized armless tRNAs are indeed functional in the nematode worm *Romanomermis culicivorax*. This situation raises several questions concerning the molecular mechanisms of co-evolution of tRNAs and their partner proteins, which ensure the maintenance of a functional protein synthesis.

This study aims the biofunctional characterization of such "bizarre" tRNAs in defining their structural properties, and in studying different aspects of their functionality, especially their interactions with CCA-adding enzymes and aaRSs from different organisms. For this purpose, *in vitro* transcripts were used for structure probing approaches, such as enzymatic and chemical probing, nuclear magnetic resonance (NMR) spectroscopy, and small-angle X-ray scattering (SAXS). We show that armless tRNAs form a hairpin-shaped secondary structure, including an internal double bulge that replaces D- and T-arms of the secondary cloverleaf structure of classical tRNAs. 3D

structures are characterized by a high intrinsic flexibility, which probably allows to compensate structural reduction.

The *Rcu* CCA-adding enzyme and mt ArgRS coding sequences have been identified, and were cloned for the first time. Recombinant proteins have been studied for their interaction with armless and cytosolic tRNAs in CCA-incorporations assays, and aminoacylation assays. We demonstrate that armless mt tRNAs represent functional molecules for CCA-incorporation, indicating adaptations of CCA-adding enzymes to armless tRNAs without losing their ability to recognize cytosolic tRNAs. Initial tests could not demonstrate aminoacylation activity of the *Rcu* mt ArgRS. However, the mt ArgRS from *R. culicivorax* exhibits a structural particularity because it lacks an important domain that normally recognizes the elbow region of tRNAs that is no longer present in armless tRNAs due to the missing D-and T-arm. This suggests a co-evolution event of both partner molecules.

2

Abbreviations

A: Adenine
A: Ampere
aaRS: aminoacyl-tRNA synthetase
APS: Ammonium persulfate
ArgRS: Arginyl-tRNA synthetase
ATP: Adenosine triphosphate
bp: base pair
BSA: Bovine Serum Albumin
C: Cytosine
$CaCl_2$: Calcium chloride
cDNA: complementary DNA
CTP: Cytidine triphosphate
Cyt: cytosolic
Da: Dalton
ddH_2O: double-distilled water
DMSO: Dimethyl sulfoxide
DNA: Desoxyribonucleic acid
dNTPs: Desoxyribonucleotide
DTT: Dithiothreitol
E. coli (*Eco*): *Escherichia coli*
EDTA: Ethylenediaminetetraacetic acid
EF-Tu: Elongation factor thermo unstable
EtOH: Ethanol
G: Guanine
GTP: Guanosine triphosphate
HDV: Hepatitis Delta Virus
HEPES: Hydroxyethylpiperazineethanesulfonic acid
HH: *hammerhead*
H. sapiens (*Hsa*): *Homo sapiens*
IEC: Ion exchange chromatography
IPTG: Isopropyl β-D-1-thiogalactopyranoside
KCl: Potassium chloride
L: liter
LB: Lysogeny broth medium
mRNA: messenger RNA
mt: mitochondrial
MTS: mitochondrial targeting sequence
$MgCl_2$: Magnesium chloride

NaAc: Sodium acetate
NaCl: Sodium chloride
Ni-NTA: Nickel Nitrilotriacetic acid
nt: nucleotide
OD_{600}: optic density at 600 nm
ORF: open reading frame
PAA: Polyacrylamide
PAGE: Polyacrylamide gel electrophoresis
PCR: Polymerase chain reaction
PEG: Polyethylene glycol
pI: isoelectric point
PNK: Polynukleotidkinase
R. culicivorax (Rcu): *Romanomermis culicivorax*
RNA: Ribonucleic acid
rRNA: ribosomal RNA
S. cerevisiae (Sce): *Saccharomyces cerevisiae*
SDS: Sodium dodecyl sulfate
SEC: Size Exclusion Chromatography
SOB: super optimal broth medium
T: Thymine
Taq: Thermus aquaticus
TBE: Tris-Borat-EDTA
TCA: Trichloroacetic acid
TEMED: N,N,N',N'- Tetramethylethane-diamine
TIPP: thermostable inorganic Pyrophosphatase
Tm: melting temperature
Tris: Trishydroxymethylaminomethane
tRNA: transfer RNA
TTP: Thymidine triphosphate
U: Uracile
UTP: Uridine triphosphate
UTR: untranslated region
v/v: volume to volume ratio
wt: wild-type
w/v: weight to volume ratio

Amino acids were abbreviated as recommended by the IUPAC-IUB Joint Commission on Biochemical Nomenclature (1984). Units were used as specified in the IUPAC compendium of Chemical Terminology. Furthermore, commonly used abbreviations have been used.

Contents

INTRODUCTION

1. Exploring the RNA world: From origins of life to contemporary RNA

Scientists have always wondered about the origin of life, and many theories have been developed. Certainly, no simple and clear answer can be given on this issue yet. Today, it is believed that ribonucleic acids (RNA) arose very early in evolution, and that they belong to the oldest molecules on Earth (Alberts B, Johnson A, Lewis J, et al., 2002; Robertson and Joyce, 2012). RNAs have long been underestimated. First, they have been perceived just as a blueprint of deoxyribonucleic acid (DNA) that allows the formation of proteins by encoding the genetic information (Crick, 1968). But due to intensive studies, we have a better understanding about RNAs now. It is nowadays known that RNAs are versatile molecules that fulfill multiple roles in living cells. Beside its role as a key component of protein biosynthesis (e.g., in the forms of mRNA, tRNA, and rRNA) (Lodish H, Berk A, Zipursky SL, et al., 2000), it can act as enzymes (Doherty and Doudna, 2001), occupy different sub-cellular structures (Nevo-Dinur *et al.*, 2012), regulate the splicing machinery (Konarska and Query, 2005), and control gene expression through a variety of mechanisms (Cannell *et al.*, 2008). Interestingly, there is increasing evidence that RNA encoded genetic information long before DNA, and has played a crucial role in the early evolution of life on Earth (Gilbert, 1986; Orgel, 1968). Our present knowledge about RNA can be told from two perspectives that belong to two different worlds. One is the "primordial RNA world" in which RNA functioned at once as information storage and biocatalyst, long before the arising of DNA, and secondly the "contemporary RNA world" in which mRNA, long non-coding RNA, and small non-coding RNA (e.g., tRNA, siRNA, miRNA, and a variety of other RNAs) play a central role (Robertson and Joyce, 2012; Eddy, 2001).

1.1. Once up one a time - The early RNA world

Since the discovery of the DNA structure by Watson and Crick in 1953 (Watson and Crick, 1953), DNA and proteins have been described as dominant macromolecules in the living cell, while RNA was thought to act only as a supporting tool to create proteins from the DNA templates (Crick, 1968). Today, we know that the expression of genetic information requires a highly complex machinery. The question is, how did this machinery arise? One theory is that an RNA world existed on Earth before modern cells arose. The term early or primordial "RNA world" was first used by W. Gilbert in 1986 to describe the hypothesis that RNA may have evolutionarily predated DNA and proteins

(Gilbert, 1986). This hypothesis is based on the breakthrough discovery of catalytic RNA that can serve not only as a genetic information carrier, but also as a catalyst that could have originally carried out both, catalysis and replication (Cech, 1986). RNA molecules that possess catalytic activity are called "ribozymes", a composition of "RNA" and "enzyme" (Joyce, 1996). A ribozyme with self-splicing activity was first discovered by T. Cech in the ciliated protozoa *Tetrahymena thermophile,* where a self-splicing RNA was found inside an intron of an mRNA transcript that can remove itself from the transcript (Cech, 1986). Another catalytic RNA was identified by S. Altman and colleagues, who were studying the bacterial ribonuclease-P complex in *Escherichia coli*, where the RNA content of the enzyme is responsible for the cleavage of the phosphodiester bond of immature pre-tRNAs (Guerrier-Takada *et al.*, 1983). T. Cech and S. Altman were honored in 1989 with the Nobel Prize in chemistry for their "discovery of catalytic properties of RNA."

A further interesting example of a ribozyme are ribosomes because their catalytic site is composed exclusively of RNA that catalyzes specifically peptide bond formation. This was confirmed with the deciphering of the 3D structure of the ribosome in 2000 (Ban *et al.*, 2000; Schluenzen *et al.*, 2000; Yusupov *et al.*, 2001). These findings revealed important insights into reaction mechanisms and evolution because it was shown that protein enzymes would not have been necessarily needed to catalyze the synthesis of new RNA at the beginning of evolution. Additionally, many critical cofactors, e.g., ATP, Acetyl-CoA, and NADH, are either nucleotides or related to them, and many components of the cell are composed partially or entirely of RNA and represent remnants of the RNA world (Cech, 2012; Yarus, 2011). Thus it seems likely that an RNA world existed initially at the beginning of the evolution of life, while DNA and proteins appeared later (Gilbert, 1986). The next question is, why and how did then proteins and DNA arise from a RNA world? Probably RNA could bind and arrange activated amino acids based on an RNA template as it is the case inside the ribosomal core. That would lead to first proteins with a faster and more efficient enzymatic activity, replacing the role of RNA. Finally, DNA could have appeared by reverse transcription from an RNA molecule, and thus could have taken over the role of information storage due to its increased stability (Alberts B, Johnson A, Lewis J, et al., 2002).

The RNA world hypothesis is widely accepted today, and the chicken and egg problem seems to be solved for the question about what was first, DNA or protein (Cech, 2012;

Lehman, 2010). A summary of probable events during the evolution of the "early RNA world" as presented by Cech is given in Figure 1.

While coding RNAs have an important role as a physical intermediate during the translation of DNA into protein, also RNA molecules that do not encode proteins, so-called non-coding RNAs (ncRNAs), were shown to be indispensable for many cellular processes (Mattick and Makunin, 2006). The analysis of genomic, transcriptomic and proteomic data revealed, that almost the entire genomic DNA is transcriptionally active in eukaryotes, but only 5 to 15 % are actually translated into proteins, whereas the vast majority of active DNA was found to be transcribed into functional ncRNAs (The ENDCODE project consortium, 2012). During the last decades, the understanding of the diversity and the role of ncRNAs has considerably expanded. A multitude of ncRNAs are known to play key roles in a number of biological processes required for cell viability and function in both, prokaryotes and eukaryotes (Mattick and Makunin, 2006; Cao, 2014).

Figure 1: RNA world model.
An RNA world model for the successive appearance of RNA, proteins and DNA during the evolution of life on Earth (modified from Cech, 2012).

1.2. Non-coding RNAs in the modern RNA world

The best known representatives of ncRNAs are likely to be transfer RNAs (tRNA) and ribosomal RNAs (rRNA). Both play a decisive role in the translation of genetic information into proteins. In 1955, Francis Crick was the first that pronounced an "adapter hypothesis". He predicted an adaptor molecule that mediates the translation of genetic information, encoded in DNA or RNA, into the sequence of amino acid of proteins (Crick, 1955). This "adapter hypothesis" was convincingly confirmed by the discovery of tRNA molecules in 1956, and its adapter function in the course of the translation process (Zamecnik *et al.*, 1956). During the 1950s, RNA was also found to be a structural component of ribosomes (Palade, 1955). Because neither tRNA nor rRNA carries instructions for specific proteins, they are referred to as ncRNAs.

Besides rRNAs and tRNAs, a large number of other ncRNAs exist in eukaryotic and prokaryotic cells. They can be grouped into long and small ncRNAs. These molecules

own a variety of important functions, and it is supposed that many of them have not been validated for their function yet (Wilusz *et al.*, 2009; Mattick and Makunin, 2006). Of particular interest for this work is the very diverse group of small regulatory RNAs (sRNAs). This group has been classified into a number of sub-categories, such as small nuclear RNAs (snRNA), small nucleolar RNAs (snoRNA), small interfering RNAs (siRNA), micro RNAs (miRNA) (Mattick and Makunin, 2005). They are involved in many cellular processes like translation, RNA splicing, DNA replication, or in gene regulation. A summary of all known types of ncRNAs is given in Figure 2.

snRNA are involved in splicing of RNA exons, and play therefore a critical role in gene regulation. The most abundant molecules of this group are U1, U2, U5 and U4/U6, which are found inside the nucleus. They are involved in the splicing of pre-mRNAs, a crucial step during the maturation of mRNAs (Valadkhan and Gunawardane, 2013). snoRNAs are mostly found inside the nucleolus, where they are involved in the processing and modification of ribosomal RNAs. snoRNAs are associated with proteins in a complex, called small nucleolar ribonucleoprotein particle (snoRNP). The modifications introduced by one of the two classes of snoRNAs (i.e., S/D box or H/ACA box families) are either methylations or pseudouridylation of specific nucleosides in immature rRNAs, which are essential for the function of the ribosome during translation (Kiss, 2002).

Micro RNAs are a class of small RNA molecules (between 22 to 26 nt long), which bind to complementary mRNAs. They often regulate gene expression by an inhibition of translation. Initially, miRNAs were found in the nematode *Caenorhabditis elegans*, but have been later identified in a wide variety of other species (e.g. in flies, mice, and humans) (He and Hannon, 2004).

siRNA are single or double stranded RNA molecules that are 20 bp to 25 bp long, and are formed by cleavage of large double-stranded RNA molecules. siRNAs are expressed in various cell types, often with the aim to destroy foreign RNA after an infection with an RNA virus. Furthermore, siRNA play a role in gene regulation via post transcriptional gene silencing through determining selectivity (McManus and Sharp, 2002). Beyond that, miRNA and siRNA are used as a major scientific tool to inhibit the expression of specific genes in cells during *in vivo* and *in vitro* experiments (Divan, 2013).

As mentioned above, another group of RNAs with catalytic activity are commonly referred to as ribozymes. In addition to their role for the origin of life, they play

important roles for replication, mRNA processing and splicing (Serganov and Patel, 2007).

A lot of interesting examples of non-coding RNA, such as riboswitches, are also found in prokaryotes. Riboswitches are RNA elements that are mostly found within the untranslated regions of mRNAs. There, they form a specific secondary and tertiary structure, and thereby recognize low molecular weight metabolites. This recognition results in a conformational change of the riboswitch, leading to an inhibition of transcription or translation. Most riboswitches where found in prokaryotes, with only some exceptions in eukaryotic cells (Serganov and Patel, 2007).

Since a lot more types of RNAs exist, and probably not all are discovered yet, RNA research is still under ongoing development (Morozova and Marra, 2008). Certainly many alternative functions of RNAs have not been clarified yet, and we are just at the beginning of understanding the complex role of RNA molecules for life. However, among all forms of ncRNAs, tRNAs belong to one of the oldest and most intensively studied molecules in living organism. Since its first mention in 1955, innumerable publications and textbook chapters have been dedicated to this fascinating molecule. Nevertheless, tRNAs still deserve our attention as new discoveries are made regularly. The following paragraph will focus on this exceptional molecule and its characteristics.

Type of RNA molecules
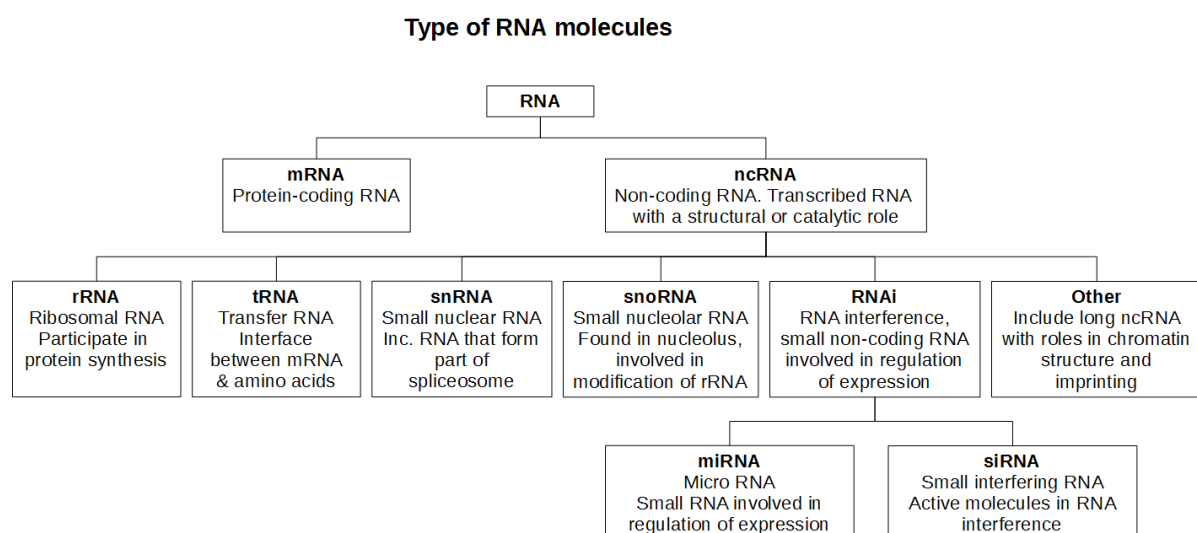
Figure 2: Schematic overview of different RNA types.
RNA can be divided in two groups, coding RNA representing messenger RNA (mRNA) and non-coding RNA including ribosomal RNA (rRNA), transfer RNA (tRNA), small nuclear RNA (snRNA), small nucleolar RNA (snoRNA), interfering RNA (RNAi), which is subdivided in micro RNA (miRNA) and small interfering RNA (siRNA), and other RNAs, including long ncRNA.

2. Transfer RNAs : canonical structure, structural evolution and origin

In principle, protein bio-synthesis follows the same procedure in all kingdoms of life. This fact is already an indication that the protein synthesis system has been developed early in evolution (Noller, 2012). An mRNA transcript is always translated in 5'→3' direction, one codon (i.e., a triplet of three nucleotides) after another. Thereby, the protein is synthesized sequentially by a chemical linkage of amino acids, one after another. tRNAs recognize only the corresponding codons by Watson-Crick base pairing that encode for the amino acids that they carry. Therefore, they represent an adapter molecule that serves as a physical link that translates mRNA information into amino acid sequences of proteins (Crick, 1970).

Today, in the era of large scale-genomics, a huge number of complete genome sequences are available from 3,316 Bacteria, 202 Archaea, 179 Eukaryote, 6,149 organelles and 4,026 Viruses (October 2016; https://www.ebi.ac.uk/genomes/). Despite their relatively short nucleotide sequences, a large diversity of gene structures and RNA secondary structures of pre- and mature tRNAs have been discovered in the three domains of life so far (Fujishima and Kanai, 2014).

The following paragraph will highlight the characteristic properties of cytosolic, mitochondrial tRNAs and tRNA-derived fragments.

2.1. Cytosolic tRNAs

Cytosolic tRNAs possess a highly conserved structure and are therefore called classical or canonical tRNAs (Giegé *et al.*, 2012). tRNAs are composed of approximately 75 - 100 nucleotides with a universal CCA-3' terminus (Jühling *et al.*, 2009). Although each tRNA molecule has a unique nucleotide sequence, the general secondary and tertiary structures are very similar to each other. The first 3D structure of a tRNA was obtained from yeast tRNA^{Phe}, and was solved by X-ray crystallography (Robertus *et al.*, 1974; Kim *et al.*, 1974). Therefore, the crystal structure of the tRNA^{Phe} is often used as a standard reference model for the 3D structure of canonical tRNAs.

Secondary structure of canonical tRNAs resembles a cloverleaf (Figure 3). Accordingly, they have various common structural features, and are composed of 6 sub-domains. The amino acid accepting stem (AAS) is composed of 7 base-pairs (bp) and terminates at the 5'-end with a pN_1 (with an additional N_{-1} in tRNA^{His} species), and at the 3'-end with the discriminator base (N_{73}) followed by the CCA-tail. Next, there is a connector domain

with 2 nt (U_8, N_9), followed by the D-stem and loop (DSL) (N_{10}-N_{25}), a 4 bp stem ending in a loop of 7 to 11 nt. This loop often contains the name-giving modified base dihydrouridine, and a sequence of the conserved residues A_{14}, R_{15}, and $G_{18}G_{19}$. The anticodon stem and loop (ASL) (N_{27}-N_{43}), consists of a 5 bp stem and a 7 nt loop containing U_{33} and the anticodon triplet N_{34}, N_{35}, N_{36}. The fifth domain is a variable region of normally 4 to 24 nt (N_{44}- N_{48}). Finally, all tRNAs contain a T-stem and loop (TSL) (N_{49}-N_{65}) with a 5 bp stem and a 7 nt loop containing the sequence $T_{54}\Psi_{55}C_{56}$ where Ψ is pseudouridine (Giegé *et al.*, 2012).

The tertiary structures of several tRNAs (∼25 PDB entries of free tRNA molecules, and ∼150 PDB entries in complex with interaction partner) were solved by crystallography or NMR spectroscopy. The shape of the three-dimensional structure of tRNAs resembles an upside down letter "L" (Figure 3). This universal structure is the result of two-by-two coaxial stacking of the helices formed by the stems. Although variations in the angle formed by the two branches are recognized, the overall tertiary structure of all tRNA molecules is rather conserved. Thereby, the tertiary interaction network maintains and stabilizes the L-shape structure of canonical tRNAs. It requires the participation of 12 phylogenetically conserved and semiconserved residues (U8, Y12, A14, R15, G18, G19, R20, R23, Y48, Ψ55, C56, and R57), and is associated with long range tertiary interactions found in the elbow of the molecule (Giegé *et al.*, 2012).
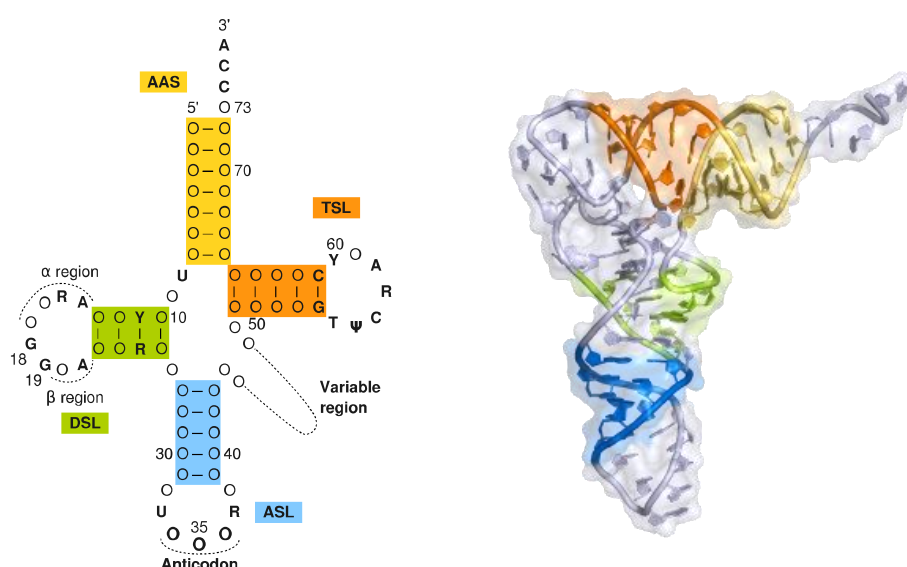
Figure 3: Secondary and tertiary structure of canonical tRNAs.
2D cloverleaf and 3D L-shape structure of canonical tRNAs. The amino acid acceptor stem (AAS), yellow; D-stem loop (DSL), green; anticodon stem loop (ASL), blue; T-stem loop (TSL), orange are highlighted in the two structures with the same color code (modified from Giegé *et al.*, 2012).

Many functional tRNAs contain a variety of chemically modified nucleosides. Nowadays more than 100 of such modified nucleosides have been identified (Machnicka *et al.*, 2013; Grosjean, 2015). Often these modifications are deaminated or methylated derivatives of the four nucleotides adenine (A), cytosine (C), guanine (G) and uracil (U), which are formed by specific modification enzymes (Bjork and Hagervall, 2014). However, the variety of modifications is huge, and may differentially affect the tRNA structure and/or function (Jackman and Alfonzo, 2013)

The different types of modifications can be subdivided into three main categories (Machnicka *et al.*, 2013). The first group comprises all modified nucleosides for which both, position and identity, are conserved in the majority of tRNA species, such as dihydrouridine (D) in the D-loop or 5-methyluridine (m^{5}U) and pseudouridine (Ψ) in the TΨC-loop. Modified residues for which only the position, but not necessarily the identity of modification is conserved, correspond to the second category. It contains uridines and purines found at positions 34 and 37 of the anticodon loop, respectively, that undergo by far the largest diversity of post-transcriptional modifications (Gustilo *et al.*, 2008). Often these hyper-modified nucleotides ensure correct decoding at the wobble position (position 43), or play roles in maintaining the reading frame (position 37) (El Yacoubi *et al.*, 2012). The third group comprises all other modified nucleotides that consist usually of simple chemical alterations, such as methylation of the base or the ribose, or isomeric derivatives. Modified residues of the third class are found at unique positions of only a limited group of tRNA species (Machnicka *et al.*, 2013).

Most of these modifications are crucial for a correct folding and the stability of tRNA molecules (Motorin and Helm, 2010). They play an important role for the functionality of a variety of cellular processes, for example by modulating interactions with other cellular macromolecules such as amino-acyl tRNA synthetases and translation factors (Giegé and Lapointe, 2009), or by ensuring the accurate decoding of mRNAs at the ribosome (Duechler *et al.*, 2016).

2.2. Mitochondrial tRNAs

So far, most attention was dedicated to the function, structure, and evolution of classical tRNAs. Nonetheless, in eukaryotes, tRNAs are not only present in the nucleus but also in organelles such as chloroplasts and mitochondria. Mitochondria encode a specific set of mitochondrial tRNAs (mt tRNA) in their own genome, and possess therefore an

appropriate own translation machinery. A very surprising discovery was made in 1980 after sequencing the mt tRNA^{Ser} from beef heart. This revealed the absence of the DSL domain (Arcari and Brownlee, 1980; Bruijn *et al.*, 1980) (Figure 4). This discovery changed completely the view on classical tRNA structures, and led to the question whether the D-armless tRNA^{Ser} is just an exception, or whether it represents a much larger portion of previously unknown tRNAs in animals. The answer to this question is the focus of attention of this chapter.
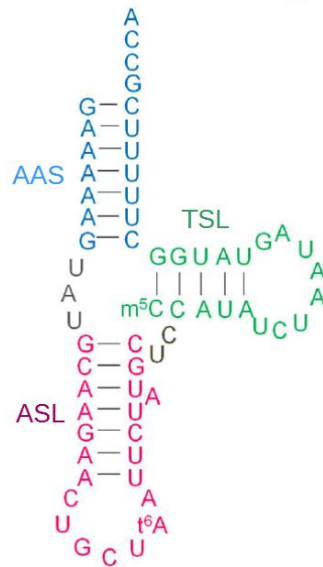
Figure 4: D-armless bovine tRNA^{Ser} (GCU).
Secondary structure of mt D-armless bovine tRNA^{Ser} (GCU) highlighting the acid acceptor stem (AAS) in blue, the anticodon stem loop (ASL) in red, and the T-stem loop (TSL) in green (modified data from tRNAdb, Jühling *et al.*, 2009).

Mitochondria are organelles that are present in nearly all eukaryotes. They are commonly described as the "powerhouse" of the cell since they generate most of the energy by supplying the cell with ATP (Tzameli, 2012). The true origin of mitochondria remains unclear. However, it is often hypothesized that mitochondria originate from an ancient endosymbiotic living proteobacterium (Gray, 2012). The presence of an own genome, also called mitogenome, supports this theory. The sizes of mitogenomes differ extremely between different species, and range from 6 kb in *Plasmodium falciparum* to over 100 kb in plant mitochondria. The average genome size of mammalian mitochondria is approximately 16 kb. Although animal mt DNA evolves about ten times faster than the nuclear genome (Brown *et al.*, 1979), they possess a well preserved gene content, encoding for 13 proteins, 2 rRNAs and 22 tRNAs (20 for the standard amino acids and 1 additional for each, leucine and serine isoacceptors).

The high amount of mt DNA copies in a cell (varies between 100 and 100,000 copies depending on cell type (Reznik *et al.*, 2016)) and its small size makes the mt genome favorable for sequence analysis. Next-generation sequencing (NGS) techniques and improved bioinformatics tools have made it quick, easy and cheap to sequence and assemble entire mitochondrial genomes from almost any eukaryotic species (Smith, 2016). Today, more than 6,000 mitogenomes are sequenced and the subject of large-scale comparative studies (Smith, 2016).

Initial sequencing studies and further computational analysis of mitochondria led to the discovery that, in contrast to cytoplasmic tRNAs, mitochondrial tRNAs show non-canonical structural features with various deviations, such as reduced size, or length variations in D-and T-loops (Wolstenholme *et al.*, 1987). It turned out that the above mentioned D-arm loss of tRNA[Ser] is not only an exception in bovine mitochondria, but is represented in most metazoans. However, the D-armless tRNA[Ser] is the biggest structural exception in animal mitochondria, while mostly all other tRNAs still occupy a cloverleaf-like structure.

Interestingly, already in the 1980s, a complete set of truncated mitochondrial tRNAs was found in the nematode worms *Caenorhabditis elegans* and *Ascaris suum*. 20 of the 22 mt tRNAs are T-armless, while both serine tRNAs lack the D-arm. It could be shown that these truncated tRNAs are indeed functional (Okimoto and Wolstenholme, 1990). Some other bizarre tRNAs with reduced size (lacking the T-arm) could also be identified in some Mollusca (Yamazaki *et al.*, 1997) and Arthropoda (Masta, 2000).

The increasing number of genomics data, and the potential of the existence of more unusual tRNA genes require efficient tRNA annotation tools. Classical annotation tools (e.g., tRNAscan-SE) are based on searching for the above mentioned conserved signature motifs of canonical tRNAs that are absent in mt tRNAs (Lowe and Eddy, 1997; Laslett and Canback, 2004; Kinouchi and Kurokawa, 2006). Thus, these approaches are highly sensitive for canonical tRNAs and report only few false positive hits in the nuclear genome, but are unsuitable for the detection of mt tRNA genes because of their miscellaneous structural deviations.
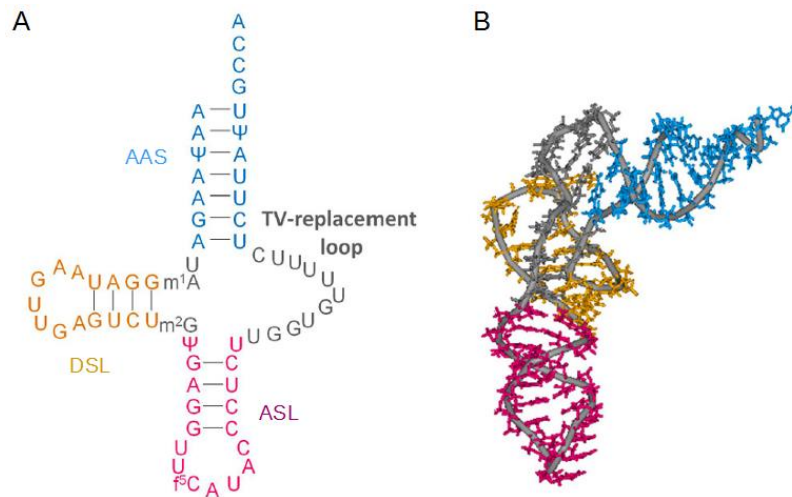
Figure 5: Secondary and tertiary structure of truncated mt tRNA[Met] in *A. suum*.
(A) Secondary structure of T-arm-lacking tRNA[Met] in *A. suum* highlighting the amino acid acceptor stem (AAS) in blue, the D-stem loop (DSL) in yellow the anticodon stem loop (ASL) in red, and the TV-replacement loop in black. (B) L-shape model of the same tRNA (adapted from Watanabe *et al.*, 2014).

In 2012, Jühling et al. developed a specialized bioinformatics tool called MiTFi (<u>Mi</u>tochondrial <u>t</u>RNA <u>Fi</u>nder) for the detection of any bizarre tRNA gene (Jühling *et al.*, 2012a). About 1,800 metazoan mitochondrial genomes within a wide range of different taxonomic groups were investigated in this analysis, resulting in a global view on the level of degeneracy of mitochondrial encoded tRNAs in metazoan through the identification of a wide range of exceptional tRNA structures (Jühling *et al.*, 2012a). A summary with the most interesting cases is shown in Figure 6. Deuterostomia, including Mammalia, possess a complete set of mt tRNA sequences with classical cloverleaf structures. Only the D-domain is missing in all tRNA[Ser1] and occasional missing in tRNA[Cys] and other tRNAs. In contrast, basal Metazoa, including Placozoa and Proifera, possess frequently tRNA[Ser1] with a classical cloverleaf structure and/or an incomplete set of mt tRNAs. Two major groups of protostomes (Lophotrochozoa and Ecdysozoa) show a high diversity in presence and absence of D- and T-domains. Nearly all taxonomic sub-classes show a lot of occasionally exceptions from the classical cloverleaf structure with missing D- or T-domains in tRNA[Cys] and other tRNAs (apart from the usually D-arm missing tRNA[Ser1]). Interestingly, in Nematoda nearly all tRNA[Ser2] lack the D-arm, and either the D- or the T-arm is lost in most of the other tRNAs.

Taxonomy	Ser1	Ser2	Cys	others	missing
Deuterostomia					
Mammalia	#^{D}	–	o^D	–	o
Testudines	#^{D}	–	–	–	–
Archosauria	#^{D}	–	–	–	–
Lepidosauria	#^{D}	–	o^D	o^D	–
Amphibia	#^{D}	–	o^D	–	–
Basal Metazoa					
Placozoa	+^{Cl}	–	–	–	–
Porifera	+^{Cl}	–	–	o^D	+
Lophotrochozoa					
Annelida	#^{D}	o^D	–	o^D	–
Brachiopoda	#^{D}	+^{D}	–	o$^{D/T}$	–
Bryozoa	#^{D}	#^{D}	o^D	o$^{D/T}$	–
Entoprocta	#^{D}	–	–	–	–
Ecdysozoa					
Diplura	#^{D}	+^{D}	o^D	o^D	–
Ellipura	#^{D}	–	o^D	–	–
Insecta	o^{Cl}	o$^{D/T}$	–	o$^{D/T}$	o
Crustacea	#^{D}	o$^{D/T}$	o$^{D/T}$	o$^{D/T}$	–
Nematoda	#^{D}	#^{D}	#$^{D/T}$	+$^{D/T}$	–

Figure 6: Exceptional structures of mt tRNA genes and loss of tRNA genes in different taxonomic groups.
'o' indicates occasional events, '+' frequent (>50%) events and '#' highlights taxa that all share the same abnormality. The 'Ser1' column summarizes tRNA^{Ser1} genes exceptionally featuring the classical cloverleaf ('Cl') or commonly lost the D-domain ('D'). Columns 'Ser2', 'Cys' and 'others' indicate tRNA genes that lost the D-domain ('D'), the T-domain ('T') or both domains ('D/T'). The 'missing' column summarizes where it was not possible to find a complete set of 22 tRNA genes within the genomes. The most interesting group for this study, the Nematodes, are highlighted in red (modified from Jühling *et al.*, 2012a).

In this study, an extreme case of structural deviations was found in the mitochondria of Enoplea, a subgroup of nematodes. The newly discovered tRNAs were predicted to lack both at once, D-arm and T-arm, and were thus called "armless" tRNAs (Figure 7). A comparison of armless tRNAs within different nematode species indicated that these minimized tRNA genes are highly conserved, and that the loss of sequences, corresponding to the structural domains, seemed to have evolved multiple times within these species (Jühling *et al.*, 2012b).

With the increased number of available sequenced mitochondrial genomes (from 1,800 in 2012 to over 6000 in 2016), more and more armless tRNA genes similar to that of Enoplea have been identified, especially in Arthropods (Xue *et al.* 2016). Most mt tRNAs

are highly truncated in these animals including, e.g., mites, spiders, and pseudoscorpions. Accordingly, these bizarre tRNA structures seem to be rather the rule than an exception in these animal lineages.

Organism	A	C	D	E	F	G	H	I	K	L1	L2	M	N	P	Q	R	S1	S2	T	V	W	Y
Dorylaimida																						
Xiphinema americanum	⊣	|	⊣	⊣	⊣	⊣	⊣	|	⊣	⊣	⊣	⊣	⊣	⊣	⊣	⊣	⊢	⊢	⊣	⊣	⊣	|
Mermithida																						
Agamermis sp BH-2006	|	⊣	⊣	⊣	|	⊣	|	|	⊣	⊣	⊣	⊣	|	⊣	⊣	|	⊢	⊢	⊣	|	⊣	|
Hexamermis agrotis	|	|	⊣	⊣	|	⊣	|	|	⊣	⊣	⊣	⊣	|	⊣	⊣	|	⊢	⊢	⊣	⊣	⊣	|
Romanomermis culicivorax	|	|	⊣	⊣	|	⊣	|	|	⊣	⊣	⊣	⊣	|	⊣	⊣	|	⊢	⊢	|	⊣	⊣	|
Romanomermis iyengari	|	|	⊣	⊣	|	⊣	|	|	⊣	⊣	⊣	⊣	|	⊣	⊣	|	⊢	⊢	|	⊣	⊣	|
Romanomermis nielseni	|	|	⊣	⊣	|	⊣	|	|	⊣	⊣	⊣	⊣	|	⊣	⊣	|	⊢	⊢	|	⊣	⊣	|
Strelkovimermis spiculatus	|	|	⊣	⊣	|	⊣	|	|	⊣	⊣	⊣	⊣	|	⊣	⊣	|	⊢	⊢	⊣	⊣	⊣	|
Thaumamermis cosgrovei	|	|	⊣	⊣	|	⊣	|	|	⊣	⊣	⊣	⊣	|	⊣	⊣	⊣	⊢	⊢	⊣	|	⊣	|
Trichocephalida																						
Trichinella spiralis	⊣	⊣	+	⊣	⊣	⊣	⊣	+	+	+	+	+	⊣	⊣	⊣	+	⊢	⊢	⊣	⊣	+	|

Figure 7: Secondary structures of predicted mt tRNAs in Enoplea.
The first row enumerates all 20 amino acids. As mitochondrial genomes encode two distinct tRNA[Leu] and tRNA[Ser] genes, both are listed twice as L1/L2 and S1/S2, respectively. Typical nematode tRNAs with a D-arm but no T-arm are indicated by (⊣). The two serine tRNAs have retained their T-arm and lack the D-arm (⊢). Structures lacking both the T-arm and the D-arm are denoted by (|). The intact clover-leaf structures in *Trichinella spiralis* are shown as (+). The used model organism in this study, *Romanomermis culicivorax* is highlighted in red (modified from Jühling *et al.*, 2012b).

2.3. Armless mitochondrial tRNAs

The discovery of armless tRNAs raised several questions concerning their functionality, and if functional, the molecular mechanisms of co-evolution of these unusual molecules and their partner proteins, ensuring the maintenance of a functional protein synthesis machinery. Related questions are for example: "Do armless tRNAs exist *in vivo*? (not only the gene, but also the transcribed RNA)", "Are they functional?", "How are they recognized by their partner proteins?", and "Are they biological relevant"?

As mentioned above, the appearance of truncated mt tRNAs has evolved to an extreme case in nematodes species. The roundworm *Romanomermis culicivorax* belongs to the group of nematode species that were predicted to carry armless mitochondrial tRNAs. In 2014, Wende and colleagues provided the first biological evidence for the existence of

armless tRNAs by sequencing RNA extracts from this worm (Wende *et al.*, 2014). A first hint for the functionality of these bizarre tRNA was the presence of a CCA-tail in each identified transcript at the 3' end. Because this sequence is not encoded in the genome, it has to be post-transcriptionally added by a CCA-adding enzyme. By consequence, the CCA-addition event exists *in vivo* in the nematode worm, and armless tRNAs are processed at this essential maturation step. Thus, the first question concerning the existence of the RNA expression of the gene, and its possible functionality could be positively considered for at least a subgroup of tRNAs.

The study presented here was designated to continue the work presented by S. Wende and colleagues, in order to characterize armless tRNAs from a structural, functional and evolutionary point of view. Therefore, two specific cases where chosen, i.e., tRNA^{Arg} and tRNA^{Ile} from *R. culicivorax*, for performing a more profound investigation. The reasons for these choices are the following. First, the complete sequences as proposed by (Jühling *et al.*, 2012b) could be confirmed for both tRNAs by sequencing of RNA extracts. Second, tRNA^{Arg} and tRNA^{Ile} belong with a length of only 45 nt and 50 nt (including CCA-tail), respectively, to the shortest tRNAs ever described, and are thus highly interesting study objects. Third, tRNA^{Arg} was chosen because aminoacylation studies of the human mt arginyl-tRNA synthetase are in progress at the host laboratory in Strasbourg. This offered the possibility to establish a comparative study between different mitochondrial arginyl-tRNA synthetases and their substrates. Finally, Wende *et al.* also proposed secondary and tertiary structure predictions of both tRNAs calculated by bioinformatic structure prediction tools (Figure 8). The tertiary structure prediction revealed that armless tRNAs may fold into an L-shape-like structure that resembles canonical tRNAs. This might be the case although the distance between the anticodon and the aminoacylation site appears to be much shorter in armless tRNAs (56 Å for tRNA^{Arg} and 46 Å for tRNA^{Ile}) compared to 63 Å for the human mt tRNA^{Arg}. The authors suggested that either the armless tRNAs possess an increased flexibility to compensate for the missing distance, or that the mt translation machinery of *R. culicivorax* has somehow adapted to the reduced tRNA size (Wende *et al.*, 2014). Thus, it appeared highly interesting to evaluate these predictions experimentally, and to confirm or to refute their predictions.
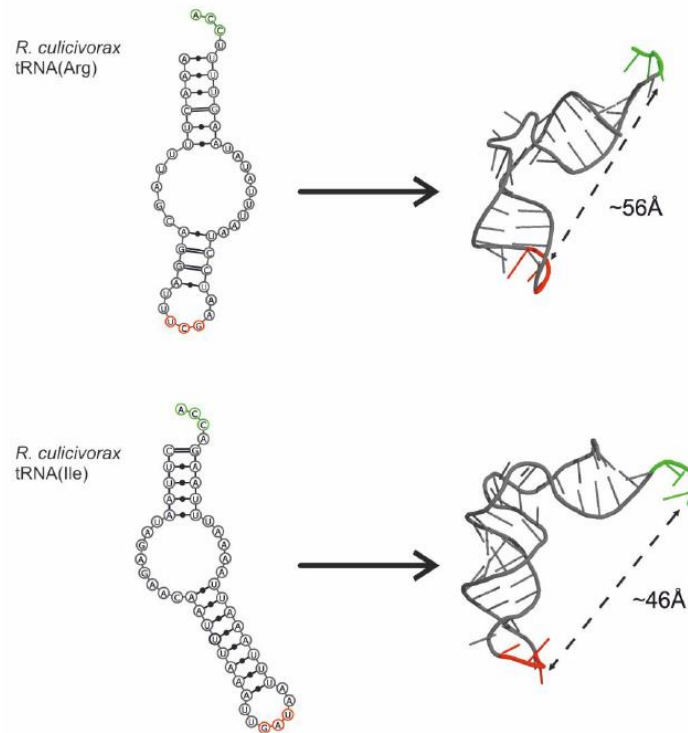
Figure 8: Structure prediction of mt tRNA^Arg and mt tRNA^Ile from R. culicivorax.
In the secondary structure models, the truncations of D- and T-arms are visible, leading to replacement bulges. The anticodon is highlighted red, and the CCA-end green. The predicted 3D structures resemble the standard L-shape of canonical tRNAs, even if acceptor- and anticodon stems show considerable deviations in distance (modified from Wende *et al.*, 2014).

2.4. tRNA-derived fragments (tRFs) - a novel class of small RNAs

The development of next-generation sequencing methods led to a dramatic progress in our understanding of the cellular transcriptome, revealing the existence of many different functional small non-coding RNAs. A novel class of such small RNAs, which is distinct from miRNAs an siRNAs, has been discovered recently by several research groups (reviewed in (Sobala and Hutvagner, 2011). These molecules result from enzymatic cleavage of mature tRNAs or precursor tRNA transcripts, and are referred to as tRNA-derived fragments (tRFs) (Kumar *et al.*, 2015). tRFs arise from cytosolic as well as mitochondrial tRNA templates (Pliatsika *et al.*, 2016), and are processed by several tRNA-specific nucleases such as Dicer (Cole *et al.*, 2009), ELAC2 (Lee *et al.*, 2009), RNase Z, RNase P (Diebel *et al.*, 2016) or Angiogenin (Yamasaki *et al.*, 2009). To date, it has been reported that expression of tRFs is regulated by cellular stresses (Emara *et al.*, 2010), cell proliferation (Lee *et al.*, 2009), or hormone stimulation (Honda *et al.*, 2015). Five structural types of fragments have been identified so far (Pliatsika *et al.*, 2016) (Figure 9): (i) 5'-halves and (ii) 3'-halves that result from Angiogenin cleavage of tRNA

24

within the anticodon loop are composed of 30–35 nt fragments (iii) 5'-tRFs and (iv) 3'-tRFs are shorter and originate from cleavages within the D- and T-arm respectively. Finally, (v) internal tRFs (i-tRFs) correspond to internal cleavages of the tRNA and vary in length (i.e., 14 - 33 nt).
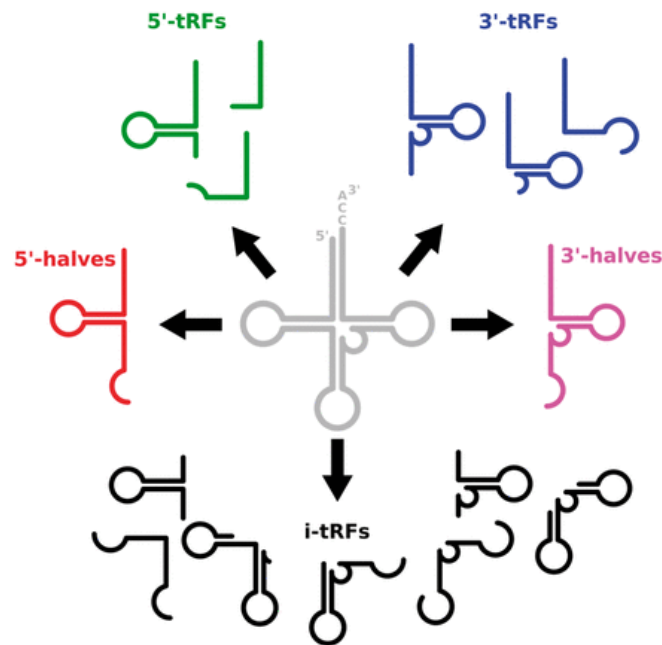
Figure 9: Structural types of tRNA derived fragments.
This is a pictorial summary of the five structural categories of tRNA fragments that are now known to arise from mature tRNAs, both mitochondrial-and nuclear-encoded ones (adapted from Pliatsika *et al.*, 2016).

The composition and abundance of these fragments is extremely versatile, and they exhibit significant changes between sexes, population origin, tissue, and disease status. It has been also shown that tRFs are not restricted to humans, but exist also in other animals (e.g., mice, flies, and worms), bacteria, fungi, yeast and plants (Haiser *et al.*, 2008; Jochl *et al.*, 2008; Thompson and Parker, 2009; Zhang *et al.*, 2009).

Their functions are diverse and still largely unknown (Nolte-'t Hoen *et al.*, 2012). Among others, tRFs have been shown to regulate cell proliferation (Lee *et al.*, 2009), to mediate RNA silencing (Gebetsberger and Polacek, 2013), tumor suppression in breast cancer cells (Goodarzi *et al.*, 2015), and to influence human translation processes (Sobala and Hutvagner, 2013; Ivanov *et al.*, 2011).

The numerous and variable features of tRFs in the cell as well as their presence in a wide variety of organisms and cell lines indicate that this new class of small RNAs probably is not just a random by-product or degradation product of tRNA processing and biogenesis, but has indeed a specific biological importance (Shigematsu *et al.*, 2014).

2.5. Evolution and origin of tRNAs

It is still unclear from where tRNA molecules originated, and how they got involved in the context of protein synthesis. Several evolutionary models have been proposed for the origin and evolution of tRNAs (Weiner and Maizels, 1999; Widmann *et al.*, 2005; Sun and Caetano-Anolles, 2008).

Since secondary structures are very similar for tRNAs, one hypothesis is, that tRNA genes arose through gene duplication. One gene that encoded an original tRNA got duplicated, and the two copies developed independently, so that ultimately tRNA molecules emerged with different amino acid specificities. This process was repeated several times during evolution (LaRue *et al.*, 1981; Di Giulio, 1995).

In contrast, Weiner and Maizels have introduced a Genomic tag Hypothesis, which suggests that tRNAs have evolved independently from two structural and functional units, (Weiner and Maizels, 1999). While one unit ("top half") includes the acceptor arm and the TΨC-arm, the other "bottom half" includes the D-arm and the anticodon arm. The "upper" unit could first have been evolved as a 3'-terminal genomic tag that marked single stranded RNA genomes for replication in a primordial RNA world as proposed by (Gilbert, 1986). Later, with the beginning of protein synthesis, the "lower" unit could have developed separately (Weiner and Maizels, 1999).

However, it is still unclear from where tRNAs originated, and an ongoing debate is still in process in the field of tRNA evolution (Weiner and Maizels, 1999; Widmann *et al.*, 2005; Sun and Caetano-Anolles, 2008; Randau and Soll, 2008; Di Giulio, 2012).

3. tRNA biogenesis and function

The biosynthesis of tRNAs comprises multiple processing steps. After its initial transcription, the tRNA transcript is processed and several modifications are performed, including the removal of its 5' leader and 3' trailer, splicing of introns (if present), CCA-tail addition, and multiple modifications of nucleotide residues. Finally, every mature tRNA is aminoacylated, i.e., the proper amino acid is added to the CCA-tail at its 3' end. Modified and aminoacylated tRNA may than be used in translation. for the synthesis of proteins (Hopper and Phizicky, 2003). After the delivery of the amino acid to the ribosome, uncharged tRNAs may be aminoacylated again, or marked for degradation by adding a second CCA triplet to its 3' end (Wilusz *et al.*, 2011).

Beside the transcription and processing of cytosolic tRNAs, tRNA biosynthesis takes also place in organelles (e.g., mitochondria and chloroplasts) (Hopper *et al.*, 2010). Since processing enzymes are coded in the nucleus, and expressed in the cytosol, they have to be imported into the organelles (Alberts B, Johnson A, Lewis J, et al., 2002). The overall function of tRNAs as well as their processing, modification, charging and translation remain the same inside organelles. However, some peculiarities regarding structures and mechanisms can be observed for proteins that are dedicated to organelles. One interest of this thesis is concentrated on direct mitochondrial tRNA-interacting proteins. The following paragraph will described the main steps of tRNA biogenesis in detail, and thereby also compare cytosolic tRNA processing enzymes (such as RNase P, RNase Z, CCA-adding enzyme) and other partner molecules in translation (such as aminoacyl-tRNA synthetases, elongation factors and ribosomes) with those from mitochondrial and bacterial origins.

3.1. From primary transcripts to functional tRNA molecules

tRNA transcription

The biosynthesis of nuclear encoded tRNAs starts with their transcription by the RNA polymerase III (Pol III) (Roeder and Rutter, 1969). Pol III is primarily guided by two transcription factors, i.e., TFIIIC and TFIIIB that recognize two internal promoter sequences (block A and B). The A-block and B-block are part of the D- and T-stems (Asin-Cayuela and Gustafsson, 2007) and loops, respectively (White, 2011).

The human mitogenome is transcribed by a specialized machinery that includes a monomeric RNA polymerase, the mitochondrial transcription factor A, and a mitochondrial transcription factor B homolog (Asin-Cayuela and Gustafsson, 2007). The human mitogenome is transcribed into three polycistronic RNA molecules, which is then processed and split into individual tRNA and RNA molecules (Ojala *et al.*, 1981). This mode of RNA processing is known as the "tRNA punctuation model" (Asin-Cayuela and Gustafsson, 2007). In general, pre-tRNA transcription products contain additional 5' and 3' RNA sequences, and in some cases tRNA precursors contain an intron in the anticodon arm, which have to be spliced out during processing of the tRNA (Abelson *et al.*, 1998).

5'- and 3'-end maturation

The ribonuclease P (RNase P) cleaves 5'-leader sequences of tRNA precursors (Altman, 2000). This ribozyme is a ubiquitous endoribonuclease, found in Archaea, Bacteria and Eukaryotes. Interestingly, RNase P is usually a ribozyme composed of a catalytic active RNA chain and at least one protein (Evans *et al.*, 2006). The crystal structure of bacterial and eukaryotic RNase P confirmed the location of the active site in the RNA part (Reiter *et al.*, 2010). Surprisingly, in mitochondria and chloroplasts of various animals and plants another type of RNase P exist. This other type is a proteinous enzymes and termed PRORP for "protein-only RNase P" (Holzmann *et al.*, 2008; Gobert *et al.*, 2010). Its counterpart, the endonuclease RNase Z removes the 3'-trailer of primary transcripts, and leaves a 3'-hydroxy group at the tRNA end (Ceballos and Vioque, 2007). In eukaryotes two different forms of RNase Z exist, i.e., a long form (RNase Z^L) and a short form (RNase Z^S). RNase Z^S is localized in the cytosol, whereas the human RNase Z^L was found in both, mitochondria and nucleus (Rossmanith, 2011). Some pre-tRNAs contain introns. These are either removed by several tRNA-splicing exonucleases, or are self-splicing group I introns in bacteria and in higher eukaryote organelles (Tocchini-Valentini *et al.*, 2009).

CCA-incorporation

In all three domains of life, mature tRNAs contain a CCA-sequence at their 3'-end to allow the correct attachment of the appropriate amino acid. These three bases are usually not encoded in the tRNA gene in eukaryotes, but have to be post-transcriptionally added during the processing of the pre-tRNA transcript (Yue *et al.*, 1996). The enzyme responsible for this process is a [ATP(CTP):tRNA nucleotidyltransferase] (CCA-adding enzyme, or a CC- and A-adding enzyme) (Tomita *et al.*, 2004; Neuenfeldt *et al.*, 2008). Thereby, the CCA-addition is performed in a highly specific, template independent manner (Xiong and Steitz, 2006). In some bacteria, e.g., *E. coli,* tRNA genes encode already the CCA sequence. Nevertheless, even in these organisms the CCA-enzyme is important because it functions as a repair enzyme for tRNAs with an incomplete CCA triplet (Zhu and Deutscher, 1987). One main interest of this work is the characterization of the CCA-adding enzyme of the nematode *R. culicivorax* (Chapter 3). Therefore, section 4 is dedicated to a more accurate description of the structural specificities and the features of this interesting enzyme.

28

tRNA modifications

Mature tRNAs can contain up to 10 % bases that are different from the usual 4 bases, i.e., adenine (A), guanine (G), cytosine (C) and uracil (U). These bases are modified by specific tRNA modification enzymes during the processing of the transcript (Jackman and Alfonzo, 2013). To date, more than more than 160 modification enzymes have been identified (Grosjean, 2015). tRNA modification enzymes can be divided into two groups. The first group ensures a stabilization of the tRNA structure, and is thus independent from the presence of the L-shaped tertiary structure. These modifications concern often nucleotides of the acceptor and the TΨC arm (Grosjean *et al.*, 1995). Modifications in these domains comprise mainly methylated nucleotides, pseudouridines, or dihydrouridines (Helm, 2006). The enzymes belonging to the second group, however, are dependent on tRNA secondary and tertiary structures. These modifications are mainly found in the anticodon arm and the D-arm (Grosjean *et al.*, 1995). Many of these enzymes can modify both, cytosolic and mt tRNAs. This group, for example, includes (guanine- N1)-methyltransferase (Trm5p) and Pseudouridylat synthase 1 (PUS1) (Fernandez-Vizarra *et al.*, 2007; Lee *et al.*, 2007). However, some are mitochondrial specific enzymes, e.g., 2-Thiouridylase 1 (MTU1) is responsible for the formation of 5-Taurinomethyl-2-thiouridine (τm5s2U) at the anticodon wobble position of mitochondrial mt tRNA[Lys] (Umeda et al., 2005).

Aminoacylation

The aminoacylation reaction is catalyzed by specific aminoacyl-tRNA synthetases (aaRS). In contrast to RNase P, RNase Z, or the CCA-adding enzyme that are all able to recognize different tRNAs, each aaRS recognizes specifically its cognate tRNA or family of tRNA isoacceptors, and esterifies the tRNA 3'-end with the specific amino acid. The aminoacylation reaction consists of a two-step reaction including the formation of an aminoacyl-adenylate intermediate, followed by the transfer of the activated aminoacyl group to either the 2′- or 3′-OH of their cognate tRNAs (Ibba and Soll, 2000).

The eukaryotic nuclear genome encodes two or three distinct sets of aaRSs. One set is specific for cytosolic, mitochondrial or chloroplastic translation. The sets can be distinguished by their sequences (Berglund *et al.*, 2009).

Experimental characterization of the mammalian mt aminoacylation systems is still at the beginning, which is probably due to the limited number of recombinant mammalian

mt aaRSs that have been obtained so far. However, the dual origin of the two partner molecules and the mechanisms of reciprocal recognition and of co-evolution of aaRS makes them very interesting study objects and deserve further attention (Florentz *et al.*, 2013). More information about structural, biophysical and functional properties of cytosolic and mitochondrial aaRS is given in section 5 and characteristic peculiarities of the arginyl-tRNA synthetases will be further reviewed in chapter 4 of this study.

Elongation factors EF-Tu

The elongation factor EF-Tu (an acronym for "elongation factor thermo unstable")/GTP complex binds and transports aminoacyl-tRNAs to the A site of the ribosome (Clark and Nyborg, 1997). EF-Tu binds to the acceptor stem and T-arm of cytosolic tRNAs (Nissen *et al.*, 1995). It has been shown that it cannot bind to a tRNA analogue missing the T-arm (Rudinger *et al.*, 1994). Interestingly, the mitochondrial counterpart of EF-Tu in nematodes has developed a different strategy to recognize T-arm missing tRNAs. In fact, nematode mitochondria possess two EF-Tu homologs: EF-Tu1 binds T-arm lacking tRNAs, while EF-Tu2 binds exclusively D-arm lacking tRNAs[Ser] (Ohtsuki *et al.*, 2002b). In *C. elegans,* EF-Tu1 presents a C-terminal extension of ~60 amino acids that likely compensates for the missing T-arm. In contrast, it is not able to bind full-size tRNAs. EF-Tu2 has an approximately 15 amino acid extension at the C-terminus and seems to be adapted especially to D-arm missing tRNA[Ser] backbones (Sato *et al.*, 2006). Interestingly, two distinct mt EF-Tu genes were also discovered in arthropods carrying T-armless and D-armless tRNAs (Ohtsuki and Watanabe, 2007).

Translation

The ribosomal translation of mRNAs is a central step of protein biosynthesis, and is found in all living organisms. Translation occurs in the cytoplasm, in mitochondria and in chloroplasts. Ribosomes are composed of proteins and RNA, and act through ribozyme activity (Ban *et al.*, 2000). They are composed of two subunits that differ in size and function. During translation, they assemble into a functional complex, wherein the large subunit links the amino acids to the nascent protein chain, and the small subunit is the location of translation where tRNA's anticodons bind mRNA (Alberts B, Johnson A, Lewis J, et al., 2002).

The mass of the ribosome is characterized by their sedimentation in centrifugation that is specified in Svedberg units (S). An overview of the subunit sizes and the RNA/protein proportion is given in Table 1. The cytosolic ribosome of eukaryotes corresponds to 80S, containing a large 60S and a small 40S subunit. Its protein:RNA mass ratio is approximately 1:1, while it consists of 4 rRNAs (i.e., 28S, 18S, 5.8S, and 5S) and 79 ribosomal proteins (Ban *et al.*, 2000; Wilson and Doudna Cate, 2012). Bacteria possess a 70S ribosome with a large subunit of 50S, and a small subunit of 30S. In contrast to their eukaryotic counterpart, they possess a higher RNA content with a protein:RNA mass ratio of 1:3. Thereby, bacterial ribosomes contain about 50 different proteins, and three rRNAs (i.e., 23S, 5S, and 16S rRNAs) (Yusupov *et al.*, 2001; Schuwirth *et al.*, 2005). The mammalian mitoribosome contains a large 39S and a small 28S subunit, together forming a 55S mitoribosome (O'Brien, 1971). Unlike eukaryotic ribosomes and their bacterial ancestors, the mitoribosome is protein rich with a protein:RNA mass ratio of 3:1, and consists of 77 proteins and 3 RNAs (i.e., 16S, 5S, and 12S) (Sylvester *et al.*, 2004). Interestingly, the solved crystal structures of human and porcine mitoribosome revealed the presence of tRNAs (tRNA[Val] and tRNA[Phe], respectively) replacing the 5S RNA when comparing with the yeast mitoribosome (Brown *et al.*, 2014; Greber *et al.*, 2015).

Table 1: Overview of the composition of ribosomes in Eukaryotes, Prokaryotes and mammalian mitochondria.
The exact size, weight and number of proteins varies from organism to organism (modified from Greber and Ban, 2016).

	Ribosome (Sedimentation coefficient and RNA:protein ratio	Molecular weight	Subunits	rRNAs	Number of proteins
Eukaryotes	80S RNA: 50 % Protein: 50 %	3.3-4.3 MDa	60S	26S-28S 5.8S 5 S	46-47
			40S	18S	33
Prokaryotes	70S RNA: 67 % Protein: 33 %	2.3 MDa	50S	23S 5S	33
			30S	16S	21
Mammalian mitochondria	55S RNA: 31 % Protein: 69 %	2.7 MDa	39S	16S CP tRNA (73-75 nt) mt tRNA[Val] (human) mt tRNA[Phe](pork)	52
			28S	12S	30

Mitochondrial ribosomal proteins are encoded in the nucleus, and post-translationally targeted into mitochondria. Additional ribosomal proteins that have evolved to replace RNAs tend to have no recognizable homologs in prokaryotic or eukaryotic cytoplasmic proteomes, and are evolving faster than cytoplasmic ribosomal proteins (O'Brien, 2002). Nematode ribosomes are even more striking in their rRNA loss, and are much more protein-enriched (Figure 10) (Watanabe, 2010; Zhao *et al.*, 2005). The figure illustrates that the amount of RNA is reduced in mammalian and *C. elegans* mitoribosomes. Only the region containing the catalytic site is highly conserved. These observations strongly suggest that enlarged mitoribosomal proteins can compensate for the deficit in mitoribosomal RNAs (Suzuki *et al.*, 2001).
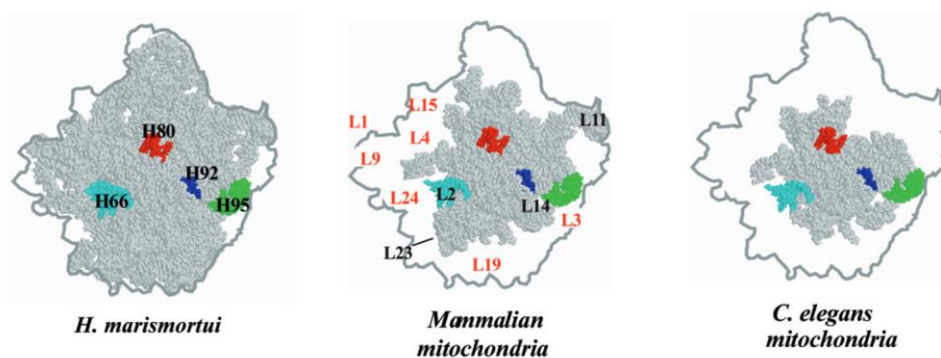
Figure 10: 3D models for large mitoribosomal RNA
3D models for large mitoribosomal RNA (gray) of mammalian (middle) and *C. elegans* (right) mitochondria, based on the crystal structure of a bacterial 50S subunit from *H. marismortui* (pdb 1FFK) (left). The outline shows an edge line of the crystal structure of the 50S subunit from the crown view. Some functional rRNA domains are colored: red, P loop; blue, A loop; green, S/R loop; light blue, L2 binding helix (H66). The topological orientation of the ribosomal protein is based on the model for the mammalian mitoribosome (adapted from Watanabe, 2010).

Alternative roles of tRNAs

Beyond their canonical role during protein biosynthesis, tRNAs can be involved in additional processes in eukaryotes, prokaryotes and archaea (Raina and Ibba, 2014). Several tRNAs participate in energy metabolism and amino acid synthesis. One example, which is found in all domains of life, although not present in all organisms, is the formation of the exceptional 21st amino acid selenocysteine, which is mostly formed indirectly through the modification of a tRNA[Ser] precursor (Sheppard *et al.*, 2008).

In bacteria, tRNAs participate in the regulation of siRNAs, that interfere in mRNA silencing during stress conditions (Lee and Feig, 2008). tRNA[Gly] is involved in cell-wall synthesis (Navarre and Schneewind, 1999). tRNA[Phe] and tRNA[Leu] are used to tag proteins

with Phe and Leu for degradation, while tRNA^{Lys} and tRNA^{Ala} are involved in remodeling membrane lipids (Roy and Ibba, 2008).

In eukaryotes, it has been shown that tRNA^{Glu} takes part in the chlorophyll and heme biosynthesis (Jahn *et al.*, 1992). tRNA^{Arg} is used for N-terminal arginylation of proteins, thus effecting cell motility, and it may contribute to cardiovascular development and angiogenesis (Karakozova *et al.*, 2006). Furthermore, specific cytosolic tRNAs are involved in the initiation of reverse transcription in retroviruses (Miller *et al.*, 2014). Mt tRNAs can interfere with a cytochrome *c*-mediated apoptotic pathway, and promote cell survival (Hou and Yang, 2013). One should also not neglect the emerging role of tRNA derived fragments that are known to be present in various organisms of all kingdoms of life, where they perform crucial and diverse functions, e.g., in the regulation of translation or stress responses (Nolte-'t Hoen *et al.*, 2012; Shigematsu *et al.*, 2014; Pliatsika *et al.*, 2016). A schematic overview about tRNA biogenesis and function is represented in Figure 11.
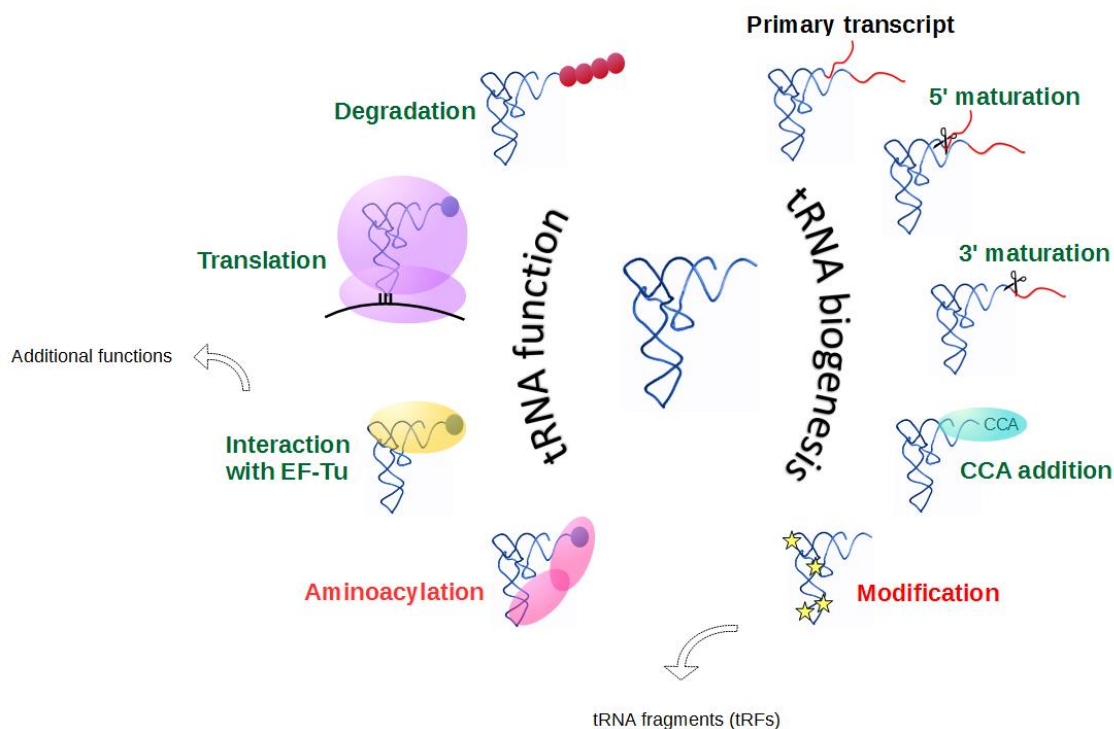
Figure 11: tRNA biogenesis and function
The 5'-sequence is removed by RNase P, whereas the 3'-end is removed by RNase Z. The CCA nucleotide sequence is added by CCA-adding enzymes at the 3'-end of tRNAs. Modification enzymes modify the tRNA. tRNA fragments (tRFs) result through the cleavage of exonucleases or cleavage enzymes. Aminoacyl-tRNA synthetases are specialized for one tRNA family and transfer the cognate amino acid to the tRNA. Finally, aminoacyl-tRNAs are delivered to the ribosome by elongation factor (EF-Tu) where they participate in protein synthesis. Despite their fundamental role in translation, mature tRNAs can fulfill additional functions. Maturation and processing steps marked in green are performed by enzymes that recognize all tRNA families, while aminoacylation and modification (red) are mostly performed by specialized enzymes.

4. Structure and function of CCA-adding enzymes

The CCA-adding enzyme catalysis the synthesis and regeneration of the nucleotide sequence C-C-A at the 3'-end of tRNAs missing one, two or all three 3'-terminal nucleotides (Sprinzl and Cramer, 1979). In several prokaryotes, this function is accomplished by separate enzymes for CC- and A-addition (CC-adding enzyme and A-adding enzyme), which share conserved motifs with CCA-adding enzymes in the N-terminal catalytic core (Bralley *et al.*, 2005). In some bacteria like *E. coli* or *Mycoplasma genitalium* the CCA terminus is encoded in all tRNA genes. An inactivation of this enzyme is not lethal for these organisms but decreases the growth rate. Thus, the CCA-adding enzyme functions here primary as a repair enzyme (Reuven *et al.*, 1997; Zhu and Deutscher, 1987; Lizano *et al.*, 2008). For eukaryotes, some archaea, and many bacteria that do not encode the 3'-terminal CCA sequence the CCA-addition is an essential step in tRNA biogenesis (Yue *et al.*, 1996; Shi *et al.*, 1998).

According to their primary sequence CCA-adding enzymes belong to the superfamily of DNA polymerases β (Holm and Sander, 1995). Enzymes of this family of all the three kingdoms, Eubacteria, Bacteria and Archaea share a common active site signature: hG[GS]x$_{(7-13)}$DhS[DE]h (x - any amino acid, h - hydrophobic amino acid) (Martin and Keller, 2004). They can be further divided into two classes. Class I includes the β-DNA polymerases, terminal deoxynucleotidyltransferases (TdT), eukaryotic poly(A) polymerases (PAP), kanamycin nucleotidyltransferases, three protein nucleotidyltransferases (GlnB-uridylyltransferase, glutamine synthase adenylyltransferase and streptomycin adenylyltransferase), and archaeal tRNA nucleotidyltransferases (Aravind and Koonin, 1999; Holm and Sander, 1995; Martin and Keller, 1996; Yue *et al.*, 1996). Beside the two highly conserved primary structural motifs (DxD and RRD; x - any amino acid) in the catalytic domain that possess all members of this class no more sequence homology can be determined. Class II enzymes represent those of bacterial and eukaryotic origin and include bacterial poly(A) polymerases, and eukaryotic and eubacterial tRNA nucleotidyltransferases (Yue *et al.*, 1996).

<u>Reaction mechanism</u>

CCA-adding enzymes recognize tRNA precursors or tRNA-like molecules, and select the correct incoming nucleotide (CTP or ATP). After nucleotide selection, the enzyme adds

two Cytosines, and terminates nucleotide incorporation by the addition of a final Adenosine. Thereby, CCA-adding enzymes do not require any nucleic acid template to fulfill this complex function (Betat *et al.*, 2010). Nucleotide incorporation by CCA-adding enzymes takes place according to a common two-metal ion mechanism as known for polymerases (Doublie *et al.*, 1998) (Figure 12). Two highly conserved carboxylates (DxD, DxE) bind and coordinate two divalent metal Mg^{2+} ions. Metal ion A subtracts the proton from the 3'-OH group of the tRNA primer, and thus facilitates a nucleophilic attack on the α-phosphate group of the incoming nucleotide. The second metal ion B stabilizes the triphosphate group of the incoming nucleotide, and facilitates the cleavage from the pyrophosphate group (Steitz, 1998).
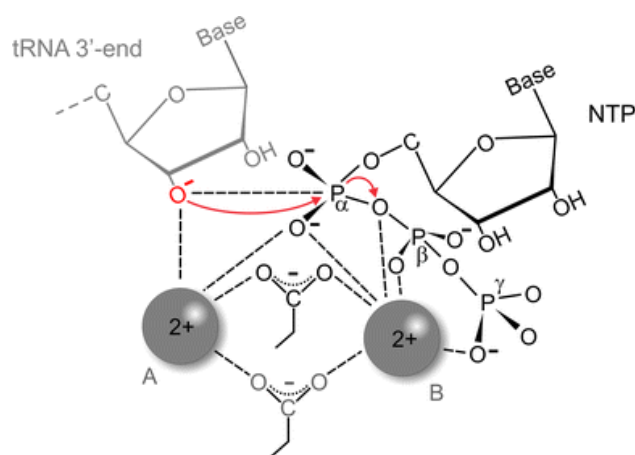
Figure 12: Schematic representation of the two-metal ion mechanism of CCA-adding enzymes.
Polymerization mechanism of CCA-addition according to the general two-metal ion-catalyzed reaction. The two metal ions (Me^{2+}, grey balls) are bound to the two catalytic carboxylates. Metal ion A deprotonates the 3'-OH group of the tRNA primer (grey), and activates the resulting 3'-O⁻ (red) for an attack at the α-phosphate of the incoming nucleotide (red arrows). The second metal ion B stabilizes the triphosphate moiety of the NTP, and facilitates the separation of the pyrophosphate group (adapted from Betat *et al.*, 2010).

Structural organization

The resolution of crystal structures of an archaeal CCA-adding enzyme (*Archaeoglobus fulgidus*), bacterial (*Bacillus stearothermophilus*) and the human CCA-adding enzyme (Li *et al.*, 2002; Augustin *et al.*, 2003; Okabe *et al.*, 2003) brought further insights into the structural organization of CCA-adding enzymes and revealed that they can be divided in four structural domains: head, neck, body and tail (Li *et al.*, 2002; Xiong *et al.*, 2003) (Figure 13). The general division into the four domains is the same for the classes I and II enzymes although differences exist between the two classes regarding the secondary structure and the mechanism of CCA-addition (Xiong and Steitz, 2006).

In class II the head domain is composed of anti-parallel β-sheets, including the catalytic site with the signature motif DxD. The neck domain is composed of α-helical elements containing the EDxxR motif, necessary for the detection of incorporated nucleotides. In contrast to class I enzymes, class II CCA-adding enzymes use amino acid side chains, which form a protein template for the selection of incoming nucleotides (Li *et al.*, 2002). The body and tail domains are responsible for tRNA recognition, which takes place exclusively via the sugar-phosphate backbone of the tRNA. This means that the CCA-adding enzyme is capable of binding any tRNA in a sequence-independent manner (Xiong and Steitz, 2006).
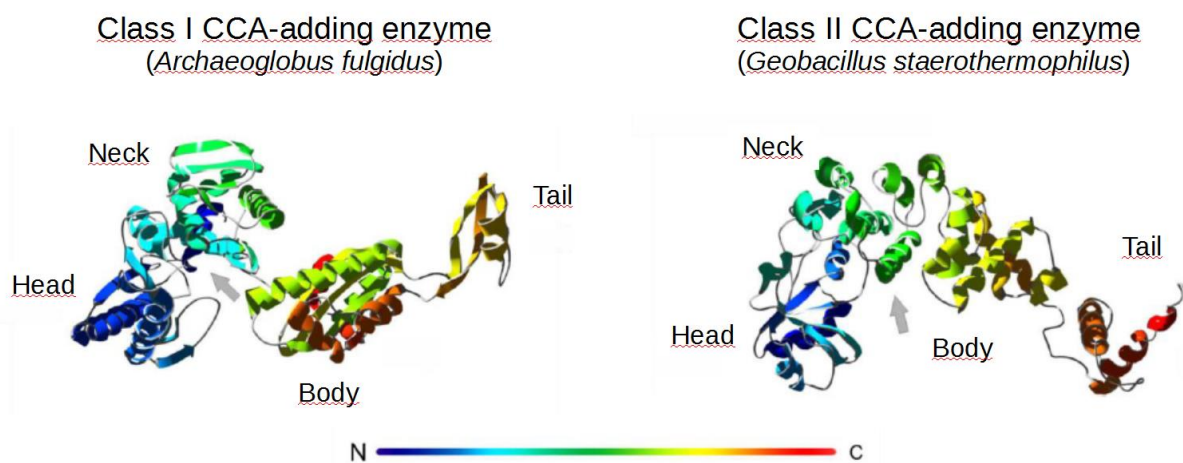
Figure 13: Structure comparison of class I and class II CCA-adding enzymes.
Crystal structures of the class I CCA-adding enzyme of *A. fulgidus* (pdb 1SZ1) (left) and the class II CCA-adding enzyme of *G. stearothermophilus* (pdb 1MIV) (right). Both enzyme classes exhibit head, neck, body and tail domains, but the allocation of secondary structure elements are quite different. The class I enzyme consists of α-helices and β-folds. The class II enzyme, on the other hand, has a seahorse-like structure and consists exclusively of α helices outside the head domain. A gray arrow points to the catalytic center of both enzymes. The enzymes are shown from the N- to the C-terminus in a rainbow pattern (from blue to red) (modified from Vörtler and Mörl, 2010).

Class I CCA-adding enzymes

The class I CCA-adding enzyme employs both an arginine side chain and a phosphate backbone of the bound tRNA to recognize incoming nucleotides. However, selection of the ribonucleotides takes place only when the tRNA primer is present. The switch from C to A addition is done through changes in the size and shape of the nucleotide-binding pocket, which is progressively altered by the elongated 3′-terminus of the tRNA (Xiong and Steitz, 2006). After incorporation of the full CCA sequence, the CCA end reaches a stabilized conformation by stacking interactions. As a result, A76 is no longer positioned

in the primer binding site and no further additions are performed (Martin and Keller, 2007; Xiong and Steitz, 2006).
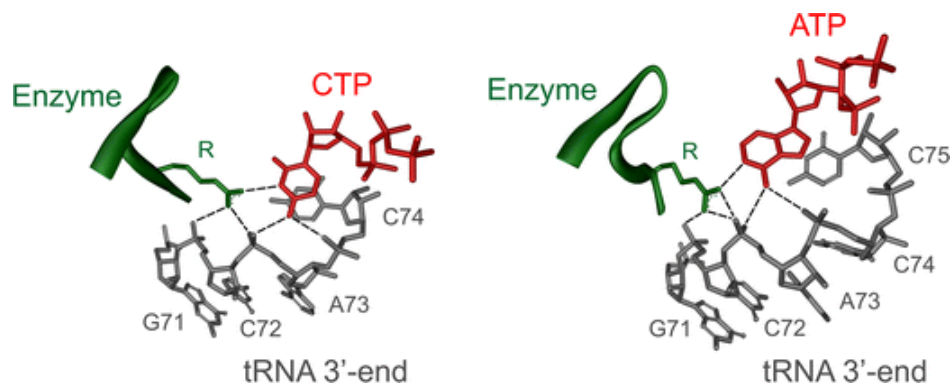
Figure 14: Nucleotide binding pocket of class I CCA-adding enzymes.
A highly conserved arginine (green) and the phosphate groups of the tRNA backbone (gray) form specific hydrogen bonds to the bound nucleotides CTP and ATP (red). The collaboration of both protein and tRNA is responsible for an efficient and accurate templating during CCA-addition. The crystal structure originates from the *A. fulgidus* CCA-adding enzyme (pdb 1SZ1) (adapted from Betat et al. 2010).

Class II CCA-adding enzymes

All members of class II nucleotidyltransferases possess a highly conserved 25 kDa N-terminal region that includes characteristic active site signature motifs A-E. Motif A represents the common signature motif of nucleotidyltransferases of the β-superfamily and contains the conserved amino acids GGxVRD and DxD, which are essential for the metal ion catalysis (Steitz *et al.*, 1994). Motif B consists of the amino acids DxxRRD, which are important for the discrimination between NTPs and dNTPs (Li *et al.*, 2002). A recent study revealed that motif C ($Dx_{(3,4)}Gx_{(9)}R$) contributes to the switch in nucleotide specificity during polymerization (Ernst *et al.*, 2015). The neck domain contains motif D, which consists of the amino acids EDxxR and plays a crucial role for nucleotide substrate specificity. It represents therefore an amino-acid based template for nucleotide selection (Li *et al.*, 2002). Less is known about motif E. It is described as a stabilizing element between the individual domains of the enzyme. Another important structural element is referred to as a flexible loop due to its high flexibility and missing conserved signature. This element is essential for the terminal A incorporation (Neuenfeldt *et al.*, 2008).

The C-terminal part is involved in the binding of the tRNA. Interestingly, this domain exhibits a high degree of variation and shows no sequence conservation when comparing CCA-adding enzymes (Yue *et al.*, 1996; Betat *et al.*, 2004).
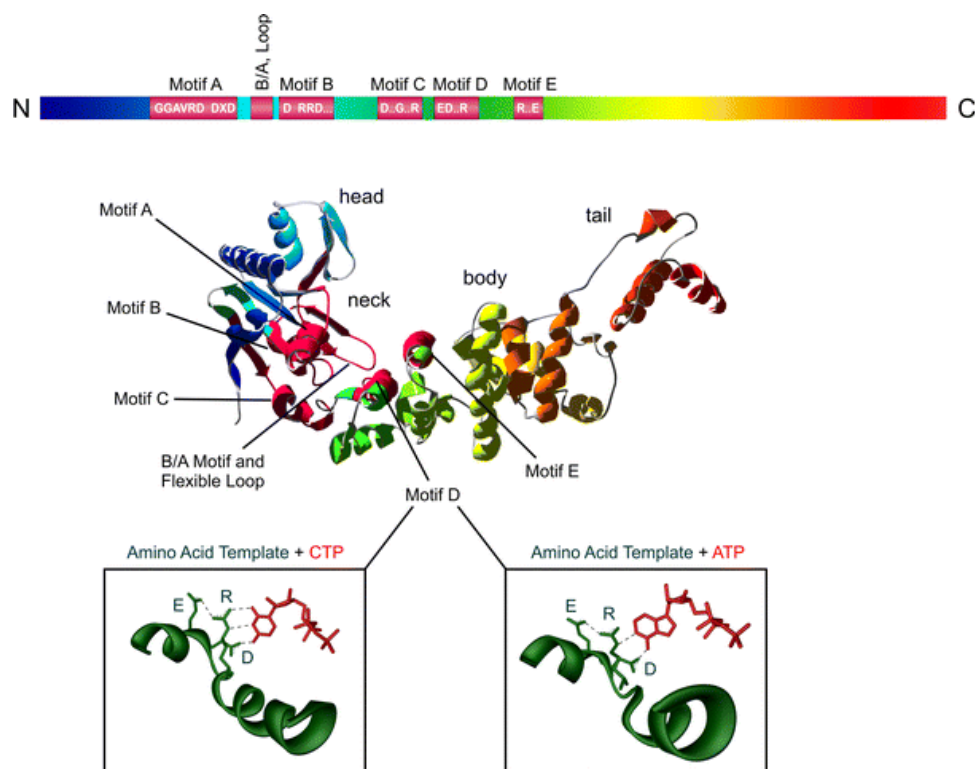
Figure 15: Structural organization of Class II CCA-adding enzymes.
The upper part of the figure shows the highly conserved motifs in red boxes from the N- to the C-terminus Furthermore, the crystal structure of the CCA-adding enzyme of *Thermotoga maritima* (pdb 3H38) is shown from the N- to the C-terminus in a rainbow pattern (from blue to red). The conserved motifs are located in the head and neck domains and are shown in dark red. The lower part of the figure shows the nucleotide binding site (green) for incoming CTP or ATP (red) in motif D. The nucleotide-binding site structure is derived from the pdb entry of the *Geobacillus stearothermophilus* CCA-adding enzyme (pdb 1MIY, 1MIW) (modified from Betat *et al.*, 2010).

From a genomic point of view, a single gene encoded in the nucleus of eukaryotic cells provides the enzyme activity for the CCA-addition of both, cytoplasmic and mitochondrial tRNAs. The mitochondrial enzyme carries an amino-terminal mitochondrial import sequence that derives from an alternative start codon for translation of the mRNA.

tRNA recognition and substrate specificity of CCA-adding enzymes
tRNAs represent the main substrates of CCA-adding enzymes. Class I as well as class II CCA-adding enzymes recognize tRNAs in a sequence-independent manner. Both, class I and II CCA-adding enzymes recognize the size, form and charge of the tRNAs. This allows binding of all different tRNA molecules (Xiong and Steitz, 2006; Betat *et al.*, 2010). Binding of tRNAs to these enzymes takes mainly place at the sugar phosphate backbone of the T-arm, the T-loop and the acceptor arm of tRNAs (Xiong and Steitz, 2006). CCA-adding enzymes do not require a complete tRNA for substrate identification, but only

the upper half of the L-shaped structure. Therefore, tRNA minihelices consisting of acceptor and T-arm of CCA-adding enzymes are also recognized as substrates (Li *et al.*, 1997; Dupasquier *et al.*, 2008; Lizano *et al.*, 2008).

It has been shown that enzymes from various organisms strictly recognize the elbow region of tRNAs formed by conserved D- and T-loops. However, many mammalian mt tRNAs lack of consensus sequences in both loops, or even miss one of the loops completely. In 2001, Nagaike and colleagues demonstrated that the human mt CCA-adding enzyme is capable to repair cytosolic tRNAs, human mt tRNAs as well as non-cognate nematode mt tRNAs that lack the T-arm. Its bacterial counterpart, in contrast, was only poorly able to process mt tRNAs, which indicates an adaptation of mitochondrial CCA-adding enzymes to the unusual structure of mt tRNAs (Nagaike *et al.*, 2001).

Alternative substrates for CCA addition are often tRNA-like molecules or hairpin structures imitating the upper half of tRNA structures. Indeed, alternative non-tRNA-like molecules have been shown to be appropriate substrates for CCA-addition. For example, the 3'-terminal RNA structure in the tobacco mosaic virus resembles a tRNA structure, which is recognized by both, *E. coli* and *S. cerevisiae* CCA-adding enzymes (Hegg *et al.*, 1990). Furthermore, CCA nucleotides are post-transcriptional added to the mRNA of rps12 in *Zea mays* (Williams *et al.*, 2000). And 65% of mature human spliceosomal U2 snRNAs carry a 3'-CCA sequence, where at least the terminal A has been added post-transcriptionally. Structure of the 3'-stem of U2 snRNAs resemble a tRNA minihelix (Cho *et al.*, 2002). The substrate requirements for the human CCA-adding enzyme were studied more in detail and revealed that transcripts lacking a tRNA-like 3′-end are also accepted for CCA addition and that the discriminator position in tRNAs, which is normally an identity element for aminoacyl-tRNA synthetases, has a great impact on CCA incorporation (Wende *et al.*, 2015). All these examples emphasize the diversity of alternative substrates of CCA-adding enzymes. However, the biological relevance of these alternative substrates for CCA addition is still unclear.

5. Structure and function of aminoacyl-tRNA synthetases

Before an amino acid can be used for protein synthesis, it must be transferred to a specific tRNA molecule. This process is of particular importance as it allows the implementation of the genetic code. Specific aminoacyl-tRNA synthetases (aaRSs) are key enzymes in this process. The aminoacylation of a tRNA is a highly specific two-step reaction. First, the amino acid is activated into an aminoacyladenylate (aminoacyl-AMP) at the expense of ATP. In the second step the aminoacyl-group is transferred from the aminoacyl-AMP to a specific tRNA molecule resulting in aminoacyl-tRNA (Ibba and Soll, 2000).

The two classes of aaRSs

Interestingly, these enzymes differ in sequence, size, shape and oligomer composition and share little sequence homology (Schimmel, 1987). They can be divided into two classes (Eriani *et al.*, 1990). Class I enzymes are mostly monomeric and contain a characteristic Rossman fold catalytic domain (Sugiura *et al.*, 2000). The Rossman fold displays two conserved signature amino acid sequences: "HIGH" and "KMSKS" (Barker and Winter, 1982; Webster *et al.*, 1984). The aminoacyl group is coupled to the 2'-hydroxyl of the substrate tRNA. Class II aminoacyl-tRNA synthetases are mostly dimeric or multimeric and share an anti-parallel beta-sheet fold flanked by alpha-helices and contain three characteristic homologous motifs. The class II enzymes attach the amino acid to the tRNA 3'-hydroxyl site.

Class I	Class II
ArgRS	AlaRS
CysRS	AsnRS
GlnRS	AspRS
GluRS	GlyRS
IleRS	HisRS
LeuRS	LysRS-II
LysRS-I	PheRS
MetRS	ProRS
TrpRS	SerRS
TyrRS	ThrRS
ValRS	

Human mt-TyrRS   Human mt-AspRS
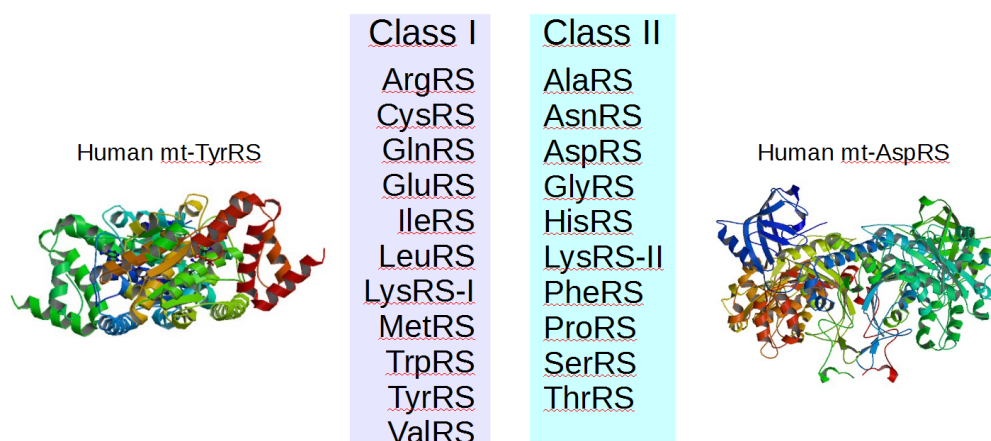
Figure 16: Schematic overview of the two classes of aminoacyl tRNA synthetases.
The 20 aminoacyl-tRNA synthetases comprise two distinct families of enzymes. Class I enzymes are characterized by an active site domain that has a Rossmann nucleotide-binding fold composed of alternating β strands and α helices. Class II enzymes are made up of a seven-stranded β sheet with flanking α helices. Classical examples of the crystal structures of the two classes are shown with the human mt TyrRS (pdb 3ZXI) and human mt AspRS (pdb 4AH6) (modified from Ribas de Pouplana and Schimmel, 2001).

40

Many efforts have been brought over decades, towards understanding of the recognition code of tRNAs by aminoacyl-tRNA synthetases. This "second genetic code" is crucial for the accuracy of translation since it allows a specific amino-acid to be linked precisely and exclusively to the corresponding tRNA (Beuning and Musier-Forsyth, 1999; Giegé and Eriani, 2001).

tRNA recognition and specific "identity elements" have been deciphered for each aaRS in *E. coli* and *S. cervisiae* and have been partially determined for other organisms, e.g., *T. thermophilus*, *C. elegans*, *A. thaliana* and *H. sapiens* (McClain, 1993; Beuning and Musier-Forsyth, 1999; Giegé *et al.*, 2012). Most aaRSs recognize their cognate tRNAs through direct interactions with the anticodon and acceptor stem regions (Rich and Schimmel, 1977; Giegé *et al.*, 1998). But also other structural regions or even concrete nucleotides can represent additional tRNA identity elements such as the variable loop region of tRNA^{Ser} (Lenhard 1999), the tRNA elbow of tRNA^{Leu} and tRNA^{Val} (Du, 2003; Fukai *et al.*, 2000), single nucleotides such as the discriminator base at position 73 (Pütz *et al.*, 1991), base pairs like G3:U70 in tRNA^{Ala} (Chihade *et al.*, 1998) or even chemically modified bases for example in the anticodon loop of *E. coli* tRNAs specific for Ile, Glu and Lys (Giegé *et al.*, 1998).

Mitochondrial aaRSs

Usually mitochondria do not encode any aaRSs in their own genome. All aaRS that are needed for mitochondrial translation, are encoded in the nuclear genome, and imported into mitochondria. Mt aaRSs are translated in the cytosol, and imported into mitochondria, thanks to a MTS, which is cleaved during the import process. The identification of a MTS is still challenging since sequence lengths and amino acid compositions are not conserved (Gakh *et al.*, 2002; Chacinska *et al.*, 2009).

In mammals, cytosolic and mitochondrial synthetases are usually encoded by two different genes. The only exceptions are LysRS and GlyRS, which are encoded by the same gene. The protein, which is dedicated to mitochondria is generated by either alternative splicing (Tolkunova *et al.*, 2000) or by processing from alternative translation start site (Mudge *et al.*, 1998). A different exception represent GlnRS, as no mitochondrial homolog could been identified in mammalian genomes so far, indicating the existence of an alternative pathway for tRNA^{Gln} formation (Nagao *et al.*, 2009; Frechin *et al.*, 2009; Bullwinkle and Ibba, 2014).

Mammalian mitochondrial aaRSs tend to show size and structural homology to their corresponding enzymes from the three domains of life. They exhibit classical signature motifs for amino acid specificity, and specific signature motifs either for class I, or for class II aaRS (Bonnefond *et al.*, 2005). The oligomeric state of mt aaRSs is generally the same as that of the cytosolic aaRSs. However, two exceptions exist, which concern mt GlyRS and mt PheRS. Mt GlyRS is dimeric like other eukaryotic cytosolic enzymes, while a heterotetrameric form is present in most bacteria (Tang and Huang, 2005). PheRS appears as a monomer in mitochondria, and thus not as a classical tetramer (Klipcan *et al.*, 2008).

The evolutionary origin of mt aaRSs has been investigated intensively, but still remains obscure. Phylogenetic analysis revealed that many mt aaRS originate from bacteria, but are not closely related to any known α-proteobacterial ancestor, suggesting that various horizontal gene transfer events took place during evolution (Brindefalk *et al.*, 2007).

A first comprehensive analysis of mt aaRS was performed in 2005, which was based on an annotation of a full set of mt aaRSs and presented a functional characterization of the mt AspRS and mt TyrRS (Bonnefond *et al.*, 2005). Results have been validated then also for several other mt enzymes. Interestingly, some mt aaRSs show slower enzymatic activity compared to their cytosolic or *E. coli* homologs (Bullard *et al.*, 1999; Bullard *et al.*, 2000).

Nowadays, crystal structures of human mt TyrRS (Bonnefond *et al.*, 2007), mt PheRS (Klipcan *et al.*, 2012), mt AspRS (Neuenfeldt *et al.*, 2013), bovine mt SerRS (Chimnaronk *et al.*, 2005), and yeast mt ThrRS (Holman *et al.*, 2016) have been solved. Although mt enzymes exhibit similar architectures when compared to their prokaryotic homologs, they can be distinguished by more electropositive surface potentials, or by enlarged grooves for tRNA accommodation. This indicates an adaptation to degenerated mt tRNAs (Neuenfeldt *et al.*, 2013).

Following the endosymbiotic theory on the origin of mitochondria, it should be possible that mt aaRSs may have preserved the ability to aminoacylate prokaryotic tRNAs, and vice versa. Indeed, it has been shown that bovine mt extracts efficiently aminoacylate eubacterial tRNAs, whereas prokaryotic enzymes are unable to aminoacylate bovine mt tRNAs (Kumazawa *et al.*, 1991). In another study, cross aminoacylation of human mt and cytosolic extracts from HeLa cell has been compared. It could be shown that 12 mt aaRSs were able to aminoacylate corresponding cytosolic tRNAs, whereas several cytosolic

aaRSs were not capable to efficiently charge mt tRNAs (Lynch and Attardi, 1976). LeuRS and LysRS activities of human mt placenta extracts were capable to charge both, *E. coli* and yeast cytosolic total tRNAs, but LysRSs from *E. coli* and yeast cytoplasm could not charge human mt tRNAs (Ibba *et al.*, 2009). These examples illustrate the higher capability of mt aaRSs to recognize cytosolic tRNAs than that of cytosolic aaRSs to recognize mt tRNAs. Rare cases of cross reactivities between both, cytosolic and mt enzymes, may be correlated to sequence homologies and/or similar structural features of mt and cytosolic tRNAs (Suzuki *et al.*, 2011).

This study focused especially on mt arginyl-tRNA synthetases because a cognate tRNA[Arg] from *R. culicivorax* was one of the tRNAs, which was also further characterized. A detailed description and characterization of classical arginyl-tRNA synthetases is presented in Chapter 4 of the results part.

6. Objectives of the study

This study aims the functional characterization of armless tRNAs in defining their structural properties and studying different aspects of their functionality, especially their interaction with CCA-adding enzymes and with the cognate aminoacyl-tRNA synthetase. For this study we chose to characterize the armless tRNA[Arg] and tRNA[Ile] from *R. culicivorax*. The objectives of this work are divided into two parts

6.1. Structural characterization of armless mitochondrial tRNAs

Our goal is to understand into which structures the unusual transcripts do fold. All known translational systems require tRNA molecules that fold into an L-shaped tertiary structure on the basis of a cloverleaf-like secondary structure. The L-shaped 3D structure is the requirement for functional activities including to be substrate and/or interactor with the macromolecules involved in translation. The armless tRNAs from *R. culicivorax* mitochondria, however, show such a strong deviation from regular structures in terms of size, of nucleotide content and cloverleaf folding, that on a theoretically basis they would not fold into a conventional three-dimensional tRNA structure. The aim of this project is to describe the actual structural features of these transcripts as a prerequisite for understanding the interplay between the tRNAs and their processing enzymes. For this purpose *in vitro* transcripts are used in structure

probing approaches, such as enzymatic and chemical probing. We will also use nuclear magnetic resonance (NMR) spectroscopy, and small-angle X-ray scattering (SAXS) to study the intramolecular interactions in armless tRNAs. These approaches will provide details about the tRNA size and shape at the 3D level and will also allow for comparison with classical tRNAs.

The elucidation of structural and functional properties of armless tRNAs will help to verify if the smallest known tRNA is compatible with life and will give further insights to possible co-evolutional processes between armless tRNA and partner proteins.

6.2. Functional study of armless tRNA maturation and aminoacylation

CCA-adding enzyme and the mitochondrial arginyl-tRNA synthetase from *R. culicivorax* will be used for functional analysis. In general, one CCA-adding enzyme recognizes two different sets of tRNAs (cytosolic and mitochondrial), while the mitochondrial aminoacyl-tRNA synthetases are specialized enzymes exclusively adapted to mitochondrial tRNAs. The gene sequence of both enzymes have yet to be identified and confirmed by PCR and sequencing methods, as the genome annotation of this particular nematode worm became only recently available and is still incompletely annotated, especially for the arginyl-tRNA synthetase. The identified gene sequences will be cloned and the corresponding proteins expressed in order to identify their functional properties in regard to armless tRNAs. For this purpose, CCA-incorporation assays and aminoacylation assays will be performed with the respective protein using *in vitro* transcribed armless tRNAs as substrate. The properties of these enzymes will be compared with those of homologous enzymes of human mitochondria and *E. coli*, respectively, already or in the process to be characterized in the two host laboratories.

Enzymes that recognize tRNAs can be divided into two groups, based on their range of recognition. Proteins like CCA-adding enzymes, EF-Tus, and ribosomes need to recognize the full variety of all tRNA molecules in an organism, and possess therefore a broad substrate spectrum. On the other hand, the range of recognition of each aaRS is restricted to only one or a few tRNAs that all bind the same amino acid. To cover both groups, one representative protein from each group has been chosen for functional and structural characterization in this study.

MATERIAL & METHODS

7. Material

Chemicals, kits, enzymes, cell material, bacterial strains, plasmids, DNA primers, media, buffers and solution as well as software used in this study are listed in the following paragraphs.

7.1. Sources for chemicals

Unless otherwise mentioned, all chemicals used in this study were purchased in the highest quality available from the following companies AppliChem (Darmstadt), Carl Roth (Karlsruhe), Sigma-Aldrich (Munich), and Merck (Darmstadt).

7.2. Kits

The following table (Table 2) contains the kits used in this study.

Table 2: Kits

Product	Source
BigDye® Terminator 1.1 Cycle Sequencing Kit	GE Healthcare
CloneJET™ PCR Cloning Kit	Thermo Scientific
GeneJET™ Gel Extraction Kit	Thermo Scientific
GeneJET™ PCR Purification Kit	Thermo Scientific
GeneJET™ Plasmid Miniprep Kit	Thermo Scientific
GeneElute™ mRNA Miniprep Kit	Sigma-Aldrich
NucleoSpin® plasmid	Macherey-Nagel
RACE DNA Purification System	Life Technologies
TOPO® TA Cloning® Kit	Life Technologies
Wizard® SV Gel and PCR clean-up System	Promega

7.3. Enzymes and tRNAs

The commercially available enzymes used in this study are listed in Table 3, and non-commercial enzymes are listed in Table 4. The utilized tRNA material is listed in Table 5.

Table 3: Commercial enzymes

Enzyme	Source
*BamH*I	New England Biolabs
*Dpn*I	New England Biolabs
*EcoR*V	New England Biolabs
*Hind*III	New England Biolabs
*Nco*I	Thermo Scientific
*Xba*I	Thermo Scientific
Pfu DNA polymerase	Fermentas and Thermo Scientific

46

Phusion High Fidelity DNA Polymerase	Thermo Scientific
RevertAid Reverse Transcriptase	Thermo Scientific
Nuclease S1	Fermentas
Ribonuclease V1	Applied Biosystems
Ribonuclease T1	Applied Biosystems
T4 DNA ligase	New England Biolabs
T4-PNK	New England Biolabs and Thermo Scientific
T4 RNA ligase I	New England Biolabs
Terminal deoxynucleotidyl transferase (TdT)	Invitrogen
Thermostable inorganic pyrophosphatase (TIPP)	New England Biolabs

Table 4: Non-commercial enzymes

Enzyme	Source
Taq DNA polymerase	In house preparation
T7 RNA polymerase	In house preparation
H. sapiens CCA-adding enzyme	In house preparation
E. coli CCA-adding enzyme	In house preparation
R. culicivorax CCA-adding enzyme	This study
E. coli mt arginyl-tRNA synthetase	Provided by S. X. Lin (Laval University, Canada)
S. cerevisiae mt arginyl-tRNA synthetase	Provided by G. Eriani (University of Strasbourg)
R. culicivorax mt arginyl-tRNA synthetase	This study

Table 5: tRNAs

tRNAs	Source
Total *E. coli* tRNA	Sigma-Aldrich
Total yeast tRNA	G. Eriani (University of Strasbourg)
R. culicivorax mt tRNA^{Arg}	C. Lorenz (University of Leipzig)
R. culicivorax mt tRNA$^{Arg\_CCA}$	This study
R. culicivorax mt tRNA^{Ile}	This study
R. culicivorax mt tRNA$^{Ile\_CCA}$	This study

7.4. Cell material

Living *Romanomermis culicivorax* worm material was provided by Edward G. Platzer (University of California, Riverside). The nematodes were snap-frozen using liquid nitrogen and stored at -80°C. *Saccharomyces cerevisiae* strains AH109 and Y187 were used in this study (Table 6).

Table 6: *S. cerevisiae* strains

Strain	Genotype	Source or reference
AH109	MATα, trp 1-901, leu2-3, 112, ura 3-52, his3-200, gal4Δ, gal80Δ, LYS2: GAL1$_{UAS}$-GAL1$_{TATA}$-HIS3, GAL2$_{UAS}$-GAL2$_{TATA}$-ADE2, URA3: MEL1$_{UAS}$-MEL1$_{TATA}$-LacZ	Clontech
Y187	MATα, ura3-52, his3-200, ade2-101, trp1-901, leu2-3, 112, gal4Δ, met–, gal80Δ, MEL1, RA3::GAL1$_{UAS}$-GAL1$_{TATA}$-lacZ	Clontech

7.5. Bacterial strains and plasmids

Bacterial strains and plasmid used in this study are listed in Table 7 and Table 8.

Table 7: Bacterial strains

E. coli strain	Genotype	Source or reference
Top10	F- *mcr*A Δ(*mrr-hsd*RMS-*mcr*BC) φ80*lac*ZΔM15 Δ*lac*X74 *rec*A1 *ara*D139 Δ(*ara-leu*)7697 *gal*U *gal*K *rps*L (Str^R) *end*A1 *nup*G	Invitrogen
BL21(DE3)	F- *ompT hsd*S$_B$ (rB- mB-) *gal* dcm (DE3)	Novagen
Rosetta™2	F- *ompT hsd*S$_B$(rB- mB-) *gal dcm* (DE3) pRARE2 (Cam^R)	Novagen
Arctic Express™(DE3)	F- *ompT hsd*S(rB- mB-) *dcm$^+$* Tet^r *gal* λ(DE3) *end*A Hte [*cpn*10 *cpn*60 Gent^r]	Agilent Technologies

Table 8: Plasmids

Plasmid	Source or reference
Used for cloning of tRNA genes	
pCR®2.1-TOPO	Invitrogen
Used for cloning of protein genes	
pET28a	Novagen
pTrcHisA	Invitrogen
pUCIDT	IDT
pDEST	Invitrogen
pJJH378	Provided by A. Brüser (University of Leipzig)

7.6. Primers

DNA primer used in this study were acquired from Biomers and Sigma and are listed in Table 9. The numbering used in the laboratory is given as well as the name, sequence in 5' to 3' direction, and the purpose of each primer. Small letters indicate restriction sites.

Table 9: Primer

N°	Primer name	Sequence (5'→3')	Purpose
M537	HH_tRNAIle_Rcu_fw1	AGACTGAAGATTTAAGCTGATGAGTC CGTGAGGACGAAACG	
M538	HH_tRNAIle_Rcu_rev1	CTCTATTAAGGACGGTACCGGGTACC GTTTCGTCCTCACGGAC	
M539	HH_tRNAIle_Rcu_fw2	CGGTACCGTCCTTAATAGAGAACAAT TTAAATTGATAATTTAAATTAA	*In vitro*
M540	HH_tRNAIle_Rcu_rev2	TCTTAAATTTTAATTTAAATTATCAA TTTAAATTGTTCTC	synthesis, and cloning of
M541	Rcu_tRNAIle_QuikChange_fw	CTAATACGACTCACTATAGGGAGACT GAAGATTTAAGCTGATGAG	tRNA^{Ile} constructs
M542	Rcu_tRNAIle_QuikChange_rev	GATGCCATGCCGACCCTCTTAAATTT	
M611	Rcu_tRNAIle_H39neu fw	TAATTTAAATTATCAATTTAAATTG	
M612	Rcu_tRNAIle_H39neu rev	GAGATGCCATGCCGACCCTC	
553	M13 fw	GTTTTCCCAGTCACGAC	Sequencing
554	M13 rev	AGCGGATAACAATTTCACACAGGA	and
L46	HDV-Ampl-fw	GGGTCGGCATGGCATCTCCAC	amplification
L768	T7_Promoter_for	GGAGATCTAATACGACTCAC	of tRNA
L769	HDV_rev	AAA CGA CGG CCA GTG CCA AG	constructs
M658	HDV+T7_fw	GTCGGCATGGCATCCTAATAC	
M577	Rcu_CCA_BamHI_fw	GCGTTAggatccATGAAAATCGATTCG CCGCAATTTCG	
M578	Rcu_CCA_BamHI_rev	CCAGCGaagcttTCATTGTTTGGAATGA ATAGGCGACC	
M732	Rcu_CCA_BamHI in yeast_for	GCGTTAggatccAATGAAAATCGATTC GCCGCAATTTCG	
M733	Rcu_CCA_HindIII in yeast_rev	GTCCAGaagcttTCAGTGGTGATGGTGA TGATGTTGTTTGGAATGAATAGGCGA CCTG	
M734	Rcu_CCA_6His-tag in yeast_rev	TCAGTGGTGATGGTGATGATGTTGTT TGGAATGAATAGGCGACCTG	Cloning and sequencing of *Rcu* CCA- adding enzyme
M735	Link_RcuCCA_6His-tag+3'UTR in yeast_rev	GAAAGTGTAATAAAAGGTCATTTTCT TTCAGTGGTGATGGTGATGATGTTGT	
M736	3'UTR ScPFK2_for	AAGAAAATGACCTTTTATTACACTTT CTATTATTAATG	
M733	3'UTR ScPFK2_MCS_rev	CAGAGGAAGCTTCGTCGATAGAGATA AAAAAAAAGAATTATAGAC	
M760	-165_Seq_MCS_pJJH378_for	GGGTAATTAATCAGCGAAGCG	
M761	+99 Seq_MCS_pJJH378_rev	GTGAGTTAGCTCACTCATTAGG	
L648	pTrcHisZ_rev_sequ	GTT CGG CAT GGG GTC AGG TG	

GSP1	ArgRS_intern_RP1	GTGCCGTCACTTTTGGATAACGG	
GSP2	ArgRS_intern_RP2	GGTCTCAAAGTTATCGAGGAGC	
GSP3	ArgRS_intern_FP1	GACCAAGTTATCGGGTGTACAGG	5'RACE PCR
AAP	Abridged Anchor Primer	GGCCACGCGTCGACTAGTACGGGIIGG GIIGGGIGG	
AUAP	Abridged Universal Amplification Primer	GGCCACGCGTCGACTAGTAC	
T10	RP ArgRS modi	gtgcAAGCTTTTACAGTTTTTCAATCG GGT	
T11	start +24 ArgRS modi	gataGGATCCATGCCGTGTCTGCCGGA TAG	
T12	start +28 ArgRS modi	gttaGGATCCATGGATAGCGTTAGCAG CATTG	
T13	start +30 ArgRS modi	ggaaGGATCCATGGTTAGCAGCATTGC AAAAGG	
T14	start +36 ArgRS modi	gtctGGATCCATGGGCACCAGCATTGG TCTG	
T15	RP C-His all	ACCGTCTCGAGCAGTTTTTCAATCGG GTCCAG	
T16	FP FL C-His pDEST	taagtccATGGGGCAACTGATTAGCCGT GAAATC	Cloning and sequencing of *Rcu* ArgRS and N-terminal variants
T17	FP 16 C-His pDEST	gctatccATGGGGGATTTTAGCGCAATT CGTCGTC	
T18	FP 17 C-His pDEST	gtcttccATGGGGTTTAGCGCAATTCGT CGTCTG	
T19	FP 18 C-His pDEST	cgtctccATGGGGAGCGCAATTCGTCGT CTGC	
T20	FP 23 C-His pDEST	atggtccATGGGGCTGCCGTGTCTGCCG GATA	
T21	FP 24 C-His pDEST	cgataccATGGGGCCGTGTCTGCCGGAT AGC	
T22	FP 25 C-His pDEST	gattgccATGGGGTGTCTGCCGGATAGC GTTAG	
T23	FP 28 C-His pDEST	cgttaccATGGGGGATAGCGTTAGCAGC ATTGC	
T24	FP 29 C-His pDEST	gataaccATGGGGAGCGTTAGCAGCATT GCAAAAG	
T25	FP 31 C-His pDEST	cattaccATGGGGAGCAGCATTGCAAAA GGCAC	
T26	pDEST FP intern	CAGCCAGCCATCGTATTCGTGG	

7.7. Media, buffers and solutions

Media, buffers and solutions used in this study are listed in Table 10 Table 11. Media were dissolved using Milli-Q water (Purification System, Millipore) and autoclaved. For solid media, 15 g/l agar was added to the media prior autoclaving.

Table 10: Media

Media	Mixture	
LB medium	10 g/l	Tryptone
	5 g/l	Yeast extract
	5 g/l	NaCl
SOC medium	20 g/l	Tryptone
	5 g/l	Yeast extract
	0.6 g/l	NaCl
	0.288 g/l	KCl
	20 mM	Glucose
After autoclaving addition of	10 mM	$MgCl_2*6H_2O$
	10 mM	$MgSO_4*7H_2O$
YPDA medium pH 6.5	10 g/l	Yeast extract
	20 g/l	Peptone
After autoclaving addition of	55.6 ml/l	Glucose 40 %
	20 ml/l	Adenosine hemisulfate 0.2 %
SD medium (-Leu)	0.67 %	Yeast nitrogen base
	0.06 %	Complete synthetic mix
	2 %	Glucose
Lithium-Sorbitol-buffer	10 mM	Tris-HCl pH 8.0
	100 mM	Lithium acetate
	1 mM	EDTA pH 8.0
	1 M	Sorbitol
Lithium-PEG-buffer	10 mM	Tris-HCl pH 8.0
	100 mM	Lithium acetate
	1 mM	EDTA pH 8.0
	40 %	PEG 3350

Table 11: Buffers and solutions

Media	Mixture	
Buffers for DNA manipulation and plasmid purification		
TBE (10x)	890 mM	Tris base
	890 mM	Boric acid
	20 mM	EDTA-Na$_2$
DNA loading buffer (5x)	30 % (v/v)	Glycerol
	0.25 % (w/v)	Bromphenol bleu
	0.25 % (w/v)	Xylene cyanol

RNA loading buffer (3x)	10 mM	Tris-HCl pH 7.6
	80 % (v/v)	Formamide
	0.25 % (w/v)	Bromphenol bleu
	0.25 % (w/v)	Xylene cyanol
Ethidium bromide solution	1 mg/l	Ethidium bromide
Taq-PCR buffer (10x)	200 mM	Tris-HCl, pH 8,8
	100 mM	$(NH_4)_2SO_4$
	100 mM	KCl
	20 mM	$MgSO_4$
	1 % (v/v)	Triton®X-100

Buffers for tRNA manipulation

3'-Tagging buffer (2x):	100 mM	Tris-HCl pH 8.0
	20 mM	$MgCl_2$
	2 mM	Hexaamminecobalt(III) chloride
	0,4 mg/ml	BSA
	25 % (w/v)	PEG 8000
Transcription buffer (10x)	800 mM	Tris-HCl pH 7.5
	220 mM	$MgCl_2$
	50 mM	DTT
	10 mM	Spermidine
	1.2 mg/ml	BSA
Dephosphorylation buffer (10x):	1 M	Imidazole-HCl pH 6.0
	100 mM	$MgCl_2$
	100 mM	β-mercaptoethanol
	1 mM	ATP
	200 µg/ml	BSA
T4-PNK buffer (1x)	50 mM	Tris-HCl pH 7.6
	10 mM	$MgCl_2$
	5 mM	DTE

Buffers for tRNA structure analysis

RNase V1 buffer (10x)	400 mM	Tris-HCl pH7.5
	100 mM	$MgCl_2$
	400 mM	NaCl
Nuclease S1 buffer (5x)	200mM	NaAc
	1.5 M	NaCl
	10 mM	$ZnSO_4$ pH 4.5

RNase T1 buffer (10x)	100 mM	Tris-HCl pH7.5
	300 mM	NaCl
	5 mM	EDTA

| In-line buffer (5x) | 500 mM | Glycine/NaOH pH 8.5 |
| | 20 mM | DTT |

| AH buffer | 100 mM | $Na_2CO_3/NaHCO_3$ pH 9.75 |

Protein purification of *R. culicivorax* CCA-adding enzyme

Lysis buffer CL	20 mM	Tris-HCl pH 7.6
	500 mM	NaCl
	10 mM	$MgCl_2$
	5 mM	Imidazole

Dissociation buffer DBC	20 mM	Hepes-KOH pH 8.0
	150 mM	KCl
	10 mM	$MgCl_2$
	5 mM	ATP
	0.5 mg/ml	Denatured *E. coli* proteins

Wash buffer CW	20 mM	Tris-HCl pH 7.6
	500 mM	NaCl
	10 mM	$MgCl_2$
	50 mM	Imidazole

Elution buffer CE	20 mM	Tris-HCl pH 7.6
	500 mM	NaCl
	10 mM	$MgCl_2$
	500 mM	Imidazole

SEC buffer	20 mM	Tris-HCl pH 7.6
	150 mM	NaCl
	10 mM	$MgCl_2$

Protein purification of *R. culicivorax* mt ArgRS

Wash buffer AW	50 mM	K_2HPO_4/KH_2PO_4 pH 7.5
	500 mM	KCl
	10 mM	β-mercaptoethanol
	10 %	Glycerol
	20 mM	Imidazole

Urea wash buffer AU	50 mM	K_2HPO_4/KH_2PO_4 pH 7.5
	500 mM	KCl
	2 M	Urea
	10 mM	β-mercaptoethanol
	10 %	Glycerol
	20 mM	Imidazole

Elution buffer AE	50 mM	K_2HPO_4/KH_2PO_4 pH 7.5
	500 mM	KCl
	10 mM	β-mercaptoethanol
	10 %	Glycerol
	400 mM	Imidazole

Dialysis buffer A1	50 mM	K_2HPO_4/KH_2PO_4 pH 7.5
	150 mM	KCl
	10 mM	β-mercaptoethanol
	1 mM	EDTA
	10 %	Glycerol

Dialysis buffer A2	50 mM	K_2HPO_4/KH_2PO_4 pH 7.5
	150 mM	KCl
	10 mM	β-mercaptoethanol
	0.1 mM	EDTA
	10 %	Glycerol

Dissociation buffer DBA	20 mM	Hepes-KOH pH 7.5
	150mM	KCl
	10 mM	β-mercaptoethanol
	20 mM	Imidazole
	10 mM	$MgCl_2$
	5 mM	ATP

Buffers for SDS-PAGE

Separating buffer (pH 8.8)	4 ml	H_20
for 2 gels	2.5 ml	Tris-base pH 8.8
	3.3 ml	Acrylamide-mix (30 %)
	0.1 ml	SDS
	0.1 ml	APS (10 %)
	0.004 ml	TEMED

Stacking buffer (pH 6.8)	2.7 ml	H_20
for 2 gels	0.5 ml	Tris-base pH 6.8
	0.67 ml	Acrylamide-mix (30 %)
	0.04 ml	SDS
	0.004 ml	APS (10 %)
	0.0004 ml	TEMED

Protein loading dye	188 mM	Tris-HCl pH 6.7
	1,9 mM	β-Mercaptoethanol
	0,2 mM	Bromphenol bleu
	30 % (v/v)	Glycerol
	6 % (v/v)	SDS

| Coomassie blue staining solution | 24,8 % (v/v) | Methanol |
| | 0,8 % (v/v) | Roti®-Blue |

| Destaining solution | 25 % (v/v) | Methanol |
| | 7 % (v/v) | Acetic acid |

10 x SDS-Electrophoresis buffer	250 mM	Tris-base
	1.92 M	Glycerol
	1 % (w/v)	SDS

Buffers for western blot analysis

2x Blotting buffer	28.8 g/l	Glycine
	6.06 g/l	Tris-base
	3.75 ml/l	20 % SDS

1x Transfer buffer	100 ml	2x Blotting buffer
	40 ml	Methanol
	60 ml	ddH$_2$O

| 10x TBS | 1.5 M | NaCl |
| | 100 mM | Tris-HCl pH 7.6 |

5x TBSTT	2.5 M	NaCl
	100 mM	Tris-HCl pH 7.6
	1 %	Triton X-100
	0.25 %	Tween 20

| Blocking solution | 3% BSA | In 1x TBS |

1x TBST	50 mM	Tris-HCl pH 7.5
	150mM	NaCl
	1 %	Tween-20

Buffers for activity tests

CCA-addition buffer (10x):	300 mM	Hepes-KOH pH 7,6
	300 mM	KCl
	60 mM	MgCl$_2$

Mitochondrial aminoacylation buffer (MRM) (5x)	50 mM	Hepes KOH pH7.5
	25 mM	KCl
	0.2 µg/µl	BSA 10 mg/ml
	1 mM	Spermidine
	12 mM	MgCl$_2$
	2.5 mM	ATP

Rcu aminoacylation buffer (MRR) (5x)	50 mM	Hepes KOH pH7.5
	30 mM	KCl
	0.2 µg/µl	BSA 10 mg/ml
	1 mM	DTT
	1 mM	Spermidine
	4 mM	$MgCl_2$
	4 -40 mM	ATP
Sce aminoacylation buffer (MRC) (5x)	50 mM	Hepes KOH pH7.5
	30 mM	KCl
	0.5 µg/µl	BSA
	2.5 mM	Spermidine
	15 mM	$MgCl_2$
	10 mM	ATP
Eco aminoacylation buffer (MRE) (5x)	50 mM	Hepes KOH pH7.5
	25 mM	KCl
	0.2 µg/µl	BSA
	1 mM	DTT
	10 mM	$MgCl_2$
	4 mM	ATP
Dilution buffer	100 mM	Hepes KOH pH 7.5
	10%	Glycerol
	5 µg/µl	BSA
	1 mM	DTT

7.8. Software and databases

Software or database	Purpose
ApE-A plasmid Editor http://biologylabs.utah.edu/jorgensen/wayned/ape/	Analysis and editing of sequences
Argus X1® V3.3.1 (Biostep)	Scanner software
Assemble2 http://bioinformatics.org/s2s/	Prediction and editing of 2D structures, 3D modelling
ATSAS 2.7.2 https://www.embl-hamburg.de/biosaxs/software.html	A program suite for small-angle scattering data analysis from biological macromolecules
BLAST® https://blast.ncbi.nlm.nih.gov/Blast.cgi	Comparison of nucleotide and protein sequences
Clustal Omega https://www.ebi.ac.uk/Tools/msa/clustalo/	multiple sequence alignment program
GenBank http://www.ncbi.nlm.nih.gov/genbank/	Search and annotation of DNA sequences
ImageQuant 5.0 GE Healthcare	Image analysis software

I-TASSER http://zhanglab.ccmb.med.umich.edu/I-TASSER/	Prediction of protein 3D structure
Lasergene 6 DNASTAR	Analysis of DNA sequences
MITOPROT https://ihg.gsf.de/ihg/mitoprot.html	Prediction of mitochondrial targeting sequences
MitoFates http://mitf.cbrc.jp/MitoFates/cgi-bin/top.cgi	Prediction of mitochondrial targeting sequences
Mfold 3.2 http://mfold.rna.albany.edu/?q=mfold	Prediction of RNA secondary and tertiary structure
OligoCalculator http://mcb.berkeley.edu/labs/krantz/tools/oligocalc.html	Calculation of oligonucleotide statistics
ProtParam http://web.expasy.org/protparam/	Computation of protein statistics
PyMOL Schrödinger (Portland, USA)	3D modelling of protein sequences
RNAfold http://rna.tbi.univie.ac.at/cgi-bin/RNAfold.cgi	Prediction of RNA secondary structure
tRNAdb / mitotRNAdb http://trnadb.bioinf.uni-leipzig.de/	Search, annotation and comparison of tRNA genes and structures

8. Methods

8.1. General nucleic acid methods

8.1.1. Measurement of DNA and RNA concentrations

DNA and RNA concentrations were estimated by measuring the absorbance at 260 nm and 280 nm using a NanoDrop®ND-1000 or NanoDrop®ND-2000 spectrophotometer (both Thermo Scientific) according to the manufacturer's instructions.

8.1.2. Extraction and precipitation of DNA and RNA

DNA and RNA fragments were purified using the phenol-chloroform extraction method (Sambrook *et al.*, 1989). A reaction volume of 200 μl was added to 200 μl of a phenol:chloroform:isoamyl alcohol (25:24:1) mix, vortexed, and centrifuged (3 min, 6000 rpm). The aqueous upper phase was transferred to a new reaction tube and treated with 200 μl chloroform, vortexed and centrifuged (3 min, 6000 rpm). After centrifugation the aqueous upper phase was transferred to a new reaction tube and the nucleic acids were precipitated by the addition of sodium acetate to 0.3 M final concentration and 2 volume of absolute ethanol. Occasionally, glycogen (1 μg/ml) was added to the reaction as a carrier to increase the efficiency of the precipitation. The solution was incubated 30 min at -20°C or 10 min at -80°C and afterwards centrifuged at 14.000 rpm for at least 20 min at 4°C. The nucleic acid pellet was washed with 70 % ethanol and resuspended after drying in ddH$_2$O. Alternatively, the nucleic acid was stored as an alcohol precipitate for several months at -80°C.

PCR products were also purified using the GeneJET™ PCR Purification Kit (Thermo Scientific), or were extracted from the gel using the GeneJET™ Gel Extraction Kit (Thermo Scientific). All purifications steps were carried out according to the manufacturer's instructions.

8.1.3. DNA sequencing

Sequencing of PCR products and plasmid DNA was carried out using the chain termination method (Sanger *et al.*, 1977). For this purpose, the BigDye® Terminator Cycle Sequencing Kit 1.1 was used according to the manufacturer's instructions. Sequencing was performed on an ABI Prism 3730-sequencing unit (Amersham

Pharmacia Biotech) at the Max Planck Institute for Evolutionary Anthropology in Leipzig. In Strasbourg, DNA samples are sequenced using the sequencing service from GATC Biotech.

8.2. DNA manipulation

Standard methods were used for plasmid isolation, restriction enzyme digestion, ligation, transformation, and agarose gel electrophoresis (Sambrook *et al.*, 1989). A schematic representation of the different PCR methods used in this study is shown in Figure.

8.2.1. PCR Methods

<u>Amplification PCR</u>

The polymerase chain reaction (PCR) allows a specific *in vitro* amplification of DNA fragments. A standard PCR consists of 50 µl reaction volume and contains the following components: 10-50 ng DNA template, 0.4 µM Primers, 0.2 mM dNTP 1x *Pfu* or *Taq* reaction buffer and between 2.5 U and 5 U *Pfu* or *Taq* DNA Polymerase. The reaction was carried out according to the following temperature-time diagram:

Initial denaturation	95°C	5 min
Denaturation	95°C	1 min
Annealing	54°C - 64°C	1 min 30 x
Elongation	68/72°C	30 sec – 2 min
Final elongation	68/72°C	5 min
Storage	10 °C	∞

The annealing temperature was set to 2°C below the melting temperature (TM) of the two primers. This temperature was calculated using the web tool "Oligo Calculator". Calculated elongation temperatures were appropriate for the used DNA polymerase: 68°C for *Pfu*, and 72°C for *Taq* DNA polymerase. All reactions were performed in a Robocycler® (Stratagene), a MJ™ thermal cycler (Biorad), or a C-1000 Touch™ thermal cycler (Biorad).

Overlap-Extension PCR

Overlap extension PCRs were performed when two DNA fragments needed to be connected. In these cases, the overlapping region of both single-stranded DNA fragments was at least 15 nt. 300-500 ng of these overlapping DNA fragments were used in the overlap extension PCR. The PCR was stopped after ten cycles and in a second step 400 nM primers that are complementary to the outer ends of the target construct were added. 20 - 25 additional PCR cycles were performed in order to amplify and extend the DNA construct. The reaction was carried out according to the temperature-time diagram described above.

QuikChange Mutagenesis PCR

QuikChange mutagenesis PCRs were used to introduce or delete DNA sequences, or to exchange base pairs in plasmid sequences. For this purpose, chemically synthesized DNA oligonucleotides were used as DNA megaprimer. The QuikChange mutagenesis method was performed using *Pfu* DNA polymerase, or Phusion® DNA polymerase in corresponding buffers. A typical reaction mixture included also dNTPs (200 nM), DNA megaprimer (500 ng) and the target plasmid (depending on size 50 to 150 ng). Reactions were carried out according to the temperature-time diagram described above. The elongation times were calculated as 30 s/kb plasmid size for both DNA polymerases, and 18-25 amplification cycles were performed.
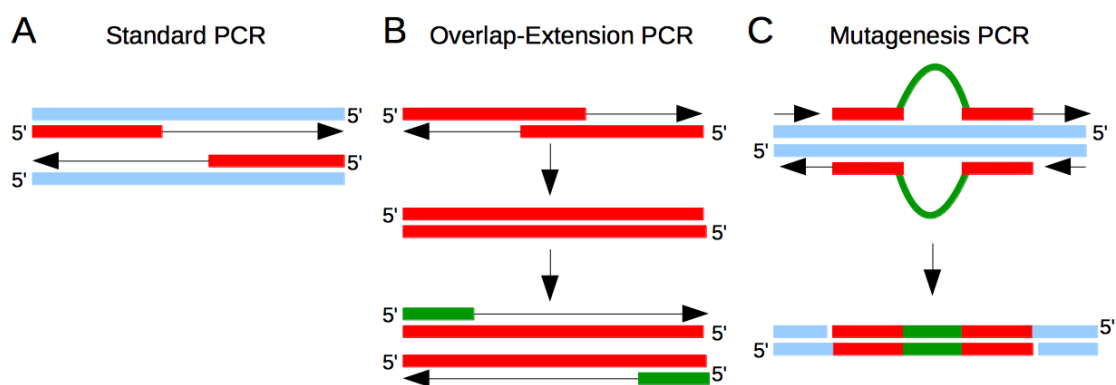
Figure 17: Schematic overview of standard PCR, overlap-extension PCR and mutagenesis PCR.
(A) Standard PCR served for simple amplification of DNA templates (blue). (B) During the first step of overlap-extension PCR, two DNA fragments (red) that overlap at their 3'-ends are elongated by a DNA polymerase. In the second step, the amplification of the product was carried out using single-stranded DNA primers (green). (C) For mutagenesis a DNA megaprimer pair that contains the mutation site (green) binds to both strands of the target plasmid DNA (blue). The primers were extended by a DNA polymerase resulting in a plasmid with the inserted mutation site.

Colony PCR

Colony PCR is an easy way to rapidly screen positive clones. For this purpose, a single bacterial colony was picked using a sterile pipet tip, dissolved in 10 µl ddH$_2$O, and incubated at 95°C for 10 min. 5 µl of this cell suspension were then used for a standard amplification PCR.

8.2.2. Cloning of DNA fragments

Standard Ligation

DNA fragments obtained by restriction digestion were inserted into the corresponding vector through ligation. For this purpose, the vector and DNA insert were treated with the same restriction endonucleases. About 50 ng of the vector was mixed with the DNA fragment in a molar ratio of 1:3 or 1:5. The ligation was carried out in a final volume of 20 µl for 10-20 min at room temperature or at 16°C for 16 h. A typical reaction contained 1x DNA ligation buffer and the corresponding amount of vector, as well as the insert DNA and 40 units of T4 DNA ligase.

Blunt end cloning

The CloneJet™ PCR Cloning Kit (Thermo Scientific) was used according to the manufacturer to clone DNA fragments obtained by standard or overlap-extension PCR into a plasmid.

TA cloning

The efficient and ligation independent cloning of (unpurified) PCR products into the pCR®2.1-TOPO vector was carried out using the TOPO TA Cloning® kit (Invitrogen) according to the manufacturer. Only PCR products generated by *Taq* DNA polymerase are suitable for this cloning method because of the necessity of 3'-dA overhangs produced by the *Taq* DNA polymerase.

8.2.3. Plasmid purification for cloning and sequencing

Plasmids were purified from a bacterial culture grown overnight at 37°C using the QIAprep Spin Miniprep kit (Qiagen) or the GeneJET™ Plasmid Miniprep Kit (Thermo Scientific), following the manufacturer's instructions. The quantity and quality of the plasmid DNA was determined as described in section 8.1.1.

8.2.4. Restriction analysis of DNA

The restriction of plasmid DNA or PCR products was carried out using restriction enzymes (New England Biolabs) according to the manufacturer's instructions. A typical 100 µl reaction mixture contained 500-2000 ng of PCR product or 250-500 ng of plasmid DNA, 1x restriction buffer, and 10 U/µl restriction enzyme. The digestion mixture was incubated at 37°C for 3h. The restriction was verified with analytical agarose gel electrophoresis, followed by purification as described in section 8.1.2.

8.2.5. Agarose gel electrophoresis

Analytical or preparative agarose gels were used for the separation of DNA molecules. The routine analysis of DNA molecules of 100 to 5.000 base pairs in size was done by electrophoresis on 1% to 2 % agarose gels (according to the expected DNA size) with 1x TBE as running buffer. The samples were loaded with 1x DNA loading buffer and a DNA ladder (2 log or 50 bp DNA ladder from New England Biolabs) was applied adjacent to the samples in order to verify the fragment sizes. The electrophoresis was carried out at 90 V for 60 min. The agarose gels contained 0.5 µg/ml ethidium bromide or 1x Gel Red solution in order to allow visualization of the DNA fragments under UV light at 254 nm.

8.3. RNA manipulation

8.3.1. RNA preparation from *R. culicivorax*

Total RNA from *R. culicivorax* was recovered using the guanidine thiocyanate method from (Chomczynski and Sacchi, 1987). 100 mg cell material was treated with 1 mL TRIZOL®, and lysed using Precellys® ceramic beads with a diameter of 1.4 mm in a FastPrep®-24 homogenizer twice for 40 s at 6 m/s. The mixture was then centrifuged for 30 min at 16,000 g and 4°C. The upper phase was transferred to a new reaction tube and 300 µl chloroform were added and mixed. The mixture was centrifuged at 16,000 g for 5 min at 4°C. The upper phase was removed and ethanol precipitation (see section 8.1.2) was performed. The pellet was taken up in 250 µl water.

8.3.2. mRNA purification from total RNA

The GenElute™ mRNA Miniprep Kit (Sigma-Aldrich) was used for the isolation of polyadenylated mRNA from previously prepared total RNA according to the manufacturer's instructions.

8.3.3. 5'-Rapid amplification of cDNA ends (RACE)

A 5'-RACE DNA purification system kit (Invitrogen) was used for the analysis of the 5'-ends of the *R. culicivorax* ArgRS mRNA according to manufacturer's instructions. Total RNA and mRNA from *R. culicivorax* was prepared as described above, and served as templates for cDNA production. First strand cDNA synthesis was primed using a gene-specific antisense oligonucleotide (GSP1). Following cDNA synthesis using SuperScript II RT, the mRNA template was degraded by digestion with a supplemented RNase mix. The first strand product was purified from unincorporated dNTPs and GSP1. TdT (Terminal deoxynucleotidyl transferase) was used to add a poly C-tail to the 3' ends of the cDNA. The tailed cDNA was then amplified by standard PCR using a nested gene-specific primer (GSP2), which anneals 3' to GSP1; and an Abridged Anchor Primer (AAP), which permits amplification from the homopolymeric tail. This allows amplification of unknown sequences between the GSP2 and the 5'-end of the RNA template. Reamplification of the PCR product can be performed using an Abridged Universal Amplification Primer (AUAP) and GSP2 or a nested GSP. The amplified PCR product was introduced by TA-cloning into the pCR®2.1-TOPO plasmid, and sequenced.
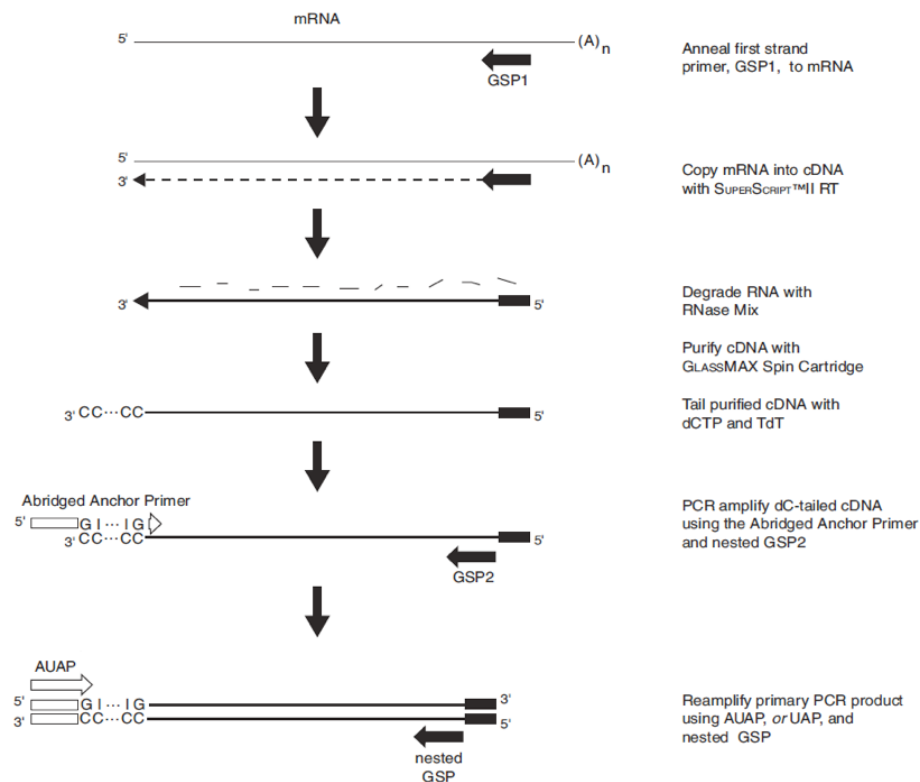
Figure 18: Schematic overview of the 5' RACE procedure.
5'-RACE cDNA synthesis starts with a gene specific primer (GSP1) in the coding region that binds in antisense direction of the mRNA template. The resulting cDNA contains the complete 5'-region. Subsequently, the mRNA is degraded by means of an RNase Mix. The remaining cDNA is purified. Then, the TdT and dCTPs are used to attach a polyC-tail to the end of the cDNA molecule. The product serves as a template in a PCR reaction. To do so, a first sense primer consisting of an oligo (dG) (Abridged Anchor Primer) and GSP2 are used for a first amplification. With the aid of the first primer, the anchor is attached to the PCR products. A second PCR provides a specific amplification by using the AUAP and a nested GSP. (Adapted from 5'-RACE DNA purification system kit manual - Invitrogen.)

8.4. tRNA manipulation

8.4.1. Construction of tRNA transcription templates

DNA templates for the production of individual tRNAs by *in vitro* transcription, included a T7 promoter for T7 RNA polymerase, a sequence for the hammerhead (HH) ribozyme, the respective tRNA sequence, and a sequence for the hepatitis delta virus (HDV) ribozyme (Figure 19).

The tRNA^{Ile} transcription template was generated by PCR extension of two overlapping primer pairs. The two resulting megaprimers were combined during overlap extension PCR. The resulting product was further amplified using primers that align to the 5'- and 3'-ends carrying overlaps that allowed cloning into a pCR®2.1-TOPO plasmid by mutagenesis PCR. The mt tRNA^{Arg} from *R. culicivorax* and the cytosolic tRNA^{Phe} from

yeast were already available on a pCR®2.1-TOPO plasmid and kindly provided by C. Lorenz and E. Lizano, respectively. The CCA sequence necessary for aminoacylation assays was introduced in the tRNA transcription templates using site-directed mutagenesis PCR.

>tRNA[Ile] transcription template
5'- GGAGATCTAATACGACTCACTATAGGGAGACTGAAGATTTAAGCTGATGAGTCCGTGAGG ACGAAACGGTACCCGGTACCGTCCTTAATAGAGAACAATTTAAATTGATAATTTAAATTAAAATTTAA GAGGGTCGGCATGGCATCTCCACCTCCTCGCGGTCCGACCTGGGCTACTTCGGTAGGCTAAGGGAGAAG CTTGGCACTGGCCGTCGTTT -3'

>tRNA[Arg] transcription template
5'- GAGATCTAATACGACTCACTATAGGGAATAAGTTTCTGATGAGTCCGTGAGGACGAAACG GTACCCGGTACCGTCAAACTTTTAGCAGGATTTCGAATCCTAATTTATATAAGTTTTGGGTCGGCATG GCATCTCCACCTCCTCGCGGTCCGACCTGGGCTACTTCGGTAGGCTAAGGGAGAAG -3'

>tRNA[Phe] transcription template
5'- GGAGATCTAATACGACTCACTATAGGGAGAAATCCGCCTGATGAGTCCGTGAGGACGAAA CGGTACCCGGTACCGTCGCGGATTTAGCTCAGTTGGGAGAGCGCCAGACTGAAGATCTGGAGGTCCTG TGTTCGATCCACAGAATTCGCAGGGTCGGCATGGATCTCCACCTCCTCGCGGTCCGA CCTGGGCTACTTCGGTAGGCTAAGGGAGAAGCTTGGCACTGGCCGTCGTTT -3'
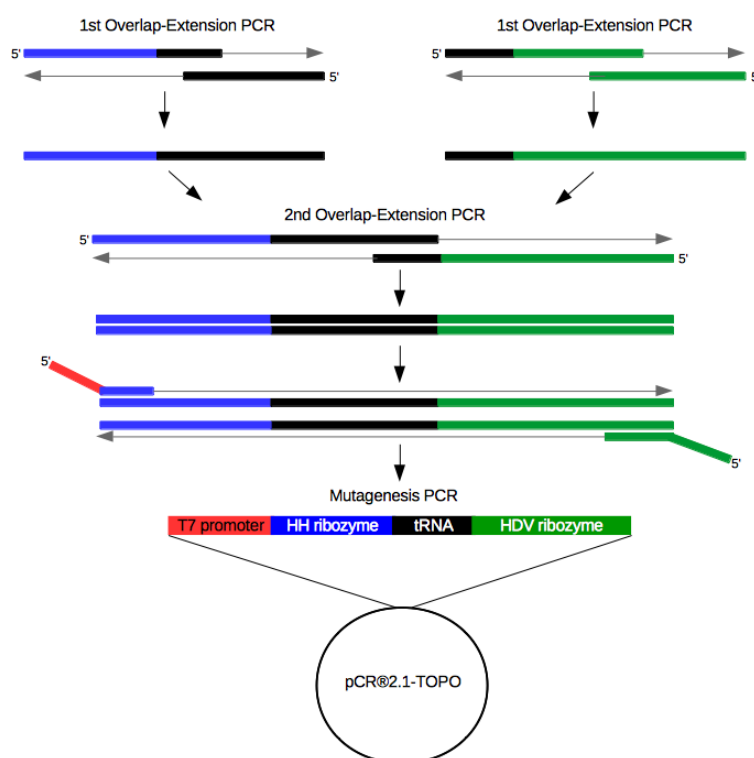
Figure 19: Construction of tRNA transcription templates.
(Upper part) tRNA[Arg], tRNA[Ile] and tRNA[Phe] transcription template sequences. (Lower part) tRNA transcription templates were generated by two combined overlap-extension PCRs followed by mutagenesis PCR in order to introduce the construct into pCR®2.1-TOPO plasmid. The components of the construct are a T7 promoter (red), a HH ribozyme sequence (blue), a tRNA gene sequence (black), and a HDV ribozyme sequence (green).

8.4.2. *In vitro* Transcription

R. culicivorax mt tRNA[Arg] and mt tRNA[Ile] transcripts were obtained by run-off transcription with T7 RNA polymerase following the protocol described in (Schürer *et al.*, 2002). The template used for the reaction consisted either of a linearized plasmid, digested with the restriction endonuclease *EcoR*V, or of a PCR fragment. In both cases, the template contained a promoter for the T7 RNA polymerase, an upstream hammerhead ribozyme sequence, the gene for the tRNA and a downstream sequence of a hepatitis delta virus (HDV) ribozyme.

The transcription reaction was carried out in a 30 µl reaction volume at 37°C for 6-16 h, and contained, in addition to the template (1 µg of plasmid DNA or 100 ng of PCR product), 1x transcription buffer, 3.3 mM DTT, 4 mM of each NTP, 1 unit of pyrophosphatase, and 50 units of T7 RNA polymerase. tRNAs were internally labelled by adding 10 µCi [γ-^{32}P]-ATP to the transcription reaction.

The self-cleaving activity of the flanking ribozymes allows the production of tRNA molecules with defined 5'- and 3'-ends. The resulting tRNAs carry a 5'-terminal hydroxyl group and a 2', 3'-cyclic phosphate group at the 3'-terminus after transcription (Schürer *et al.*, 2002). To overcome a low ribozyme cleavage efficiency due to a possible missfolding, 10 denaturing/renaturing cycles of 3 min at 60°C / 3 min at 25°C were performed on the 30 µl sample following transcription. The reaction products were separated on a denaturing (8 M urea) polyacrylamide gel ("sequencing gel"). tRNAs were then extracted from the gel as described in 8.4.4.
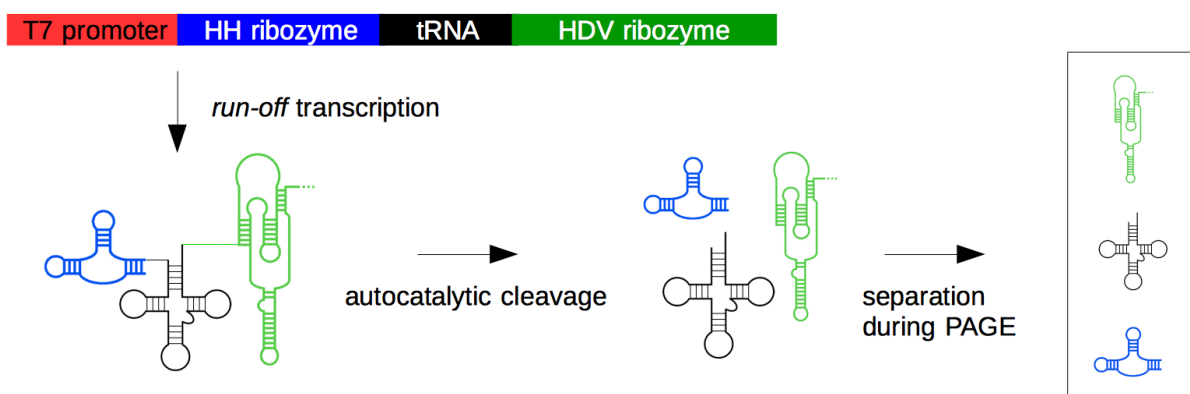

Figure 20: Schematic representation of the preparation of *in vitro* transcribed tRNAs.
The *in vitro* transcription templates consist of a T7 RNA polymerase promoter (red), a hammerhead (HH) ribozyme sequence (blue), the gene for the tRNA (black) and a hepatitis delta virus (HDV) ribozyme sequence (green). RNA products are separated on a denaturing PAA-gel.

8.4.3. Separation of RNA via denaturing PAGE and detection

The preparative separation of RNA was carried out by gel electrophoresis in a 10 %, 12.5 % or 15 % denaturing polyacrylamide gel (8 M urea in 100 mM Tris-Borate, 2 mM EDTA, pH 8.3). The samples were completed with 5 µl RNA loading buffer and electrophoresis was performed in vertical chambers at 20-40 W with 1x TBE as running buffer until the xylene cyanol reached the lower part of the gel. Radiolabeled RNA was subsequently detected by autoradiography. For this purpose, the gel located on a glass plate was wrapped in a polyethylene film, on which a phosphor screen was placed. The exposure was carried out in a cassette overnight at 4°C. The visualization of RNA bands was performed with a Phosphor imager (Storm 860TM Optical Scanner or Typhoon Scanner). The position of non-labelled RNA bands was determined by UV shadowing. For this purpose, the gel was transferred onto white paper. The nucleic acid bands were visible as a shadow upon irradiation with UV light of 254 nm.

8.4.4. Extraction of RNA from denaturing polyacrylamide gels

tRNA-bands of interest were excised from gel with a sterile scalpel, and placed into an Eppendorf tube. RNA was eluted by overnight incubation in 400 µl ddH$_2$O at 4°C under shaking. After recovery of the supernatant, RNA was precipitated with ethanol.

8.4.5. 3'–end dephosphorylation

The co-transcriptional self-cleavage of the terminal HDV ribozyme cassette results in a 2',3'-cyclic phosphate at the 3'-end of the tRNA transcripts. The 3'-terminal cyclophosphate was removed by the phosphatase activity of T4 PNK (polynucleotide kinase). A 3'–end dephosphorylation reaction was carried out in a 50 µl volume incubation for 6 h at 37°C. The reaction mixture contained up to 500 pmol of RNA, 10 units of T4 PNK and 1x dephosphorylation buffer. The efficiency of the reaction was verified by running a sub-sample on a 10 % polyacrylamide denaturing gel. The removal of the phosphate group leads to a reduced net charge, which results in a lower electrophoretic mobility of the dephosphorylated tRNAs as compared to the untreated tRNAs. Once dephosphorylation was completed, tRNAs were purified by phenol-chloroform extraction followed by ethanol precipitation.

8.4.6. 5'-end labeling of tRNAs

5'-end labeling of tRNAs was performed in a 30 µl reaction with PNK buffer A (50 mM glycine-NaOH pH 8.5, 2 mM DTT), 1.5 µg BSA, 6.7 mM DTT, 10 µCi [γ-^{32}P]-ATP, 10 units T4 polynucleotide kinase, and 10 µg RNA (extracted from PAA gel). The reaction mixture was incubated at 37°C for one hour. The separation of RNA was performed in 10 % denaturing PAGE followed by the isolation from gel.

8.5. Determination of tRNA structures

8.5.1. Native polyacrylamid-gelelectrophoresis (native PAGE)

Native polyacrylamide gels electrophoresis was performed to elucidate the conformation of tRNA transcripts. 5 µl of native RNA loading dye was added to the purified tRNA samples. Separation was performed in a 15 % native polyacrylamide gel with 0.5x TBE as running buffer at 4°C. Detection was performed by autoradiography.

8.5.2. Enzymatic analysis

Ribonuclease V1 cleavage

Ribonuclease V1 (RNase V1) from *Naja oxiana* was used to detect paired nucleotides in tRNA structures. Prior to use, tRNAs were denatured 2 min at 65 °C, and then cooled down to room temperature. The reaction mixture (20 µl) was prepared on ice in RNase V1 reaction buffer in the presence of 1 µg of total tRNA from *E. coli*, 0.005 U RNase V1 and 40 pmol of 5´-labeled tRNA. The reaction was carried out at 5°C, 15°C, or 37°C for 5 minutes. The reaction was stopped with the addition of 5 µl RNA loading dye, and immediately frozen at -20°C. Reaction products were separated on 15 % denaturing PAA gel.

Nuclease S1 cleavage

Nuclease S1 from *Aspergillus oryzae* catalyzes the nonspecific endonucleolytic cleavage of single-stranded DNA and RNA at phosphodiester bonds. The catalysis requires the presence of zinc ions. Prior to use, tRNAs were denatured 2 min at 65 °C, and then cooled down to room temperature. 20 µl of a reaction mixture contained 1x nuclease S1 reaction buffer, 1 µg of total tRNA from *E. coli*, 40 pmol of 5´-labeled tRNA, and 5 U nuclease S1. The reaction was incubated at 5°C, 15°C, or 37°C for 5 minutes. The

reaction was stopped with the addition of 5 μl RNA loading dye, and immediately frozen at -20°C. Reaction products were separated on 15 % denaturing PAA gel.

Ribonuclease T1 cleavage

Ribonuclease T1 (RNase T1) from *Aspergillus oryzae* cleaves single-stranded RNA downstream (3' side) of guanine residues. A typical reaction mixture (10 μl) contained 1x RNase T1 reaction buffer, 1 μg of total tRNA from *E. coli*, 40 pmol labeled tRNA and 5 U RNase T1. The reaction mixture was incubated at 5°C, 15°C, or 37°C for 5 minutes, stopped with the addition of 5 μl RNA loading dye, and immediately frozen at -20°C. Reaction products were separated on 15 % denaturing PAA gel.

8.5.3. In-line probing

In-line probing assays rely on non-enzymatic self-cleavage of RNA under mild alkaline conditio (Regulski and Breaker, 2008) Intrinsic higher reactivity of phosphodiester bonds in single-stranded domains are linked to higher flexibility of RNA chains as compared to double-stranded or higher-ordered domains. 40 pmol of 5'-labeled tRNA were incubated in a 10 μl volume containing 1x in-line probing buffer, and 1 μg of total tRNA from *E. coli*. The reaction was incubated at room temperature. 2 μl samples were taken after 15 h, 24 h, and 40 h. 5 μl of RNA loading dye were added to stop the reaction. Separation and analysis of reaction products were performed on 15 % denaturing PAA gel.

8.5.4. Alkaline hydrolysis

Radioactively labeled tRNA molecules were hydrolyzed in a strong alkaline environment to generate a systematic (but still statistic) cleavage at each phosphodiester bond. Co-migration of the cleavage fragments on denaturing gels enables an assignment of the reaction products generated by enzymatic and chemical cleavages. The reaction leads to a "ladder" as the RNA is cleaved after each nucleotide. The reaction was carried out at 90°C for two minutes in a 10 μl reaction volume containing a strongly alkaline buffer, 1 μg total tRNA from *E. coli*, and 40 pmol of 5'-labeled RNA. The reaction was stopped with the addition of 5 μl RNA loading dye. The analysis of the hydrolysis products was carried out on 15 % denaturing PAA gel.

8.5.5. Nuclear magnetic resonance (NMR) spectroscopy

Proton NMR spectra of armless tRNAs were measured in collaboration with Dr. Elke Durchardt-Ferner from the laboratory of Prof. Jens Wöhnert (Goethe University Frankfurt). The method is based on the principle that the nuclei of some atoms (e.g. ^{1}H, ^{13}C, ^{19}F) can change its spin states (resonate) when placed between the poles of a powerful magnet. The spinning nuclei will align with or against the applied field, and thereby creating an energy difference. This energy difference can be measured. An NMR spectrum is a plot of the radio frequency (chemical shift in ppm) applied against absorption (intensity). A signal in the spectrum is referred as a resonance. The number of signals indicates how many different types of hydrogen are in the molecules. This means that hydrogens that resonate at the same applied field are magnetically and chemically equivalent. Positions of signals indicate the type of hydrogen. For example, primary and secondary H resonate at 0.9 ppm and 1.3 ppm, respectively, while aromatic H resonate between 6 - 8.5 ppm (Levitt, 2013).

For NMR measurements, 1.05 mg of tRNA^{Arg} and 1.17 mg of tRNA^{Ile} were dissolved in 500 µl buffer containing 25 mM phosphate and 50 mM KCl at pH 6.2. The final concentration of tRNA was 100 µM. Mg^{2+} ions were added in chloride form to reach a final concentration of 2 mM. The solution was transferred to a Wilmad 508CP NMR microtube, and NMR spectra were recorded in a Bruker AV 950 NMR spectrometer. Data was collected at different temperatures between 5°C and 25°C.

8.5.6. Small angle X-ray scattering (SAXS)

SAXS measurements were performed in collaboration with Dr. Claude Sauter (IBMC/CNRS, University of Strasbourg) at the SWING beamline, SOLEIL synchrotron (Saint-Aubin, France). tRNA^{Arg} and tRNA^{Ile} samples were concentrated using centrifugation in an Amicon Ultra-4 (cut off 3K) at 5000 rpm to a final concentration of 6 mg/ml (tRNA^{Arg}) and 3.5 mg/ml (tRNA^{Ile}) in 200 µl buffer containing 50 mM Hepes pH 7.4 and 5 mM MgCl$_2$. 70 µl and 50 µl of these solutions containing tRNA^{Arg} and tRNA^{Ile}, respectively, were loaded onto a size exclusion chromatography (SEC) HPLC column (BioSEC3-150, Agilent) in order to separate monomers from aggregates. Elution was performed using an Agilent HPLC system at 0.2 ml/min in the concentration buffer, as well as in a similar buffer containing 150 mM KCl. Samples were exposed to an X-ray beam directly downstream to the SEC column and the resulting scattering signal was

collected (240 images of 1 min exposure). The scattering signal from the buffer (=background) was collected as well to be subtracted from the RNA signal. The scattering curve, I(q) results then from the subtraction of the buffer from the sample signal. SAXS images were processed with FOXTROT, and resulting curves were analyzed with the package ATSAS 2.7.2 (Petoukhov *et al.*, 2012), including various tools e.g., to evaluate the integral parameters from Guinier plots such as radius of gyration Rg (PRIMUS) (Konarev *et al.*, 2003), and to evaluate the particle distance distribution function P(r) (GNOM) (Svergun, 1992). 3D model reconstructions were obtained using the DAMMIF software (Franke and Svergun, 2009). Atomic models were compared with SAXS curves using CRYSOL (Svergun *et al.*, 1995). A schematic representation of the experimental setup of a typical SAXS analysis is shown in Figure 21.
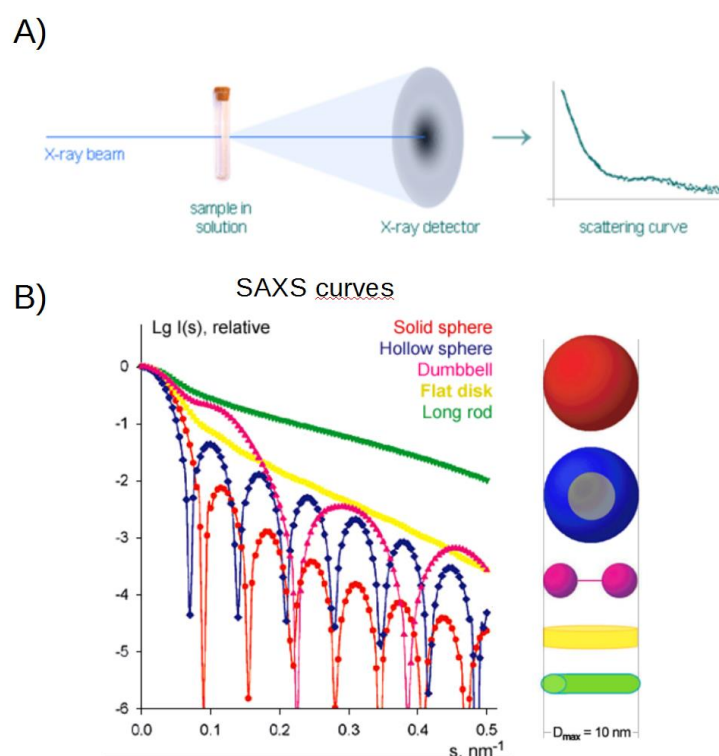
Figure 21: Experimental setup of typical SAXS analysis.
(A) Schematic representation of a SAXS experiment. The sample is exposed to X-rays and the scattered radiation is registered by a detector. The result is a scattering curve from which a low resolution model can be created. (Modified from biosax.com) (B) Characteristic SAXS curves for five objects of different shapes but same D_{max} and same molecular weight (modified from Svergun and Koch, 2003).

8.6. *E. coli* culture and transformation

8.6.1. Plating

To cultivate *E. coli*, LB-agar plates supplemented with the necessary corresponding antibiotics were used and inoculated with transformation products, or with bacteria stored in glycerol. The plates were incubated overnight at 37°C.

8.6.2. Liquid cultures

Incubation of *E. coli* in liquid cultures was usually performed at 37°C and shaking at 200 rpm. A pre-culture was grown overnight in a volume of 5 ml LB from a single colony. Main cultures were incubated for several hours until the desired optical density was reached. The growing temperature for main cultures varied between 13 °C and 37°C, and was adapted to the corresponding *E. coli* strain used for protein expression (see section 8.6.6).

8.6.3. Storage

LB agar plates were stored at 4°C for 3-5 days. Liquid cultures (1 ml) were stored under glycerol (40 % final concentration) at -80°C.

8.6.4. Chemical transformation of *E. coli*

Chemically competent *E. coli* cells were prepared following the calcium chloride method described by (Sambrook *et al.*, 1989) aliquoted and stored at -80°C. Up to 50 ng of purified plasmid (or the ligation mixture, see section 8.2.2) was directly used for transformation of competent Top10 *E. coli* cells. 10 µl of plasmid solution or ligation mixture were added to 200 µl of competent cells and gently mixed. The cells were incubated on ice for 20 min. Afterwards, a heat shock was performed for 30 sec at 42°C in a water bath followed by incubation on ice for 3 min. 800 µl of SOC medium was added, and the cells were incubated at 37°C for 1 h under shaking. Finally, 100 µl cells were plated on LB plates with the appropriate antibiotic for the resistance gene present on the transferred plasmid. LB plates were incubated at 37°C overnight.

8.6.5. Transformation by electroporation of *E. coli*

To transform electro-competent *E. coli* cells, corresponding bacterial aliquots were thawed on ice. The cells were mixed, either with the plasmid DNA, or with the ligation product. Subsequently, the mixture was transferred to a previously cooled electroporation cuvette (1 cm), and electroporation was performed in an electroporator (E. coli Pulser, Bio-Rad) according to the manufacturer's instructions. After electroporation, the cells were rinsed from the cuvette with 1 ml of SOC-medium. LB-agar plates with the corresponding antibiotic for selection of the transformants were spread out with 100-500 µl of the transformation product, and the plates were incubated overnight at 37°C.

8.6.6. Expression of recombinant proteins in *E. coli*

The expression protocol of recombinant proteins was adapted to the different expressing *E. coli* strains used in this study.

	BL21 (DE3)	Rosetta™2	Arctic Express™ (DE3)
Preculture	Inoculation of 5 ml LB containing corresponding antibiotic, growth at 37°C overnight	Inoculation of 5 ml LB containing Cam + corresponding antibiotic, growth at 37°C overnight	Inoculation of 5 ml LB containing Gm + corresponding antibiotic, growth at 37°C overnight
Main culture	Inoculation of 800 – 2000 ml LB medium containing the appropriate antibiotic with 4-5 ml preculture, growth at 37°C	Inoculation of 800 – 2000 ml LB medium containing the appropriate antibiotics with 4-5 ml preculture, growth at 30°C	Inoculation of 800 – 2000 ml LB medium containing NO antibiotics with 4-5 ml preculture, growth at 30°C
Induction	Growth until OD_{600} = 0.6 or 1.5 (for late induction); addition of 1 mM IPTG (final concentration)	Growth until OD_{600} = 0.6 or 1.5 (for late induction); addition of 1 mM IPTG (final concentration)	Growth until OD_{600} = 0.6; addition of 1 mM IPTG (final concentration)
Expression	Growth at 37°C for 3 h	Growth at 30°C for 3 h	Growth at 13°C for 16 h
Harvest	Centrifugation for 15 min at 3500 x g and 4°C, storage at -20°C until use.	Centrifugation for 15 min at 3500 x g and 4°C, storage at -20°C until use.	Centrifugation for 15 min at 3500 x g and 4°C, storage at -20°C until use.

8.7. Handling of *S. cerevisiae*

8.7.1. Gene construct

For expression in yeast the plasmid pJJH378 (kindly provided by A. Brüser, University of Leipzig) was used. The plasmid contains an inducible Gal promoter and the gene sequence of a phosphofructokinase subunit (PFK2), which was removed by *BamH*I and *Hind*III digestion and replaced by the *Rcu* CCA-adding gene sequence equally digested by *BamH*I and *Hind*III. The gene construct contained still the 3' untranslated region (UTR) of the PFK2 gene (about 100 nt after the N-terminal 6xHis-tag and stop codon) to allow a successful termination of translation.

8.7.2. Transfection of *S. cerevisiae*

S. cerevisiae strain AH109 and Y187 were transfected with pJJH378 plasmid containing the *Rcu* CCA-adding enzyme coding sequence. Cells were thawed on ice, and 1 μl of plasmid (100-200 ng/μl) and 150 μl of LiPEG were added. The cell suspension was vortexed, and incubated for 20 min at room temperature. 17.5 μl DMSO was added, and the solution was shortly vortexed before the heat shock treatment was performed at 42°C for 15 min. Cells were centrifuged at 2000 rpm for 2 min, and the supernatant was removed. The cell pellet was re-suspended in 100 μl H_2O, and plated on SD(-Leu) agar plates. Agar plates were incubated at 30°C together with a bowl filled with H_2O. Cell growth was verified after 3-4 days.

8.7.3. Protein overexpression in *S. cerevisiae*

A preculture of the *S. cerevisiae* AH109 or Y187 strain was used to inoculate 5 ml of SD selection medium (-Leu), and incubated overnight with shaking at 180 rpm at 30°C. Overnight cultures were vortexed for 0.5–1 min to disperse cell clumps. 50 ml aliquots of YPDA medium were inoculated with the preculture to a final OD_{600} of 0.001. The culture was incubated overnight until an $OD_{600} = 2$ was reached. Cells were centrifuged at 400 rpm for 20 min. Protein expression was induced by the addition of the same YPDA medium volume supplemented with 2 % galactose. Cells were harvested after growth of 24 h ($OD_{600} = 15$) by centrifugation at 4000 rpm for 20 min at 4°C. The cell pellet was stored at -20°C.

8.8. *In vitro* translation

The Easy Express® Protein Synthesis Kit from Qiagen was used for *in vitro* synthesis of the *Rcu* CCA-adding enzyme following the manufacturer's instructions.

8.9. Protein Methods

8.9.1. Purification of *Rcu* CCA-adding enzyme

Gene construct

The CCA-adding enzyme coding sequenced was available with a N-terminal 6xHis-tag sequence in the pET28b vector (kindly provided by O. Götze), and was cloned in this study into a pTrcHis A plasmid, also with N-terminal 6xHis-tag sequence. Protein expression in the pET system was controlled by a T7 promoter, and therefore appropriate for *E. coli* (DE3) strains that express T7 RNA polymerase, and are controlled by a Lac regulatory construct. In contrast, protein expression on pTrcHis vectors was directly under the control of a *trc* promoter. The expression is induced for both constructs by the addition of IPTG. The resulting proteins have a molecular weight of 53 kDa and a theoretical pI of 8.5 or 7 for the recombinant protein translated from pET28b or pTrcHis A vector, respectively.

Affinitychromatography via ÄKTA

The cell pellet obtained from overexpression (section 8.6.6) was thawed on ice and resuspended in 5 ml binding buffer. The cell suspension was mixed with 5 g Zirconia/Silica beads and lysed with a FastPrep®-24 homogenizer for 30 s at 6 m/s. The supernatant was separated from the cell pellet by centrifugation at 42,000 rpm for 40 min. The protein solution was further clarified from particles by filtering through a 0.22 μm syringe filter. The lysate was diluted 1:2 with binding buffer and loaded onto a His Spin Trap column, which was equilibrated in lysis buffer CL. The column was washed with 40 ml of dissociation buffer DBC (1 ml/min), followed by 20 ml of wash buffer CW (2 ml/min). The protein was eluted with 15 ml elution buffer CE in 1 ml fractions (1 ml/min).

Affinity chromatography via Batch-method

The cell pellet obtained from overexpression (section 8.6.6) was thawed on ice and resuspended in 5 ml lysis buffer CL. The cell suspension was mixed with 5 g Zirconia/Silica beads and lysed with a FastPrep®-24 homogenizer for 30 s at 6 m/s. The supernatant was separated from the cell pellet by centrifugation at 42,000 rpm for 40 min. The protein solution was further clarified from particles by filtering through a 0.22 µm syringe filter. The lysate was diluted 1:2 with lysis buffer CL containing denatured *E. coli* proteins (0.1 mg/ml final concentration). 2 ml of Ni-NTA slurry (1 ml bed volume) were pipetted into a 15 ml tube and briefly centrifuged. The supernatant was removed and 2 ml of lysis buffer CL were added. After centrifugation the supernatant was removed. 8 ml of cell lysate were added to the matrix and gently mixed by shaking (200 rpm on a rotary shaker at 4°C for 60 min). The mixture was centrifuged and washed 2 times with 2.5 ml washing buffer CW. All centrifugation steps were carried out for 2 min at 1000 rpm. The whole procedure was performed in a cooling room at 4 °C.

The lysate-Ni-NTA mixture was loaded onto a column with the bottom outlet capped. The bottom cap was removed and the flow-through was collected for SDS-PAGE analysis. The column was washed twice with 2 ml dissociation buffer DBC, followed by two wash steps with 2 ml wash buffer CW. All wash fractions were collected. The protein was eluted 4 times with 1 ml elution buffer CE. The eluate was collected in 4 tubes and analyzed together with the other fractions by SDS-PAGE.

Size-exclusion chromatography

Size-exclusion chromatography (SEC) was performed to separate the *Rcu* CCA-adding enzyme from remaining protein contaminations and to remove imidazole from elution buffer. A HiLoad 16/60 Superdex 75 pg column (1 column volume = 120 mL) was equilibrated with 250 ml SEC buffer. Subsequently, 2 ml of the elution fractions (obtained from affinity chromatography) were injected. The elution was performed in 0.5 ml fractions, and the elution fractions were stored until use at 4°C.

Concentration and storage

Before the concentration procedure was performed, the absorbance and concentration of the protein solution was determined at OD_{280} (NanoDrop) using the theoretical extinction coefficient ($\varepsilon = 43047$). The protein containing fractions were transferred into

a dialysis membrane tube (cut off 30 kDa) and directly put onto a bed of high molecular weight polyethyleneglycol (PEG) 20,000 chips (e.g. 10 g per 5 ml). Incubation time (in general 1 h) was adapted, if necessary, to reach the favored volume reduction. Samples with *Rcu* CCA-adding enzyme were either stored in SEC-buffer at 4°C or were supplemented with 40 % (v/v) glycerol and stored at -20°C.

8.9.2. Purification of *Rcu* mt ArgRS

<u>Gene construct</u>

The coding sequence of the full length *Rcu* mt ArgRS and its variants were cloned with a C-terminal 6xHis-tag in pET28a vector under the control of an inducible T7 promoter. A codon optimized full length gene sequence for expression in *E. coli* was generated and synthesized using the IDT services. Additionally, codon modified variants were cloned into the pDEST vector with an N-terminal 6xHis-tag and were also under the control of an inducible T7 promoter. The different protein variants varied in the length of their N-terminal sequence. They were transferred into different *E. coli* strains, and expressed as mentioned in section 8.6.6.

<u>Affinity chromatography</u>

After cultivation and recombinant protein expression, cells were harvested by centrifugation and resuspended in 30 ml of buffer AW. Two protease inhibitor tablets (Roche) were added. Cell lysis was performed by sonication on ice 8 times for 10 sec at 120 V with a pause of 30 sec between each sonication step. The cell suspension was centrifuged at 35,000 g for 40 min at 4°C. The supernatant was loaded onto a 5 ml NiNTA resin column (QIAGEN), which was equilibrated in buffer AW. Afterwards the column was washed with 40 ml urea wash buffer AU (1 ml/min), followed by 20 ml dissociation buffer DBA (1 ml/min) and 20 ml wash buffer AW (2 ml/min). The protein was eluted using 15 ml elution buffer AE in 1 ml fractions (1 ml/min).

<u>Dialysis and Concentration</u>

Fractions containing the *Rcu* ArgRS were pooled and dialyzed against 500 ml dialysis buffer A1 overnight. The buffer was exchanged by fresh buffer A1 and dialysis was continued for 2 h. In a final dialysis step, the buffer was replaced by 500 ml dialysis buffer A2 and the protein was dialyzed additional 2h. The protein solution was

concentrated by means of centrifugation using Amicon® Ultra-4 (cut-off: 30 kDa) at 5000 x g. The protein concentration was determined at OD_{280} (NanoDrop) using the theoretical extinction coefficient of *Rcu* ArgRS ($\varepsilon = 39100$).

8.9.3. Protein Separation in SDS-polyacrylamide gel electrophoresis

The separation of proteins, depending on their size was performed as described in (Sambrook *et al.*, 1989) on a SDS-polyacrylamide gels. The gels contained a 10 % resolving gel solution (pH 8.8) and a 4 % stacking gel solution (pH 6.8). Protein samples were mixed with 5x protein loading buffer and boiled at 95°C for 5 min. Samples were then briefly centrifuged and loaded onto the gel. Electrophoresis was performed with 1x TGS as running buffer at 100 V and 180 V for the stacking and resolving gels, respectively. To visualize the protein bands, the gel was stained with SDS-staining solution for at least 30 min, and then washed with destaining buffer.

8.9.4. Western blot analysis

The Trans-blot Turbo Transfer System from Biorad was used for the detection of His-tagged proteins. Samples were prepared as described in 8.9.3 and separated on a Mini-Precast Gel (Biorad) at 200 V. The transfer to the membrane was performed following the manufacturer's instructions. For immuno detection, the PVDF membrane was blocked with 5 % milk in 1x TBST for 30 min. Incubation with the HRP-conjugated primary Anti-His antibody (abcam) (diluted 1:10,000 in 1x TBST + 1% milk) was performed at 4°C overnight. After incubation, the membrane was washed three times with 1% TBST, and briefly dried on Whatman paper. The Pierce ECL Western Blotting Substrate 1 and 2 (Thermo Scientific) were mixed at a 1:1 ratio and added to the membrane. After incubation of 1 minute excess reagent is drained. The membrane was covered in a clear plastic wrap and exposed to X-ray film.

8.10. Protein aectctivity assays

8.10.1. CCA-incorporation assay

An assay contained 1x CCA reaction buffer, 1 mM NTPs, 4 pmol of radioactively labeled tRNA and 50 ng of enzyme. The reaction was incubated between 30 min and 2h at 30 °C in a final volume of 10 µl. The reaction was stopped by precipitating the RNA with

ethanol/0.3 M NaAc and centrifugation at 14,000 rpm for 20 min at 4°C. The precipitated RNA pellet was directly resuspended in RNA loading buffer and then separated on denaturing PAA gels. The reaction products were visualized using autoradiography.

8.10.2. Aminoacylation assay

Before starting the aminoacylation reaction the *in vitro* synthesized tRNAs were denatured for 1 min at 60 °C and then slowly renatured at room temperature (at least min 4 min) to improve the correct refolding of tRNAs. An assay contained between 27 and 40 pmol tRNA, 500 µM arginine and 25 µM radioactively labeled ^{3}H L-arginine (40 ci/mmol), and 1x reaction buffer. The aminoacylation reaction mixture was equilibrated to 25 °C before the addition of enzyme to a final volume of 50 µl. Aliquots of 10 µl were removed at varying time points and spotted onto Whatman 3MM papers whetted with 5% TCA. These papers were placed immediately in a cold 5 % TCA solution for 10 min. The TCA solution precipitates the tRNA. Free amino acids remain in the solution. The papers are washed 2 times with 5% TCA and then dehydrated by rinsing with ethanol. The dried papers were put in counting vessels containing 2.5 ml of scintillation liquid (Ecoscint 0™, National diagnostics). The radioactivity corresponding to amino acid charged to the tRNA, fixed on the paper, was measured in a scintillizer (LS6500, Beckmann Coulter) for 1 min per assay.

However, there were indications that the arginyl-tRNA synthetases used in this study was sensitive to the ratio ATP/Mg^{2+} in the reaction buffer. So the reaction buffer was adjusted for each of the synthetases. MRE and MRC buffer was used for *E. coli* and for *S. cerevisiae* ArgRS respectively. For *R. culicivorax* ArgRS MMR buffer with varying Mg^{2+} concentration was used.

RESULTS

CHAPTER 1: Genomic analysis of the nematode worm *R. culicivorax*

Romanomermis culicivorax is a nematode roundworm. The phylum Nematoda consists of two classes: Chromadorea, which include, e.g., *Caenorhabditis elegans* and *Ascaris suum*, and Enoplea, which include, e.g., *Trichinella spiralis* and *R. culicivorax* (Schiffer *et al.*, 2013) (Figure 22)*. R. culicivorax* inhabits freshwater environments like ponds and lakes. While its original habitat is situated in the United States, particularly in Louisiana, Florida, and Utah, humans have distributed the species around the world (Levy R *et al.*, 1979).

 R. culicivorax is an obligatory endoparasite and penetrates a broad range of mosquito species. Its body is long and narrow, with a whitish color. Its body size ranges from 5 up to 25 mm. *R. culicivorax* undergoes four molts during the first 3-6 weeks while it grows up from the first instar larvae stadium to an adult. During this time, the infective preparasite stage hatches from eggs as a second-stage larva, and swims freely in fresh water until it finds a host, i.e., a mosquito larvae (e.g. different Aedes and Anopheles species). Upon successful contact, the preparasite attaches to the mosquito larvae by means of a stylet, and enters the hemocoel through a hole cut into the host's cuticle. The parasite then matures inside the host during the following 7-8 days. Afterwards, the postparasitic stage emerges by rupturing a hole in the host's cuticle through simple mechanical pressure, which is always lethal for the host. After its emergence, the free-living larvae molts again, and finally reaches the adults stage, and thereby sexual maturity. After mating in fresh water and laying eggs, the parasitic life cycle restarts again (Shamseldean and Platzer, 1989).

As mentioned above, *R. culicivorax* can infest different mosquito species, which are transmitters of major infectious diseases, e.g., malaria and dengue. It has been shown that *R. culicivorax* can infest Anopheles and larvae of other species under laboratory as well as under natural conditions (Kobylinski *et al.*, 2012). Malaria is a highly infectious disease caused by parasites belonging to the *Plasmodium* type, and is commonly transmitted by the bite of an infected female *Anopheles* mosquito. Therefore, *R. culicivorax* is of considerable interest because of its potential to be used as a biological remedy against these insect's pest (Petersen and Chapman, 1979; Kamareddine, 2012). Even if *R. culicivorax* would be able to theoretically reduce the prevalence of malaria within the human population, the effectiveness of this parasite to

act against malaria vectors is often dependent on biological limitations in his habitat (e.g. temperature, humidity, polluted environments, and natural enemies) (Petersen and Cupello, 1981).
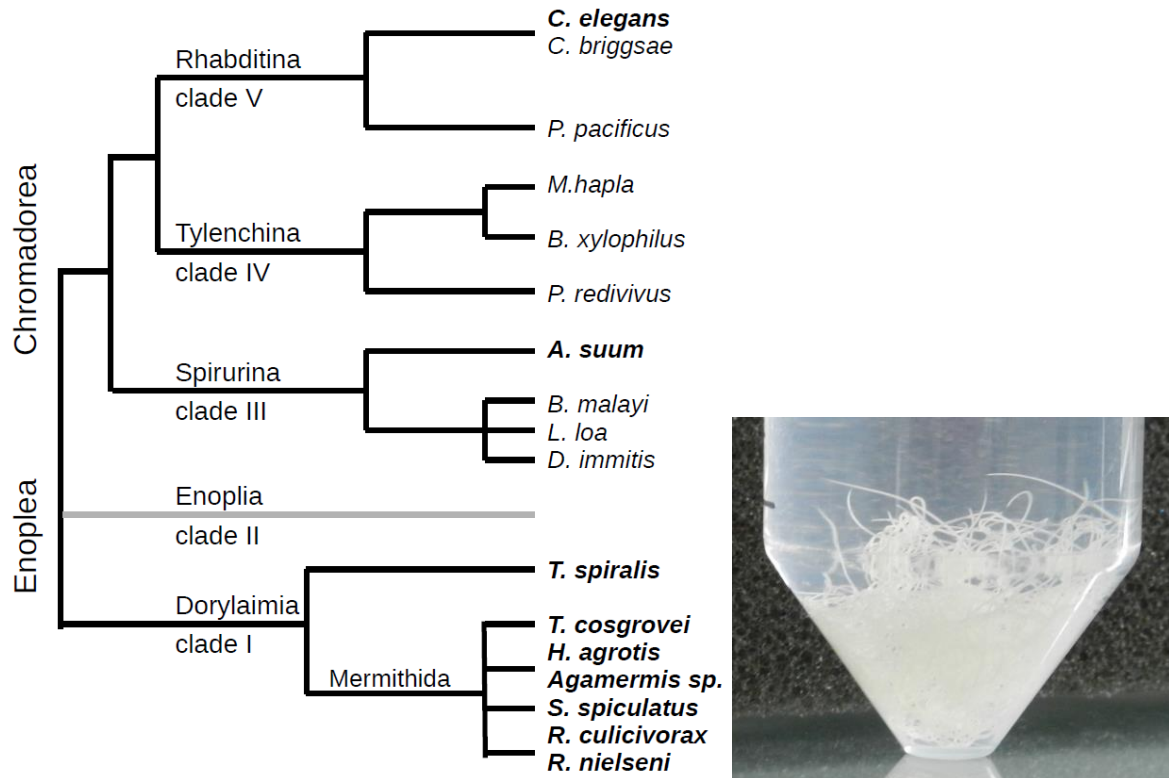

Figure 22: *R. culicivorax* and a simplified phylogenetic tree of the phylum Nematoda.
(Left) The phylogeny, simplified from (Schiffer *et al.*, 2013), emphasizes the position of the main species of interest in this study: species from the Mermithida *(such as R. culicivorax)*, *T. spiralis*, *A. suum* and *C. elegans*. (Right) *R. culicivorax* animals were kindly provided by G.E. Platzer (University of California, USA). Photo was taken by S. Wende.

Beside this, *R. culicivorax* is of high interest for genomic research because its mitochondrial genome and genes exhibit various peculiarities.

Its mitochondrial genome was sequenced and analyzed already in the 1980s. This revealed (as it is the case for most other animals) the presence of genes for 13 structural proteins, whose products are predicted to contribute to the electron transport chain and oxidative phosphorylation, two ribosomal RNAs (rRNA), and 22 transfer RNAs (tRNAs) molecules (Powers *et al.*, 1986). The mitochondrial genome size is particularly large with 26 kb as compared to other nematodes worms with an average size of 14-18 kb (Hyman, 1988). The unusual large size extension is probably caused by several tandem duplications within the mt DNA (Hyman *et al.*, 1988; Azevedo and Hyman, 1993).

In contrast to former genome annotations, a recently updated version annotated mt tRNA genes with an extremely reduced size. Throughout the 22 mt tRNA genes, 11 correspond to D-armless tRNAs, 2 correspond to T-armless tRNAs, and 9 correspond to tRNAs missing both arms (Jühling *et al.*, 2012b). It appears that tRNA^{Arg} and tRNA^{Ile} belong to those that miss both arms. Chapter 2 focuses on the structural properties of these tRNAs, which are one of the main interests of this study.

9. Analysis of mitochondrial small and large rRNA in *R. culicivorax*

The discovery of shortened tRNA genes in Nematodes in general, led to the presumption that the mitochondrial translation machineries of these parasitic worms could differ considerably from that in plants or mammals. In fact, not only tRNAs but also other ncRNA genes are of shorter size. Indeed, the rRNA components of nematode mitoribosomes are among the smallest characterized thus far, indicating that some of the nematode mt ribosomal proteins are likely to be recruited to compensate for the reduced size of the mt rRNAs during evolution (Okimoto and Wolstenholme, 1990; Okimoto *et al.*, 1992; Okimoto *et al.*, 1994; Suzuki *et al.*, 2001). Thus, it is of high interest whether reduced rRNAs are also present in the mitoribosome of *R. culicivorax.* Both genes, coding for the small and large rRNA, were compared herein to those from *C. elegans,* representing the shortest rRNAs identified so far. Additionally, they were compared to human mt rRNA genes, which serve as a reference. Thereby, the estimation of rRNA gene sizes was based on the annotations that are available at the NCBI database (www.ncbi.nlm.nih.gov).

This analysis revealed that both annotated rRNAs of *R. culicivorax* are shorter than these of *C. elegans*. The large rRNA is with 839 nt more than 100 nt shorter than this of *C. elegans* (953 nt). The length of the small rRNA is with 662 nt slightly shorter compared to its counterpart in *C. elegans* (697 nt). Both mt rRNA genes from both nematodes are significantly shorter than those from human mitochondria, which are of 954 nt and 1,559 nt for the small and large rRNA gene, respectively (see Table 12 for a detailed overview). We hypothesize that the reduction in size of the mitochondrial RNA content (for tRNA and rRNA sequences) in *R. culicivorax* is potentially correlated to an increased protein content in the mitoribosome as it was shown for other mammals (Okimoto *et al.*, 1992; Wolstenholme *et al.*, 1994; Suzuki *et al.*, 2001). However, this hypothesis has still to be verified for *R. culicivorax*.

Table 12: Size comparisons of mt rRNA genes from *R. culicivorax*, *C. elegans*, and *H. sapiens*

Organism	Size of large mt rRNA gene	Size of small mt rRNA gene
R. culicivorax	839 nt	662 nt
C. elegans	953 nt	697 nt
H. sapiens	1,559 nt	954 nt

The nuclear genome of *R. culicivorax* has been sequenced and published in 2013 (Schiffer *et al.*, 2013). The annotations for several protein coding genes that are relevant for this study are still incomplete, or only partially correct. Unfortunately, this makes an accurate analysis of the nuclear encoded genes, which should be analyzed in this study to a challenging task. However, the mRNA sequences coding for proteins characterized in this study were determined by reverse transcription on RNA extracts, and were then verified by an own annotation using the original RNAseq data (see Chapter 3 and 4).

CHAPTER 2: Structural characterization of armless mt tRNAs

This chapter is dedicated to the structural investigation of armless mitochondrial tRNAs of the nematode *R. culicivorax*, with special regards to tRNA^{Arg} and tRNA^{Ile}. This study continues the work of Frank Jühling and Sandra Wende about the bioinformatic prediction of truncated tRNAs, and the initials hints for their biological existence (Jühling *et al.*, 2012b; Wende *et al.*, 2014).

In the following paragraphs a comparative tRNA gene analysis is presented and in a second part the secondary and tertiary structure of armless tRNAs are identified using enzymatic and chemical probing as well as biophysical methods such as nuclear magnetic resonance (NMR) spectroscopy and small angle X-ray scattering (SAXS).

10. Primary sequence analysis of armless mt tRNA genes

In order to obtain a better structural overview of these extremely truncated tRNAs, alignments were built containing a variety of tRNA^{Arg} or tRNA^{Ile} genes from different organisms. The comparisons is based on alignments presented in 2012 by Jühling and colleagues for all mt tRNA genes of several nematode worms of the Mermithidae family (i.e. *Romanomermis nielseni*, *Hexamermis agrotis*, *Strelkovimermis spiculatus*, *Thaumamermis cosgrovei, and Agamermis sp. BH-2006*) that are closely related to *R. culicivorax* (Jühling *et al.*, 2012b). Here we focus especially on the tRNA^{Arg} and tRNA^{Ile}, while the peculiarities of both tRNAs are highlighted through a comparison with several other mitochondrial and cytosolic tRNA gene sequences. These alignments that are presented below include therefore also mt tRNA sequences of nematodes that are more distantly related, e.g., *Caenorhabditis elegans, Ascaris suum, and Trichinella spiralis*. Furthermore, the annotated mt tRNA^{Arg} and tRNA^{Ile} genes of some arthropods, more precisely, of two mites (*Pireneitega taishanensis and Dermatophagoides farina*), a spider (*Tetragnatha nitens*), and a pseudoscorpion (*Paratemnoides elongates*) are included into this alignment. In addition, a typical human mt tRNA is added as a reference for typical metazoan mt tRNAs. Moreover, cytosolic tRNAs of classical model organisms, such as *C. elegans*, *Homo sapiens*, *Saccharomyces cerevisiae*, and *Escherichia coli* were added to complete the comparative analysis between cytosolic, mitochondrial and armless tRNAs. The complete overview of all tRNAs showing the different gene sequences and their alignments with each other are shown in Figure 23. It can be clearly seen that the nucleotide composition of each tRNA differs strongly from one organism to another. Only anticodons of tRNAs of similar

isoacceptor families are conserved among each other.

The alignment of cytosolic tRNA gene sequences was included since these tRNAs represent a group with the classical cloverleaf secondary structures, with strongly conserved lengths of structural domains, and served thus as reference for this analysis. The domains (i.e., acceptor/anticodon/D/T-stem) of the cloverleaf structure are highlighted in specific colors to facilitate the discrimination of these domains.

When taking a closer look on mt sequences, it is obvious that the mammalian human mt tRNA^{Arg} and tRNA^{Ile} genes are still quite similar to cytosolic tRNAs. However, the sequence content in the D- and T-domains is different, the domains appear to be shorter, and conserved motifs (e.g., the TΨC motif in the T-loop) are absent.

Interesting examples for reduced tRNA genes can be found in the roundworms *C. elegans, A. suum,* and *T. spiralis*. Although the D-stems of their tRNAs are still conserved with 4 base pairs, the D-loop is shortened to 4 – 7 nt (except in *C. elegans* mt tRNA^{Arg}). The T-domain of both tRNA families is significantly reduced, and a stem is even absent, since no base pairs and thus no stem can be formed. Instead of the presence of a classical domain, T-arms and variable loops are replaced by elements of 7-13 nt that are called TV-replacement loops (Wolstenholme *et al.*, 1994).

In recent years, a complete set of truncated tRNAs genes have been also identified in the mitochondrial genome of some arthropods (Masta, 2000; Klimov and Oconnor, 2009). Here, four different species have been chosen to represent this phylum. The complete loss of the T-domain in tRNA^{Arg} and tRNA^{Ile} of *T. nitens* and *P. elongates* is very striking, and only a highly reduced D-arm is still present. Particularly, in both mite species, *D. farinae* and *P. taishanensis,* most tRNA genes are clearly shortened. The T-stem-loop (TSL) and D-stem-loop (DSL) are completely absent. A small D-stem consisting of 3 base pairs is present only in the tRNA^{Ile} of *D. farinae*.

The mt tRNA sequences of *R. culicivorax* and the other Mermithids are extremely shortened compared to other mitochondrial and to cytosolic tRNAs. Both, the classical DSL and TSL regions are completely lost and replaced by short replacement loops with a length of 4-15 nucleotides. The identified sequences of mt tRNA^{Arg} and mt tRNA^{Ile} from *R. culicivorax* consist of 42 nt and 47 nt, respectively. Both sequences have a very low G and C content of 24 % for tRNA^{Arg} and 13 % for tRNA^{Ile}, and their calculated (by means of OligoCalculator) melting temperatures are very low, with approximately 27°C for both tRNAs. In contrast, classical tRNAs with a balanced nucleotide content have a melting temperature of about

75°C and mitochondrial tRNAs from higher eukaryotes exhibit a melting temperature of about 55°C (Yokogawa *et al.*, 2010). Interestingly, the optimal range of temperature for the development of *R. culicivorax* is 21°C-33°C (Platzer, 2007). Thus, it is possible that armless tRNAs are stabilized by base modifications or other (so far unknown) factors.

Figure 23: Alignment of cytosolic and mitochondrial tRNA^Arg and tRNA^Ile gene sequences.
The 18 selected tRNA^Arg and tRNA^Ile gene sequences from *R. culicivorax, R. nielseni, H. agrotis, S. spiculatus, T. cosgrovei, A. sp. BH-2006, P. taishanensis, D. farina, T. nitens, P. elongates, C. elegans, A. suum, T. spiralis, H. sapiens, S. cerevisiae,* and *E. coli* are aligned according to secondary structural domains (acceptor stem, orange; D-stem, green; anticodon stem, blue; anticodon, bold; T-stem, red). As the CCA triplet is not encoded in the eukaryotic tRNA genes it was added manually for reasons of clarity (modified from Jühling *et al.*, 2012b).

11. Construction of DNA templates and *in vitro* transcription of tRNAs without 3'-CCA-end

In order to elucidate the secondary and tertiary structures of both armless tRNAs, these molecules were produced by *in vitro* transcription. The tRNA gene containing plasmids or PCR products that served as template for *in vitro* transcription were synthesized and cloned into a pCR®2.1-TOPO vector following the protocol described in section 8.4.1. Therein, the sequence encoding the tRNA gene, flanked upstream by a hammerhead-ribozyme sequence and downstream by a HDV-ribozyme sequence, is located downstream of a T7 promoter. While the T7 promoter ensures the binding of the T7 RNA polymerase and defines the transcription start, both ribozymes self-cleave autocatalytically after transcription and make thus sure that produced tRNA molecules possess homogeneous 5`- and 3`-ends (Schürer *et al.*, 2002). Transcription and the following purification of the transcript was performed as described in section 8.4.2. The overall quality of the RNA preparations was assessed by electrophoresis on a denaturing 12.5 % PAA-gel. This method allows first evaluation about RNA quantities. A typical result of RNA migration using a denaturing gel system is shown in Figure 24 A. In this example, the RNA was internally radioactively labeled with α-^{32}P-ATP. The resulting bands represent tRNA molecules (tRNA^{Phe} from yeast in lane 1 as control, mt tRNA^{Ile} in lane 2 and mt tRNA^{Arg} in lane 3) as well as the RNA molecules corresponding to the cleaved hammerhead ribozyme and HDV-ribozyme, respectively, are all clearly identifiable. The ribozymes have different sizes, because their nucleotide sequences have been adapted to the corresponding tRNA sequences to ensure an exact cleavage of the specific tRNA ends, and to facilitate the size discrimination between RNA products. Bands corresponding to RNA products of larger size probably represent transcription products in which the ribozyme cleavage did not occur. These bands are very weak and can be neglected. The released tRNAs were excised from the gel and purified. The yield from a typical 30 µl reaction volume of transcription was about 300 pmol of tRNA molecules. The yeast cytosolic tRNA^{Phe} was prepared as a positive control for the transcription procedure, and served later as an activity control for the CCA-incorporation assays.

The tRNA gene transcription product carries a 5'-hydroxyl group, which can be converted to a radioactively labeled 5'-phosphate. This property required for structure probing assays. At the 3'-end, a 2', 3'-cyclic phosphate group is generated during the ribozyme cleavage, which has to be removed by dephosphorylation with T4 PNK if the tRNA is used

in functionality assays. The removal of the phosphate group can be monitored by denaturing PAGE because the missing phosphate group leads to a reduced net charge of the transcript, which leads to a lower electrophoretic mobility compared to untreated RNA. The different migration profiles of phosphorylated (P) and dephosphorylated (DP) tRNA transcripts are monitored in Figure 24 B.
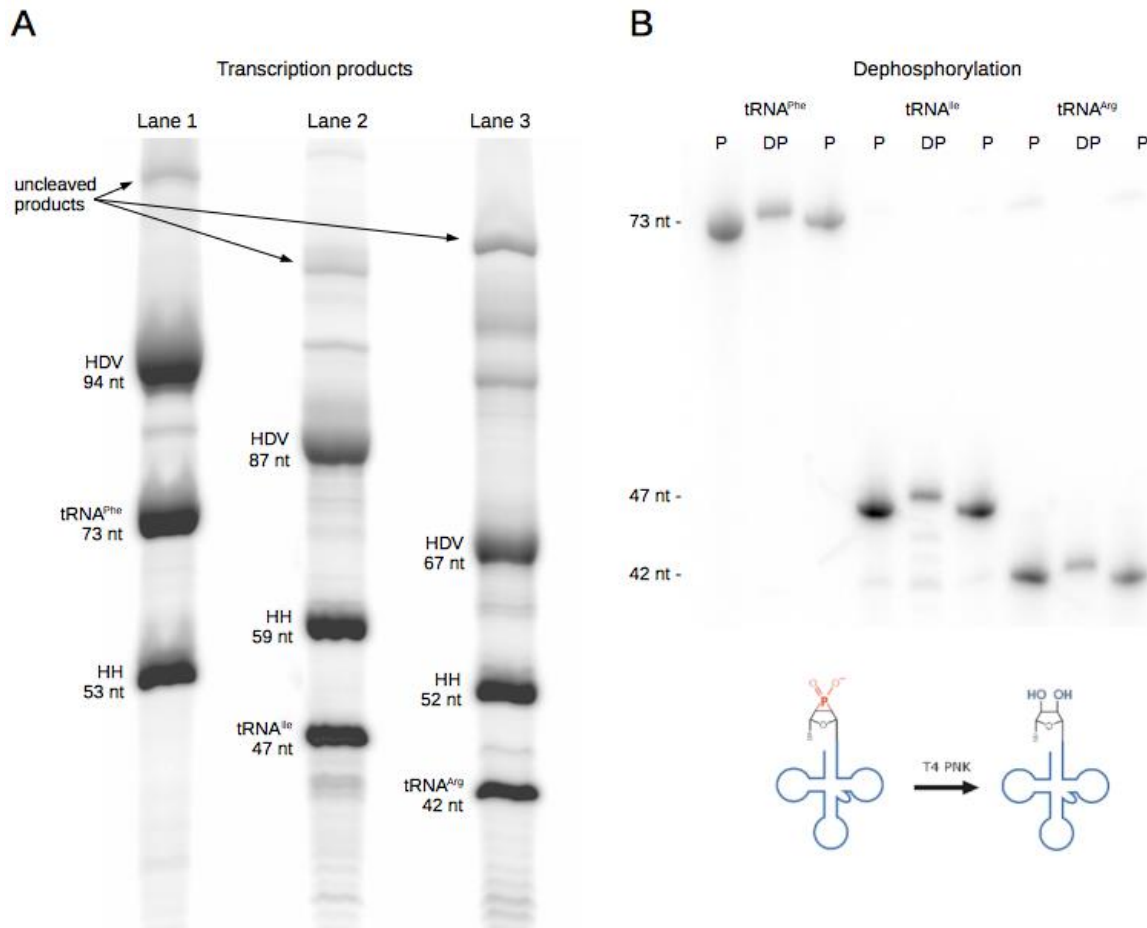

Figure 24: 12.5 % PAA gel after *in vitro* transcription and dephosphorylation of tRNA transcripts.
(A) After autocatalytic ribozyme cleavage, transcription products were separated on a 12.5 % denaturing PAA gel. Individual reaction products were visualized by autoradiography. The transcribed tRNA[Phe] from yeast with a size of 73 nt served as a length standard (lane 1). Furthermore, the cleavage of both the HDV ribozyme (94 nt) and HH ribozyme (53 nt) from the tRNA[Phe] after transcription can be detected. In lane 2 and 3 the transcription of mt tRNA[Ile] (47 nt) and mt tRNA[Arg] (42 nt) is visible. The size of the ribozymes was adapted to the size of the tRNAs to allow the identification of the transcription products in the gel. (B) tRNA transcripts were dephosphorylated by T4 PNK in order to remove the terminal 2', 3'-cyclic phosphate group, which remains after the ribozyme cleavage. Dephosphorylated tRNAs (DP) migrate slower than untreated tRNAs (P) carrying the 2', 3'-cyclic phosphate in a denaturing PAA gel because of a missing negative charge.

12. Structural analysis of armless mitochondrial tRNAs

Conformation and structures of armless mitochondrial tRNA[Arg] and tRNA[Ile] of the nematode *R. culicivorax* were analyzed via native PAGE, enzymatic probing, in-line probing, NMR, and SAXS. The results are discussed in the following sections.

12.1. Analysis of RNA conformation by native PAGE

In native gels, RNA electrophoretic mobility depends not only on the size of RNA molecules, but also on their secondary structures. Therefore, polyacrylamide gel electrophoresis under native conditions provides a useful method for studying nucleic acid conformations. In particular, heterogeneity with respect to certain conformations can be detected. Basically, compact folded RNAs run much faster through a native gel compared to unstructured RNAs, even if both have the same molecular weight. Accordingly, it can be assumed that an altered electrophoretic mobility or the presence of multiple bands represents different structural conformations of a single RNA species and may indicate changes in structures of the RNA molecules (Woodson and Koculi, 2009).

The secondary structure of tRNA[Arg] and tRNA[Ile] was investigated by native gel electrophoresis on a 12.5 % polyacrylamide gel (Figure 25). One concrete band is visible for both tRNAs. Even a different treatment of denaturation/renaturation of the RNA molecules (either slowly cooling at room temperature (RT) or fast cooling on ice after denaturation at 65°C) did not affect the migration behavior and thus the RNA conformation. As no additional bands are visible for tRNA[Arg] and tRNA[Ile] it can be suggested that both tRNA molecules adopt only one conformation.
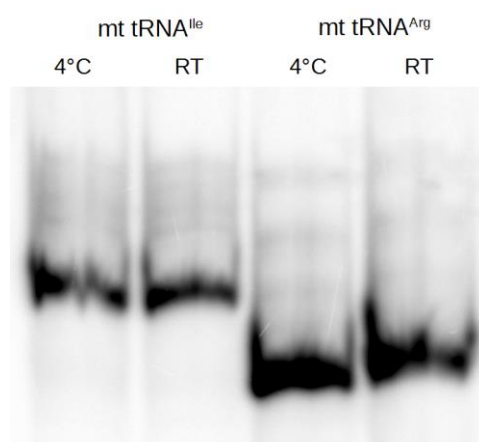

Figure 25: Analysis of armless tRNAs in a 12.5 % native PAGE.
Mt tRNA[Arg] and tRNA[Ile] from *R. culicivorax* are heated for 2 min at 65°C, cooled down either to room temperature (RT) or to 4°C and loaded onto a 12.5 % native PAA gel before migration.

12.2. Secondary structure analysis by enzymatic probing

The secondary structure of an RNA molecule can be determined by means of enzymatic structural analysis. In this case, specific nucleases are used in order to allow the accurate determination of single-stranded nucleotides and of nucleotides involved in higher ordered domains (unpaired and paired nucleotides respectively) in an RNA molecule. To study the secondary structure of mt tRNA^{Arg} and mt tRNA^{Ile} both molecules were labeled at their 5'-end with γ-^{32}P-ATP.

Nuclease S1 was used for the identification of single-stranded regions in the tRNAs. Additionally, RNase V1 was used to cleave nucleotides that are present within double-stranded or stacked regions of the tRNAs. For each enzymatic cleavage it is important that the enzymes cut statistically not more than once per molecule (Ehresman et al., 1987). Therefore, total tRNA from *E. coli* was added as competitor to regulate the occurrence of cuts in a tRNA molecule. Negative controls were set up without any enzyme. The digestion mixtures were incubated for 5 min at 4°C, 15°C, and 30°C. The resulting RNA fragments were separated in a 15 % denaturing PAA gel. Positions of residues digested by the nucleases could be mapped to individual nucleotides through the comparison of RNase digestion profiles with an RNase T1 ladder and the alkaline hydrolysis profile of both tested tRNAs.

Figure 26 andFigure 27 represent the enzymatic probing profiles for mt tRNA^{Arg} and mt tRNA^{Ile}, respectively. Green bars mark the cleavage sites that result from nuclease S1 digestion. Positions that are cleaved by RNase V1 are marked by red bars. In order to facilitate the evaluation of the results, the identified cleavage sites are indicated by arrows in the same color code in a secondary structure prediction determined *in silico* using the RNAfold program.

The cleavage profiles of both tRNAs vary slightly at different temperatures. At 4°C, both tRNAs seem to have more stable conformations, however, enzymes are also less active. The optimal activity temperature of nucleases is about 30°C, which is, however, very close to the calculated melting temperature of about 27°C of the armless tRNAs (see above). Therefore, performing the experiments at 15°C seems to be the best compromise between optimal activity temperature for the nucleases and an optimal temperature for stable tRNA conformations. Nuclease S1 cleaves the tRNA^{Arg} molecules in three different regions. Two of them are located in predicted single stranded regions including the anticodon loop (C_{19}-A_{22}) and the bulge region (U_{30}-A_{32}). The third one is a single cleavage site after

position A_2, which is localized in the acceptor stem. Apparently, RNase V1 cuts significantly at several positions. Some are located in the predicted double stranded regions like the anticodon stem (G_{13}/G_{14} and C_{24}-U_{26}) and the acceptor stem (A_{37}/G_{38}). Surprisingly, some cleavages took place in bulge regions, i.e., such as in position U_6-A_8 and A_{27}. Since the U_6-A_8 region contains many U nucleotides, and is located opposite of A_{27}, internal interactions may be formed in the bulge, which could have been recognized by RNase V1. Control incubations performed under the same conditions in absence of nuclease S1 and RNase V1 and T1 confirm that no degradation of tRNA molecules took already place.

The results of the enzymatic probing analysis of mt tRNA[Arg] indicate that nuclease S1 is preferentially active in predicted single-stranded region (anticodon loop and bulge), while RNase V1 cuts preferentially in stem regions (anticodon and acceptor stem), except for one region, which is located in the bulge. Since not every region in the mt tRNA[Arg] molecules could be determined structurally by enzymatic probing, further investigation using more sensitive methods were necessary (see the following sections).
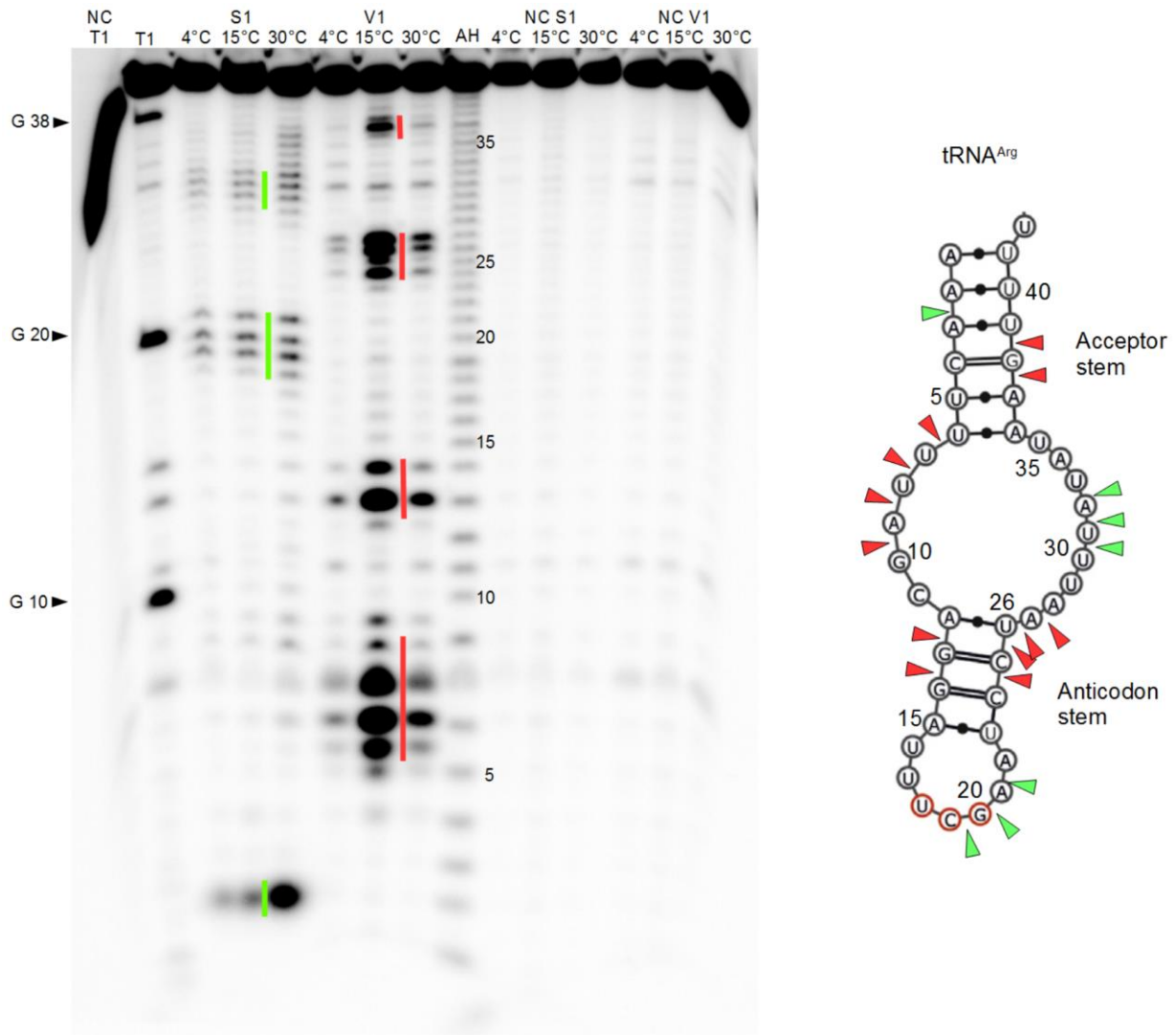
Figure 26: Enzymatic structure probing analysis of mt tRNA^Arg.
(Left) Autoradiogram of 15 % PAA gel resulting from enzymatic probing of mt tRNA^Arg. 5'-labelled mt tRNA^Arg from *R. culicivorax* was subjected to nuclease S1 and RNase V1 digestion at varying temperatures (4°C, 15°C, and 30°C), to RNase T1 digestion as well as alkaline hydrolysis (AH). Negative controls (NC) contain no enzyme. tRNA positions were precisely mapped with the T1 and alkaline ladders. Green and red bars indicate cleavage sites for nuclease S1 and RNase V1, respectively. (Right) The same positions are marked in the RNAfold 2D structure prediction by arrows using the same color code. The numbering of the nucleotides is straight forward, starting with nucleotide 1 at the 5'-end.

In the cleavage profile of tRNA^Ile, nuclease S1 cuts in 3 regions: between U_2 and G_{10}, which belongs partially to the acceptor stem and bulge region, in the anticodon loop at A_{25} and U_{26}, and in the 3'-end of the acceptor stem downstream of nucleotides A_{44} and A_{45}.

RNase V1 leads to cleavages mainly in the predicted anticodon stem at positions A_{14}, U_{17}-A_{20}, U_{31}-A_{33}, U_{36}, and in the acceptor stem at positions U_3, A_4 and U_{43}. Surprisingly, RNase V1 cuts after U_6 and A_7 that are also cleaved by nuclease S1, and which are located in the bulge region of the 2D model.
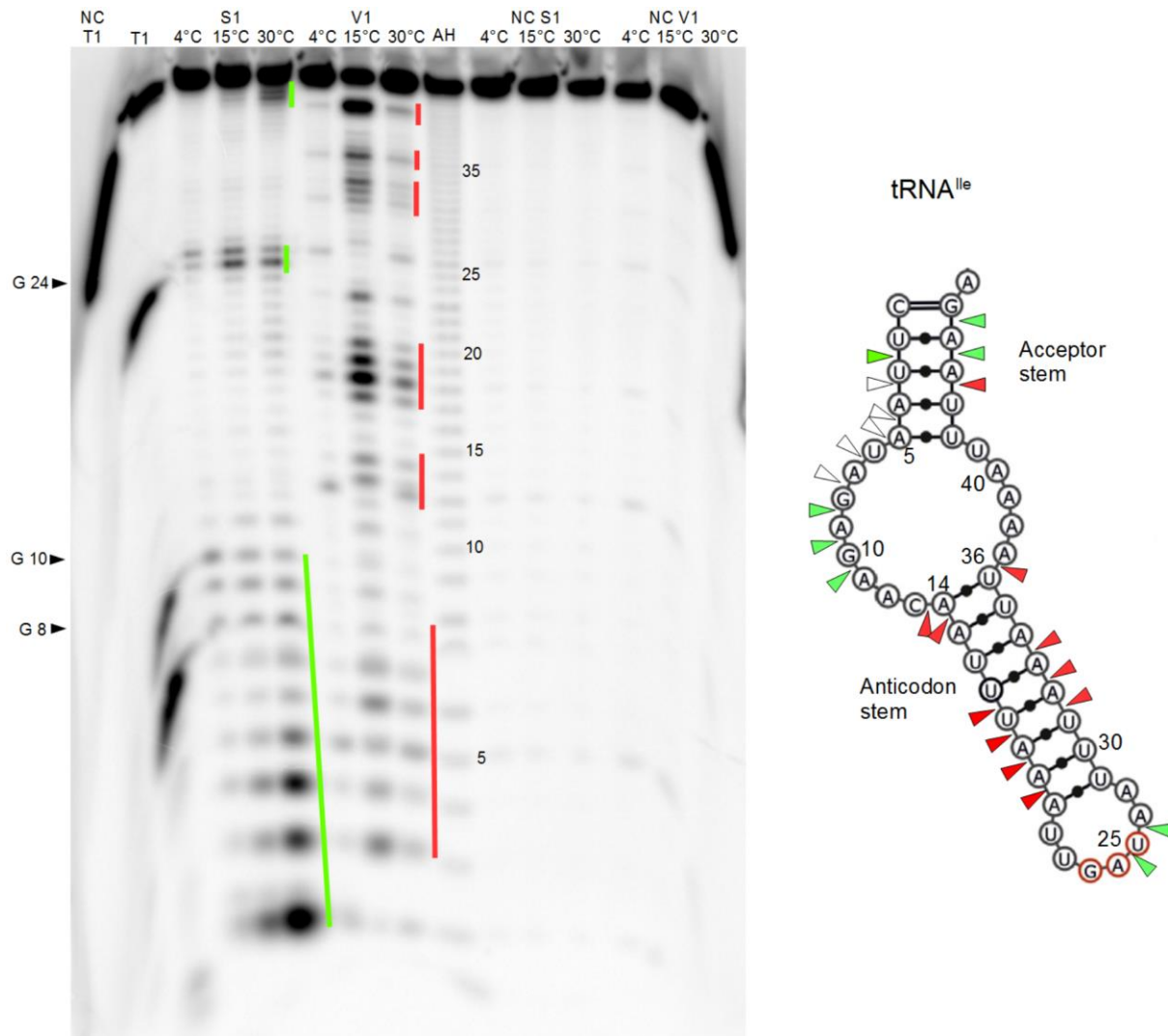
Figure 27: Enzymatic structure probing analysis of mt tRNA^Ile.
(Left) Autoradiogram of 15 % PAA gel resulting from enzymatic probing of mt tRNA^Ile. 5'-labelled mt tRNA^Ile from *R. culicivorax* was subjected to nuclease S1 and RNase V1 digestion at varying temperatures (4°C, 15°C, and 30°C), to RNase T1 digestion as well as alkaline hydrolysis (AH). Negative controls (NC) contain no enzyme. tRNA positions were precisely mapped with the T1 and alkaline ladders. Green and red bars indicate cleavage sites for nuclease S1 and RNase V1, respectively. (Right) The same positions are marked in the RNAfold 2D structure prediction by arrows using the same color code. White arrows indicate positions that are cleaved by nuclease S1 as well as RNase V1. The numbering of the nucleotides is straight forward, starting with nucleotide 1 at the 5'-end.

The results of the enzymatic probing analysis of mt tRNA^Ile reveals that nuclease S1 and RNase V1 cut mostly at different positions in the tRNA molecule. Although nuclease S1 is preferentially active in single-stranded regions, and RNase V1 in double-stranded regions, a few contradictory cleavages happen, and suggest that the enzymatic cleavage pattern of tRNA^Ile does not fit completely with the secondary structure predictions. Further investigations were performed in order to determine the structure of armless tRNAs more in detail.

12.3. Secondary structure analysis by in-line probing

A simple - and compared to the S1 probing more reliable - chemical technique to analyze secondary structure is in-line probing (Regulski and Breaker, 2008). RNAs are incubated at slightly alkaline pH, and the spontaneous cleavage of the sugar backbone by adjacent $2'$- hydroxyl groups is monitored. Single stranded regions will faster degrade over time because they are more flexible and unstable than double stranded RNA.

For in-line probing structure analysis the tRNAs were radioactively labelled at the 5'-end, incubated in alkaline conditions and the cleavage fragments were analyzed by electrophoresis on a 15 % denaturing PAA gel.

Results from in-line cleavage for mt tRNA^{Arg} and tRNA^{Ile} are shown in Figure 28 and Figure 29. During the incubation in the alkaline environment the cleavage pattern for mt tRNA^{Arg} appears exclusively in areas where loops (anticodon) and bulges were predicted. These positions are located between U_6-C_{11}, U_{17}-A_{21} and A_{27}-U_{35}.

Looking at the in-line profile of mt tRNA^{Ile} one can observe that, similar to mt tRNA^{Arg}, cleavages occur only in areas that were predicted as single-stranded regions. These regions correspond to positions between U_6-C_{13}, U_{23}-U_{26} and A_{36}-U_{41}, indicating that the in-line probing results for both mt tRNAs correlate perfectly with their computationally predicted secondary structure.

One striking result is that both tRNAs behave in an unexpected manner regarding their chemical stability. Indeed, it is well known that RNAs are more sensitive to chemical hydrolysis at 5'-CpA-3' or 5'-UpA-3' sequences than at any other sequence (Kaukinen *et al.*, 2002). Despite, there are six of these sequences in tRNA^{Arg} and four in tRNA^{Ile}, their natural cleavage (degradation) is very restricted. This suggests that both tRNAs are chemically stable, which is very different from other mitochondrial tRNAs, especially those from human (Motorin and Helm, 2010; Helm and Attardi, 2004).
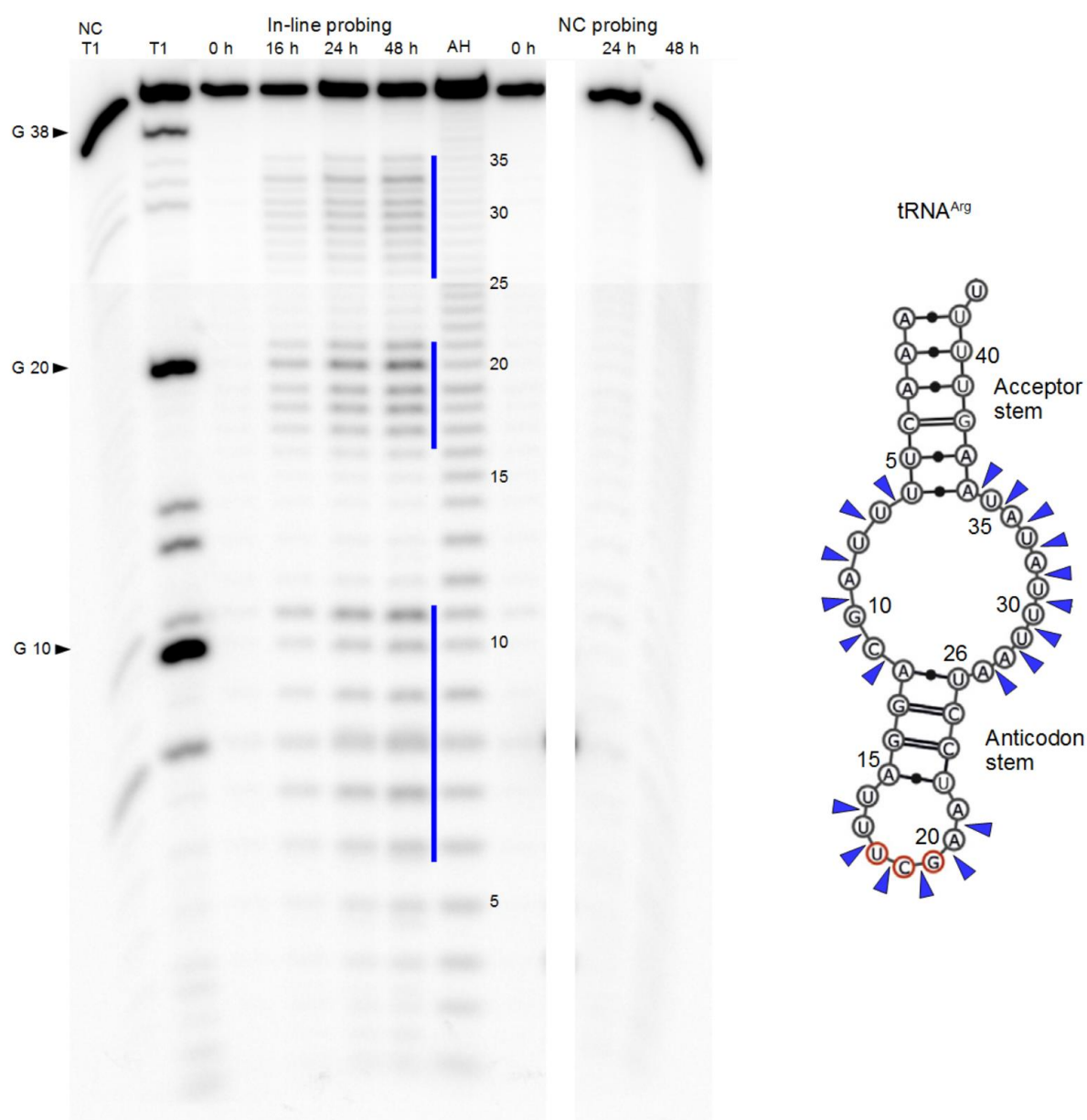
Figure 28: In-line probing analysis of mt tRNA^Arg.
(Left) Autoradiogram of 15 % PAA gel resulting from in-line probing of mt tRNA^Arg. 5'-labelled mt tRNA^Arg from *R. culicivorax* was subjected to in-line probing conditions and samples were taken at different time points (0h, 24h, and 48h). The mt tRNA^Arg was also subjected to RNase T1 digestion and alkaline hydrolysis (AH). In negative controls (NC) probing buffer was replaced by H_2O. tRNA positions were precisely mapped with the T1 and alkaline ladders. Blue bars indicate the hydrolysis pattern. (Right) The same positions are marked in the RNAfold 2D structure prediction by arrows with the same color code. The numbering of the nucleotides is straight forward starting with nucleotide 1 at the 5'-end.
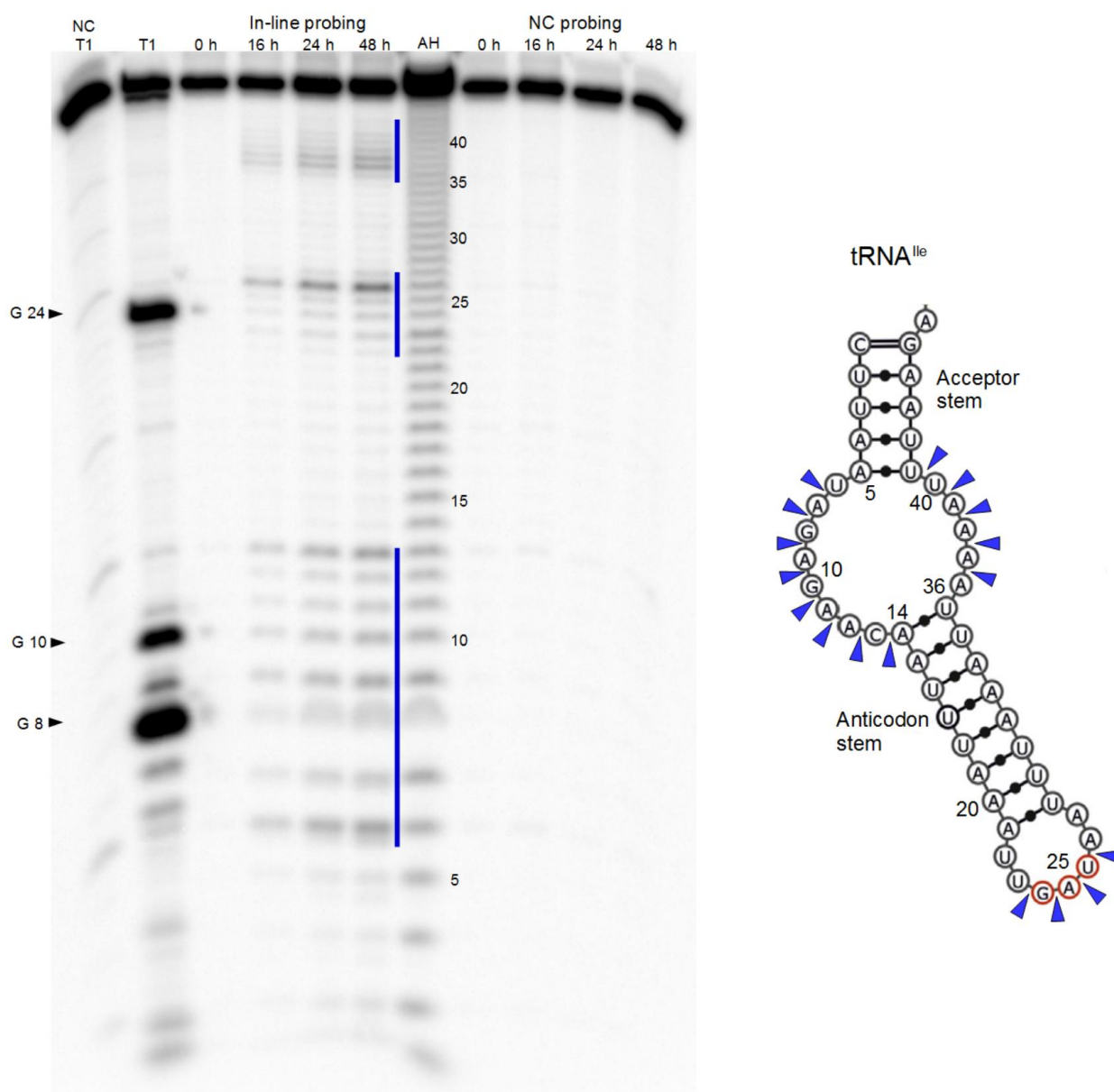
Figure 29: In-line probing analysis of mt tRNA^{Ile}.
(Left) Autoradiogram of 15 % PAA gel resulting from in-line probing of mt tRNA^{Ile}. 5'-labelled mt tRNA^{Ile} from *R. culicivorax* was subjected to in-line probing conditions and samples were taken at different time points (0h, 16h, 24h, and 48h). The mt tRNA^{Ile} was also subjected to RNase T1 digestion and alkaline hydrolysis (AH). In negative controls (NC) probing buffer was replaced by H$_2$O. tRNA positions were precisely mapped with the T1 and alkaline ladders. Blue bars indicate the hydrolysis pattern. (Right) The same positions are marked in the RNAfold 2D structure prediction by arrows with the same color code. The numbering of the nucleotides is straight forward starting with nucleotide 1 at the 5'-end.

12.4.   tRNA structure analysis by NMR

NMR spectroscopy provides a powerful tool to analyze the hydrogen-bonded structures of tRNAs in solution (Puglisi and Puglisi, 2007). The proton spectra of mt tRNA[Arg] and tRNA[Ile] from *R. culicivorax* were analyzed using NMR spectroscopy. Also the effects of temperature and Mg^{2+} ions on the structure of these tRNAs was investigated.

12.4.1. Effect of temperature and Mg^{2+} to the proton spectra of mt tRNA[Arg]

The complete ^{1}H spectra of tRNA[Arg] at different temperatures are shown in Figure 30 A. The spectra are characterized by several peaks that appear between 14.2 and 12.2 ppm. The major peaks are numbered from 1 to 7. Typical Watson-Crick A-U base pairs resonate upfield of 13 ppm, while G-C base pairs resonate upfield of 12 ppm. Therefore, all H bonds, represented by the peaks in the spectra, participate in canonical Watson-Crick base pair interactions.

The first spectrum is measured at 5°C. The temperature of the sample is then increased gradually up to 25°C. Upon raising the temperature to 25°C, which is close to the calculated melting temperature of tRNA[Arg], resonances decrease (e.g., peak 1 and 4), or even completely disappear (one shoulder of peak 3). This is probably due to the "melting" effect of the secondary structure at higher temperatures. A slightly increase at higher temperatures is detectable for the peaks 6 and 7 between 12 and 13.2 ppm. This effect is possibly associated with the gain or stabilization of H bonds. Peak 2 and 5 showed no change during the measurements.

It has been shown that millimolar Mg^{2+} concentrations have the ability to stabilize RNA tertiary structures (Romer and Hach, 1975; Stein and Crothers, 1976). In order to verify whether this is also true for armless tRNAs, the effect of magnesium ions to the proton spectrum of tRNA[Arg] was measured at 10°C and 25°C (Figure 30 B). At 10°C, no significant difference is measured in presence of 2 mM Mg^{2+} compared to the spectra at the same temperature without Mg^{2+}. Also the spectra measured at 25 °C with and without Mg^{2+} are similar to each other. Only peak 3 and 4 are increased, suggesting stabilized H bonds. For the remaining resonances no detectable changes are observed in the presence of Mg^{2+}.
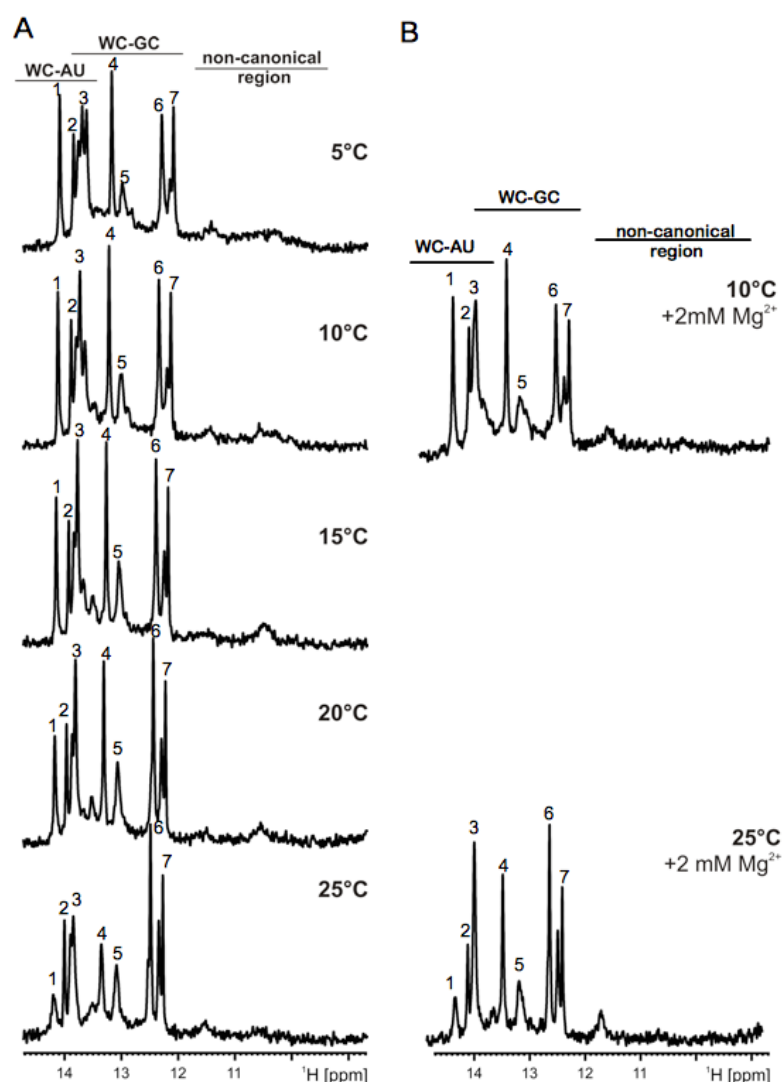
Figure 30: ¹H spectra of mt tRNA^{Arg} measured by NMR spectroscopy.
(A) Temperature dependence of the ¹H spectrum of mt tRNA^{Arg} from *R. culicivorax*. Temperatures at which each spectrum was recorded are indicated (B) Effect of 2 mM Mg2+ on the NMR spectra of mt tRNA^{Arg}. The tRNA spectra were collected in a buffer containing 25 mM phosphate and 50 mM KCl at pH 6.2. Major peaks are numbered from 1 to 7.

12.1.1. Effect of temperature and Mg^{2+} to the proton spectra of mt tRNA^{Ile}

The proton spectra of mt tRNA^{Ile} was measured at 5°C, 10°C, 15°C, and 25°C (Figure 31 A). The effect of different temperatures on this tRNA is shown in Figure A. Five main peaks (numbered from 1 to 5) are present between 13.8 and 12.75 ppm, indicating that this tRNA consists only of classical Watson-Crick base pairs. Three resonances (i.e., peak 1, 3, and 4) showed a loss of intensity with increasing temperatures. While this difference is low for peak 3, peaks 1 and 4 are completely lost at 25°C. At this temperature, which is close to the melting temperature, the tRNAs probably melt and loss their ordered state, which is associated with a loss of secondary and possibly tertiary base pair interactions.
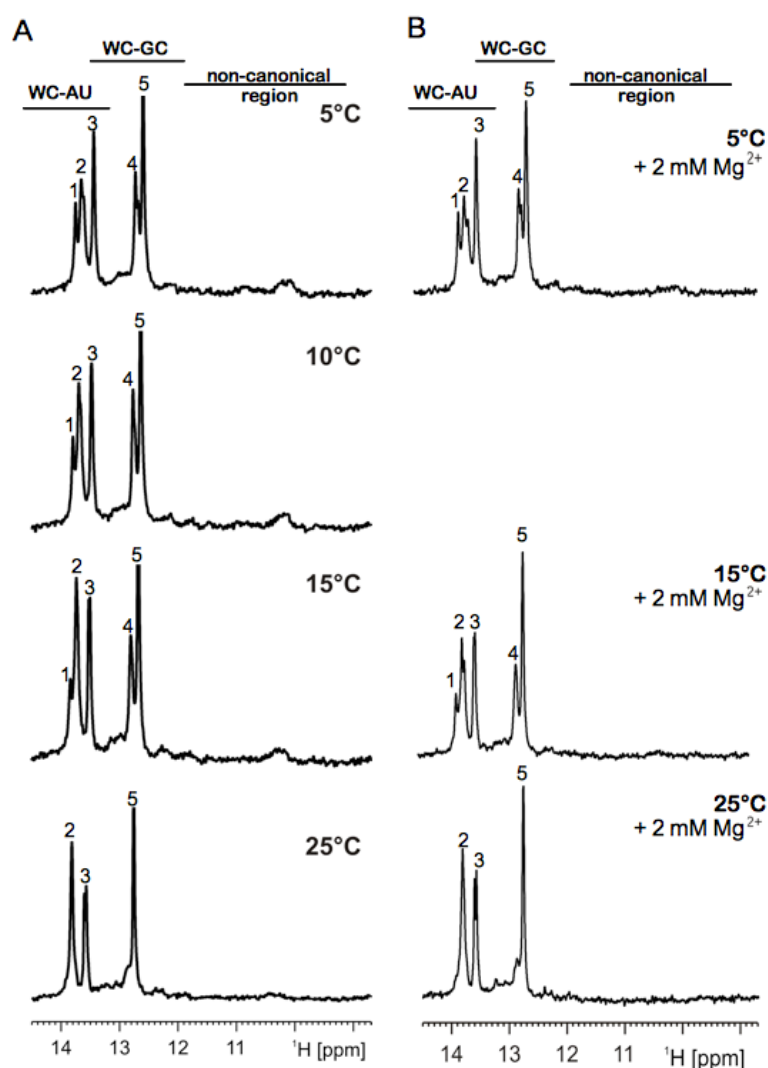
Figure 31: ¹H spectra of tRNAᴵˡᵉ measured by NMR spectroscopy.
(A) Temperature dependence of the ¹H spectrum of tRNAᴵˡᵉ from *R. culicivorax*. Temperatures at which each spectrum was recorded are indicated (B) Effect of 2 mM Mg²⁺ on the NMR spectra of mt tRNAᴬʳᵍ. The tRNA spectra were collected in a buffer containing 25 mM phosphate and 50 mM KCl at pH 6.2. Major peaks are numbered from 1 to 5.

In contrast, peak 2 shows an improved resolution at higher temperatures. It seems that this change has a stabilizing effect to the H bonds associated to this peak. No detectable changes are observed for peak 5.

After the addition of Mg²⁺ to a final concentration of 2 mM the proton spectra of mt tRNAᴵˡᵉ was measured at 5°C, 15°C, and 25°C (Figure 31 B). Magnesium has no significant effect on the structure of mt tRNAᴵˡᵉ at low temperature. There are only minor changes detectable at moderate temperatures compared to the spectra without magnesium. Peaks 2 and 3 are slightly decreased at 15 °C, and peak 5 is slightly increased at 25 °C. Potentially, magnesium has simultaneously a degrading, and a stabilizing effect on different H bonds in the tRNA structure represented by these peaks.

12.2.   tRNA structure analysis by SAXS

Armless mt tRNA samples were further studied by small-angle X-ray scattering (SAXS), a method that allows for structural characterization of biological molecules in solution, by providing information on the size and shape (Putnam *et al.*, 2007; Lipfert and Doniach, 2007; Mertens and Svergun, 2010). Additionally, commercial cytosolic yeast tRNA[Phe] was analyzed with SAXS and the measured parameters were compared to those that were obtained for armless tRNAs. Because low salt concentrations may provoke aggregation problems during SAXS measurements, the behavior of both tRNAs was measured with and without the presence of 150 mM KCl.

12.2.1. Separation by chromatography

Before the SAXS measurements were started, a HPLC was setup on line with the SAXS cell. The elution of molecules by size exclusion chromatography (SEC) was used to separate individual populations, and to obtain more monodisperse samples along SEC peaks. The HPLC profiles of the four tRNA samples (mt tRNA[Arg/Ile], with/without KCl) are shown in Figure 32. Three peaks appeared in the HPLC profiles of tRNA[Arg] and two peaks for the tRNA[Ile] samples. These peaks represent different populations of the molecules, which likely correspond to monomers (peak 2), dimers or multimers (peak 1 and 0). The presence of salt in the buffer does not significantly change the HPLC profile of both tRNAs.
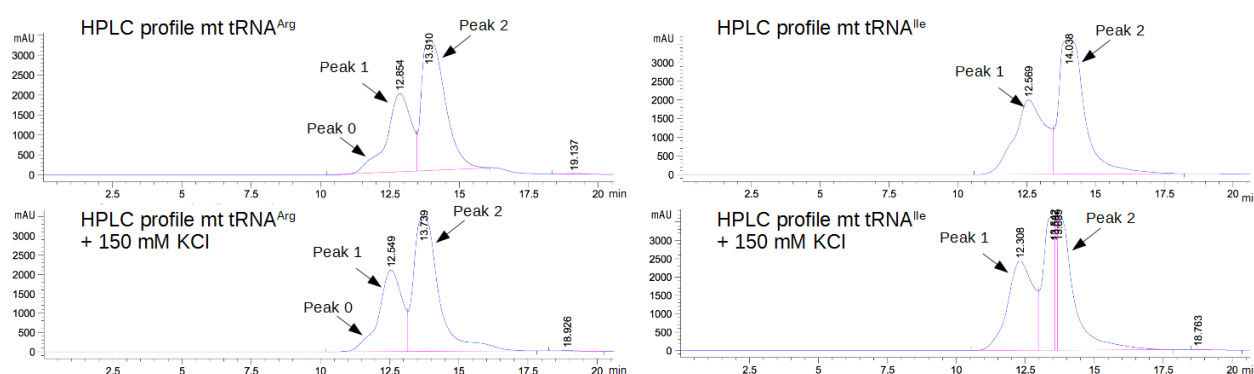
Figure 32: Figure HPLC-SEC profile of mt tRNA[Arg] and mt tRNA[Ile].
HPLC-SEC profile of mt tRNA[Arg] (left) and mt tRNA[Ile] (right) without KCl (above) and with 150 mM KCl (below). Sample injection was 50-70 µl at 6 mg/ml for tRNA[Arg] and 3 mg/ml for tRNA[Ile]. The tRNA[Arg] sample is a mixture of at least three populations as indicated by the three peaks. The tRNA[Ile] sample is a mixture of at least two populations as indicated by the two peaks.

12.2.2. SAXS data collection

The resulting data from an SEC-SAXS experiments represent a time series of SAXS intensity curves (blue lines in Figure 33). Additionally, a corresponding radius of gyration (Rg) curve can be estimated for each image (red and orange lines in Figure 33).

A plateau in the Rg curve indicates a stable conformation of the molecules in the corresponding peak. Such a plateau is measured for peak 1 of mt tRNA[Arg] between the SAXS signals 126-143 and in presence of KCl between 124-132. Peak 2 forms a plateau between 160-181 and with 150 mM KCl between 154-173. For mt tRNA[Ile], a plateau for peak 2 can be observed between the SAXS signals 159-181 and presence of KCl between 144-180. No clear plateau is visible for peak 1. Instead, the signal decreases slowly but continuously. This suggests that the molecules causing this signal have no uniform size or shape, and may forming dimers or multimers. However, the signals in presence of KCl between 101 and 109 were used for the calculation of the SAXS curve.
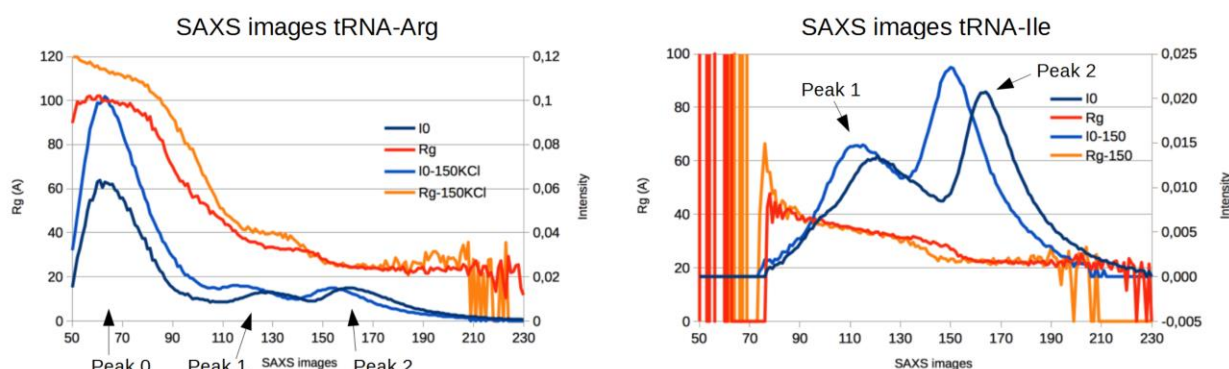

Figure 33: SAXS images of tRNA[Arg] and tRNA[Ile].
SAXS images of mt tRNA[Arg] (left) and mt tRNA[Ile] (right) are represented as a function of intensity at zero scattering angle I(0), (red line without KCl, orange line in presence of 150 mM KCl) and as a function of the radius of gyration Rg in Å, (dark blue line without KCl, light blue line in presence of 150 mM KCl).

The scattering signal of images within a plateau of the Rg curves as mentioned above were averaged, and used to generate characteristic SAXS curves as representatives of every tRNA population (peak 1 and 2 of tRNA[Arg] and tRNA[Ile] in presence and absence of KCl). A commercial cytosolic tRNA[Phe] from yeast was also analyzed with SAXS and served as a reverence for comparison with armless tRNAs.

The SAXS curves obtained from peak 1 and peak 2 are separated in two diagrams shown in Figure 34. The recorded scattering profiles spanned a q-range from ~0.02 Å^{-1} to ~3 Å^{-1}, where q = 4π sin(θ)/λ (2θ is the scattering angle, and λ is the wavelength of the incident radiation). The resulting SAXS curves, characteristic for each tRNA are compared with each other. A significant difference is visible in the shape of the scattering curves

104

produced by the samples in peak 1 and 2. The curves that result from peak 2 resemble the curve obtained from tRNA^{Phe}. They resemble a convex shape, whereas the curves that result from peak 2 populations possess a concave shape. An increased slope at very low angles (beginning of the curve), as it is the case for peak 1 curves, is often a sign of aggregation in the sample.

The shape of the SAXS curves is directly related to the shape of the molecule. The shape of the curve corresponding to the tRNA^{Phe} is characteristic for a rod-shaped molecule. The curves of both armless tRNAs present in peak 2 are similar to the curve of tRNA^{Phe}, indicating that armless tRNAs possess a similar shape to that of a classical tRNAs.
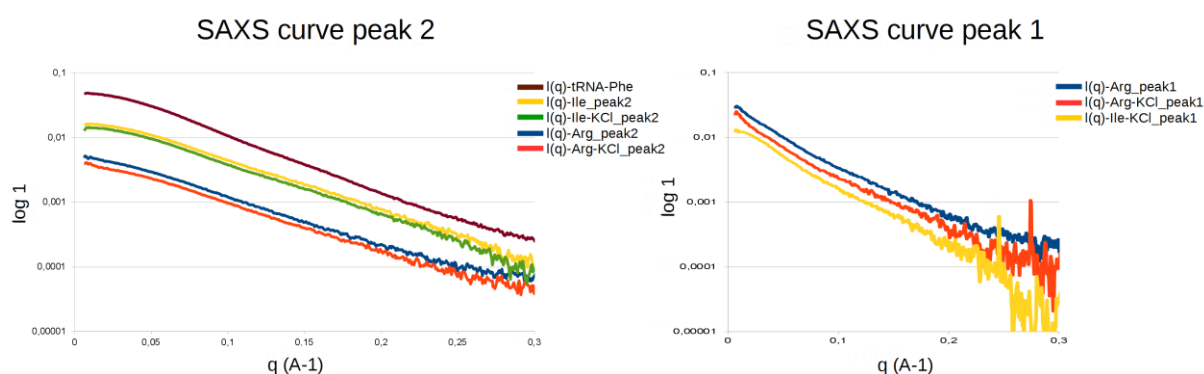

Figure 34: Characteristic SAXS curves of each tRNA population.
Comparison of the experimental SAXS curves obtained for yeast tRNA^{Phe} (violet) and for tRNA population from peak 2 (left) and peak 1 (right) of HPLC-SEC, including mt tRNA^{Ile} (yellow), and mt tRNA^{Ile} +KCl (green), mt tRNA^{Arg} (blue), and mt tRNA^{Arg} +KCl (red). Shape of SAXS curves is directly related to the shape of the molecule. While tRNA populations from peak 2 seem to reassemble a classical tRNA (cyt tRNA^{Phe}), SAXS data of tRNA populations from peak 1 result in a curve characteristic for aggregates.

The generated SAXS curves of each tRNA population were used to determine the radius of gyration Rg, the pair-distribution function P(r), and the maximal intramolecular distances D$_{max}$. The results are presented in the following sections.

12.2.3. The Guinier plot

The lowest resolution (low angle) portion of SAXS curves is dictated by a single size parameter, the radius of gyration, which is the square root of the average distance of each scatterer (atom) from the particle center. The Guinier plot of log(I(q)) against q^2 gives a straight line from which Rg and I(0) can be extracted. This leads to a direct estimation of the overall size of the tRNA molecules. Figure 35 shows the Guinier plots of yeast tRNA^{Phe} and those that were obtained for peak 1 and peak 2 of mt tRNA^{Arg} and tRNA^{Ile} in presence of 150 mM KCL.

The radius of gyration is 24.2 Å for tRNA^{Phe}, while Rg observed for both armless tRNAs in peak 2 is clearly lower with ~22 Å. Interestingly, the overall particle size of the armless tRNAs present in peak 1 seems to be higher than that of tRNA^{Phe} as indicated by the significantly increased Rg of 38.2 Å (tRNA^{Arg}) and 36.2 Å (tRNA^{Ile}). These increased values are probably due to aggregation or a dimerization of the molecules from this population. The quality of the fit is indicated by the lower green line that corresponds to the standard deviation. The flatter this line, the better the quality of the Guinier fit. An excellent fit is obtained for tRNA^{Phe}, but also for experimental data from peak 2 of both armless tRNAs. The tRNA population presented in peak 2 clearly corresponds to a monomer in solution. In contrast to that, the Guinier fit of the data for peak 1 (tRNA^{Arg} and tRNA^{Ile}) shows outliers, which results in an uneven line. The lack of linearity can be a sign for interparticle interactions, which is already indicated by the increased Rg for these molecules.
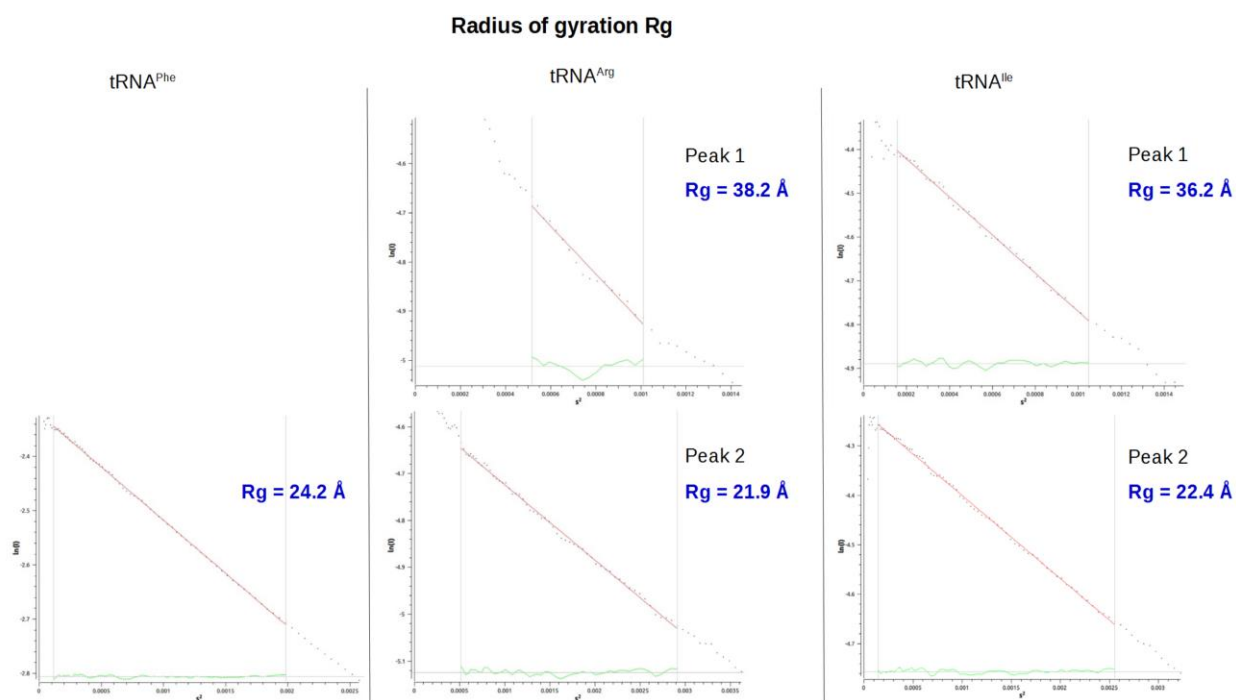
Figure 35: Guinier plots of *Sce* tRNA^{Phe}, *Rcu* tRNA^{Arg}, and *Rcu* tRNA^{Ile}.
Guinier plots, derived from SAXS curves indicating the radius of gyration Rg for yeast tRNA^{Phe}, *Rcu* tRNA^{Arg} from two populations (peak 1 and peak 2) and *Rcu* tRNA^{Ile} from two populations (peak 1 and peak 2). The quality of the fit is indicated by the lower green line that corresponds to the standard deviation.

12.2.4. The pair-distance distribution function

The pair-distance distribution function P(r) is directly calculated through a Fourier transformation of the scatting curve I(q) into real space. It provides direct information

about the distribution of distances within atoms that compose the molecule weighted by their respective electron densities. The Fourier transformation indicates therefore the average distance between electrons inside the tRNA molecule, and the maximum intramolecular distance (D_{max}). This information can be used to obtain an estimation of the shape of the molecule by *ab initio* modelling.

The average distance in the P(r) corresponds to the Rg and is indicated by the peak in the diagrams shown in Figure 36. The estimated Rg for tRNA^{Arg} and tRNA^{Ile} from peak 2 are 21.8 Å and 22.9 Å, respectively, and thus very close to the value for tRNA^{Phe} with Rg = 24 Å. The tRNA populations of peak 1, however, have an increased Rg with 32 Å for tRNA^{Arg} and 33.9 Å for tRNA^{Ile}, as already observed in the Guinier plot.

The D_{max} for classical tRNAs represents in general the distance between the A of the CCA-tail and the base 35 in the anticodon. The calculated D_{max} for tRNA^{Phe} is with 85 Å significantly higher than for tRNA^{Arg} and tRNA^{Ile} (both from peak 2) with D_{max} = 68 Å and 76 Å, respectively. However, it should be considered that the analyzed armless tRNAs do not carry the CCA-tail. It is questionable whether this sequence can compensate the missing length of about 10-20 Å to reach the D_{max} of tRNA^{Phe}. Interestingly, the spatial distribution of one nucleotide is estimated 3-4 Å. We assume that armless tRNAs carrying the CCA-tail are close to the D_{max} of tRNA^{Phe} and are probably able to compensate the missing distance. The D_{max} of the other tRNA population from peak 1 is significantly increased with 100 Å, indicating aggregated tRNA molecules.
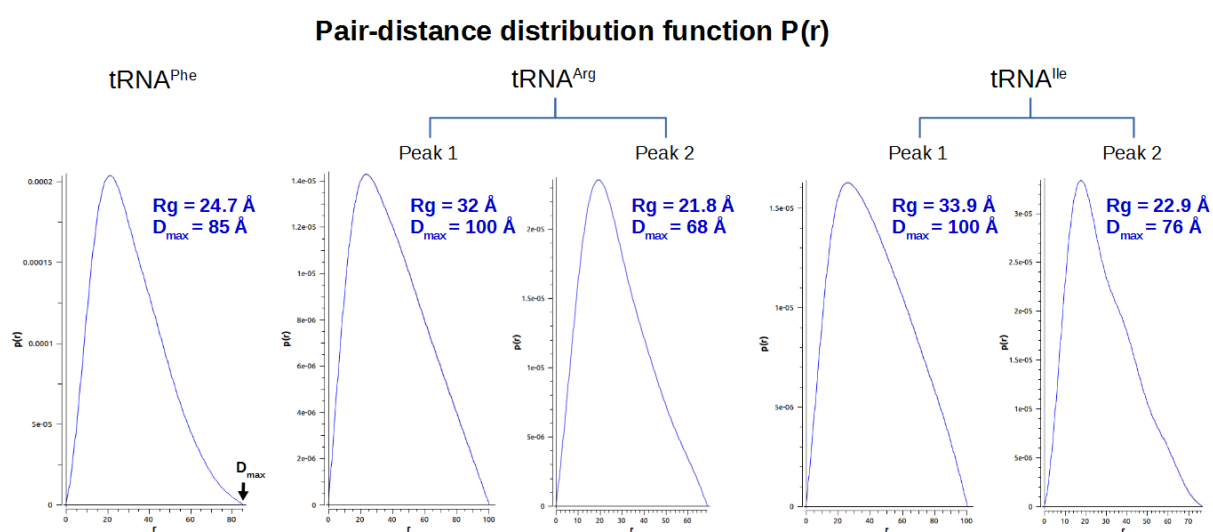

Figure 36: Pair-distance distribution functions of Sce tRNA^{Phe}, *Rcu* tRNA^{Arg}, and *Rcu* tRNA^{Ile}.
Pair-distance distribution functions, derived from SAXS curves indicating Rg and D_{max} for yeast tRNA^{Phe}, *Rcu* tRNA^{Arg} from two populations (peak 1 and peak 2) and *Rcu* tRNA^{Ile} from two populations (peak 1 and peak 2).

The obtained SAXS parameters are summarized in Table 13. This table contains, beside the presented parameters above, also those that were determined for the tRNA samples that did not contain 150 mM KCl in the buffer solution.

Table 13: Summary of parameters obtained from SAXS measurements.

Sizes, derived from Guinier and Fourier transformation for tRNA[Phe], and different tRNA[Arg] and tRNA[Ile] populations (peak 1 and 2) in absence or presence of 150 mM KCl are given in Ångström. Guinier transformation indicates overall size of tRNA molecules. Fourier transformation indicates the average distance between electrons inside tRNA molecules, and the maximum intramolecular distance (D_{max}). tRNA[Arg] and tRNA[Ile] molecules do not carry a CCA-tail. Bold numbers indicate results that are detailed analyzed in this study.

	tRNA[Phe]	tRNA[Arg] peak 1	tRNA[Arg] peak 1 + 150 mM KCl	tRNA[Arg] peak 2	tRNA[Arg] peak 2 + 150 mM KCl	tRNA[Ile] peak 1 + 150 mM KCl	tRNA[Ile] peak 2	tRNA[Ile] peak 2 + 150 mM KCl
Guinier trans-formation	**24.2 Å**	39.6 Å	**38.2 Å**	24.2 Å	**21.9 Å**	**36.2 Å**	22.1 Å	**22.4 Å**
Fourier trans-formation P(r) in Rg	**24.7 Å**	34.6 Å	**32 Å**	22.5 Å	**21.8 Å**	**33.9 Å**	22.6 Å	**22.9 Å**
Dmax	**85 Å**	110 Å	**100 Å**	69 Å	**68 Å**	**100 Å**	76 Å	**76 Å**

12.2.5. 3D modeling

SAXS is also used to determine the structure of a particle in terms of average particle size and shape. Based on measured and calculated SAXS parameters, we were able to determine *ab initio* molecular envelops for all three analyzed tRNAs. Resulting 3D models consist of pseudo atoms, or beads that reproduce the experimental scattering curve.

Several series of models can be created that fit the experimental data. Figure 37 shows nine representative 3D models obtained for tRNA[Arg] and tRNA[Ile] and 5 SAXS models obtained for tRNA[Phe], as well as its crystal structure at 1.9 Å resolution (pdb 1EHZ). SAXS models of tRNA[Phe] are very similar to each other but seem to adopt a different, slightly more open conformation, compared to the classical L shape represented by the crystal structure. This is probably due to resolution limitations of the SAXS method, and due to the fact that the analysis is performed in solution to allow more flexibility in the tRNA backbone.

The 3D SAXS models that were obtained for the armless tRNAs seem to be smaller in size compared to the SAXS models of the tRNA[Phe], which corresponds to the determined data

for Rg and D$_{max}$ (which are smaller for the armless tRNAs). Nevertheless, the overall shape is similar to that of the cytosolic tRNAs and resembles a curved tube that was termed the "boomerang" shape, in memory of the initial crystal structure description of the yeast tRNA^{Asp} (Moras *et al.*, 1980), and because it suggests a higher flexibility in the angle of armless tRNAs that would probably allow to compensate for the reduced tRNA sequence content.
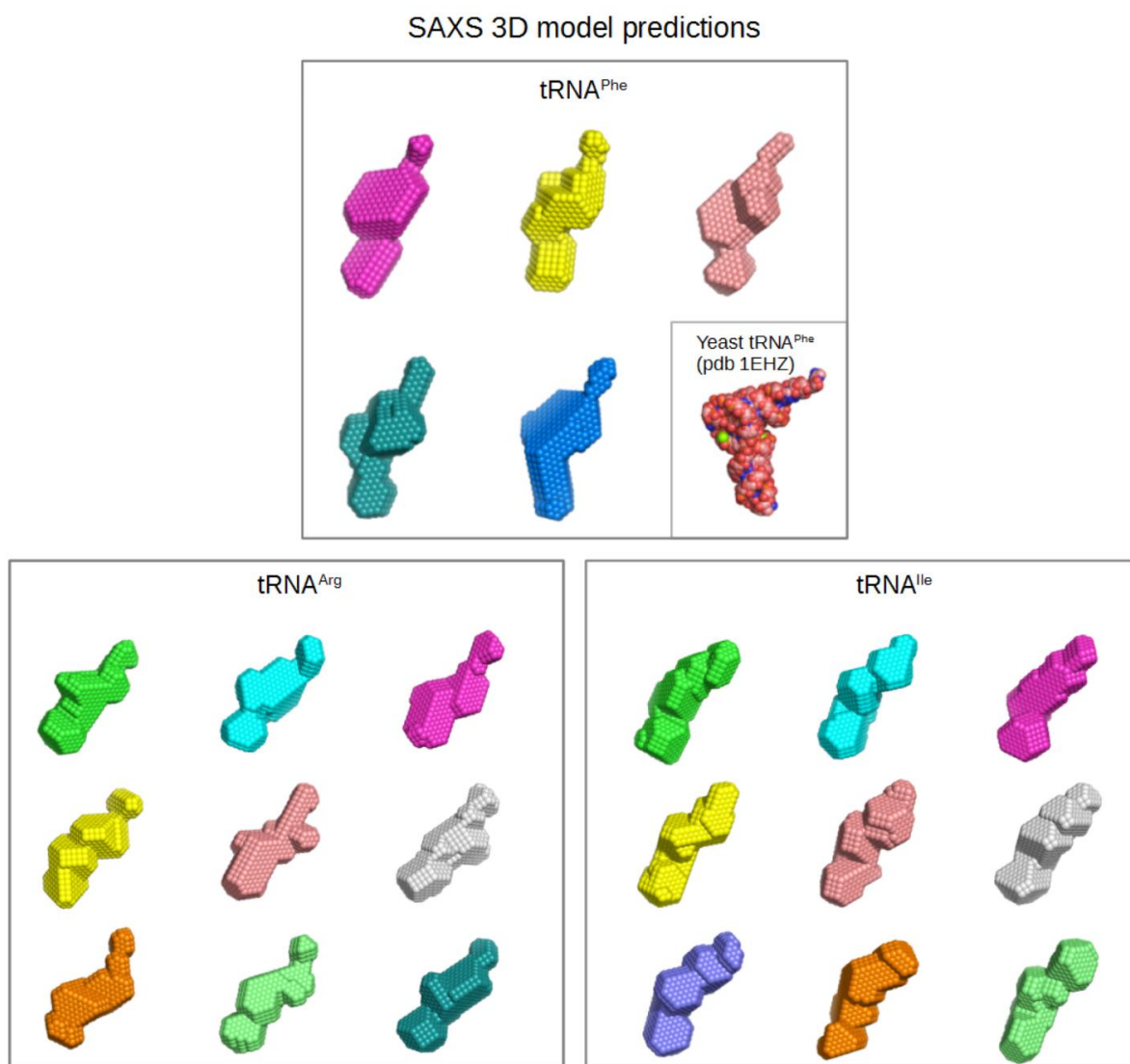
Figure 37: Low-resolution 3D electron density map for Sce tRNA^{Phe}, *Rcu* tRNA^{Arg}, and *Rcu* tRNA^{Ile}.
SAXS data analysis allows *ab initio* determination of molecular envelops for Sce tRNA^{Phe}, *Rcu* tRNA^{Arg}, and *Rcu* tRNA^{Ile}. 5 and 9 different models are shown for tRNA^{Phe} and tRNA$^{Arg/Ile}$, respectively. Furthermore, the crystal structure of Sce tRNA^{Phe} is included (pdb 1EHZ). SAXS 3D models consist of pseudo atoms, or beads that represent the experimental scattering curve. SAXS models of armless tRNAs seem to be smaller in size compared to the SAXS models of the tRNA^{Phe}, while the overall shapes are similar to each other and resembles a "boomerang" shape.

13. Discussion

Transfer RNAs play a major and essential role in protein biosynthesis. The accuracy of their functionality is mostly directly correlated with a correct folding into precisely defined secondary and tertiary structures that are recognized by several proteins. Thus, the detailed determination of structural features is of high importance for the understanding of tRNA functions. In a more general sense, RNA folding is important for any RNA function. Moreover, and per se, RNA folding and 3D organization of RNA undergoes a very large variety of possibilities, which makes a major difference with DNA structures. It is thus of interest to explore if very small tRNAs possess unprecedented folding features or if they are based on already known motifs and features.

The discovery of armless tRNA, missing both, D-and T-arm, leads to the question in which 2D and 3D structure they fold, and whether, despite from their reduced size, they represent functional molecules that can still be recognized by important interacting proteins. One aim of this thesis was to elucidate the structural properties of armless mitochondrial tRNA[Arg] and tRNA[Ile] from the nematode worm *R. culicivorax*.

13.1. Structural characteristics of *in vitro* transcribed mt tRNA[Arg] and mt tRNA[Ile]

Structural properties of *in vitro* transcribed mt tRNA[Arg] and mt tRNA[Ile] from *R. culicivorax* were analyzed using appropriate methods, such as enzymatic and chemical (in-line) probing to identify secondary structures, and biophysical methods like NMR spectroscopy and SAXS to identify tertiary interactions, and to analyze the 3D shape of these molecules. The results of enzymatic structure probing revealed that the cleavage pattern of RNase V1 digestion is mainly specific for regions predicted as double-stranded. The nuclease S1 is mainly active in the single-stranded regions of the predicted secondary tRNA structures. Although, a few regions remained undigested or were ambiguously cleaved by this nuclease, making a complete structural determination of both armless tRNA substrates a difficult task. Nuclease S1 is known for its partially unspecific cleavage pattern (M. Mörl, personal communication) Nevertheless, we conclude that the cleavage profile of enzymatic probing corresponds at least partially to the 2D structure of armless tRNAs that was predicted by *in silico* analyses (Wende *et al.*, 2014).

The in-line structure probing approach was used to complete the 2D structure profile of armless tRNAs for regions that could only ambiguously be resolved by enzymatic probing.

This technique uses the natural tendency for RNAs to degrade slowly through a nucleophilic "in-line" attack of the 2'OH to the phosphorus center (Regulski and Breaker, 2008). The speed of this reaction is strongly dependent on the structural environment of each RNA linkage: single-stranded RNA degrades faster because of missing of stabilizing base pair interactions. Interestingly, in-line probing revealed a very detailed and clear result for secondary structure profiles of both studied mt tRNAs. Exactly three regions could be determined to be accessible for degradation. These regions correspond perfectly with single stranded sequence stretches in bulge regions and anticodon loops of the secondary structure prediction for both mt tRNAs (Wende *et al.*, 2014). In-line probing is thus preferable to nuclease S1 for the analysis of single-stranded domains.

Surprisingly, no internal tertiary interactions in the bulge regions were detected by this approach. In general, the 3D structure of classical tRNAs is stabilized by long-range base pair interactions, and base stacking, especially between D- and T-loop regions (Giegé, 2008). Although both, D-and T-arm, are missing in armless tRNAs, we initially supposed that specific tertiary interactions would be needed to allow a formation of stable 3D structures. However, based on our results, this seems not to be the case, which could be confirmed by NMR spectroscopy (see below).

Another striking observation was that the structures appeared to be stable and robust under different conditions since no alternative conformations and no unspecific damage/degradation could be detected, despite their primary composition in favor of ApU sequences due to high A and U nucleotide content (76 % and 87 % for tRNA[Arg] and tRNA[Ile], respectively). Usually, ApU and CpU sequences are preferred cleavage positions in RNA molecules (Sissler *et al.*, 2008). This high stability of armless tRNAs is a very particular characteristic compared to other *in vitro* transcribed mt tRNAs (Sampson and Uhlenbeck, 1988; Derrick and Horowitz, 1993; Alexandrov *et al.*, 2006; Bhaskaran *et al.*, 2012), and is further discussed in section 13.2 of this chapter.

Regarding enzymatic and in-line structure probing analysis, we conclude that both, mt tRNA[Arg] and mt tRNA[Ile] from *R. culicivorax* form a hairpin-shaped secondary structure. This includes an internal double bulge replacing both, the D- and T-arm, in the secondary cloverleaf structure as compared to classical tRNAs. We found no hints for any internal long-range nucleotide interaction.

NMR spectroscopy is a powerful technique to detect tertiary intramolecular interactions and has been widely applied for structure determination of proteins, DNA, and RNA so far (Varani *et al.*, 2004). In this study NMR spectroscopy was used for the structural analysis of *Rcu* armless mt tRNA[Arg] and mt tRNA[Ile].

The results of this investigation revealed that all detected resonances corresponding to nucleotide interactions in both tRNAs were present between 14-12 ppm in the ^{1}H spectra, corresponding to classical Watson-Crick AU and GC base pair interactions.

Here, again the armless tRNAs show an overall stable conformation even under different conditions (absence and presence of Mg^{2+}). Mg^{2+} ions are known to stabilize the tRNA structure (Draper, 2004). However, this effect could not be observed here because no significant change in the spectra of both tRNAs (with and without Mg^{2+}) was detected.

Only the change in temperature had an impact on the conformation of the tRNAs. This was monitored by resonance that disappeared at higher temperatures (20-25°C), which was close to the calculated melting temperature (Tm=27°C) of both tRNA molecules. Decreasing resonances correspond to the loss of nucleotide interactions and indicate a melting effect of the corresponding molecules.

In conclusion, the NMR measurements confirm that the analyzed armless mt tRNAs are exclusively composed of classical Watson-Crick base pairs forming helices that contribute to the secondary structure. No signal for long-range base interactions was detectable, suggesting the absence of internal tertiary interactions in the bulge regions. This absence is remarkable since such interactions usually stabilize 3D structures of RNAs, and in particular tRNAs (Westhof and Auffinger, 2001; Giegé *et al.*, 2012).

SAXS was used to measure physical characteristics related to shapes and tertiary dimensions of classical and armless mt tRNAs. This method allows to compare determined physical parameters as well as calculated 3D shapes representing molecular envelopes with the features of classical tRNAs. The results of the size exclusion chromatography (SEC-)SAXS experiments revealed the existence of different tRNA populations (three for tRNA[Arg], and two for tRNA[Ile]). The SAXS parameters Rg, P(r), and D_{max} determined for each population indicate that they correspond to tRNA monomers (peak 2) and to tRNA dimers or multimers (peak 0 and 1). tRNA aggregates are characterized by significantly increased values for the determined parameters.

For comparison with the classical tRNA^{Phe} only the values obtained for the monomeric tRNA populations were used. The overall size (Rg) derived from the Guinier transformation and the pair–distribution function for armless tRNA molecules is slightly lower compared to tRNA^{Phe} indicating a more compact shape of armless mt tRNAs compared to the classical tRNA.

Another interesting result represents the determination of D$_{max}$ of the tRNA molecules. The D$_{max}$ calculated by SAXS for tRNA^{Phe} was 85 Å. This is significantly increased compared to the D$_{max}$ of 75 Å that can be determined for the crystal structure of the same tRNA. This raises the question, how this difference can be explained? The distance between the ends of the two arms is usually 75 Å, and corresponds to the distance between phosphates 76 and 34 in the crystal structure of yeast tRNA^{Phe}, which adopts an L-shape with an angle of 90° (pdb 1EHZ) (Shi and Moore, 2000). Indeed, it has been demonstrated that the tRNA^{Phe} core can exhibit higher intrinsic flexibility in solution (Friederich *et al.*, 1998). We suggest that D$_{max}$ effectively reflects the opening of the angle of this tRNA molecule, which is probably more important in solution than in a crystal, which selects a priori a more stable form. We suggest a similar intrinsic flexibility for armless tRNAs, which concerns mainly the hinge of these molecules. The presence of many A/U nucleotides, and the simultaneous absence of nucleotide interactions within the bulge regions support this hypothesis.

The maximal distances determined for armless tRNAs seem extremely small with 68 Å and 76 Å compared to tRNA^{Phe} (D$_{max}$=85 Å). However, it should be considered that in contrast to tRNA^{Phe}, armless tRNA transcripts do not carry a CCA-tail. Since the size of an individual nucleotide is approximately 3-4 Å, the maximal distance of armless tRNAs could be extended theoretically by approximately 10 Å. This hypothesis has to be confirmed by SAXS analysis of armless tRNAs carrying the CCA-tail. If we consider an increased intrinsic flexibility for armless tRNAs with a CCA-tail, the maximum size of these molecules in solution would be comparable to that of classical tRNAs. These molecules are probably no longer restricted to the typical L-shape, but possess a more relaxed form that is more likely to correspond to a boomerang-shaped structure. We suppose that this characteristic intrinsic flexibility of armless tRNAs allows interactions with important partner proteins, and preserves therefore tRNA biosynthesis and protein translation processes in nematode mitochondria.

Scattering data provide only low-resolution structural information, and cannot be used to define a detailed 3D structure. A computational generated 3D structure prediction was published for the mt tRNA^{Arg} and mt tRNA^{Ile} (Wende *et al.*, 2014). Thus, it would be interesting to compare experimental SAXS data with computed SAXS profiles data that are based on these 3D structure predictions. Preliminary data suggest that computed SAXS data fit well with the experimentally obtained SAXS profiles. This indicates that structural predictions are very close to the actual structure of armless mt tRNAs (C. Sauter, personal communication).

A next step, to determine structures of armless mt tRNAs in higher resolution implies the application of X-ray crystallography. While different crystal structures already exist for various different cytosolic tRNAs (Giegé *et al.*, 2012) no crystal structure is available for a complete mitochondrial tRNA, except for the human mt tRNA^{Val} and the porcine mt tRNA^{Phe}, which were co-crystallized in the mitoribosome complex. For both tRNAs the structure is incomplete since the elbow region could not be resolved (Brown *et al.*, 2014; Greber *et al.*, 2015). So far, the experimental verification of secondary and tertiary structures of mt tRNAs is mainly based on native gel electrophoresis, enzymatic digestion, chemical probing, and NMR spectroscopy (Bruijn and Klug, 1983; Bonnefond *et al.*, 2008; Messmer *et al.*, 2009; Ohtsuki *et al.*, 2002a).

The attempt to crystallize armless tRNAs is certainly a difficult but exciting challenge. However, the unexpected high stability of these tRNAs is an excellent prerequisite that they represent good substrates for this analysis in future.

13.2. Stability of armless mt tRNAs

As mentioned above, a striking observation was the fact that analyzed armless tRNAs are highly stable, and that they can be incubated over several days in an unfavored environment without their complete degradation. This is a very unusual characteristic for many *in vitro* transcribed mt tRNAs that are generally more sensitive and unstable compared to native tRNAs (Sampson and Uhlenbeck, 1988; Derrick and Horowitz, 1993; Alexandrov *et al.*, 2006; Bhaskaran *et al.*, 2012). This sensitivity is especially true for mammalian mt tRNAs because they are all A, U and C rich, while mt tRNAs from plants for example, have a more random nucleotide content (Pütz *et al.*, 2010).

Posttranscriptional modifications of tRNAs can increase the stability of correct tRNA structures, and are simultaneously necessary for various biochemical processes, such as

114

an accurate translation and a correct processing of tRNAs (Kirino and Suzuki, 2005; Helm, 2006). Many mt tRNAs exhibit several different modifications, which seem to be of great importance (Suzuki and Suzuki, 2014). For the nematode *A. suum*, e.g., it has been shown that the modification m^1A_9 is indispensable for the structure and function of most mt tRNAs (Sakurai *et al.*, 2005). Furthermore, for mt tRNA^{Arg}, additional modifications have been detected, e.g., m^1A_8, $\Psi_{22, 26, 29, 35}$, $\Psi(U)_{35, 51}$, and m^1G_{34} (Suzuki and Suzuki, 2014). Several modifications have also been determined for mt tRNA^{Ile}. For example, the bovine mt tRNA^{Ile} includes, among others, modifications at positions m^1G_9, $m^2_2G_{26}$, Ψ_{27}, t^6A_{37}, and m^1A_{58} (Watanabe *et al.*, 1997)(Figure 38).
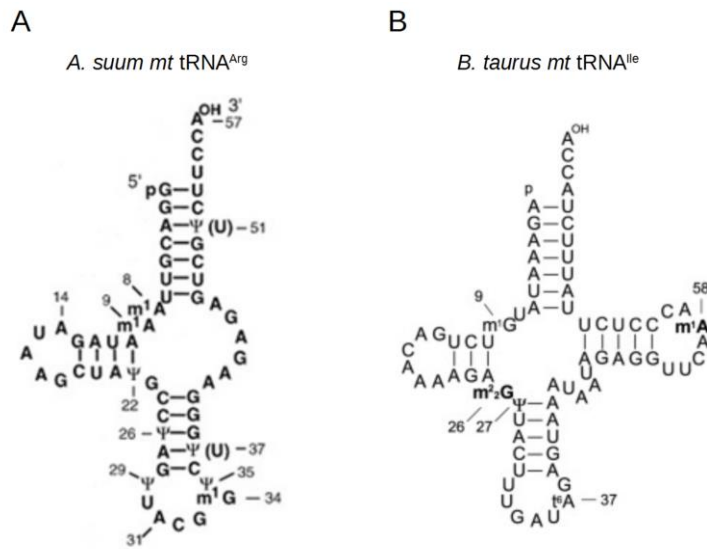

Figure 38: Modified nucleotides in 2D structure of *A. suum* mt tRNA^{Arg} and *B. taurus* mt tRNA^{Ile}.
(A) Post-transcriptional modifications of *A. suum* mt tRNA^{Arg}. The positions of modified nucleotides m^1A, m^1G, m^2_2G, and Ψ are indicated. Letters in parentheses indicate residues partially modified. (B) Post-transcriptional modifications of bovine mt tRNAIle. Newly identified modified bases are represented in bold type. The positions of modified nucleotides m^1A, m^1G, m^2_2G, t^6A, and Ψ are indicated (modified from Watanabe *et al.*, 1997; Suzuki and Suzuki, 2014).

It would be interesting to verify whether armless mt tRNAs are also modified *in vivo* in *R. culicivorax* and if so, whether these modifications have an influence on the structure and stability of the tRNA transcript and their structures.

13.3.   Evolution of armless mt tRNAs

The motivation to study characteristic structural and functional features of armless mt tRNAs from *R. culicivorax* was based on the previous findings regarding the degeneracy of mt tRNA genes (Jühling *et al.*, 2012a). In general, most animal mt tRNAs, possess some special features compared to cytosolic tRNAs. They have shortened loop sequences and stem sequences, and structural domains are less conserved. A very prominent example is

the mt tRNA[Ser] that is lacking the complete D-arm in most animal mitochondria. During the recent years, other mt tRNAs with extremely truncated sequences have been identified also in other animal lineages. Even complete set of all mt tRNAs to be truncated tRNAs were identified, especially in molluscs, arthropods, and nematodes, which exhibit mt tRNAs with the most extreme reduction of tRNA gene sizes (Yamazaki *et al.*, 1997; Masta, 2000; Wolstenholme *et al.*, 1987; Jühling *et al.*, 2012b).

The high diversity of mt tRNA genes led to the conclusion that armless mt tRNAs seem not to be an exception only, but are actually the general rule for many organism (Jühling *et al.*, 2012b). The observation that truncated mt tRNA genes are very conserved in many organisms throughout different animal lineages led to the consideration to accept "bizarre" tRNAs as "normal" situation.

The discovery of these reduced tRNA sequences (which is in many studies still based on computational predictions only) raises the question, where (i.e., in which animal linages), how, and why armless mt tRNAs did arise during evolution. It is still a challenging task to give a complete and satisfying answer to these questions. Theories about mt tRNA evolution are very complex. However, it was shown that the evolution of mt tRNAs is also highly dependent on evolutionary aspects of the organisms. This may explain the high diversity of sequences and structures, e.g., when comparing plant and animal mt tRNAs (Salinas-Giegé *et al.*, 2015).

However, the answer whether reduced mt tRNA sequences appear only in phylogenetic niches (such as extremely truncated mt tRNAs that have been identified only in nematodes and arthropods, so far) or also in other species will surely soon be better understood thanks to the incredible improvement of sequencing and bioinformatics tools. This will led to an increased availability of mitochondrial genome sequences, and thus to an improved identification of maybe even unknown tRNA structures. Since extremely reduced mt tRNAs have only been discovered in the last few years, it is very likely that more and more truncated tRNAs will be found in the near future, maybe even in organisms that have already been studied, but in which no complete set of mt tRNA genes could be identified yet.

The tRNA degeneracy is highly interesting in the context of adaptation and co-evolution partner proteins. During tRNA biosynthesis, tRNAs have to be recognized by a variety of proteins, such as maturation enzymes, modification enzymes, aminoacyl-tRNA

synthetases, elongation factors, and ribosomes. The flexibility of the interplay between tRNAs and their interacting partner proteins is probably one factor for the occurrence of armless tRNAs. If partner proteins had not evolved the ability to compensate for the RNA, the prerequisite that would have favored the evolution of armless tRNAs would not exist. However, this process is certainly the result of co-evolutional events between both, mt tRNAs and partner proteins. Hereby, tRNA structures are probably mostly governed by enzymes that have to recognize all tRNAs at once (e.g., CCA-adding enzymes, elongation factors, and ribosomes), and not by enzymes that interact only with one or a subset of tRNAs (e.g., aminoacyl-tRNA synthetase) (Watanabe *et al.*, 2014). It could already be shown that two nuclear encoded EF-Tu homologs exist in nematode mitochondria. They are specialized to D-arm or T-arm lacking mt tRNAs thanks to a C-terminal extensions (Ohtsuki and Watanabe, 2007; Watanabe *et al.*, 2014). Another example are enlarged proteins that compensate for reduced 12S and 16S rRNA sequences in mammalian mitoribosomes (Mears *et al.*, 2002; Sharma *et al.*, 2003). The different mode of compensation of interacting proteins may represent one explanation why truncated mt tRNAs have evolved, but further investigations are still needed to better understand the exact binding and recognition between armless mt tRNAs and their co-evolved partner proteins (Fujishima and Kanai, 2014).

CHAPTER 3: Structural and functional characterization of the mt CCA-adding enzyme from *R. culicivorax*

This chapter will address the characterization of the mt CCA-adding enzyme from *R. culicivorax* (*Rcu*). The newly identified open reading frame (ORF) coding for the *Rcu* CCA-adding enzyme has been cloned and analyzed for this study. Several expression and purification studies were performed to establish an optimal protocol. The subsequent functional characterization was examined via activity assays, also known as CCA-addition assays. To ensure a comparative study, human and *E. coli* CCA-adding enzymes were included, and their activity on armless tRNAs was analyzed

Preliminary work for this study

As previously mentioned, a draft genome annotation for *R. culicivorax* was published only shortly before the beginning of this study (Schiffer *et al.*, 2013). However, until now a complete and verified genome assembly is still missing, making the identification of protein coding genes a challenging task. Yet, based on the available data, a putative gene sequence encoding for a CCA-adding enzyme was identified and was composed of eight exons. A reverse transcription PCR reaction on isolated mRNA was performed by O. Götze at the Institute of Biochemistry, University of Leipzig, in order to verify the protein coding sequence. O. Götze was able to isolate and sequence two variants, a long variant with a length of 1434 nt and a splice variant, missing one exon of 159 nt. Figure 39 shows a sequence alignment of both *Rcu* protein variants in comparison with the human CAA-adding enzyme. This sequence analysis revealed that the splice variant lacked important sequence motifs (flexible loop and motive B), which are characteristic for CCA-adding enzymes (see below). Furthermore, expression of the short protein variant in bacterial cells was not possible. Thus, this study was continued with the long protein variant. A putative mitochondrial targeting sequence (MTS) was predicted with a high probability (0.94) using the MitoProt online tool. The cleavage site of the MTS for the mitochondrial *Rcu* CCA-protein was chosen accordingly to the cleavage site of the human mitochondrial CCA-adding enzyme. This resulted in a protein sequence with an alternative translation start very similar to the well characterized human protein.

Figure 39: Multiple sequence alignment of identified *Rcu* and *Hsa* CCA-adding enzymes.
Clustal Omega was used to build the multiple sequence alignment. Grey, predicted mitochondrial targeting sequence; red, alternative translation start for mt CCA-adding enzymes, yellow, deletion of 53 amino acids in the splice variant. Sequence motifs are marked in blue frames. Conserved nucleotides are indicated by "*", strongly similar amino acids are indicated by ":", weakly similar amino acids are indicated by ".".

13. Sequence alignment and comparison of CCA-adding enzymes

First, sequence comparisons of the amino acid composition of biochemically characterized CCA-adding enzymes from *Escherichia coli (Eco), Saccharomyces cerevisiae (Sce), Caenorhabditi elegans (Cel), Homo sapiens (Hsa)* and the newly identified *Romanomermis culicivorax* (*Rcu*) CCA-adding enzyme were performed. For this purpose, protein sequences were aligned to each other using the online tool Clustal Omega, and analyzed for similarities and differences. The *Rcu* CCA-adding enzyme shows the highest sequence similarity to the human CCA-adding enzyme with an overall sequence identity of 46 %. Sequences of bacterial and yeast enzymes are more different to the worm enzyme with both only around 20 % identity. A high level of sequence identity were identified especially in the N-terminal domain of all analyzed enzymes. In class II CCA-adding enzymes, this domain usually corresponds to the catalytic center carrying five highly conserved motifs A-E. This alignment was used to verify whether the *Rcu* enzyme

sequence is similar to these of other CCA enzymes or whether additional domains are required to compensate for armless tRNAs, as is the case for e.g., the EF-Tu in *C. elegans.* The identified long protein variant of the *Rcu* CCA-adding enzyme possesses all the characteristic motifs A-E in the catalytic center with conserved amino acids and a non-conserved flexible loop region (Figure 40). However, no additional sequence domains or other particularities could be identified at the sequence level.
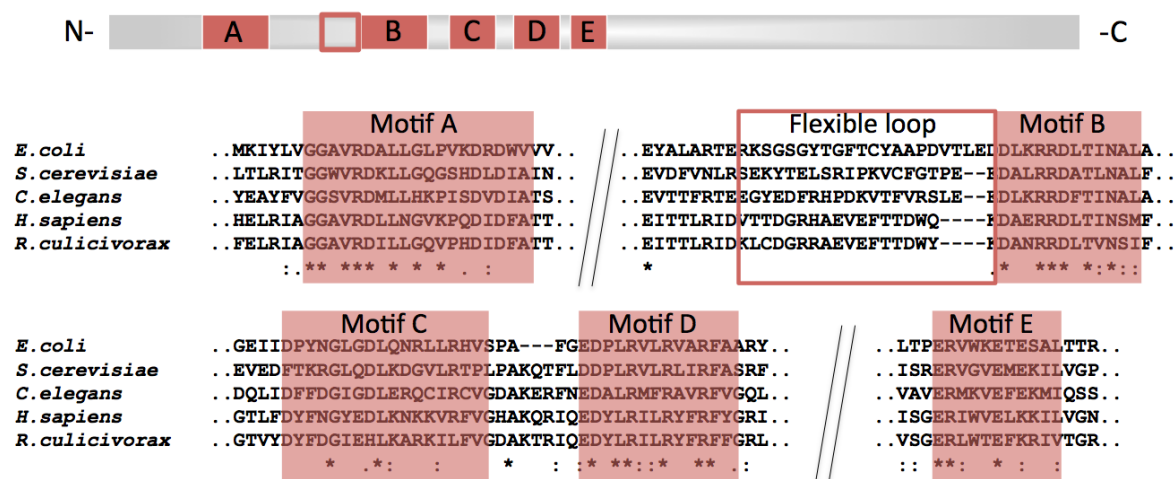
Figure 40: **Alignment of the catalytic center of CAA-adding enzymes.**
Biochemically characterized CCA-adding enzymes are compared based on their amino acid sequence of motif A-E (highlighted in red) in the catalytic center. The flexible loop region is indicated by a red box. Conserved nucleotides are indicated by "*", strongly similar amino acids are indicated by ":", weakly similar amino acids are indicated by ".".

The I-TASSER protein structure prediction algorithm (Zhang, 2008) was used to build a 3D structure prediction model of the *Rcu* CCA-adding enzyme (Figure 41). The program is a template-based modeling using PDB structure entries. The I-TASSER model prediction proposed five different models for the *Rcu* CCA-adding enzyme, consisting mainly of α-helices. A superposition of these models revealed high structural similarities in the N-terminus but different conformations of the C-terminus. This result is in agreement with the results obtained from the sequence alignments (above), which showed that the *Rcu* protein has a conserved N-terminus, which is similar to other CCA-adding enzymes. A superposition of the I-TASSER model 1 with the crystal structure of a bacterial CCA-adding enzyme from *Geobacillus stearothermophilus* (pdb 1MIV) shows that the similarity is not only found at the sequence level but also in the structural organization of the enzyme.
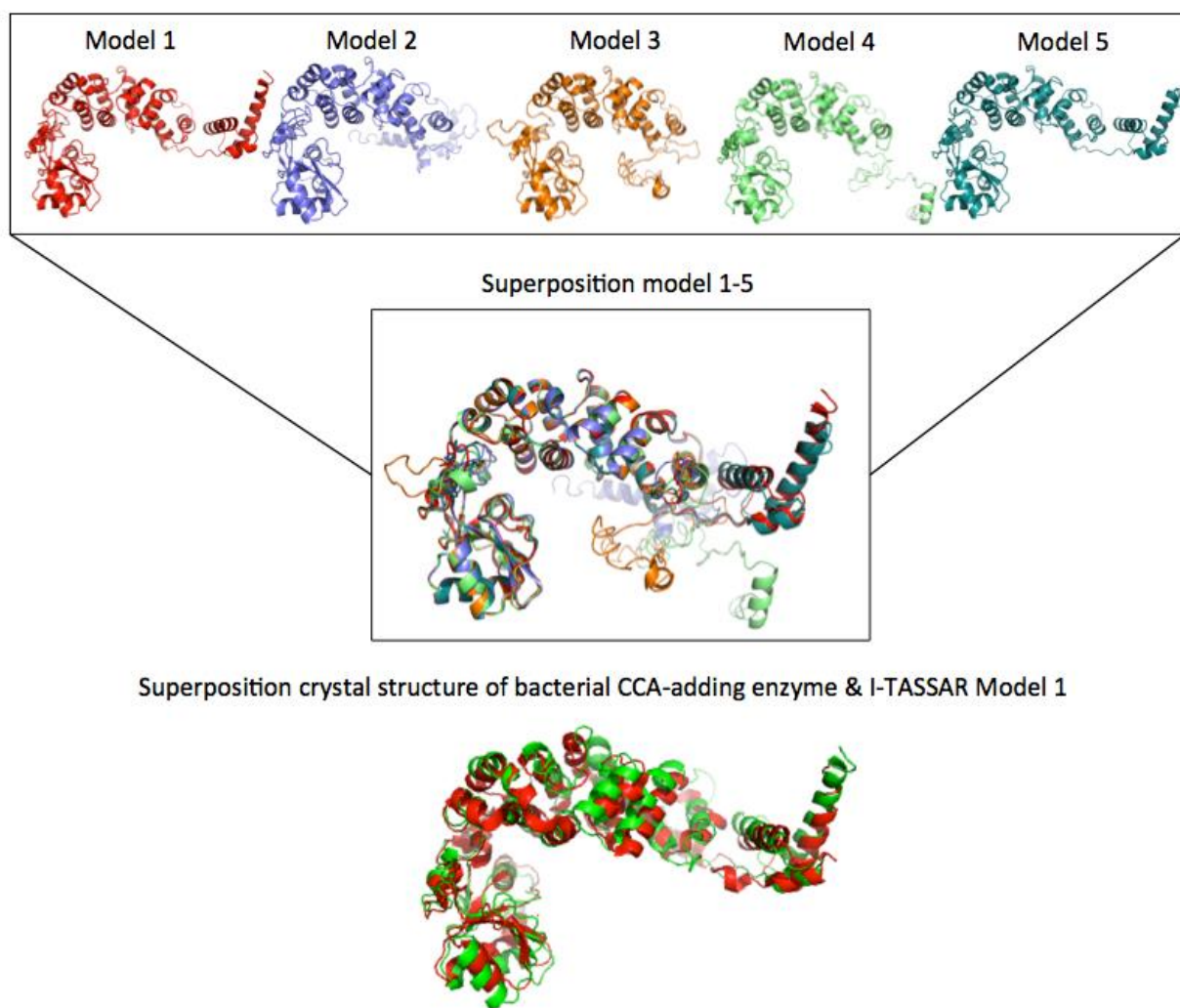
Figure 41: I-TASSER 3D models of *Rcu* CCA-adding enzyme
(Top) Five different 3D structure prediction models were obtained for the *Rcu* CCA-aading enzyme using the I-TASSER online tool. (Middle) Superposition of the five 3D models (same color code as used before). (Below) Superposition of crystal structure of CCA-adding enzyme from *G. stearothermophilus* (pdb 1MIV) (red) and 3D model 1 of *Rcu* CCA-adding enzyme (green).

14. Cloning, expression and purification of the recombinant CCA-adding enzyme

The identified gene sequence of the open reading frame (ORF) of the *Rcu* CCA-adding protein was cloned into a pTrc-His A plasmid during this study following the protocol described in section 8.9.1. The recombinant protein sequence carries an N-terminal 6xHis-tag, which is used for purification by means of affinity chromatography on nickel columns. Protein expression is under the control of a *trc* promoter in this construct. The same gene sequence was also available on a pET28a vector designated for expression under the control of a strong T7 promoter.

Intensive studies on eukaryotic and bacterial CCA-adding enzymes led to the establishment of well-functioning expression and purification protocols in the host

laboratory in Leipzig (Lizano *et al.*, 2008; Neuenfeldt *et al.*, 2008). These protocols were also used for the production of the recombinant *Rcu* protein. However, since these protocols did not provide a satisfactory yield of proteins, intensive studies were undertaken in order to optimize the quantity and purity of the isolated protein.

14.1. Expression in *S. cerevisiae*

Since the *Rcu* CCA-adding enzyme originate from an eukaryotic organism, we assumed that this protein, would probably show good expression rates in an eukaryotic system. Therefore, expression and purification studies in the yeast strains AH109 were attempted. The cloning and expression protocol was performed as described in 8.7.3. The results of the SDS-PAGE analysis (data not shown) reveal that it was not possible to determine on the SDS-gel whether the recombinant protein was overexpressed. In addition, no dominant protein band corresponding to the size of the *Rcu* CCA-adding enzyme (53 kDa) was present in the elution fractions. Thereon, the experiment was repeated with another *S. cerevisiae* strain (Y187). But here again, no protein was purified with the corresponding size. Therefore, it is questionable whether the protein was sufficiently overexpressed in both yeast strains. In summary, it can be concluded that yeast is not suitable for the expression and purification of the *Rcu* CCA-adding enzyme.

14.2. *In vitro* protein translation

In parallel to the expression studies in yeast, an *in vitro* expression system was used for the production of the protein. The two protein containing plasmids pET28a and pTrcHis A containing the *Rcu* CCA-enzyme coding sequence were each added to a reaction mix (using the Easy Express® Protein Synthesis Kit) and incubated at 37°C for 1 h. The functionality of the kit was checked by performing a positive-control reaction containing a PCR product encoding the 32 kDa elongation factor EF-Ts with a C-terminal 6xHis-tag. In a negative control, no DNA template was added. The results were analyzed by SDS-PAGE (Figure 42).

The results show a dominant band of about 32 kDa in the positive control that corresponds to the size of the EF-Ts. Thus the *in vitro* translation reaction was functional. However, no difference could be observed between the samples containing the pET28a or the pTrcHis A vector and the negative control. This indicates that *in vitro* protein translation of the *Rcu* CCA-adding enzyme was not successful.
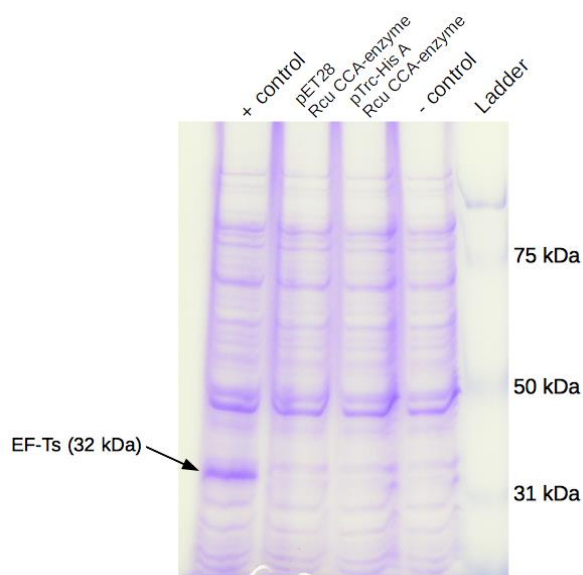
Figure 42: *In vitro* translation of the *Rcu* CCA-adding enzyme.
The Easy Express® Protein Synthesis Kit (Qiagen) was used for the production of the *Rcu* CCA-adding enzyme. The plasmids pET28a and pTrcHis A containing the ORF of the *Rcu* CAA-enzyme were subjected to the reaction mixture (supplied with the kit). A positive control contained a PCR product encoding the 32 kDa elongation factor EF-Ts protein. In a negative control, no DNA template was added. Samples were taken after 1 h of incubation at 37°C, and loaded onto a 12.5 % SDS-gel. The protein ladder was loaded on the lanes designated with "Ladder" (sizes are indicated on the right side of the gel). The expected size of the *Rcu* CCA-adding enzyme containing the N-terminal 6xHis-tag is 53 kDa, but could not be detected in the gel.

14.3. Expression in *E. coli* BL21 (DE3)

Escherichia coli BL21 (DE3) was chosen for the overexpression of the recombinant protein. The bacterial culture was grown under standard conditions (37°C, induction at OD_{600} = 0.6, and harvest after 3 h). Purification was performed in phosphate buffer at pH 6.5. on an ÄKTA purifier system as described in 8.9.1. Both, overexpression as well as purification of the recombinant CCA-adding enzyme was controlled on SDS-PAGE (Figure 43). The protein could be expressed, which was verified by a visible band at the corresponding size (53 kDa) in the SDS-PAGE. However, the majority of the protein was only present in the pellet fraction after disruption and centrifugation of the cells, suggesting that the protein is not soluble under these conditions and may be sequestered as insoluble aggregates within inclusion bodies.

A dominant band of about 60 kDa appeared in the elution fractions in the SDS-gel, probably representing a heat shock protein (Hsp). Hsp60, corresponding to GroEL in *E. coli* is a well-characterized chaperone with ~60 kDa and, which appears in the pathway of misfolding and aggregation (Fenton and Horwich, 2003).
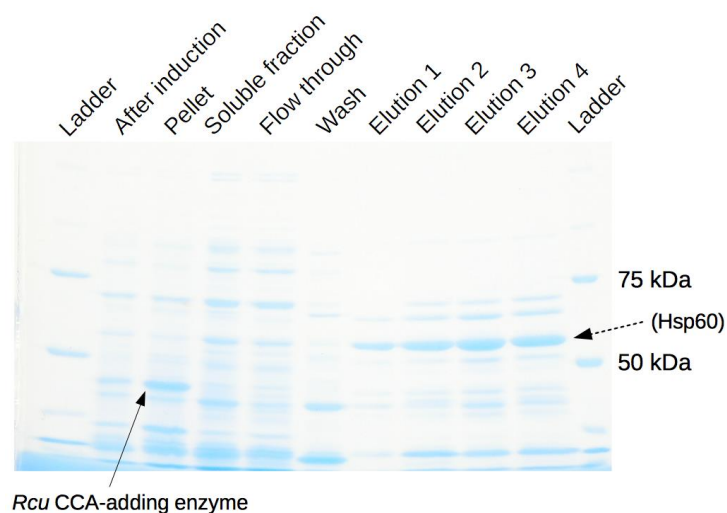
Figure 43: Expression and purification of the *Rcu* CCA-adding enzyme in Bl21 (DE3).
E. coli BL21(DE3) cells transformed with the plasmid pET28a carrying the ORF for the *Rcu* CCA-adding enzyme were used for expression and purification. Samples were taken during expression (after induction), after sonication and centrifugation (soluble fraction and pellet fraction) and during purification (flow through, wash, and elution fractions), and were loaded onto a 12.5 % SDS-gel. The expected size of the *Rcu* CCA-adding enzyme containing the N-terminal 6xHis-tag is 53 kDa and an arrow indicates its putative presence. A dotted arrow indicates the presence of a possible heat shock protein (Hsp60), whose identity was not clarified. The protein ladder was loaded on the lanes designated with "Ladder" (sizes are indicated on the right side of the gel).

In order to increase the yield of soluble recombinant protein, another expression method was performed. During the "late induction" method, the gene expression is induced in a late log phase culture, which have been shown to contribute to protein quantity and solubility (Galloway *et al.*, 2003). Otherwise the bacterial culture was treated as described before. The expression and purification was controlled by SDS-PAGE (Figure 44).

Using the late-induction method, the amount of soluble product could indeed be increased. Furthermore, more protein contaminations were eliminated compared to the standard method, although two large protein contaminations remained in the elution fractions, indicating that the *Rcu* enzyme fractions were still not pure enough for assays.
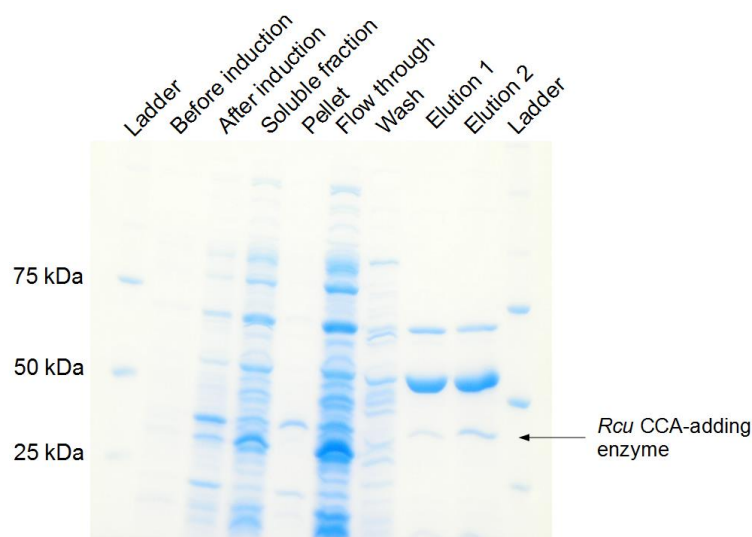
Figure 44: Expression and purification of the *Rcu* CCA-adding enzyme in Bl21 (DE3) following the late-induction protocol.
E. coli BL21 (DE3) cells transformed with the plasmid pET28a carrying the ORF of the *Rcu* CCA-adding enzyme were used for expression and purification. Samples were taken during expression (before and after induction), after sonication and centrifugation (soluble fraction and pellet fraction) and during purification (flow through, wash, and elution fractions), and were loaded onto a 12.5 % SDS-gel. The expected size of the *Rcu* CCA-adding enzyme containing the N-terminal 6xHis-tag is 53 kDa. The protein ladder was loaded on the lanes designated with "Ladder" (sizes are indicated on the left side of the gel).

14.4. Expression in *E. coli* Rosetta-gami 2

The eukaryotic codon usage of the *Rcu* protein could lead to problems in expression in *E. coli*. In order to limit this factor, a special *E. coli* strain was used that contains codons rarely used in *E. coli*. The Rosetta-gami 2 strain allows for enhanced disulfide bond formation and enhanced expression of eukaryotic proteins. This strain carries an additional plasmid, pRARE2, which supplies tRNAs with rare codons, AUA, AGG, AGA, CUA, CCC, GGA, and CGG under the control of their native promoter. Indeed, the *Rcu* CCA-adding gene sequence carries 40 of these rarely used codons.

The use of the Rosetta-gami 2 cells resulted in an improvement of the expression rate of the *Rcu* CCA-adding enzyme (Figure 45). However, the presence of protein contamination could not be reduced, which is illustrated by the strong band at 60 kDa in the SDS-gel. The size of 60 kDa corresponds to the *E. coli* chaperone GroEL.
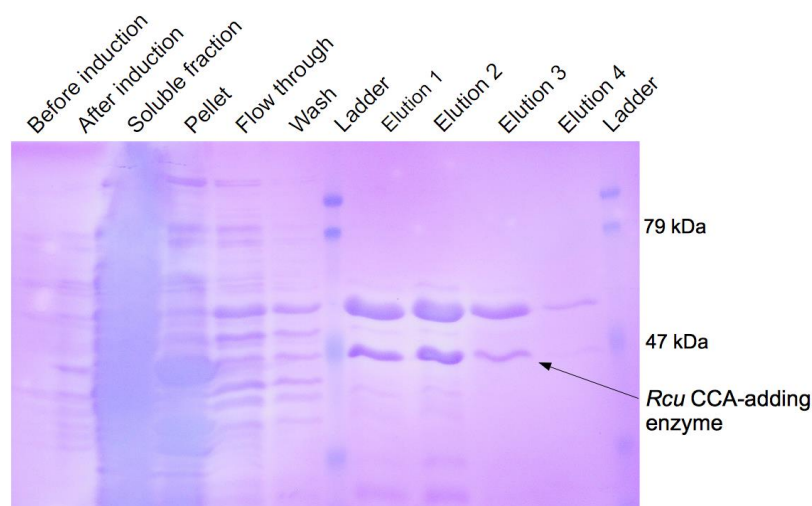
Figure 45: Expression and purification of the *Rcu* CCA-adding enzyme in Rosetta-gami 2.
E. coli Rosetta-gami 2 cells transformed with the plasmid pTrc-His A carrying the ORF of the *Rcu* CCA-adding enzyme were used for expression and purification. Samples were taken during expression (before and after induction), after sonication and centrifugation (soluble fraction and pellet fraction) and during purification (flow through, wash, and elution fractions), and were loaded onto a 12.5 % SDS-gel. The expected size of the *Rcu* CCA-adding enzyme containing the N-terminal 6xHis-tag is 53 kDa. The protein ladder was loaded on the lanes designated with "Ladder" (sizes are indicated on the right side of the gel).

In addition to the different bacterial strains and the different expression methods described in the previous paragraphs, several other purification methods were tested, using different buffer systems (containing phosphate, Tris-base, or Hepes), different supplements (salts, detergents) and different purification strategies (e.g. Ion-exchange-chromatography, ammonium–sulfate precipitation). However, none of these changes could significantly improve the purity of the protein elution.

14.5. Expression in *E. coli* Arctic Express (DE3)

Cultivation at lower temperatures, potentially increase the yield of active, and soluble recombinant protein (Schein, 1989). Arctic Express was used, a cold-adapted *E. coli* strain that derived from BL21-Gold competent cells. This strain, allows for high-level expression of heterologous proteins that tend to be insoluble. It co-expresses the chaperones Cpn10 and Cpn60 from the psychrophilic bacterium, *Oleispira antarctica*. These proteins have high amino acid identity with the *E. coli* GroEL and GroES chaperones but possess high protein refolding activities at temperatures of 4–12°C (Hartinger *et al.*, 2010).

The Arctic Express (DE3) strains are designed for expression of recombinant proteins from an inducible T7 promoter. A pET28a vector containing a N-terminal His-tagged gene sequence was used for transformation. Various purification methods (using different combinations of buffer systems) have been performed to reach the highest purity.

The final protein purification protocol involved three steps: first, incubation of the cell lysate in binding buffer, including denatured *E. coli* proteins; second, purification using an affinity tag on a nickel matrix in a batch system, including a wash step with dissociation buffer (containing 5 mM ATP), and finally separation by Size-exclusion chromatography.

Samples were taken during expression and purification and loaded on a 12.5 % PAA-gel. A single band is visible at the corresponding size (53 kDa). Using western blot analysis the presence of the CCA-adding enzyme was successfully verified (result not shown). The protein containing fractions were concentrated to a final concentration of 75 µg/µl. The purified protein was subsequently used for CCA-incorporation assays.
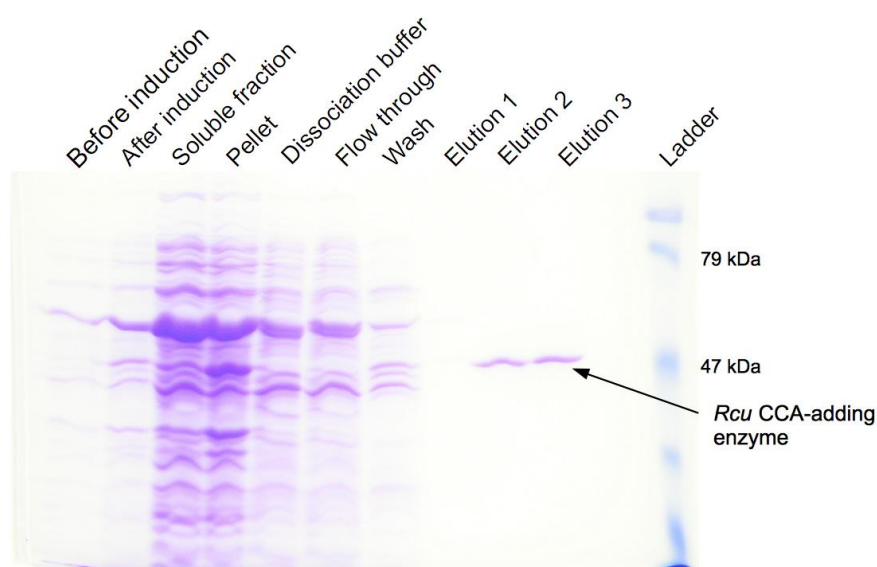
Figure 46: Expression and purification of the *Rcu* CCA-adding enzyme in Arctic Express.
E. coli Arctic Express cells transformed with the plasmid pET28a carrying the ORF of the *Rcu* CCA-adding enzyme were used for expression and purification. Samples were taken during expression (before and after induction), after sonication and centrifugation (soluble fraction and pellet fraction) and during purification (flow through, wash, and elution fractions), and were loaded onto a 12.5 % SDS-gel. The expected size of the *Rcu* CCA-adding enzyme containing the N-terminal 6xHis-tag is 53 kDa. The protein ladder was loaded on the lanes designated with "Ladder" (sizes are indicated on the right side of the gel).

15.   Activity test of the recombinant CCA-adding enzyme from *R. culicivorax*

A nucleotide-incorporation assay was performed in order to test the activity of the purified *Rcu* CCA-adding enzyme. For this purpose, the two elution fractions of the *Rcu* CCA-adding enzyme obtained from the previous purification procedures were first tested on a well-established standard substrate for CCA-addition, the classical tRNA[Phe] from yeast (Nagaike *et al.*, 2001; Lizano *et al.*, 2008). Additionally, *E. coli* and human CCA-adding enzyme were used as positive controls. The results are shown in (Figure 47).

Nucleotide incorporation results in a different migration behavior of the tRNA in the gel, which is indicated by a shift between the control incubation of tRNA^{Phe} without enzyme (mock) and the tRNA samples that were incubated with protein, and where nucleotides were incorporated. Such a shift was detected for tRNA^{Phe} incubated with *Eco*, *Hsa* and *Rcu* CCA-adding enzymes. Therefore, it can be concluded that the *Rcu* CCA-adding enzyme is active on classical tRNAs.
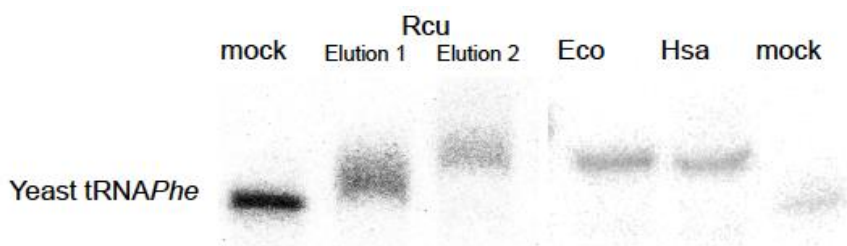

Figure 47: CCA-incorporation assay with yeast tRNA^{Phe}
Autoradiograms of yeast tRNA^{Phe} subjected to different CCA-adding enzymes are shown. The tRNA was incubated respectively with CCA-adding enzymes from *R. culicivorax* (*Rcu*), *E. coli* (*Eco*), and *H. sapiens* (*Hsa*), respectively and without any enzyme (mock) for 120 min at 37°C and then separated on a 10 % PAA gel. A migration shift between the negative control and tRNA incubated with protein indicates a change in the nucleotide length and thus the incorporation of nucleotides.

A further activity test based on the described armless mitochondrial tRNAs from *R. culicivorax* was performed to determine whether these tRNAs can be substrates for the human, bacterial or worm enzyme. For this purpose, internally radioactively labeled *Rcu* mt tRNA^{Arg} and *Rcu* mt tRNA^{Ile} were used. The reaction was stopped after 30, 60 and 120 min, and samples were loaded onto a 10 % PAA gel, and visualized by autoradiography (Figure **48**).
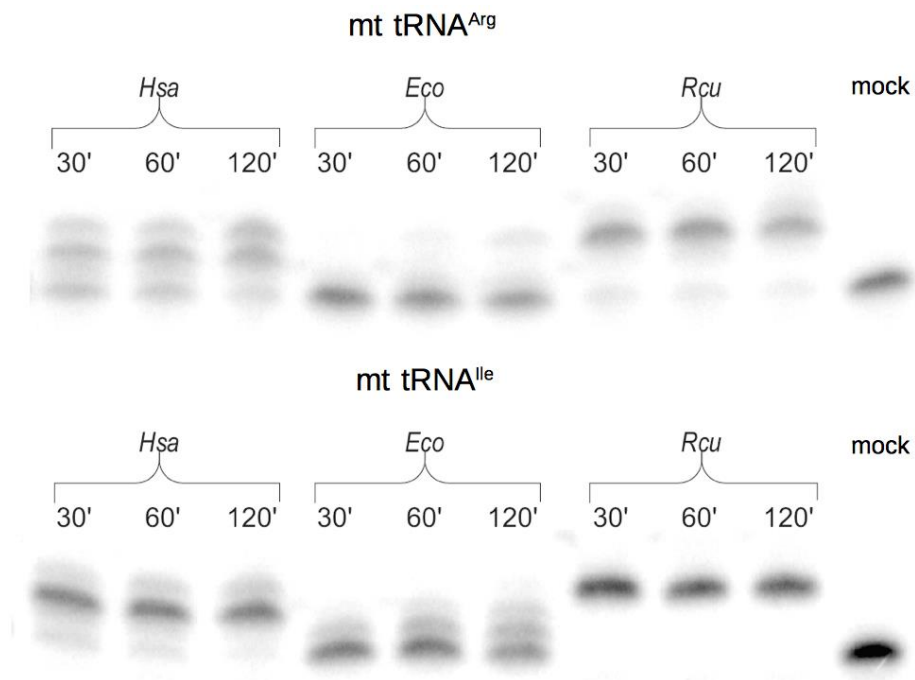
Figure 48: CCA-incorporation assay of armless *Rcu* mt tRNA[Arg] and mt tRNA[Ile].
Autoradiograms of *Rcu* mt tRNA[Arg] and mt tRNA[Ile] subjected to different CCA-adding enzyms are shown. tRNAs were incubated each with CCA-adding enzymes from *H. sapiens* (*Hsa*), *E. coli* (*Eco*), *R. culicivorax* (*Rcu*), and without any enzyme (tRNA mock) for 120 min at 37°C, and then separated on a 10 % PAA gel. A migration shift between the negative control and tRNA incubated with protein indicates a change in the nucleotide length and thus the incorporation of nucleotides.

The results show that the human enzyme is able to recognize both tRNAs, but CCA addition is not complete after 2 h, neither for mt tRNA[Arg] nor for mt tRNA[Ile]. The bacterial enzyme is also not able to add the complete CCA sequence during the prescribed incubation time. It recognizes the armless tRNAs only weakly. In contrast, the *R. culicivorax* enzyme accepts its cognate tRNAs as substrate, and nucleotide incorporation is finished already after 30 min.

16. Discussion

16.1. Preparation of mt CCA-adding enzyme from *R. culicivorax*

The newly identified ORF coding for the *Rcu* CCA-adding enzyme was cloned for overexpression and purification of the corresponding mature protein. Standard purification protocols for the human and bacterial CCA-adding enzymes, well established in the host laboratory in Leipzig (Lizano *et al.*, 2008; Neuenfeldt *et al.*, 2008), could not be applied for the purification of the *Rcu* CCA-adding enzyme due to low protein quantity, and due to the inability to eliminate bacterial contaminations. These correspond mainly to heat shock proteins (bacterial chaperones). Analyses of large-scale protein expression trials demonstrated that purification of eukaryotic proteins in bacterial cells can be difficult in high yield. Only 10 % of eukaryotic proteins can be expressed in *E. coli* in soluble form (Galloway *et al.*, 2003; Graslund *et al.*, 2008). Additional factors should be considered that might alter the expression of a eukaryotic protein in a prokaryotic hosts, e.g., codon bias or codon preference, stability of mRNAs and protein folding (Sahdev *et al.*, 2008; Khow and Suntrarachun, 2012). Additionally, the right choice about the buffer system used for protein purification is often a critical question because an appropriate buffer solution can help to improve the stability and can protect the integrity of protein molecules (Graslund *et al.*, 2008). Accordingly, several expression and purification strategies were tested, including different expression systems (*E. coli* BL21 (DE3), Rosetta-gami 2, Arctic Express (DE3), and yeast cells), different expression methods (standard, late or cold induction), different buffer compositions (different pH, buffer, salts), and several purification approaches (Affinity chromatography via HPLC or batch purification, IEC, and SEC). Unfortunately, neither the expression in *E. coli* BL21 (DE3) or Rosetta-gami 2 strains, nor in yeast cells worked optimally. In addition, no change in the expression approaches or buffer compositions led to a significant improvement of expression and purification of *Rcu* CCA-adding enzymes. Only the use of *E. coli* Arctic Express cells resulted in a sufficient yield of soluble protein. This improved protein solubility is probably due to the low growth temperatures, and due to the co-expression of GroEL/GroES chaperone homologues that promote proper refolding of the recombinant protein (Ferrer *et al.*, 2003). A disadvantage of this strategy is that these chaperones are often co-purified (Haacke *et al.*, 2009), which was also the case in this study. The undesired co-purification of chaperones seemed to be a very serious and

general problem that is described in different publications. Different solutions were proposed how co-purification can be prevented (Joseph and Andreotti, 2008; Hartinger *et al.*, 2010; Rial and Ceccarelli, 2002; Belval *et al.*, 2015). These protocols are, however, often specially adapted to a certain protein of interest, and are therefore not applicable for any protein in general. In the case of the *Rcu* CCA-adding enzyme, a combination of the methods described by (Rial and Ceccarelli, 2002; Joseph and Andreotti, 2008) turned out to be the most successful approach to reduce the amount of unwanted chaperone contamination. This method includes incubation of the soluble protein fraction with denatured *E. coli* proteins, and an additional washing step with a special dissociation buffer. The denatured *E. coli* proteins are added to compete with the recombinant protein for binding to the chaperones, and thereby may facilitate the release of chaperones from the expressed recombinant protein. The dissociation buffer contained 5 mM ATP because it could be shown that GroEL/GroES activity is ATP-dependent (Tyagi *et al.*, 2009). The purification protocol is finalized by size exclusion chromatography, which is necessary to allow the complete elimination of chaperone contaminations in elution fractions.

16.2. Functional characterization of CCA-adding enzymes

Purified protein was tested for its ability to incorporate nucleotides to the 3'-end of armless tRNAs (in vitro transcripts lacking the CCA). For a comparative analysis, classic cytosolic tRNAs, human mt and *Eco* CCA-adding enzymes were purified and included into this study.

The results show that the *Rcu* CCA-adding enzyme is active, and able to recognize armless tRNAs as well as a cytosolic tRNA. The incorporation of the "CCA" sequence was completed for all substrates. However, heterologous *Hsa* and *Eco* CCA-adding enzymes seem not to be fully compatible with armless tRNAs. These results comply with the theory of an evolutionary adaptation of the *Rcu* CCA-adding enzyme to the unusual structure of armless tRNAs, or a co-evolution of both partners. Interestingly, Tomari and colleagues obtained a similar result when studying the mt CCA-adding enzyme from the nematode *C. elegans*. They could demonstrate that *C. elegans* CCA-adding enzymes exhibit a broad substrate specificity toward nematode mt tRNAs lacking the entire T- or D-arms (Tomari *et al.*, 2002). However, also those CCA-adding enzymes can still recognize canonical tRNAs.

The results of the CCA-incorporation assay demonstrate that the human CCA-enzyme weakly recognizes armless mt tRNAs and partially adds nucleotides. In contrast, the bacterial enzyme does not recognize the armless tRNAs as its substrate. *E. coli* does not possess any unusual tRNAs, but only classical tRNAs that are present in its cytosol. The fact that the *Eco* CCA-adding enzyme does not recognize armless mt tRNAs from *R. culicivorax* suggests that the ability to modify unconventional tRNAs was not acquired by bacterial enzymes during evolution. Interestingly, it could already been shown that the *Eco* enzyme does also not recognize other animal mt tRNAs that show even less structural deviations than nematode mt tRNAs (Nagaike *et al.*, 2001).

In contrast to bacterial CCA-adding enzymes, eukaryotic CCA-adding enzymes have to recognize two sets of tRNAs, cytosolic tRNAs with highly conserved structures, and simultaneously mt tRNAs partially lacking highly conserved sequences, which is considered to be important for CCA addition (Li *et al.*, 1996). Another study has shown that the human mt CCA-adding enzyme efficiently repairs mt tRNAs besides cytosolic tRNAs (Nagaike *et al.*, 2001). Thus, eukaryotic mitochondrial CCA-adding enzymes have probably adapted evolutionarily to their cognate mt tRNAs. The adaptation of the human CCA-adding enzyme to animal mt tRNA structures results in a relaxed substrate specificity, which may explain the partial ability to recognize armless tRNAs from *R. culicivorax*. Interestingly, this lowered substrate specificity toward tRNAs seems to be a characteristic feature also of other mitochondrial enzymes, such as mt aminoacyl-tRNA synthetases (Kumazawa *et al.*, 1991) and elongation factors (Schwartzbach and Spremulli, 1991).

Since the CCA-adding enzyme from *R. culicivorax* recognizes both, cytosolic as well as armless mt tRNAs, we assume that this enzyme has adapted to the reduced size of armless tRNAs without losing the ability to recognize classical tRNAs and their extended structures. Consequently, no complete adaptation, which is exclusively intended for the recognition of armless tRNAs, happened during evolution. A decisive difference to the elongation factor EF-Tu in other nematodes is that the *Rcu* CCA-adding enzyme is not structurally distinguished from its bacterial counterpart (no additional or missing domains), while the mitochondrial EF-Tus from, e.g., *C. elegans* show a C-terminal elongation. This raises the question for the decisive factor that led to this rather slight adaptation. Possible answers to this question will be discussed in the next section, where differences between *Rcu* and *Eco* CCA-adding enzymes are examined.

The various approaches applied in this thesis work to establish an optimal expression and purification protocol for the preparation of the *Rcu* CCA-adding enzyme, as well as for the initial experiments to test protein functionality in regards to cytosolic and armless mt tRNAs, provide an excellent basis for further characterization of these enzymes.

Purified *Rcu* CCA-adding enzyme can be used to characterize its nucleotide incorporation activity with different tRNA substrates by determining kinetic parameters, i.e., K_m and k_{cat}. These values need to be compared to those already determined for the *E. coli* and human CCA-adding enzymes in combination with canonical and bovine mt tRNAs (Nagaike *et al.*, 2001). It has been shown that the human mt CCA-adding enzyme recognized efficiently mt tRNAs with non-conserved T-loop and unusual structures, while the *Eco* CCA-adding enzyme recognized only cytosolic tRNAs. As an outlook, a comparative study on different CCA-adding enzymes from human, *E. coli* and *R. culicivorax* in combination with armless mt tRNAs and other (mt) tRNA substrates would complete the characterization of *Rcu* CCA-adding enzymes, and could, e.g., help to validate its superior efficiency for CCA-incorporation also for other unconventional tRNA structures.

16.3. Structural characterization of *Rcu* CCA adding enzyme in an evolutionary context

The amino acid sequence of the *Rcu* CCA-adding enzyme was aligned to other CCA-adding enzymes from different organisms. These alignments contributed to understand the secondary organizations of these enzymes. In comparison with the human mt CCA-adding enzyme, an overall sequence identity of 46 % can be observed for the *Rcu* CCA-adding enzyme. In particular, the N-terminal domain, typically corresponding to the catalytic site (responsible for the recognition and addition of nucleotides) has a high level of identity (66 %), while the C-terminal domain is more variable. It was shown that substrate binding of CCA-adding enzymes takes place at its low conserved C-terminal region (Tomita *et al.*, 2004; Tretbar *et al.*, 2011). I-TASSER analysis revealed 5 putative 3D models, of the *Rcu* CCA-adding enzyme. All of them exhibit different conformation of the C-terminal, indicating a putative high flexibility of this domain. Thus, we suspect that a flexible C-terminus of the *Rcu* CCA-adding enzyme has adapted to allow for recognizing armless tRNAs. It would be interesting to verify this hypothesis by creating protein chimeras, e.g., by exchanging C-terminal parts of *Eco* CCA-adding enzymes with these

from *Rcu* CCA-adding enzymes. The study of several enzyme chimeras, including exchanges in N-terminal and/or C-terminal regions has been successfully performed already, and helped to decipher the role of these domains in CCA-adding enzymes (Betat *et al.*, 2004; Neuenfeldt *et al.*, 2008; Toh *et al.*, 2009).

Studies on the CCA-adding enzyme from *E. coli* have also shown that it is possible to delete large portions of the C-terminal region without losing the CCA-adding activity (Betat *et al.*, 2004). The generation of C-terminal deletion variants of the *R. culicivorax* enzyme would bring further insights into the importance of this part for recognizing and processing armless tRNAs.

Other highly interesting methods that can be used to measure, e.g., protein interaction, enzymatic activity, or conformational changes are, e.g., fluorescent labelling of proteins (FRET) (Toseland, 2013; Jager *et al.*, 2006), Electron paramagnetic resonance (EPR), and electron spin resonance (ESR) spectroscopy. Especially, the EPR/ESP approach has been applied for a CCA-adding enzymes already (Ernst *et al.*, 2015). These methods may help to understand inter-domain movements and, to determine the structural features of the *Rcu* CCA-adding enzyme more in detail.

CHAPTER 4: Structural and functional characterization of the mitochondrial arginyl-tRNA synthetase from *R. culicivorax*

Arginyl-tRNA synthetases (ArgRS) catalyze the esterification of arginine amino acid to their cognate tRNAs. Aminoacylation is typically achieved by a two-step reaction: the amino acid is first activated, and then transferred to the tRNA molecule. Together with the glutamyl-tRNA synthetase (GluRS) and glutaminyl-tRNA synthetase (GlnRS), ArgRS represents a peculiarity of this rule. It has been shown for some organisms that these synthases require their cognate tRNAs already for the first step of amino acid activation (Mehler and Mitra, 1967; Kern and Lapointe, 1980; Rath *et al.*, 1998). Several crystal structures of cytosolic ArgRSs from different organisms (e.g., *S. cerevisiae, H. sapiens, E. coli,* and *T. thermophilus)* have been solved, either in free form or in complex with their substrates (Delagoutte *et al.*, 2000; Shimada *et al.*, 2001b; Kim *et al.*, 2014; Bi *et al.*, 2014). This contributed considerably to a better understanding about structural organizations, mechanisms of arginine activation, and aspects of tRNA recognition. The crystal structure of a typical ArgRS is shown in Figure **49**.

ArgRSs belongs to the class I aminoacyl-tRNA synthetase family and are monomeric enzymes. The structure of ArgRSs is predominantly composed of α-helices, and can be divided into three major domains. The N-terminal domain, also called "additional domain" is probably involved in the recognition of edge-regions of tRNAs that is formed by long range nucleotide interactions between the D- and T-loop (Cavarelli *et al.*, 1998). The second domain is a catalytic domain, which contains the typical sequence motifs "HIGH" and "KMSKS". The HIGH sequence is often equivalent to "HVGH" of some organism, and is probably involved in binding of ATP (Oguiza *et al.*, 1993). The classical KMSKS motif, which constitutes the active site, is missing or differs in some ArgRS sequences, e.g., FKTRS in cytosolic ArgRS of *H. sapiens* as well as *C. elegans* (Kim *et al.,* 2014). Finally, the C-terminal anticodon binding domain is implicated in specific tRNA recognition.

The last chapter of this study is dedicated to the structural and functional characterization of the mt arginyl-tRNA synthetase from *R. culicivorax.* The special interest in the ArgRS of this worm is not only due to intensive studies performed (or in progress) at the host laboratory in Strasbourg on other ArgRSs of different species, but also because the cognate mt tRNA[Arg] represents one of the shortest identified tRNA molecules known so far. Therefore, it is of high interest to explore putative structural and functional adaptations of this enzyme in regard to armless tRNAs. During this study, the

sequence of the mt arginyl-tRNA synthetase from *R. culicivorax* was identified, cloned, expressed and purified for the first time. The protein sequence has been analyzed and compared to heterologous enzymes. Its activity when interacting with different tRNA substrates was tested, and compared to cytosolic ArgRSs from bacterial and eukaryotic species.
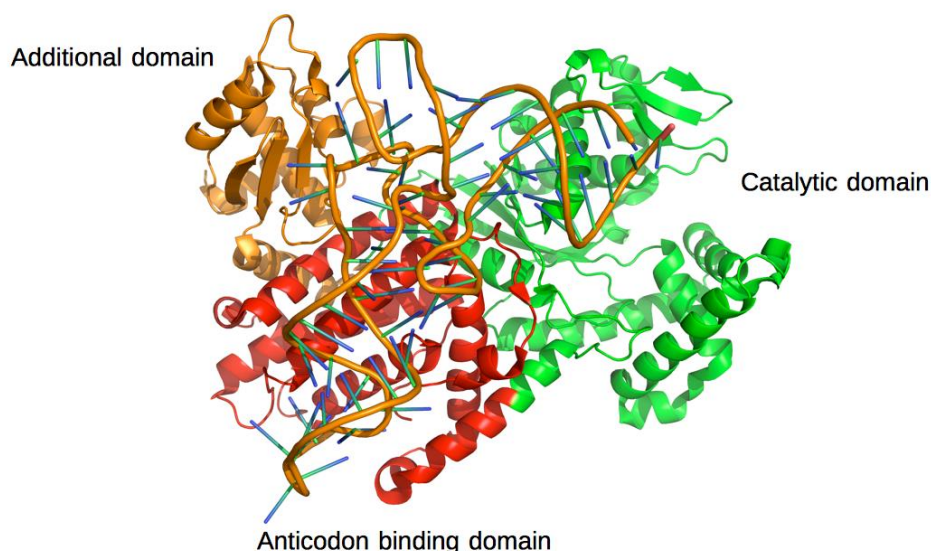

Figure 49: Crystal structure of cytosolic *S. cerevisiae* ArgRS and its cognate tRNA[Arg].
The 2.2 Å crystal structure of cytosolic yeast ArgRS in complex with its cognate tRNA[Arg] (pdb 1F7V). Main domains are indicated by different colors: additional domain (orange), catalytic domain (green), anticodon-binding domain (red).

17. Identification of mitochondrial ArgRS from *R. culicivorax* and sequence comparison

Two open reading frames (ORF) that code for putative ArgRS proteins were previously identified using next-generation sequencing of the nuclear genome as well as the transcriptome of *R. culicivorax* (Schiffer *et al.*, 2013). One ORF encodes an amino acid sequence for a protein that is similar to cytosolic ArgRS from other organisms (data not shown). The second ORF consisted of two fragments coding for sequences that resemble the N- and C-terminus of an ArgRS with mitochondrial origin. These fragments were chosen for further analysis. A merged sequence consisting of the N- and C-terminal part was inserted into a multiple sequence alignment, made of ArgRS sequences from 92 completed genomes, which cover the phylogeny of all kingdoms of life (Bacteria, Archaea, and Eukarya). This alignment reveals that the N- and C-terminus correspond indeed to a mt ArgRS protein, while the validity of an internal linker sequence of 12 aa between both

136

parts remained unclear. Thus we decided to verify the gene sequence using reverse transcription on total RNA and mRNAs extracted from *R. culicivorax*. For this purpose, gene specific primers were designed that are complementary to the 5'-end of the N-terminus and to the 3'-end of the C-terminus to cover the full length of the coding sequence. A PCR fragment with the size of ~1,500 bp appeared after PCR amplification and was sequenced (Figure 50). It turned out that the initially annotated gene sequence is only partially correct. The dubious internal sequence was solved and could be corrected. Furthermore, a 5' RACE PCR was performed to obtain the full-length sequence of the RNA transcript (data not shown). No alternative start codon was detected with this technique and confirmed thus the correctness of the predicted start codon. Additionally, the original RNAseq data that were kindly provided by P. Schiffer (University of Cologne) was used to build a new transcriptome annotation. This allowed to confirm the mt ArgRS sequence, which was identified by both previously mentioned PCR approaches. The newly identified complete protein sequence from *R. culicivorax* was aligned to other mt ArgRS sequences from *C. elegans*, *H. sapiens,* and *S. cerevisiae* to search for conserved sequence motifs, and to identify possible sequence peculiarities.

Figure 50: Identification of mt ArgRS sequence from *R. culicivorax*.
(Left) 10 % agarose gel with PCR product obtained after reverse transcription PCR on purified total RNA and mRNA from *R. culicivorax*. The size of the identified PCR fragment corresponds to the expected size of the ArgRS nucleotide sequence of 1521 bp. (Right) Sequence alignment of predicted and identified protein sequence of the *Rcu* mt ArgRS. The red box indicates the linker sequence that was corrected after sequencing of the reverse transcription product.
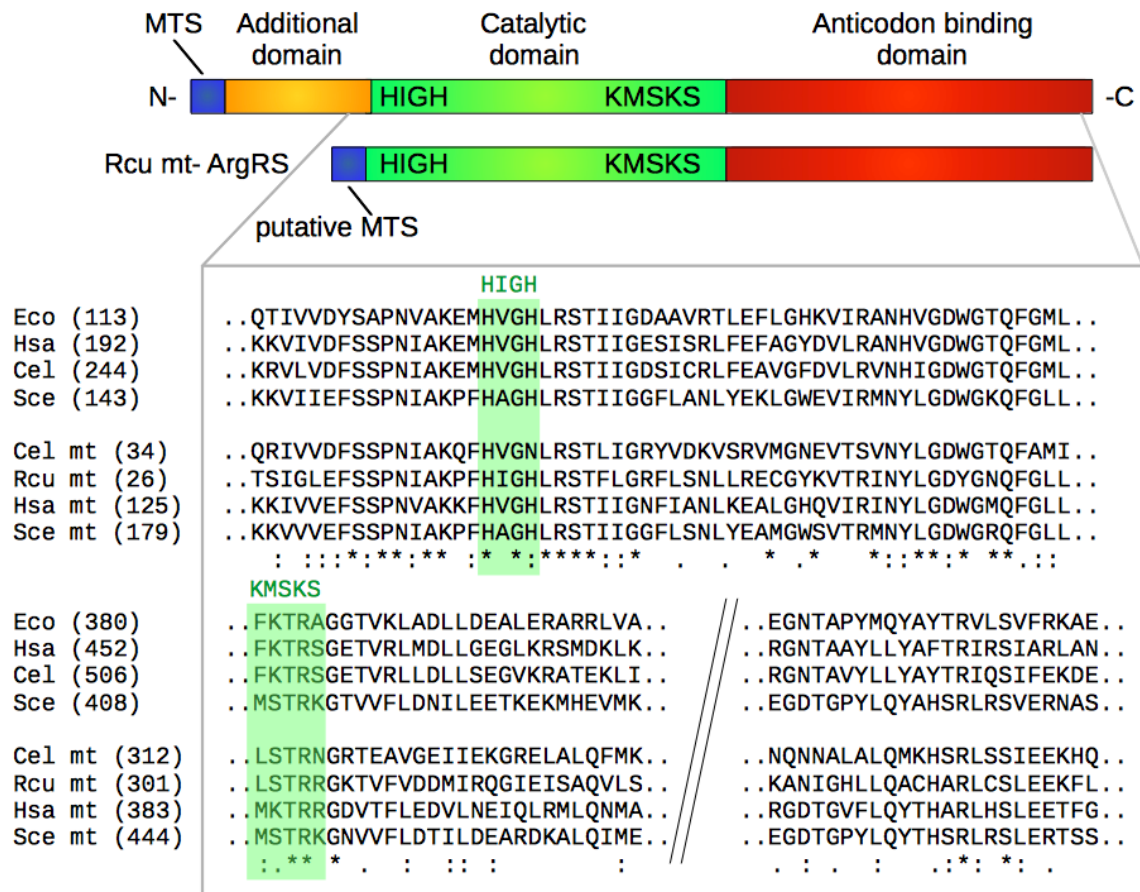
137

Figure 51: Schematic overview and sequence alignment of ArgRS.
(Top) Schematic representation of the functional domains of mt AspRS compared to mt ArgRS from *R. culicivorax.* An mt ArgRS is typically composed of a mitochondrial targeting sequence (MTS) (blue) that is cleaved after mitochondrial import, an additional domain (orange), a catalytic domain (green), and an anticodon binding domain (red). (Below) Cytosolic and mitochondrial ArgRS from different organism are compared based on their amino acid sequence. The conserved sequence motifs of class I synthetases, i.e., "HIGH" and "KMSKS", are highlighted in green boxes. Conserved nucleotides are indicated by "*", similar amino acids are indicated by ":" in the bottom line. Numbers in brackets indicate positions of the first residues in the given alignment in the amino acid sequence of corresponding ArgRS. *Eco, Escherichia coli; Hsa, Homo sapiens; Sce, Saccharomyces cerevisiae; Cel, Caenorhabditis elegans, Rcu, Romanomermis culicivorax.*

Additionally, bacterial and cytosolic ArgRS from *C. elegans*, *H. sapiens,* and *S. cerevisiae* were used to complete this comparative analysis (Figure 51). The alignment reveals that the *Rcu* mt ArgRS possesses conserved residues that correspond partially to the typical sequence motifs "HIGH" and "KMSKS". In this case the last motif is equivalent to LSTRRG. It is striking that the *Rcu* mt ArgRS exhibits the smallest size in the alignment with only 507 aa (58 kDa). Another rather small enzyme is the mt ArgRS from *C. elegans* with 512 aa. The remaining enzymes are longer than 570 aa. This size difference is particularly remarkable in the additional domain, which is completely absent in the *Rcu* mt ArgRS sequence. Only a few residues remain, which may form a putative mitochondrial targeting

sequence (MTS). This domain is also absent in the protein sequence of the mt ArgRS in *C. elegans.* It has been shown in a crystal structure of the cytosolic yeast ArgRS that the additional domain, which is apparently missing in *R. culicivorax* and *C. elegans,* presumably recognizes the elbow region of the tRNA (Cavarelli *et al.*, 1998; Delagoutte *et al.*, 2000)*.* The elbow region arises from the interactions of the D- and T-stem-loops, and stabilizes the canonical L-shape of tRNA tertiary structures. Interestingly, the additional domain is a unique structural feature of ArgRS and not present in other class I aaRSs. Mt tRNAs from *C. elegans* and *R. culicivorax* probably do not build a typical elbow region due to the missing D-and T-stem loops, suggesting that the mt ArgRS of these nematodes may have evolutionary adapted to armless tRNAs.

The *Rcu* ArgRS protein sequence was used as input for the computational structure prediction tool I-TASSER (Zhang, 2008) to create a possible 3D structure model (Figure 52 A). The predicted tertiary structure is mainly composed of alpha helices, and its composition is compared to the crystal structure of the yeast ArgRS (pdb 1BS2) (Figure 52 B). The high structure similarity is probably a result of the template-based approach modeling of the program. Nevertheless, the I-TASSER structure prediction demonstrates the absence of the additional domain in the N-terminal part of the *Rcu* mt ArgRS. Instead, a single alpha helix replaces this domain in the N-terminus, which may represent a putative targeting signal for mitochondria. A docking model of the *Rcu* mt ArgRS and yeast tRNA[Phe] was constructed (Figure 52 C) and compared to the crystal structure of the cytosolic yeast ArgRS in complex with its cognate tRNA[Arg] (Figure 52 D). It shows that a classical tRNA would theoretically fit into the recognition pocket of the 3D model prediction, which indicates a high structural similarity between the catalytic domain and the anticodon binding domain of yeast and *Rcu* ArgRS. The most striking difference between both structures is the missing N-terminal domain in the nematode enzyme. As mentioned above, this domain is involved in recognition of the elbow region of classical tRNAs (Cavarelli *et al.*, 1998). We hypothesize that this ability is probably not necessary for the recognition of armless tRNAs anymore, because these do not possess the classical D- and T-loops, and thus probably also not the canonical elbow structure.
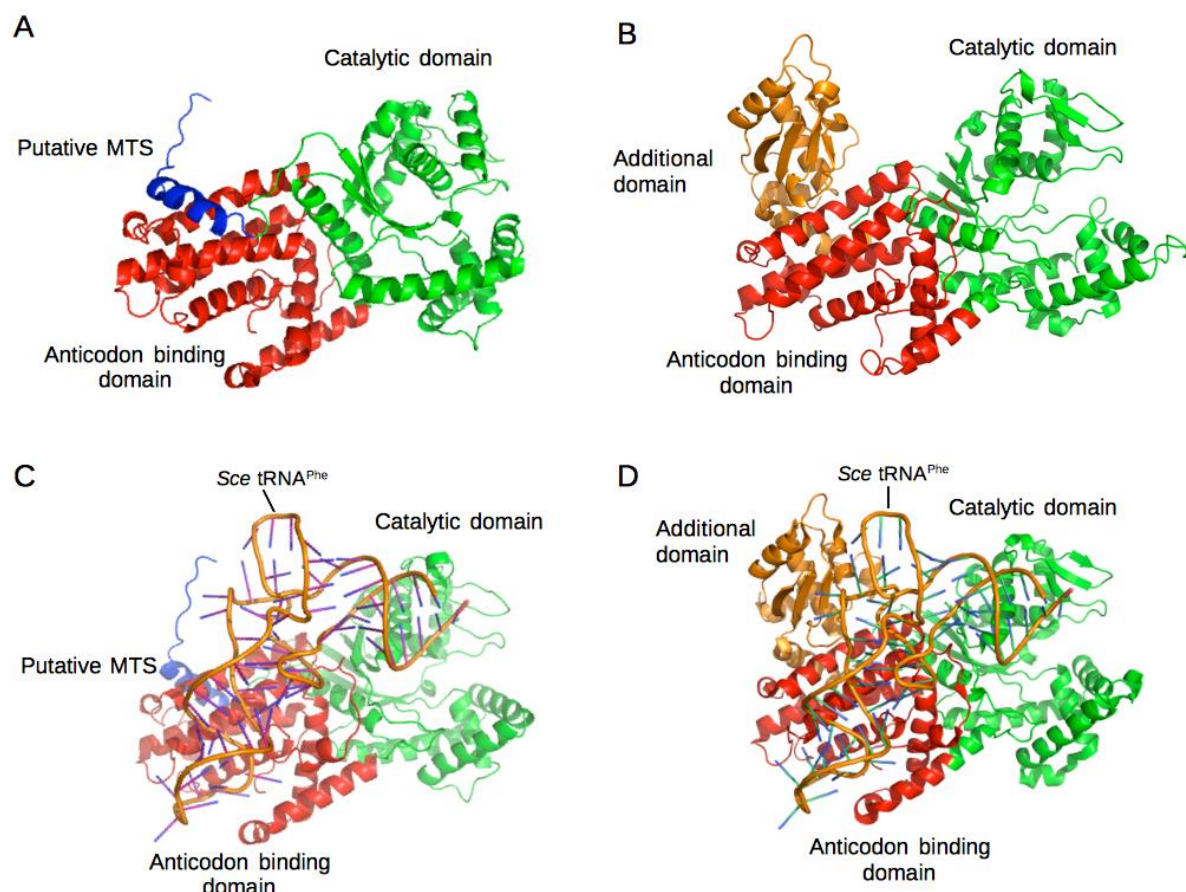
Figure 52: 3D structure prediction of *Rcu* mt ArgRS.
(A) I-TASSER structure prediction for *Rcu* mt ArgRS. (B) The crystal structure of cytosolic yeast ArgRS (pdb 1BS2) is used for structural comparison. (C) Docking model of the *Rcu* mt ArgRS 3D prediction and yeast tRNA^Phe. (D) Crystal structure of cytosolic yeast ArgRS in complex with its cognate tRNA^Phe (pdb 1F7V). Compared to the yeast ArgRS, a loss of the additional domain in the Rcu mt ArgRS structure prediction is particularly noticeable, indicating a possible evolutionary adaptation to armless tRNAs. Main domains are indicated by different colors: putative mitochondrial targeting sequence (MTS) (blue), additional domain (orange), catalytic domain (green), anticodon binding domain (red).

18. Cloning, expression and purification of *Rcu* mt ArgRS

18.1. Cloning of different ArgRS variants

Various mt enzymes possess an N-terminal MTS, which is cleaved during the import into mitochondria, resulting in a mature protein (Chacinska *et al.*, 2009; Schmidt *et al.*, 2010). The knowledge about the cleavage site is an important prerequisite for the design of protein variants that are compatible with efficient production in bacterial strains (Gaudry *et al.*, 2012). The identification of the correct cleavage site is not always straight forward since the MTS is variable in size and lacks common consensus sequence (Gavel and Heijne, 1990). Although cleavage site motifs follow loose rules, it has been observed that

MTSs often possess an increased content of arginine residues and positively charged amino acids, which may form amphiphilic helices (Fukasawa *et al.*, 2015).

In the case of the *Rcu* mt ArgRs it was difficult to predict a MTS using conventional bioinformatics tools. The prediction tools TargetP (Emanuelsson *et al.*, 2000), Predator (Small *et al.*, 2004), and TPpred2 (Savojardo *et al.*, 2014) did not detect a targeting signal, while Mitoprot (Claros and Vincens, 1996) and MitoFates (Fukasawa *et al.*, 2015) predicted a cleavage site at D16 (Mitoprot) and L23 (MitoFates), but only with a low probability (0.17 and 0.024, respectively). However, the putative presence of an amphipathic helix in the N-terminal part of the *Rcu* mt ArgRS supports the hypothesis that the N-terminal sequence represents a MTS. To identify a transcript sequence which is most suitable for expression in bacterial strains, different cleavage sites were introduced within or downstream of the identified amphipathic helix, resulting in various protein variants that vary in length of their N-terminal sequence (Figure 53). The protein variants are named after the corresponding cleavage site. The protein coding sequence for P24, V30, and G36 was first cloned into a pET28a plasmid with an N-terminal 6xHis-tag. Additionally, the full-length (FL) protein variant was cloned in this vector because it was not verified whether the N-terminal sequence represents indeed a MTS. Since the influence of the N-terminal His-tag on the structure or activity of the ArgRS variants could not be estimated, other variants (D16, C25, D28 and S29) were cloned into a pDEST plasmid with a C-terminal 6xHis-tag. The expression of all protein variants was under the control of a T7 promoter in both plasmids.
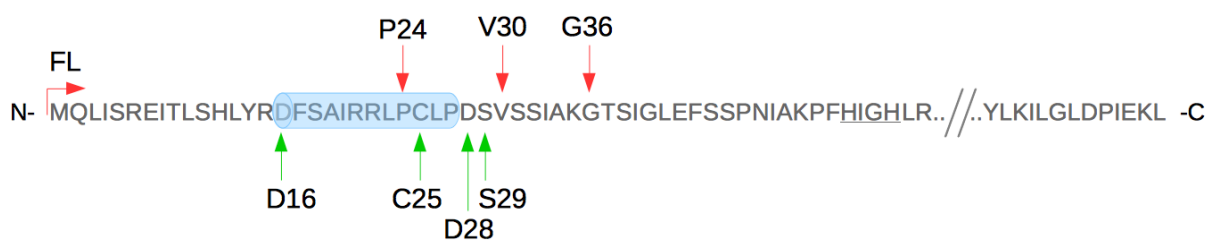

Figure 53: Protein variants of *Rcu* mt ArgRS possessing different N-terminal start sites.
Schematic overview of the manually introduced cleavage sites that result in the creation of different protein variants, varying in the length of their N-terminal sequence. The variants are named after the corresponding cleavage site (protein P24 for example starts with P24, etc.) and are cloned into a pET28a (red arrows) and pDEST vector (green arrows). The sequence forming an α-helix (blue barrow) and the conserved motif "HIGH" (underlined) are highlighted.

18.2.   Expression of FL, P24, V30, G36 in *E. coli*

The gene sequences of full-length ArgRS and variants P24, V30, and G36 were cloned into a pET28a vector with a N-terminal 6xHis-tag. These constructs were transferred into BL21 (DE3) and Arctic Express (DE3) *E. coli* strains. Expression was performed following the described protocol in 8.6.6. Cell extracts containing the expressed protein variants were disrupted through sonication, and were centrifuged afterwards. Soluble fractions as well as cell extract of disrupted cells were loaded and separated in a 10 % SDS-gel. Protein bands were detected by Western blot analysis using anti-His antibodies (Figure 54). In BL21 cells, only the full-length protein was expressed, however, it was not present in the soluble fraction. No bands are detected for the other proteins variants suggesting that they are probably unstable, toxic or are degraded in *E. coli* BL21.
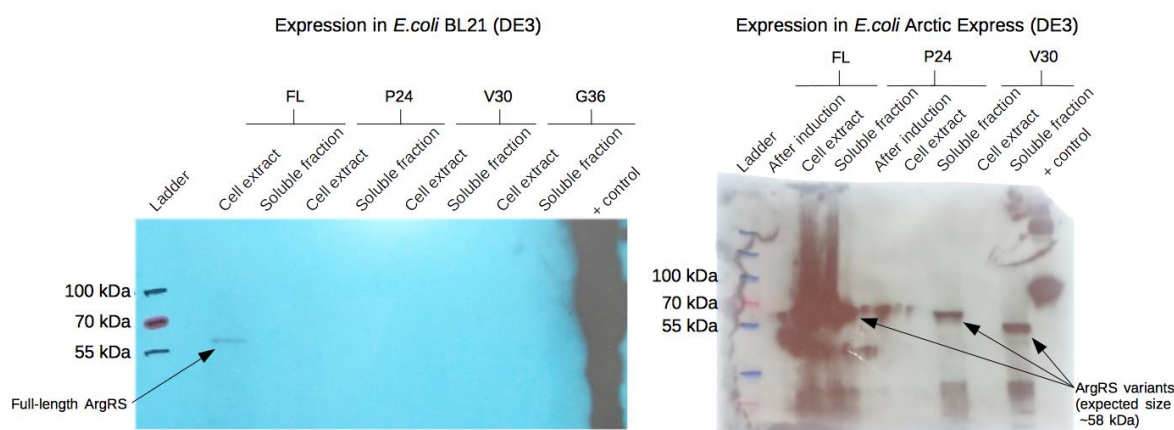
Figure 54: Solubility test of recombinant expressed protein variants FL, P24, V30, and G36.
FL, P24, V30, G36 are expressed in BL21 (DE3) (left) and Arctic Express (DE3) (right). Cell extracts and soluble cell lysate fractions were loaded and separated onto a 10 % SDS-gel and detected by Western blot analysis using anti-His antibodies. The expected size of the *Rcu* mt ArgRS variants containing the N-terminal His-tag is 58 kDa. Arrows indicate the position of the mt ArgRS variants. Protein ladder was loaded on the lanes designated with "Ladder" (sizes are indicated on the left side of the blots).

Expression in Arctic Express cells leads to an increased solubility at least for variant P24 and V30. The full-length protein is probably also expressed and soluble, but the result remains unclear due to an overload of corresponding samples onto the gel. Dominant bands appear at the expected size for ArgRS variants of 58 kDa, except for V30, which appears to be smaller than expected. A re-sequencing of the corresponding plasmid revealed a point mutation that introduced an early stop codon resulting in a shorter amino acid sequence, and thus in a smaller protein size.

18.3. Expression of D16, C25, D28, and S29 in *E. coli*

It is generally accepted that codon usage biases are different when comparing different species. It reflects the composition of the respective genomic tRNA pool. Thus, four codon optimized mt-ArgRS genes named, i.e., D16, C25, D28, and S29, were cloned into a pDEST plasmid with a C-terminal His-tag and used for bacterial expression to ensure fast translation rates and high accuracy.

Expression was performed in Rosetta2 (DE3) and Arctic Express (DE3) cells following the described protocol in section 8.6.6. Cell extracts and soluble fractions, obtained after cell lysis and centrifugation, were loaded onto a 10 % SDS-gel. Protein bands were detected by Western blot analysis using anti-His antibodies (Figure 55). The protein variants D16, D28, and S29 are expressed in both bacterial strains. However, in Rossetta2 (DE3) the expressed proteins were detected only in the cell extract fraction, indicating that these protein variants are not soluble in this strain under the tested conditions. In contrast, the expression in Arctic Express (DE3) cells results in an increased solubility of all protein variants with one exception. Only variant C25 was not expressed in both bacterial strains. As variants D16 and S29 showed the best expressions rate and solubility in Arctic Express cells, they were chosen for purification and further analysis.
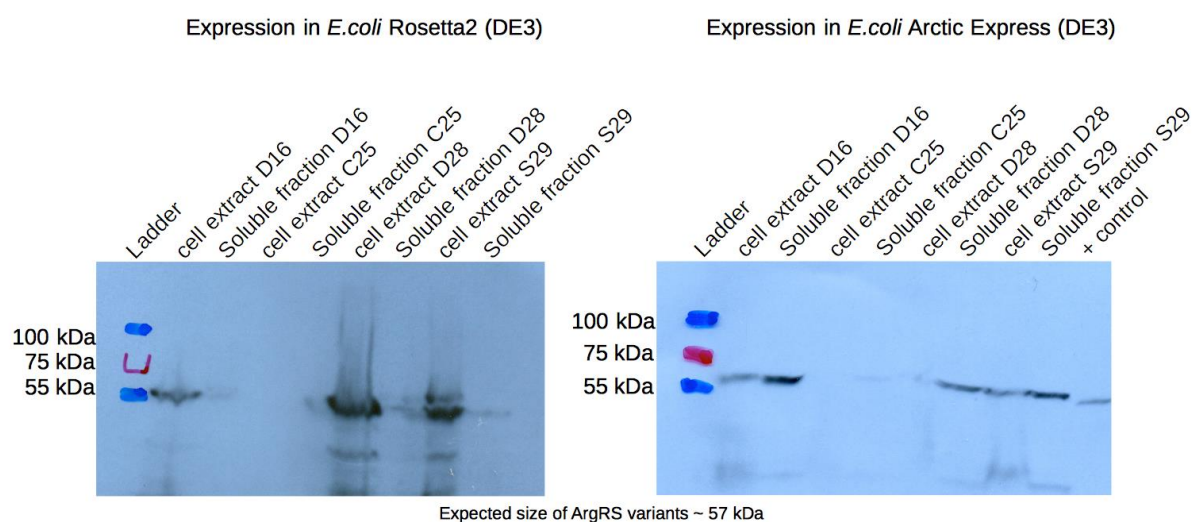

Figure 55: Solubility test of recombinant expressed protein variants FL, P24, V30, and G36.
FL, P24, V30, and G36 are expressed in Rosetta2 (DE3) (left) and Arctic Express (DE3) (right). Cell extracts and soluble cell lysate fractions were loaded and separated onto a 10% SDS-gel and detected by Western blot analysis using anti-His antibody. The expected size of the *Rcu* mt ArgRS variants containing the N-terminal His-tag is about 57 kDa. The protein ladder was loaded on the lanes designated with "Ladder" (sizes are indicated on the left side of the blots).

18.4.   Purification of *Rcu* ArgRS variants D16 and S29

Bases on previous experiences with the purification of the *Rcu* CCA-adding enzyme, it became clear that the preparation of recombinant proteins from Arctic Express can cause problems because protein expression is associated with the co-expression of chaperons Cpn60 and Cpn10. Therefore, the protocol that was established earlier in this study for the preparation of the Rcu CCA-adding enzyme was applied for the purification of *Rcu* mt ArgRS variants. However, the application of this method could not significantly improve the release of chaperons from the synthetase.

In 2015, a purification protocol was published describing a method, which allows the release of Cpn60 from expressed protein using urea at a sub-denaturing concentration (Belval *et al.*, 2015). This method was applied and optimized for the purification of *Rcu* mt ArgRS variants. The final protocol that allows almost entirely eliminating chaperons (visible as dominant band at 60 kDa in the soluble fraction in Figure 56 and Figure 57) consists of three washing steps. The first washing buffer contains 2 M urea, followed by a washing step with dissociation buffer, and a final step include washing with classical buffer that is already used for cell lysis. The protein was eluted in elution buffer. All steps were examined on an ÄKTA purifier system. Several samples were taken during preparation of D16 and S29 ArgRS variants, and loaded onto a 10 % SDS-gel (Figure 56 and Figure 57).
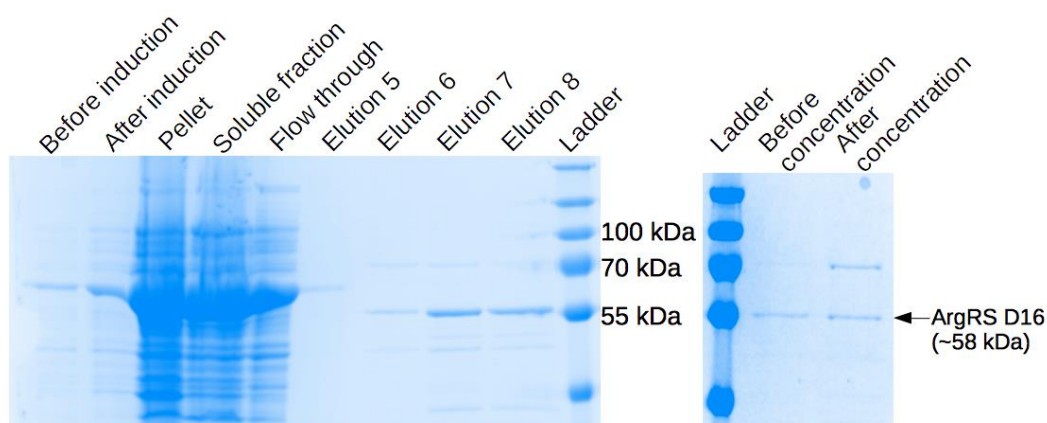

Figure 56: Expression, purification and concentration of the *Rcu* mt ArgRS variant D16.
(Left) *E. coli* Arctic Express (DE3) cells transformed with the plasmid pDEST carrying the *Rcu* mt ArgRS D16 coding sequence were used for expression and purification. Samples were taken during expression (before and after induction), after sonication and centrifugation (pellet fraction and soluble fraction) and during purification (flow through, and elution fractions 5-8), and were loaded onto a 10 % SDS-gel. The protein ladder was loaded on the lanes designated with "Ladder" (sizes are indicated between both gels). (Right) Samples obtained before and after concentration of the eluted protein were loaded onto a 10 % SDS-gel. The expected size of the *Rcu* mt ArgRS D16 variant is 58 kDa (indicated by an arrow).

Protein elution for both protein variants was almost pure. Only weak protein contaminants were still present (Figure 56: elution 7 and 8; Figure 57: elution 12 and 13). Since the quantity of both protein variants was very weak after purification, they were concentrated by centrifugation (Amicon Centricon cut off 30 kDa). Samples were taken before and after the concentration procedure and loaded onto a 10 % SDS-gel (Figure 56 and Figure 57). It turned out that it was not possible to concentrate the variant D16. Eventually, concentration through centrifugation is not an appropriate method for this protein variant. In contrast to that, S29 was well concentrated, but as a result, the remaining impurities were also concentrated and are clearly identifiable in the gel. The protein concentration was measured and the portion of the *Rcu* mt ArgRS was estimated at 0.08 mg/ml. The prepared S29 variant was used for aminoacylation assays.
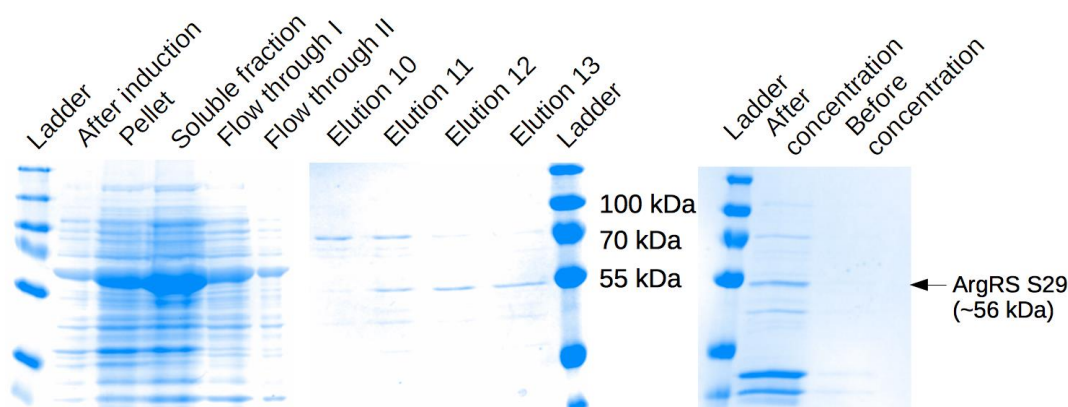

Figure 57: Expression, purification and concentration of the *Rcu* mt ArgRS variant S29.
(Left) *E. coli* Arctic Express (DE3) cells transformed with the plasmid pDEST carrying the *Rcu* mt ArgRS S29 coding sequence were used for expression and purification. Samples were taken during expression (before and after induction), after sonication and centrifugation (pellet fraction and soluble fraction) and during purification (flow through, and elution fractions 10-13), and were loaded onto a 10 % SDS-gel. The protein ladder was loaded on the lanes designated with "Ladder" (sizes are indicated between both gels). (Right) Samples obtained before and after concentration of the eluted protein were loaded were loaded onto a 10 % SDS-gel. The expected size of the *Rcu* mt ArgRS S29 variant is 56 kDa (indicated by an arrow).

19. Aminoacylation assays

The purified enzyme was used in aminoacylation assays in order to verify whether the protein can aminoacylate its cognate and other tRNA substrates. For that purpose, *Rcu* armless tRNA$^{Arg\_CCA}$ carrying the CCA tail was prepared. Commercial total tRNA from *E. coli*, and total tRNA from yeast (kindly provided by G. Eriani, University of Strasbourg) were used in parallel in these assays.

Since no positive controls are available to verify the functionality of the *Rcu* mt ArgRS and the *Rc*u mt tRNA^{Arg} in aminoacylation assays, it was absolutely necessary to test whether

the experimental setup is functioning. Therefore, assays with cytosolic ArgRS from *S. cerevisiae* and *E. coli* were integrated, and aminoacylation activity was verified for their cognate tRNA substrates as well as for *Rcu* armless tRNA^{Arg}.

An aminoacylation assay using 10 nM *Sce* ArgRS (kindly provided by G. Eriani, University of Strasbourg) and 30 pmol of tRNA was performed in MRC buffer. This buffer is adapted for cytosolic enzymes and is characterized by an [Mg^{2+}]/[ATP] ratio of 1.5. Samples were taken after 0 min, 4 min, 8 min, 15 min, and 20 min of incubation at 25°C. The results of the assay are shown in (Figure 58), revealing that the yeast ArgRS is not active on the *Eco* or *Rcu* tRNA substrates, but efficiently aminoacylates its cognate tRNAs, (even up to 52 pmol, indicating that the initial calculated tRNA^{Arg} concentration was underestimated). However, yeast synthetase is active at least on its cognate tRNA, suggesting that the experimental set up is appropriate.
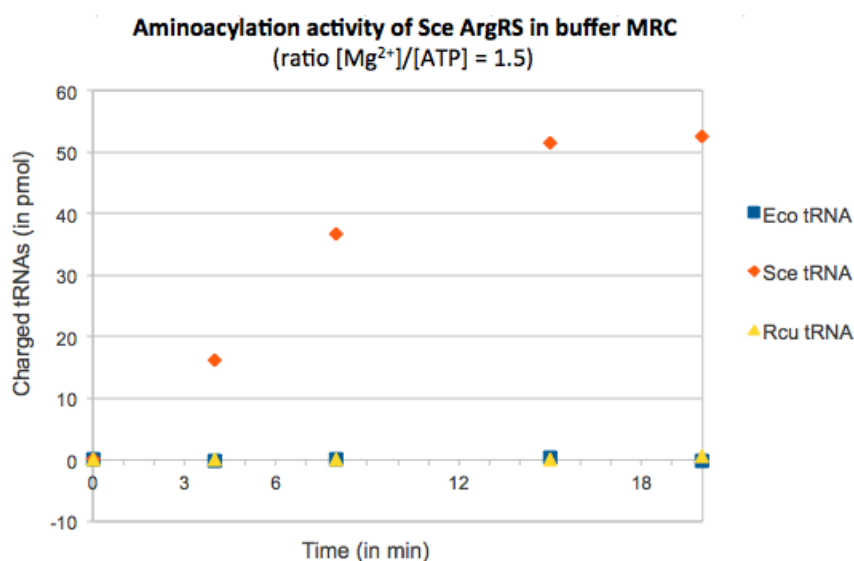

Figure 58: Aminoacylation activity of *Sce* ArgRS.
Aminoacylation assay was performed using 10 nM *Sce* ArgRS and 30 pmol tRNA^{Arg} from *E. coli*, *S. cerevisiae*, and *R. culicivorax* in buffer MRC. Aliquots of 10 μl have been taken after 0, 4, 8, 15 and 20 min.

Eco ArgRS (kindly provided by S. X. Lin, CHUL, Québec) was used to test the arginylation activity on different tRNA substrates in an additional assay. In a first attempt, the enzyme was applied in the same buffer conditions as described before: 40 pmol of tRNA was subjected to 100 nM *Eco* ArgRS in MRC buffer. The results are shown in Figure 59. About 8 pmol of yeast tRNA is charged by *Eco* ArgRS, which corresponds to 20 %. No activity is detected for the armless tRNAs or the cognate *Eco* tRNAs. Actually, arginylation in *E. coli*

146

is a well-established system and shows normally excellent aminoacylation activity. We suspected that commercial purchased *Eco* tRNAs were damaged or otherwise not useable. For subsequent experiments, total *Eco* tRNAs were prepared in house and tested. Test aminoacylation reactions on freshly prepared Eco tRNAs have been performed by A. Gaudry, University of Strasbourg (Figure 60).
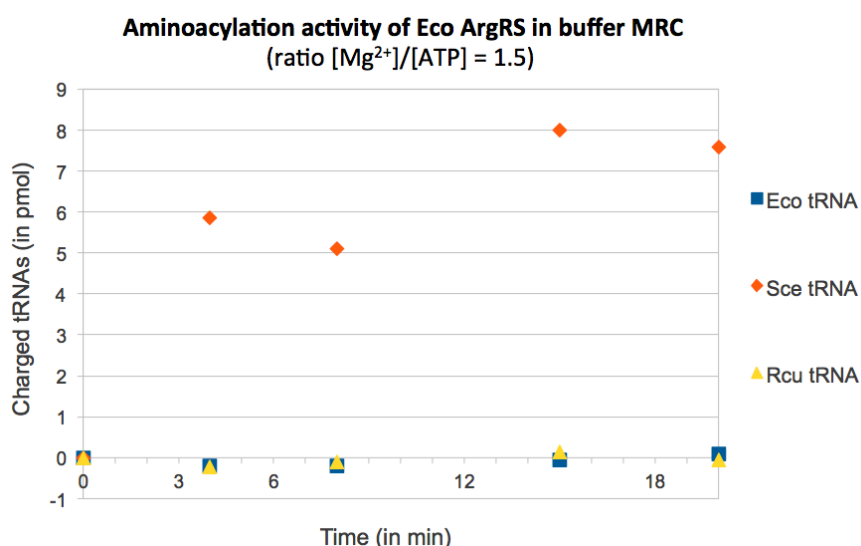

Figure 59: Aminoacylation activity of *Eco* ArgRS.
Aminoacylation assay was performed using 100 nM *Eco* ArgRS and 40 pmol tRNA[Arg] from *E. coli*, *S. cerevisiae*, and *R. culicivorax* in buffer MRC. Aliquots of 10 µl have been taken after 0, 4, 8, 15 and 20 min.

Proper buffer conditions for the *E. coli* enzymes in activity assays have been described before (Igloi and Schiefermayr, 2009). These protocols revealed an adapted $[Mg^{2+}]/[ATP]$ ratio of 2.5, but no substantial change of the other buffer components. An adapted buffer (named MRE) was prepared and tested again with *Eco* ArgRS and the three different tRNA substrates. The results are shown in Figure 60.

The enzyme efficiently aminoacylates its cognate tRNA (in house preparation). Interestingly, the *Eco* ArgRS does also recognize yeast tRNAs in the adapted MRE buffer. Up to 58 pmol tRNA are charged, corresponding to an increase of approximately 10-fold, compared to the test performed with the MRC buffer. These results indicate that arginyl-tRNA synthetases are probably sensitive to buffer conditions, especially to the $[Mg^{2+}]/[ATP]$ ratio, which needs apparently to be optimized for every ArgRS.

The *E. coli* enzyme shows no activity with the *Rcu* tRNAs. We assume that the armless *Rcu* mt tRNA[Arg] represents probably not an appropriate substrate for the *E. coli* enzyme due to its extreme size reduction.
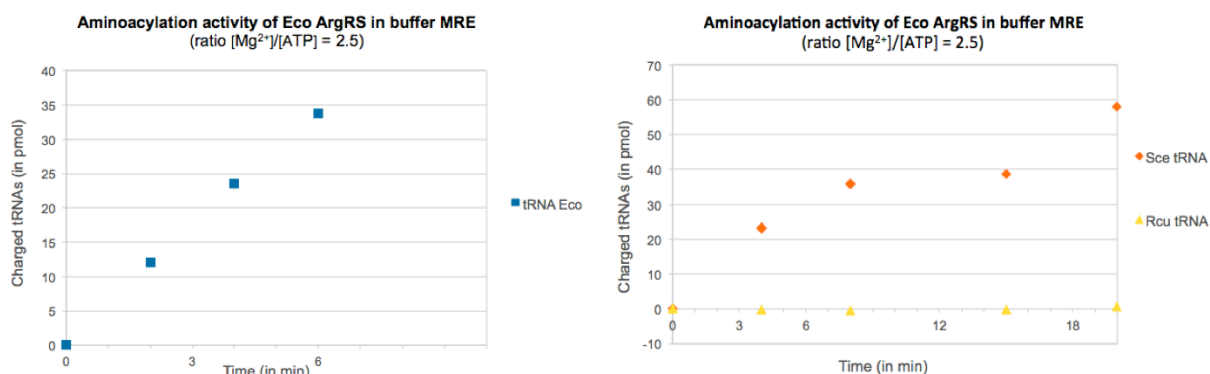
147

Figure 60: Aminoacylation activity of *Eco* ArgRS in adapted buffer.
(Left) Aminoacylation assay was performed using 1 nM *Eco* ArgRS and 60 pmol *Eco* tRNA[Arg] in buffer MRE. Aliquots of 10 µl have been taken after 0, 2, 4, and 6 min (assay performed by A. Gaudry). (Right) Aminoacylation assay was performed using 100 nM *Eco* ArgRS and 40 pmol tRNA[Arg] from *S. cerevisiae*, and *R. culicivorax* in buffer MRE. Aliquots of 10 µl have been taken after 0, 4, 8, 15 and 20 min.

We suspected that *Rcu* ArgRS may be also sensitive for buffer composition, and performed a test series using 10 µl of purified *Rcu* ArgRS S29 and 24 pmol of tRNA[Arg] by varying [Mg^{2+}]/[ATP] ratio from 1 to 10 (Figure 61). However, no enzyme activity could be detected in any of the tested condition. The *Rcu* enzyme was also not active on *Eco* and *Sce* tRNA extracts (data not shown), suggesting that all tested conditions are not optimal for the enzyme yet, that the enzyme quality or quantity was insufficient, or that the tRNAs do not represent appropriate substrates.
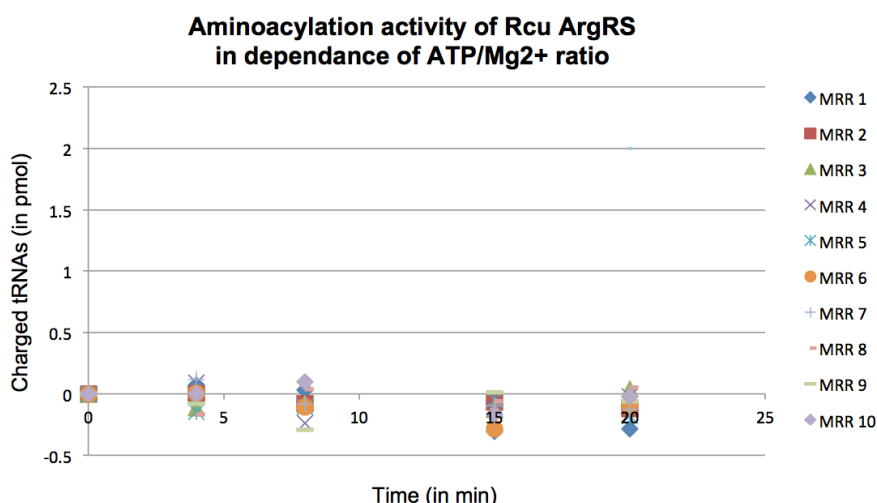

Figure 61: Aminoacylation activity of *Rcu* ArgRS in adapted buffer.
Aminoacylation assay was performed with 10 µl of *Rcu* mt ArgRS S29 eluate and 30 pmol *Rcu* tRNA[Arg] in buffer MRR with varying Mg^{2+} concentrations ([Mg^{2+}]/[ATP] ratio of buffer MRR 1 = 1, [Mg^{2+}]/[ATP] ratio of buffer MRR 2 = 2, etc.). Aliquots of 10 µl have been taken after 0, 4, 8, 15 and 20 min.

148

20. Discussion

20.1.   Identification and preparation of *Rcu* mt ArgRS

The initial (published) annotation predicted two fragments that showed similarity for N-terminal and C-terminal parts compared to ArgRS sequences from other organism, that were identified by multiple sequence alignments. Nevertheless, a linker sequence between both fragments remained unclear, but could successfully be identified by reverse transcription PCR. In addition, the *Rcu* mt ArgRS sequence was complemented and confirmed by an own annotation, based on the original RNA-seq data. These studies led to the identification of the nucleotide sequence coding for the *Rcu* mt ArgRS, and revealed the first complete and verified sequence of an aminoacyl-tRNA synthetase from *R. culicivorax.* This protein is available for structural and functional analysis now.

Many proteins that are translated in the cytosol but dedicated to mitochondria, carry often a N-terminal MTS, which leads to a mature protein after cleavage of the precursor protein (Schmidt *et al.*, 2010). With regards to protein characterization, the determination of correct cleavage sites is not only important for efficient expression and purification of the mature proteins, but also for the determination of their activities. Several cleavage motifs are known. However, they lack a common consensus sequence (Gavel and Heijne, 1990). MTSs are often characterized by positively charged amino acids and may form amphiphilic helices. This and other sequence features are used by bioinformatics tools for the prediction of cleavage sites (Fukasawa *et al.*, 2015).

It was extremely difficult to identify the precise cleavage site of the *Rcu* mt ArgRS sequence. Commonly used prediction tools either did not detected a precise cleavage site at all (TargetP, Predotar, and TPpred2), or predicted a cleavage site only with a low probability (MitoProt, MitoFates). In some cases a wrongly predicted cleavage site led to weak protein amounts after bacterial expression. Only the correction by the removal or addition of several N-terminal amino acids, as it was the case for the human mt LysRS (Bullard *et al.*, 2000; Yao *et al.*, 2003) and the human mt AspRS (Gaudry *et al.*, 2012; Neuenfeldt *et al.*, 2013) led to soluble active proteins. The identification of the correct cleavage site demands special caution and should be moreover experimentally determined. For this reason, eight *Rcu* mt ArgRS variants, which differ in the definition of their N-terminus of the mature proteins (lacking the putative MTS), were cloned and tested for expression, purification and activity. However, it should also be considered that

the putative MTS of the *Rcu* mt ArgRS may not be cleaved and that a full-length protein is active in *R. culicivorax*.

We observed that most variants were not suitable for expression in BL21 (DE3) and Rosetta (DE3) *E. coli* strains, as they were not detectable by Western blot analysis or they were only present as aggregates in the pellet fraction. The best yield, sufficient for purification, was obtained by expression in *E. coli* Arctic Express cells at low temperature for the protein variants D16, D28, and S29. Several other studies reported already about the increased solubility of recombinant expressed protein in this bacterial strain (Gopal and Kumar, 2013; Belval *et al.*, 2015).

However, the main disadvantage of this cell line is that the two cold-adapted chaperons Cpn60 and Cpn10, which are co-expressed to allow the proper folding of the recombinant protein, are also often co-purified and thus impair the purity of the eluted protein solution. An appropriate purification protocol has to be adapted for every recombinant expressed protein when using this cell line because the described protocols in the literature and also the newly developed protocol for the purification of the *Rcu* CCA-adding enzyme with denatured proteins and dissociation buffer did not led to an improved purification. The only protocol that finally led to a significantly release from chaperons consisted of a washing step with 2M urea in combination with a dissociation buffer. The urea concentration is under denaturing condition, and is compatible with affinity chromatography on nickel columns (Belval *et al.*, 2015). Only one of the numerously tested variants, i.e., S29, was finally achieved in very small quantities and could be used for initial aminoacylation assays.

20.2. Functional characterization of *Eco*, *Sce* and *Rcu* (S29) ArgRS interacting with armless mt tRNA[Arg]

Aminoacylation assays were performed in order to characterize arginylation activity of the prepared mt-ArgRS variant S29 from *R. culicivorax*. The protein was subjected to *in vitro* transcribed armless mt tRNA[Arg_CCA] and total tRNA extracts from *E. coli* and yeast. Arginylation of *S*ce and *Eco* ArgRS have been intensively studied already (Sissler *et al.*, 1996, 1998; McShane *et al.*, 2016; Tamura *et al.*, 1992; Aldinger *et al.*, 2012), and have thus been used in this study to monitor and confirm the functionality of the experimental setup and to perform a comparative analysis of the test results. *Eco* and *Sce* ArgRSs have therefore been tested with their cognate tRNAs as well as with armless tRNAs from

R. culicivorax. We confirmed that both cytosolic enzymes recognize their cognate tRNAs as substrates.

We could also show that the *E. coli* and yeast enzymes have optimal activities in distinct buffers with $[Mg^{2+}]/[ATP]$ ratio of 2.5 and 1.5, respectively. This observation is of particular importance for the *E. coli* synthetase, where the charging level increases 10-fold in low $[Mg^{2+}]/[ATP]$ MRE buffer compared to high $[Mg^{2+}]/[ATP]$ MRC buffer. We conclude that reaction buffers are not only important for maintaining pH and solubility of enzymes, but also may influence enzyme activity, and therefore need to be carefully selected and optimized for each aaRS.

However both, *Eco* and *Sce* ArgRS, did not recognize the armless tRNA[Arg] from *R. culicivorax*. We assume that truncated tRNAs are probably not appropriate substrates due to missing structural identity elements, which have been reported to be important for tRNA[Arg] recognition. Indeed, identity elements determine the specific recognition between aminoacyl-tRNA synthetases and tRNAs (Vasil'eva and Moor, 2007). In most tRNAs, the majority of recognition determinants are located in the anticodon and the acceptor stem region (Giegé *et al.*, 1998). In addition to leucine and serine, arginine is genetically encoded by six different codons, which means that a corresponding synthetase must be able to recognize six different tRNA molecules with six different anticodons. This leads to the assumption that additional identity elements are required, beside those present in anticodons and acceptor stems, to maintain nevertheless specificity (McShane *et al.*, 2016).

It has been demonstrated for *Eco* tRNA[Arg] that identity elements are present in three distinct regions: within C_{35} and G/U_{36} in the anticodon loop, within the discriminator base G_{73} or C_{73}, which contribute only modestly to recognition, and within A_{20} in the single-stranded region of the D-loop (Tamura *et al.*, 1992). A_{20} is highly conserved among the tRNA[Arg] species in most organisms (Sprinzl, 1998), and is one of the major identity elements of tRNA[Arg] (Shimada *et al.*, 2001a). Since classical D-arms and loops are not present in armless tRNAs[Arg], arginylation activity of *Eco* ArgRS seems to be strongly dependent on the presence of this major recognition element at position 20, and because it has been shown elsewhere that *Eco* ArgRS could not recognize animal mt tRNA[Arg] (Buck and Nass, 1969; Igloi and Leisinger, 2014), it was likely that the *Eco* enzyme did not aminoacylate the armless mt tRNAs from *R. culicivorax* due to the absence of A_{20}.

Interestingly, tRNA^{Arg} does not exhibit a conserved A$_{20}$ in S. *cerevisiae* and most animal mitochondria. Instead, this nucleotide is often replaced by U, dihydrouridine (D), or C at position 20 (Sprinzl, 1998). It has been demonstrated that C$_{35}$ and G/U$_{36}$ in yeast tRNA^{Arg} are essential for aminoacylation, and therefore represent major identity elements (Sissler *et al.*, 1996). *Rcu* tRNAs^{Arg} possesses both identity elements (i.e., C$_{35}$ and U$_{36}$), and should therefore theoretically be accepted by *Sce* ArgRS. However, armless mt tRNAs^{Arg} are not aminoacylated by this enzyme. This leads to the question, whether specific recognition elements exist for mt arginyl tRNAs. In 2014, Igloi and Leisinger presented a large study on identity rules of mt tRNAs^{Arg} from a wide range of animal taxa, and revealed that identity elements of metazoan mt tRNAs^{Arg} stayed highly conserved during evolution. Their identity elements resemble those that have been identified for the cytoplasmic system in yeast. However, the authors hypothesize that alternative identity elements, or a modulated recognition mechanism may exist for nematode mt tRNAs (Igloi and Leisinger, 2014).

Concerning armless tRNAs^{Arg} from *R. culicivorax* it is possible that major identity elements are present in the anticodon loop, which is supported by the presence of conserved nucleotides C$_{35}$ and U$_{36}$. It would be interesting to study, and to identify the presence of possible other identity elements for *Rcu* tRNA^{Arg}, once enzyme activity is determined. For this purpose, different tRNA mutants that carry point mutations could be prepared and tested. However, it should be considered that probably not only single nucleotides are responsible for tRNA recognition, but the whole particular tRNA architectures of armless tRNAs may play an important role.

So far, no enzyme activity could be obtained for *Rcu* mt-ArgRS neither with armless mt tRNAs, nor with cytosolic tRNAs under the tested conditions. Several reasons may be responsible for this phenomen: (i) It is possible that the quantity or quality of the enzyme was not sufficient. The preparation of this enzyme variant, i.e., S29, was performed under suboptimal conditions. Expression was only possible in Arctic Express cells, and yielded only in low quantities. Additionally, eluted protein was still contaminated by other proteins, whose impact on structure and functionality of the ArgRS is unknown. Further investigations are needed to improve the yield and purity of *Rcu* mt ArgRS.

 (ii) It could be possible that S29, which represents the protein variant that is best producible by protein preparation compared to the other tested protein variants, is only

poorly active. Therefore, further protein variants need to be screened to identify alternatives that can be expressed and purified, and that are suitable for activity analysis. (iii) Since we were able to show that *Eco* ArgRS is sensitive to the buffer conditions, we conclude that adapting buffer conditions is crucial for studies on all involved synthetases. Therefore, a series of tests with different buffer compositions, varying in the ratio of $[Mg^{2+}]/[ATP]$, was performed. However, the S29 variant showed no activity under any of the tested conditions. (iv) The *in vitro* transcribed tRNA substrates were carefully prepared, following the described protocol. However, it is still unknown whether *Rcu* ArgRS accepts *in vitro* products, or only *in vivo* synthesized tRNAs carrying posttranscriptional modifications. Although, it is usually possible to aminoacylate unmodified substrates, the impact of modification is still unclear and is maybe much more important for the stability of armless tRNAs. Each of the mentioned problems still needs to be further investigated to ultimately perform successful aminoacylation studies.

An interesting alternative assay to classical aminoacylation assays would be binding tests, in which the affinity of enzymes to the tRNAs could be determined, as described by (McShane *et al.*, 2016). In such an experiment, also referred to as electrophoretic mobility shift assay (EMSA), tRNAs and enzymes are incubated together, and separated by electrophoresis. A shift between both samples (tRNAs with and without enzyme) would indicate tRNA binding. Since aminoacylation is normally a two-step reaction, one could additionally detect the activation of amino acids. However, it has been shown that ArgRSs require usually tRNAs for amino acid activation. If this is a characteristic also for *Rcu* mt-ArgRS, it would make this analysis to perform more challenging.

20.3.   Co-evolution of *Rcu* mt ArgRS and armless tRNAs

Once the complete protein sequence of *Rcu* mt-ArgS was identified, it was compared and aligned to other ArgRSs of different organisms. A multiple sequence alignment revealed that the mt-ArgRS sequence that we propose for *R. culicivorax,* can be assigned to a subgroup of cytosolic and mitochondrial sequences from eukaryotes, and is more distant to bacterial ArgRS sequences. The conserved sequence motif "HIGH" and an eqivalent sequence to the conserved "KMSKS" motif could be identified in this comparison. Nevertheless, a striking observation was made in the N-terminal region of the nematode protein. Typically, the N-terminal region contains a structural domain of about 100 amino acids, which is unique among the class I of aaRSs (Bi *et al.,* 2014). It has been

demonstrated by crystal structure analysis that this additional N-terminal domain interacts with the D-loop of tRNAs, and is thus involved in the recognition of the elbow region (outer corner of the L-shape), formed by long range D- and T-loop interactions in classical tRNAs (Cavarelli *et al.*, 1998; Shimada *et al.*, 2001a). A sequence comparison and an I-TASSER 3D structure prediction demonstrate that this additional domain is not present in the *Rcu* enzyme, and seem to be also absent, or at least truncated, in equivalent enzymes of at least one other nematode (*C. elegans*). The loss of this structural domain may indicate a co-evolutionary adaptation to armless tRNAs[Arg] in which the typical elbow region does not exist.

Interestingly, recent studies revealed that co-evolution interferes with different mutation rates between mitochondrial and nuclear DNA encoded factors in animals, indicating that nuclear encoded proteins have a higher mutation rate, and evolve therefore faster than their cytosolic counterparts (e.g., mitochondrial ribosomal proteins as compared to cytosolic ribosomal proteins, or mt aaRS compared to cyt aaRS) (Levin *et al.*, 2014; Adrion *et al.*, 2016). Beside the animal mitoribosome, that seems to compensate reduced RNA content by an extension of protein content (Sharma *et al.*, 2003; Mears *et al.*, 2006), other proteins, e.g., involved in interactions with mt tRNAs, are known for their mitochondrial-nuclear co-evolution. Examples of these proteins, for which co-evolutionary processes related to truncated mt tRNAs have been reported, are elongation factors EF-Tu1 and EF-Tu2 in the nematodes *C. elegans* and *Trichinella* (Ohtsuki *et al.*, 2001; Arita *et al.*, 2006). Both, mt EF-Tu1 and mt EF-Tu2, possess a specific C-terminal extension which allows these enzymes to interact with mt tRNAs lacking T- or D-arms (Watanabe *et al.*, 2014). Furthermore, one single enzyme, i.e., the mammalian mt SerRS, can recognize canonical tRNAs[Ser] as well as D-armless mt-tRNAs[Ser]. This particular recognition mechanism is accomplished through small N- and C-terminal extensions (Chimnaronk *et al.*, 2005). The given examples show a tendency to an increased protein content in nuclear encoded mt proteins, which is supposed to compensate for the loss of RNA content in mitochondria (Suzuki *et al.*, 2001). This is in contrast to the observation that we made for the *Rcu* mt ArgRS, where the protein content is reduced. The intended function of an extra domain (recognition of the elbow region) appears to be no longer necessary for the functionality of this protein, resulting in a loss of this domain. However, it is possible that this evolutionary adaptation is not limited to *Rcu* mt ArgRS, but may also be the case for other mt ArgRS of species carrying armless mt tRNAs as already indicated in *C. elegans*.

CONCLUSION & PERSPECTIVES

21. The role of tRNAs in the RNA world

Since the central dogma of molecular biology was proposed in 1950, the role of RNAs in protein synthesis has been widely appreciated. Fundamental research has shown how important different RNAs are for these processes. While mRNAs are essential for the transcription process and rRNAs built up ribosomes, tRNAs represent the physical linkage between the genetic code and the amino acid sequence of proteins during translation (Lodish H, Berk A, Zipursky SL, et al., 2000).

tRNAs and rRNAs belong to the group of non-coding RNAs (ncRNAs), because they are not translated into a protein. Beside them, a variety of other ncRNAs (e.g., snRNAs, RNAi, miRNAs, and siRNAs), were shown to be indispensable for many cellular processes (Mattick and Makunin, 2006).

Even though tRNAs represent one of the oldest molecule discovered in all domains of life, they are still fascinating study objects (Fujishima and Kanai, 2014). Classical tRNAs are characterized by a cloverleaf secondary structure, which is composed of 4 domains: the amino acid accepting stem, the D-arm, the anticodon arm, and the T-arm. Their tertiary structures resemble the letter "L". This general structure is mainly conserved over all kingdoms of life. In eukaryotes, protein translation is not restricted to the nucleus, but also takes place in organelles, such as chloroplasts and mitochondria. Mitochondria encode a specific set of tRNAs in their own genome, and possess an appropriate translation machinery. In contrast to cytoplasmic tRNAs, metazoan mt tRNAs show unusual structures with reduced sizes, and can even lack complete arms. More and more unusual mt tRNAs, which exhibit extremely truncated sequences, have been discovered in different animal lineages over the last years (Yamazaki *et al.*, 1997; Masta, 2000; Wolstenholme *et al.*, 1987; Jühling *et al.*, 2012b). Truncated mt tRNAs have evolved to an extreme case in nematode species. The roundworm *Romanomermis culicivorax* belongs to the group of nematode species, that were predicted to carry truncated mt tRNAs that even lack both, D-arm and T-arm, and were thus called "armless" tRNAs. Armless tRNAs were predicted to be considerably smaller than their cytosolic counterparts with about 45 nt as compared to 76 nt. This discovery has led to many questions concerning their functionality as well as the molecular mechanisms of co-evolution that I tended to answer during this thesis work.

156

21.1. Do armless tRNAs exist *in vivo*?

The improvement of specialized bioinformatics tools allows now for the detection of bizarre tRNA genes. This led to the discovery of the shortest tRNA genes identified, lacking both lateral arms (Jühling *et al.*, 2012a; Jühling *et al.*, 2012b). These discoveries are mainly based on computational predictions. Structural or functional experimental validations were not performed for most of these predicted mt tRNAs, so far.

However, S. Wende and colleagues were able to show recently, that such putative tRNA genes are indeed transcribed in *R. culicivorax.* They could prove the existence of six of these armless mitochondrial tRNAs by sequencing of RNA extracts using 5'- and 3'-RACE PCR (Wende *et al.*, 2014). Each of the identified *in vivo* transcripts carried the nucleotides C-C-A at its 3' end, while not encoded in the mt genome. This study provides therefore first hints for the existence of functional armless mt tRNAs *in vivo*. Their structural and functional characterization were the main objectives of this study. These results lead to a significant contribution to the knowledge about these specific molecules, whose role has not been fully elucidated, yet.

21.2. Do armless tRNAs fold into classical structures?

The approaches used in this study provided details about the size and shape of the armless mt tRNAs, and led to the reconstruction of secondary and tertiary structure predictions. This allowed us to compare structural properties with those from classical tRNAs, and to identify the minimal architectural requirements of tRNA structures, that are still compatible with their functionality.

Based on the performed secondary structure analysis, we conclude that armless mt tRNAs in *R. culicivorax* form a hairpin-shaped secondary structure. This includes an internal double bulge replacing both, D- and T-arms, in the secondary cloverleaf structure as compared to classical tRNAs. We found no hint for any internal long-range nucleotide interactions, which could be confirmed by additional NMR measurements. We conclude that armless mt tRNAs are exclusively composed of classical Watson-Crick bases pairs forming helices that contribute solely to the formation of secondary structures.

Scattering data obtained from SAXS analysis provided physical parameters that allowed the reconstruction of low-resolution 3D models. In contrast to the L-shape structure of cytosolic tRNA, the tertiary structure models of armless tRNAs resemble rather a

boomerang-shape. This suggests that armless mt tRNAs possess high intrinsic flexibility, that can compensate the predicted truncated maximal distance between the extremities despite their reduced size. Thus, intrinsic flexibility probably facilitates armless tRNAs to interact with partner proteins, and preserves therefore tRNA biosynthesis and protein translation processes in nematode mitochondria.

21.1. Are armless tRNAs biological relevant?

During this study, *Rcu* CCA-adding enzymes and mt ArgRS coding sequences have been identified, and were cloned for the first time. The recombinant proteins have been studied for their interaction with cognate and cytosolic tRNAs in CCA-incorporations assays and aminoacylation assays, respectively. These experiments could be performed only after establishing appropriate expression and purification protocols. The capacity to recognize different tRNA substrates has been compared to the activity of heterologous enzymes from human, yeast, and *E. coli*.

We could show that the *Rcu* CCA-adding enzyme is active, and can efficiently recognize armless tRNAs as well as a cytosolic tRNA, indicating a broad substrate specificity. However, heterologous *Eco* and *Hsa* CCA-adding enzymes seem to be not or only partially compatible with armless tRNAs. We conclude that the incorporation of nucleotides by CCA-adding enzymes works best with the cognate enzyme, and that the *Rcu* enzyme has adapted to the small size of armless mt tRNA during evolution. This study provides therefore *in vitro* evidence for a biological relevance of armless mt tRNAs, especially in terms of CCA-adding processes.

We supposed that *Rcu* mt ArgRS possesses a MTS, like many other mt proteins do, to allow for their import into mitochondria. Many efforts have thus been made to identify a protein variant (deprived of the putative MTS) that is most compatible with expression and purification protocols. So far, only one of the different tested enzyme variants, i.e., S29, could be obtained in low quantity and quality. However, it could be used for aminoacylation assays. The results of this initial study reveal that the *Rcu* enzyme does not recognize either armless tRNAs, nor cytosolic tRNAs under the tested conditions. A comparative analysis with cytosolic ArgRS from yeast and *E. coli* showed that both enzymes have optimal activities in distinct buffers with $[Mg^{2+}]/[ATP]$ ratio of 2.5 and 1.5, respectively. These initially obtained data lead to our assumption that reaction buffers have to be carefully selected and optimized for each ArgRS. Since both, *E. coli* and yeast

ArgRS, do not aminoacylate armless tRNAs[Arg], we suppose that truncated tRNAs are not an appropriate substrate, most likely due to missing identity elements.

21.3. Did evolutionary adaptation take place?

Possible co-evolution events have been revealed during this study, concerning mostly tRNAs and proteins that are partner in the mitochondrial translation machinery.

Identified sequences of the *Rcu* CCA-adding enzyme, and the mt ArgRS have been analyzed using multiple sequence alignments, including heterologous enzymes from different organism as references. Furthermore, bioinformatic structure prediction tools have been used to build 3D models of these enzymes to provide insights into their co-evolution with armless tRNAs.

Compared to other class II CCA-adding enzymes, the *Rcu* CCA-adding enzyme shows high sequence similarity, especially in its N-terminal catalytic core, while the C-terminal domain, which is involved in tRNA recognition, is less conserved. A high flexibility of the C-terminal region may be a possible reason why the *Rcu* CCA-adding enzyme has adapted to armless mt tRNAs without losing its ability to recognize cytosolic tRNAs at the same time. However, it is almost impossible to determine, based only on sequence comparisons, whether the C-terminal part contains the decisive factor that is responsible for the recognition of armless tRNAs. This is the case because CCA-adding enzymes usually show a high degree of variation, but no sequence conservation when comparing their C-terminal regions among each other. It is conceivable, that through the creation of protein mutants or protein chimeras, specific elements of the Rcu CCA-adding enzymes that play a decisive role in the recognition of armless tRNAs, will be identified.

Typically, the structure of ArgRSs contains an additional N-terminal domain. It is involved in the recognition of the edge-region of tRNAs. Both, Sequence comparison and a 3D structure prediction highlight that this additional domain is missing in the *R. culicivorax* enzyme. It seems that the loss of this structural domain indicates a co-evolutionary adaptation to armless tRNA[Arg], for which the typical elbow region does not exist. It will become possible to explore this hypothesis, once active *Rcu* mt ArgRS will be obtained. However, the main structural differences between classical and *Rcu* mt ArgRS concerning tRNA recognition are schematically represented in Figure 62. The figure illustrates the characteristic loss of the N-terminal domain for the *Rcu* mt ArgRS, in combination with the ability of armless tRNAs to compensate the typical distances between the acceptor

stem and anticodon stem through an increased intrinsic flexibility. We hypothesize that these structural adaptations of both, synthetase and tRNA, lead to a possible interaction between enzymes and armless mt tRNAs in *R. culicivorax*.
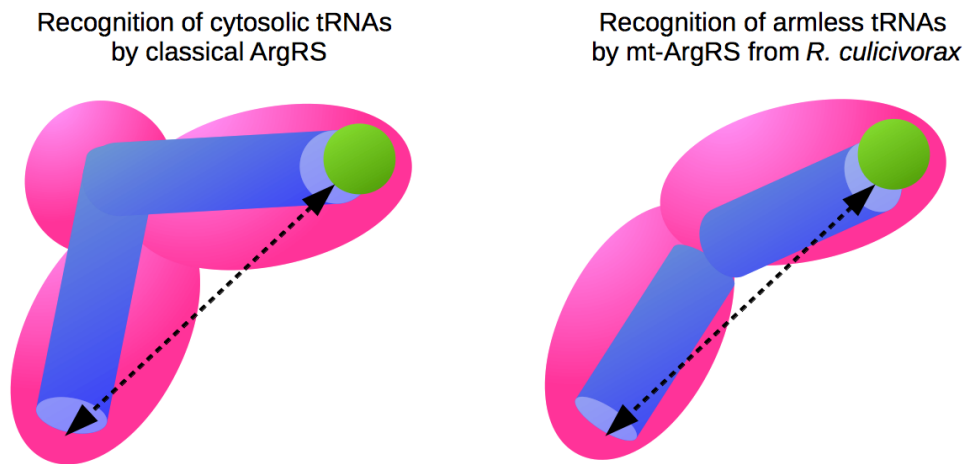

Figure 62: Schematic representation of possible recognition mode of armless tRNAs in ArgRS. (Left) Classical ArgRSs possess an additional N-terminal domain that interacts with the edge region of classical tRNAs, which folds into a typical L-shape 3D structure. (Right) In contrast, mt ArgRS from *R. culicivorax* has completely lost the additional N-terminal and its cognate tRNA will probably fold into a boomerang-shape 3D structure. The distance between the extremities of acceptor stem and anticodon loop (dotted arrows) is probably compensated by the predicted intrinsic flexibility of the armless tRNA based on the SAXS analysis. ArgRSs are represented in pink, tRNA molecules in blue, aminoacid in green.

During translation, tRNAs interact with several sites of the ribosome. It would be thus very interesting to elucidate how recognition of armless mt tRNAs is achieved in the nematode ribosome. It has already been shown that animal mitoribosomes compensate a reduced mt RNA content through an increased protein content. We found indications that the rRNA content is also reduced in *R. culicivorax*, and suppose a ribosomal organization similar to that of animal mitoribosomes. We assume that a combination of an adapted mitoribosome (high protein, low RNA content) together with the proposed high intrinsic flexibility of armless tRNAs may facilitate tRNA recognition in *R. culicivorax*, and thus supports a functional translation process.

21.1. Do armless tRNAs fulfill alternative functions?

It has already been shown that bacterial, eukaryotic, mitochondrial, and even viral tRNAs can fulfill alternative functions in the cell. Beside their conventional role in protein biosynthesis, several tRNAs participate, e.g., in energy metabolism, amino acid synthesis,

regulation of transcription, translation processes, and protein degradation (Kirchner and Ignatova, 2015).

Latest studies in RNA research revealed that small non-coding RNAs play an highly important role in cellular processes. The development of breakthrough next-generation sequencing (NGS) technologies combined with RNA biochemical studies has dramatically advanced our understanding of the cellular transcriptome, and revealed the existence of various different small non-coding RNAs with divers functions (Derks *et al.*, 2014).

Armless mitochondrial tRNAs should be considered as members of this family of molecules. We can therefore assume that armless tRNAs from *R. culicivorax* could also perform alternative functions. Until today, new forms and functions of small non-coding RNAs are discovered regularly. Almost a new research field has been developed with the discovery of tRNA-derived fragments, which are involved in a variety of metabolic processes with different functions in various organisms of all kingdoms of life (Nolte-'t Hoen *et al.*, 2012; Shigematsu *et al.*, 2014; Pliatsika *et al.*, 2016). It is possible that armless tRNAs give rise to such tRFs, or function in a similar manner. This demonstrates that much more work is required to completely understand contribution of armless mt tRNAs to cellular functions.

22. General conclusion and perspectives

The present work has contributed to decipher structural properties of armless mitochondrial tRNAs. Furthermore, the functionality of the *Rcu* CCA-adding enzyme has been determined. Aminoacylation activity of the *Rcu* mt ArgRS could not be proven, so far. Structural particularities of both tRNA interacting partner proteins have been elucidated and suggest evidence for co-evolutionary adaptation of the proteins and armless tRNAs. However, this work still represents a starting point for more profound studies as many questions still remain unanswered.

Since this thesis work was part of a joint PhD program between the University of Leipzig and the University of Strasbourg, biological aspects concerning armless mt tRNAs and their interacting partner proteins will be further elucidated in both host laboratories.

In Leipzig, Oliver Hennig will further study and characterize the enzymatic activity of the *Rcu* CCA-adding enzyme by determining kinetic parameters during his thesis work. Characteristic features of armless tRNAs (not only from *R. culicivorax*) and enzymes chimeras will play a central role for his work to determine, e.g., recognition modes and

parameters. In Strasbourg, Agnès Gaudry will continue to determine optimal assay conditions to allow a characterization of enzymatic activities of the *Rcu* mt ArgRS. It would be also very interesting to analyze characteristic features of other partner proteins that interact with armless tRNAs in *R. culicivorax*, such as EF-Tu, RNase Z, or RNAse P. Here, the group of Philippe Giegé in Strasbourg is already in progress to analyze the mt RNase P of this interesting nematode worm. Additionally, further studies are needed to finally verify 3D structures of armless tRNAs in detail. The collaboration with Claude Sauter (University of Strasbourg) represented already a great starting point for an initial tertiary structure analysis, but can be continued, e.g., with crystallographic studies. As shown in this study, armless mt tRNAs are very stable, and may therefore represent appropriate substrates for crystal structure analysis.

Transfer RNAs play a central role in the origin and evolution of fundamental biological processes, and have fascinated many scientists for over 60 years now. Since they belong to the class of RNAs, they have already largely contributed to our understanding in RNA structure and biology (Phizicky and Hopper, 2015). The fact that tRNAs, and RNAs in general, have a great influence on our organism is clearly shown by the long list of Nobel Prize laureates who have been awarded for their work in the field of RNA biology. For example, for the discoveries concerning the molecular structure of nucleic acids (Wilkins, Crick and Watson in 1962), for the discovery of the catalytic properties of RNAs (S. Altman, T. R. Check in 1989), for the discovery of RNA interference (A. Z. Fire and C. C. Mello in 2006), and for studies of the structure and function of the ribosome (A. Yonath, V. Ramakrishnan, and Thomas A. Steitz in 2009), just to mention a few of them.

Many other discoveries concerning, e.g., RNA biogenesis, processing and regulation (reviewed in (Phizicky and Hopper, 2015) are very interesting and crucial for our understanding of RNA biology. The discovery of armless tRNAs in mitochondria, and their structural as well as functional characterization, represent also very exciting discoveries in my opinion.

I am sure that with the development of new technologies or the improvement of already existing tools (e.g., NGS tools, spectrometric methods, growth conditions, and others), many new discoveries are just waiting to be investigated, and will further delight our understanding about tRNA and RNA biology.

RÉSUMÉ & ZUSAMMENFASSUNG

Résumé

Les ARN de transfert (ARNt) jouent un rôle fondamental dans la biosynthèse des protéines. Ils sont en effet des partenaires clés de la machinerie ribosomique de la traduction de l'information génétique en protéines, en fournissant les acides aminés spécifiques permettant la synthèse progressive de la chaîne peptidique à partir du message codé sur l'ARN messager. Molécules « adaptatrices » imagées d'un point de vue théorique comme une nécessité par Francis Crick en 1958 avant même leur découverte, les ARNt ont fait l'objet d'études incessantes depuis lors et restent aujourd'hui encore au centre de nombreuses découvertes (Crick, 1955; Phizicky and Hopper, 2015). Ces petits ARN non codants ont, de manière classique une structure largement conservée avec une constitution moyenne de 75 nucléotides. Leur structure secondaire ressemble à une feuille de trèfle, qui se compose de quatre tiges et trois boucles: la tige acceptrice, sur laquelle sera estérifié l'acide aminé correspondant à l'ARNt, le bras D, le bras de l'anticodon, qui reconnaît et s'associe aux codons de l'ARN messager, et le bras T. La structure tertiaire ressemble à la lettre L, l'anticodon étant à l'une des extrémités et la fixation de l'acide aminé se faisant à l'autre (Giegé *et al.*, 2012). Les structures secondaires et tertiaires sont complétées par l'action d'une série d'enzymes de maturation et de modifications post-transcriptionnelles. Les ARNt matures sont alors substrats de la famille d'enzymes, les aminoacyl-ARNt synthétases, qui chargent les ARNt avec leur acide spécifique. Chez les eucaryotes, il coexiste une machinerie de synthèse protéique cytosolique et une machinerie dans les organelles, tels que les chloroplastes et les mitochondries. Ainsi, il existe également des jeux d'ARNt dédiés à ces synthèses, partiellement ou totalement codés par les génomes de ces organelles (Salinas-Giegé *et al.*, 2015). Les mitochondries, en particulier des animaux, codent pour un ensemble complet d'ARNt dans leur propre génome permettant une traduction appropriée de l'information génétique de l'ADN mitochondrial.

Alors que les ARNt cytoplasmiques ont des motifs structuraux fortement conservés, les ARNt des mitochondries des animaux présentent des structures inhabituelles, des dégénérescences et bizarreries diverses. Nombreux sont ceux qui ont une taille réduite, ont perdu des éléments de structures typiques, ou ont perdu des domaines complets. Un

cas extrême de ces écarts structuraux a été trouvé dans les mitochondries d'Enoplea (une classe de vers nématodes). Ces ARNt nouvellement découverts sont dépourvus aussi bien du bras D que du bras T et ont été appelés ARNt "manchots". *Romanomermis culicivorax* correspond à un représentant des Enoplea dans le génome mitochondrial duquel de nombreux gènes d'ARNt prédisent l'existence de tels ARNt manchots (Jühling *et al.*, 2012b). Des premiers indices quant à l'existence d'ARNt manchots dans des extraits de *R. culicivorax* ont rapidement été apportés par le séquençage de petits ARN, et de leur possible activité biologique, par la démonstration d'un événement de maturation post-transcriptionnelle, à savoir l'incorporation du triplet terminal CCA non codé par le gène (Wende *et al.*, 2014).

L'objet de cette thèse concerne la caractérisation d'ARNt "manchots" portant sur leurs propriétés structurales et l'étude de différents aspects de leur fonctionnalité, en particulier leur interaction avec deux enzymes partenaires, l'ARNt nucleotidyltransferase (CCAse) - une enzyme de maturation, et l'aminoacyl-ARNt synthétase. Pour cette étude, nous avons choisi de caractériser les ARNt^{Arg} et ARNt^{Ile} mitochondriaux de *R. culicivorax*. Dans un premier temps la structure en solution des deux ARNt (obtenu par transcription *in vitro*) a été établie. Les approches telles que le sondage enzymatique et chimique, la spectroscopie de résonance magnétique nucléaire (RMN), et la diffusion des rayons X aux petits angles (small angle X-ray scattering ou SAXS) ont été utilisées. Ceci a permis de définir les éléments de structure secondaire, de rechercher des interactions intramoléculaires ainsi que d'aborder les enveloppes globales de structures tridimensionnelles. Les protéines partenaires, à savoir la CCAse de *R. culicivorax* et l'arginyl-ARNt synthétase mitochondriale ont été identifiés à partir d'un génome partiellement annoté, et clonés par amplification à partir d'ARN total extrait du ver, et surexprimées afin de défricher certaines de leurs propriétés fonctionnelles, en particulier leur capacité à reconnaître les ARNt manchots comme substrats. Ainsi, des essais d'incorporation de CCA et d'aminoacylation ont été effectués. Certaines propriétés de ces enzymes sont également comparées à celles des enzymes homologues d'*E. coli*, de la levure et de la mitochondrie humaine (en cours d'étude dans les laboratoires hôtes) afin de décrypter les relations évolutives des couples ARNt manchots/protéines partenaires de *R. culicivorax*.

Analyse de la structure de deux ARNt manchots

Afin d'étudier la structure des ARNt^{Arg} et ARNt^{Ile} de *R. culicivorax*, les gènes correspondants ont été clonés et les ARN obtenus par transcription *in vitro*. Trois approches différentes et complémentaires d'analyses structurales ont été utilisées : i) les sondages enzymatique et chimique (in-line probing), ii) la spectroscopie RMN et iii) la diffusion des rayons X aux petits angles (SAXS).

Les approches de sondage enzymatique et chimique sont des méthodes permettant l'étude de la structure en identifiant les régions de l'ARN en simple ou double brin. Les résultats de cette analyse ont révélé que les deux ARNt forment une structure secondaire en forme d'épingle à cheveux comprenant un double renflement (bulge) aux endroits remplaçant les deux bras latéraux dans une structure secondaire en feuille de trèfle classique. Les données collectées par cette approche n'ont pas permis de détecter la présence d'interactions nucléotidiques internes au sein des renflements. Les structures sont stables et robustes (pas de dégradations, pas de conformations alternatives) malgré leur composition primaire très biaisée en faveur des nucléotides A et U (76 % et 87 % pour ARNt^{Arg} et ARNt^{Ile} respectivement).

En utilisant la spectroscopie RMN qui est une technique puissante pour détecter les interactions intramoléculaires tertiaires nous pouvons confirmer que les ARNt manchots possèdent exclusivement des paires de bases classiques Watson-Crick formant les hélices de la structure secondaire. Aucun signal en faveur de paires de bases inhabituelles n'a été détecté, suggérant l'absence d'interactions tertiaires dans les zones des renflements. Cette absence est remarquable puisque de telles interactions servent à stabiliser les structures 3D des ARN et des ARNt en particulier.

Le SAXS nous a servi à mesurer certaines caractéristiques physiques reliées à la forme et aux dimensions de la structure 3D des ARNt. Cela nous a permis de calculer des formes 3D (enveloppes moléculaires) pour chacun des deux ARNt qui, sans être identiques, sont très comparables à celles obtenues par l'analyse SAXS d'un ARNt « classique » (ARNt^{Phe} de levure). Etonnamment, la dimension maximale de ces objets en solution (correspondant à la distance maximale entre les atomes les plus éloignés dans la structure) est du même ordre. Une différence concerne une plus grande variabilité des enveloppes pour les ARNt manchots, suggérant une plus grande flexibilité intrinsèque de la structure 3D.

Les résultats obtenus par les différentes méthodes utilisées montrent que les transcrits *in vitro* des ARNt manchots ont apparemment une structure très simple, qui se compose de

paires de bases classiques de type Watson-Crick formant deux hélices séparées par un renflement central, que les structures ne contiennent pas de connexions tertiaires internes particulières qu'elles sont chimiquement stables et ne conduisent pas à des structures secondaires alternatives. Au niveau 3D cependant une plus grande souplesse/flexibilité anticipe une adaptabilité plus importante pour l'interaction avec les protéines partenaires.

L'ARNt nucleotidyltransferases (CCAse) de *R. culicivorax*

Habituellement, dans les eucaryotes un seul gène de la CCAse existe codant à la fois pour l'enzyme cytosolique et une enzyme mitochondriale. L'enzyme mitochondriale est produite à partir d'un codon d'initiation alternatif et contient une «séquence d'adressage mitochondrial" (MTS), localisée à l'extrémité N-terminale. La MTS est clivée au cours du processus d'importation, résultant en une protéine mature. Le seul gène codant pour une CCAse que nous avons détecté dans le génome nucléaire de *R. culicivorax* possède un site de clivage très similaire à celui de l'enzyme humain lequel nous avons utilisé pour le clonage.

La séquence protéique résultant du gène cloné a été alignée à d'autres CCAses de différents organismes. Ces alignements ont permis de conforter l'organisation secondaire. En comparaison avec la CCAse mitochondriale humaine nous constatons une identité de séquence globale de 46 %. En particulier, le domaine N-terminal, correspondant classiquement au site catalytique (responsable et de l'addition des nucléotides) a un taux d'identité élevé (66 %) alors que le domaine C-terminal, dont la fonction est de la reconnaitre les ARNt, présentent un degré élevé de variation. Les séquences de la bactérie et de la levure sont plus éloignées de la séquence du ver avec seulement 21 % d'identité.

La séquence du gène de la CCAse a été clonée en vue d'une surexpression et purification de l'enzyme mature correspondante. Un protocole de purification pour les CCAse humaines et bactériennes bien établi dans le laboratoire hôte à Leipzig n'a pas pu être appliqué pour la purification de l'enzyme de *R. culicivorax* en raison du faible rendement et de l'impossibilité d'éliminer des contaminants bactériens. Par conséquent, plusieurs souches bactériennes ont été testées en vue d'une expression suffisante, et un protocole de purification mis au point. La protéine finalement purifiée et a été testée pour ses capacités à incorporer des nucléotides C-C-A à l'extrémité 3' des ARNt manchots (transcrits *in vitro* dépourvus du CCA). Pour une analyse comparative, un ARNt classique

cytosolique ainsi que les CCAses mitochondriale humaine et d'*E. coli* ont aussi été purifiées et testées.

Les résultats montrent que l'enzyme de *R. culicivorax* est active: elle est capable de reconnaître les ARNt manchots et reconnaît également les ARNt classiques. L'incorporation de la séquence CCA se fait de manière complète pour tous les substrats. Cependant, fait intéressant, les CCAses hétérologues ont beaucoup de difficultés à reconnaître les ARNt manchots. Alors que l'enzyme humaine reconnaît encore faiblement les ARNt bizarres et ajoute partiellement les nucléotides CCA, l'enzyme bactérienne ne reconnaît pas du tout les ARNt manchots comme substrat.

Ces résultats sont en faveur soit d'une adaptation évolutive de l'enzyme du ver à la structure inhabituelle de ses ARNt mitochondriaux soit d'une coévolution des deux partenaires. Le fait que l'enzyme d'*E. coli* ne reconnaisse pas les ARNt mitochondriaux manchots de *R. culicivorax*, suggère que l'évolution n'a pas permit à cette enzyme de s'adapter à ces ARNt non classiques, due à l'absence de mitochondrie chez les bactéries. Contrairement à l'enzyme humaine, qui elle s'est adapté évolutivement à ses ARNt mitochondriaux bizarres. D'où leur capacité partielle à reconnaître les ARNt manchots de *R. culicivorax*.

L'arginyl-ARNt synthétase (ArgRS) mitochondriale de *R. culicivorax*

La séquence du gène de l'ArgRS mitochondriale de *R. culicivorax* a été prédite par annotation du génome, puis complétée et corrigée par une annotation propre basée sur les données d'origine RNA-seq et par PCR à transcription inverse. Le gène ainsi défini a été cloné en vue de la surexpression de la protéine à des fins d'analyse enzymatiques. La séquence protéique a alors été comparée et alignée à d'autres ArgRS de différents organismes à l'aide d'outils bio-informatiques. Alors que la séparation entre les grands groupes d'espèces est peu visible pour les ArgRS, la séquence d'ArgRS que nous proposons pour *R. culicivorax* se trouve dans un sous-groupe de séquences cytosoliques et mitochondriales d'eucaryotes et est très distante des séquences d'ArgRS bactériennes.

Habituellement, la structure secondaire d'une ArgRS est composée d'un domaine catalytique, d'un domaine de liaison à l'anticodon et d'un domaine N-terminal qui est impliqué dans la reconnaissance de l'ARNt. Ce dernier domaine est absent dans l'enzyme de *R. culicivorax* et est également absent ou tronqué pour les enzymes équivalentes dans d'autres nématodes. De manière intéressante la reconnaissance de l'ARNt se fait au

niveau du coude du L, formé par l'interaction des boucles D et T d'un ARNt classique. Cette perte pourrait signifier une adaptation aux ARNt manchots (pour lesquels le coude du L n'existe pas) et représente peut-être un indice pour un événement co-évolutif entre ARN et protéine partenaire.

Comme d'autres protéines qui sont dédiés aux mitochondries, l'ArgRS porte aussi une «séquence d'adressage mitochondrial" (MTS) à l'extrémité N-terminale. Dans ce cas il était plus difficile à identifier le précis site de clivage. Pour cette raison, 8 variantes de l'ArgRS qui diffèrent dans la définition de l'extrémité N-terminale de la protéine mature (dépourvue du MTS), ont été clonés et testés pour l'expression, la purification et l'activité. Nous avons observé que seulement quelques variantes ne s'agrègent pas et juste une seule variante que nous avons nommé S29, a pu être obtenu en très faibles quantités et a été testé.

Les tests d'aminoacylation ont été effectués avec l'enzyme purifiée et l'ARNt^{Arg} manchot et l'ARNt totaux d'*E. coli* et de la levure. Pour contrôler et comparer la fonctionnalité de l'essai, les ArgRS d'*E. coli* et de la levure ont été également utilisées et testées avec leurs ARNt homologues et celui de *R. culicivorax*. Les enzymes d'*E. coli* et de la levure ont des activités optimales dans des tampons distincts, où les rapport [Mg^{2+}]/[ATP] sont de 2,5 et 1,5, respectivement. Alors que nous avons pu confirmer que chacune de ces deux enzymes reconnaissent leur substrat homologue, mais que aucune de ces deux enzymes ne reconnait pas le transcrit de l'ARNt^{Arg} de *R. culicivorax*. En outre, l'enzyme de *R. culicivorax* n'était active ni avec les ARNt manchots ni avec les ARNt classiques. Cela peut avoir plusieurs raisons. Entre autre il est possible que la quantité ou la qualité de l'enzyme ne soit pas suffisante ou que cette enzyme soit également sensible aux conditions de la réaction. Nous avons donc effectué une série de tests avec des compositions de tampon différentes. Mais jusqu'à présent l'enzyme ne montre aucune activité dans les conditions testées.

Conclusion & Perspectives

Nos travaux apportent des éléments en faveur d'une réalité biologique pour les ARNt les plus petits au monde, du moins en ce qui concerne des informations de structure et la maturation par la CCAse. Nos travaux ont également permis de déchiffrer des éléments de coévolution entre les partenariats ARN/protéine de la machinerie traductionnelle des mitochondries.

Grâce aux résultats obtenus on comprend mieux leurs caractéristiques structurelles aussi bien des ARNt que des deux protéines étudiées. Les approches utilisées dans cette étude ont fourni des détails sur la taille et la forme des ARNt mitochondriaux manchots. À partir de ces investigations nous sommes capable de reconstruire une prédiction de structure secondaire et tertiaire. Cela permet une comparaison avec les structures des ARNt classiques et d'identifier les éléments les plus minimes d'un ARNt qui sont compatible avec la vie. En effet, il a déjà été montré que des mini-hélices d'ARNt peuvent être des substrats pour la CCAse et être aminoacylées. Ceci suggère que la taille et la structure ARNt manchots tels que découverts dans les Enoplea ne sont peut-être pas les formes les plus petites d'ARNt qui existent dans le vivant. D'autres études sont nécessaires afin de résoudre la structure 3D de manière détaillée. À ce jour, aucune structure cristalline complète d'un ARNt mitochondrial n'existe, ce qui rend cette démarche un challenge important mais difficile.

Pour la première fois nous avons purifié des protéines recombinantes de *R. culicivorax*, en particulier la CCAse et l'ArgRS mitochondriale et nous avons étudié leur interaction avec les ARNt. Les deux protéines du ver ressemblent en séquence et structure plus à leurs homologues d'eucaryote en particulier celles d'autres nématodes. Cependant nous avons identifié des changements structuraux pour les deux enzymes, qui pourraient être l'expression d'une adaptation aux ARNt manchots.

Concernant la CCAse, il nous reste à vérifier si l'extrémité C-terminale de la CCAse est en effet un facteur responsable pour l'acceptance des ARNt manchots comme substrat. Cependant nous pouvons conclure que l'incorporation de nucléotides par la CCAse fonctionne le mieux avec l'enzyme apparentée comme l'enzyme du ver qui s'est adaptée apparemment à la taille réduite des ARNt mitochondriaux manchots au cours de l'évolution.

L'étude de l'arginyl-ARNt synthétase nous a fourni des indications en termes de coévolution des protéines. Concernant le changement structural de l'ArgRS, il semble que la perte du domaine N-terminal soit une adaptation évolutive à la perte des deux bras de cet ARNt bizarre. Nous serons en mesure d'explorer cette hypothèse, une fois qu'une ArgRS mitochondriale active de *R. culicivorax* sera obtenue. Au cours des tests d'aminoacylation les autres enzymes d'*E. coli* et de la levure ont aminoacylé les ARNt classiques mais pas l'ARNt manchot, nous en concluons que sa déviation structurelle est probablement trop extrême pour ces enzymes.

Enfin, les petits ARN non-codants jouent un rôle de plus en plus important dans notre vie. Ils sont impliqués dans une variété des processus métaboliques avec différentes fonctions. Les petits ARNt mitochondriaux manchots devrait faire partie à ce membre de cette famille de molécules. Nous pouvons donc supposer que les ARNt manchots de *R. culicivorax* peuvent également exécuter des fonctions alternatives. Leur caractérisation structurale et fonctionnelle mène certainement à une contribution importante à ces molécules spécifiques dont leur rôle n'a pas encore été complètement élucidé.

Zusammenfassung

Transfer RNAs (tRNAs) übernehmen eine wichtige Rolle bei der Proteinbiosynthese, indem sie die spezifischen Aminosäuren für die schrittweise Synthese der Peptidkette bereitstellen und somit als Bindeglied zwischen dem genetische Code der Boten-RNA (mRNA) und der Aminosäuresequenz der Proteine fungieren. Bereits vor ihrer Entdeckung um 1958, wurde die Notwendigkeit bestimmter "Adapter" Moleküle von Francis Crick vorausgesagt (Crick, 1955). Seitdem waren diese faszinierenden Moleküle von entscheidender Bedeutung für viele Entdeckungen und sie sind nach wie vor Zentrum zahlreicher Studien (Phizicky and Hopper, 2015). Diese kleinen nicht-codierende RNAs besitzen eine charakteristische hoch konservierte Struktur mit durchschnittlich 75 Nukleotiden. Die Sekundärstruktur ähnelt einem Kleeblatt, das aus vier Domänen besteht: dem Akzeptor-Stamm, auf dem die Aminosäure an die tRNA geladen wird, dem D-Arm, dem Anticodon-Stamm, welcher die Codons der mRNA erkennt und verbindet, und dem T-Arm. Die Tertiärstruktur gleicht dem Buchstaben L, wobei der Anticodon-Stamm die eine Achse und der Akzeptor-Stamm die andere Achse der L-Struktur bildet (Giegé *et al.*, 2012). Sekundär- und Tertiärstruktur werden von zahlreicher Reifungs- und Modifikationsenzymen erkannt und prozessiert. Reife tRNAs sind auch Substrate von Aminoacyl-tRNA-Synthetasen. Diese Familie von Enzymen beladen die tRNA mit ihrer spezifischen Aminosäure. In Eukaryoten koexistiert neben der zytosolischen Proteinsynthesemaschinerie auch solch eine Maschinerie in den Organellen, wie den Chloroplasten und den Mitochondrien. Folglich gibt es ein zusätzliches Set an tRNAs, welches komplett oder teilweise auf dem Genom dieser Organellen kodiert ist und für deren Proteinsynthesen bestimmt ist. Vor allem tierische Mitochondrien, kodieren einen vollständigen Satz von tRNAs in ihrem eigenem Genom, welches für die richtige Übersetzung der genetischen Information der mitochondrialen DNA verantwortlich ist (Salinas-Giegé *et al.*, 2015).

Während die zytosolischen tRNAs hochkonservierte Strukturmotive haben, zeigen die tRNAs von tierischen Mitochondrien ungewöhnlichen Strukturen und Eigenarten. Viele mitochondriale tRNAs haben eine reduzierte Größe und typische Strukturelemente sind teilweise oder komplett verloren gegangen. Ein extremer Fall dieser minimalisierten tRNAs wurde in den Mitochondrien von Enoplea, welche zur Klasse der Nematoden gehören, gefunden. Diesen neu entdeckten tRNAs fehlen sowohl der D-Arm, als auch der

T-Arm. Sie wurden deshalb „armlose" tRNAs genannt. Der Rundwurm *Romanomermis culicivorax* ist ein typischer Vertreter der Enoplea, in dessen mitochondrialem Genom solche armlosen tRNAs vorhergesagt wurden (Jühling *et al.*, 2012b). Die Existenz dieser armlosen tRNAs wurde durch Sequenzierung von RNA Extrakten aus *R. culicivorax* nachgewiesen. Außerdem konnte gezeigt werden, dass zumindest ein post-transkriptioneller Reifungsprozess erfolgt, was auf eine mögliche biologische Aktivität der kleinen tRNAs hindeutet (Wende *et al.*, 2014).

Das Ziel dieser Arbeit ist die Charakterisierung von „armlosen" tRNAs. Dabei sollen vor allem ihre strukturellen Eigenschaften und ihrer Funktionalität, insbesondere in Bezug auf ihre Interaktion mit Partnernproteinen, wie der tRNA-Nukleotidyltransferase und der Aminoacyl-tRNA-Synthetase untersucht werden. Für diese Studie wurden beispielhaft die armlose mitochondriale tRNA[Arg] und tRNA[Ile] aus *R. culicivorax* charakterisiert. Zunächst wurde die Struktur der beiden tRNAs, die durch *in vitro* Transkription hergestellt wurden, mit Hilfe verschiedener Methoden, wie dem enzymatischen und chemischen Probing, der Kernspinresonanzspektroskopie (NMR) und der Kleinwinkel-Röntgenstreuung (SAXS) analysiert. Dies erlaubte uns ihre Sekundärstruktur zu definieren, sowie intramolekulare Wechselwirkungen und den globalen Umfang ihrer dreidimensionalen Struktur zu bestimmen. Die Partnerproteine, wie die tRNA-Nukleotidyltransferase und die Arginyl-tRNA-Synthetase, wurden aus dem teilweise annotiertem Genom von *R. culicivorax* kloniert und exprimiert. Darüber hinaus wurden einige ihrer Eigenschaften identifiziert, vor allem in Bezug auf ihre Funktionalität gegenüber armlosen tRNAs. So wurden z.B. CCA-Additionstest und Aminoacylierungstest durchgeführt. Die strukturellen und funktionellen Eigenschaften wurden mit denen homologer Proteine aus *E. coli*, der Bäckerhefe (*S. cerevisiae*) und denen aus humanen Mitochondrien (die ebenfalls in den jeweiligen Arbeitsgruppen untersucht werden) verglichen. Dies gab uns auch die Möglichkeit die evolutionären Beziehungen von zwischen armlosen tRNAs und ihren Partnerproteinen aus *R. culicivorax* zu charakterisieren.

Strukturanalyse von armlosen mitochondrialen tRNAs

Um die Struktur der mt tRNA[Arg] und tRNA[Ile] aus *R. culicivorax* zu untersuchen, wurden die entsprechenden Gene kloniert und durch *in vitro* Transkription hergestellt. Drei

verschiedene Methoden wurden für eine komplementäre Strukturanalysen verwendet: i) enzymatisches und chemisches Probing, ii) NMR-Spektroskopie und iii) SAXS.

Enzymatisches und chemisches Probing sind spezifische Verfahren, um einzel- oder doppelsträngige Bereiche in der Sekundärstruktur einer RNA zu identifizieren. Die Ergebnisse dieser Analysen zeigen, dass beide tRNAs eine Haarnadel-ähnliche Sekundärstruktur bilden mit einer zentralen Ausbuchtung (bulge), die die beiden seitlichen Arme in einer klassischen Kleeblattstruktur ersetzt. Die Ergebnisse dieser Methoden zeigen auch, dass offenbar keine internen Wechselwirkungen der Nukleotide innerhalb der Ausbuchtung gebildet werden. Die Strukturen sind stabil und robust (keine Beschädigungen, keine alternativen Konformationen) trotz ihrer primären, sehr einseitigen Zusammensetzung aus A und U Nukleotiden (jeweils 76 % und 87 % für tRNA^{Arg} und tRNA^{Ile}).

Mittels NMR-Spektroskopie, welches eine sehr gute Methode ist, um tertiäre intramolekulare Wechselwirkungen zu identifizieren, konnten wir bestätigen, dass die armlosen tRNAs für die Ausbildung der Sekundärstruktur ausschließlich klassische Watson-Crick-Basenpaarungen eingehen. Es wurde kein Signal für ungewöhnliche Basenpaarungen nachgewiesen, was auf eine Abwesenheit von tertiären Wechselwirkungen in dem Bereich der Ausbuchtung hindeutet. Solche Wechselwirkungen werden normalerweise oft für die Stabilisierung der 3D-Strukturen von RNAs und insbesondere tRNAs eingesetzt.

Mit Hilfe von SAXS wurden einige interessante physikalische Eigenschaften der tRNA, wie Größe, Form, sowie die Dimension ihrer 3D-Struktur gemessen. Dadurch konnten wir 3D-Modelle mit niedriger Auflösung konstruieren, und diese mit dem 3D-Modell einer „klassischen" tRNA vergleichen, das ebenfalls mittels SAXS generiert wurde. Obwohl die 3D-SAXS Modelle der armlosen tRNAs mit der einer „klassischen" tRNA (tRNA^{Phe} aus der Hefe) nicht identisch sind, sind sie in ihrer Form doch sehr ähnlich. Ein erster offensichtlicher Unterschied, den wir festgestellt haben, betrifft die größere Variabilität des Umfangs der armlosen tRNAs, welches auf eine größere innere Flexibilität hindeutet. Was dazu führt, dass die 3D Struktur der armlosen tRNAs nicht einer typischen L-Form, sondern eher einer „Boomerang-Form" ähnelt.

Die Ergebnisse der unterschiedlichen Methoden, zeigen dass die *in vitro* transkribierten armlosen tRNAs offenbar eine sehr einfache Struktur haben, die sich aus zwei Helices mit klassischen Watson-Crick Basenpaarungen zusammengesetzt. Die zwei Helices werden

durch eine zentrale Ausbuchtung getrennt, die keine spezifischen internen tertiären Basenpaarungen enthält. Die Struktur der armlosen tRNAs ist chemisch stabil und bildet augenscheinlich keine alternativen Sekundärstrukturen. Jedoch nehmen wir aufgrund der konstruierten 3D-Struktur eine größere Flexibilität für die Interaktion mit Partnerproteinen an.

Die tRNA Nukleotidyltransferase (CCA-addierendes Enzym) aus *R. culicivorax*

Die CCA-Sequenz am 3'-Ende einer tRNA ist eine wichtige Voraussetzung für deren Aminoacylierung. Sie ist in den meisten Organismen nicht kodiert, sondern wird mit Hilfe des CCA-addierenden Enzyms post-transkriptionell addiert (Betat *et al.*, 2010). Üblicherweise existiert bei Eukaryoten ein Gen, welches sowohl für das zytosolische, als auch das mitochondriale kodiert. Das mitochondriale Enzym wird von einem alternativen Startcodon transkribiert und enthält eine mitochondriale Import-Sequenz (mitochondrial Targeting-Sequence, MTS) am N-terminalen Ende. Die MTS wird während des Importprozesses gespalten, wodurch ein „reifes" Protein entsteht. Das für das CCA-addierende Enzym kodierende Gen, welches wir in dem Kerngenom von *R. culicivorax* identifiziert haben, besitzt eine Spaltungsstelle, die der des menschlichen Enzyms sehr ähnlich ist. Diese Spaltungsstelle wurde für eine Klonierung des Gens verwendet. Die Proteinsequenz des CCA-addierendes Enzyms aus *R. culicivorax* wurde mit der von homologen Proteinen aus anderen Organismen verglichen. Im Vergleich mit dem human mitochondrialen CCA-addierenden Enzym konnten wir eine 46 %-ige Sequenzidentität feststellen. Insbesondere der N-Terminus, der typischerweise, die katalytisch aktiven Domänen enthält (Erkennung und die Prozessierung der tRNAs) ist zu 66 % identisch, während die C-terminale Domäne, ein erhöhtes Maß an Variabilität darstellt. Die Sequenzen der entsprechenden Enzyme aus *E. coli* und *S. cerevisiae* sind jeweils nur mit 21 % zu der Proteinsequenz aus *R. culicivorax* identisch.

Die Gensequenz des CCA-addierenden Enzyms wurde für die Überexpression und Reinigung des entsprechenden Enzyms kloniert. Reinigungsprotokolle, welche bereits für das humane und das bakteriellen CCA-addierende Enzym in der Leipziger Arbeitsgruppe etabliert waren, konnten aufgrund von niedriger Ausbeute und bakteriellen Verunreinigungen für die Reinigung des Enzyms aus *R. culicivorax* nicht übernommen werden. Es wurden daher mehrere Bakterienstämme getestet, um eine ausreichende Expression zu erzielen und alternative Reinigungsprotokolle wurden dementsprechend

entwickelt. Ein Protokoll, welches die Verwendung eines speziellen Dissoziationspuffers enthielt, gefolgt von einer Gelfiltration führte zur erfolgreichen Reinigung des Proteins.

Das gereinigte Protein wurde im Hinblick auf seine Kapazität getestet, die CCA Sequenz an das 3'-Ende der armlosen tRNAs zuzufügen. Für eine vergleichende Analyse, wurden zusätzlich zu den armlosen tRNAs auch eine klassisches zytosolische tRNA verwendet. Außerdem wurde das humane sowie ein bakterielles CCA-addierende Enzym gereinigt und getestet.

Die Ergebnisse dieser Tests zeigen, dass das *R. culicivorax* Enzym in der Lage ist, sowohl die armlosen tRNAs als auch die klassischen tRNAs zu erkennen und zu prozessieren. Die Einarbeitung der CCA-Sequenz ist für alle Substrate vollständig abgeschlossen. Interessanterweise haben im Gegensatz dazu die heterologen Enzyme große Schwierigkeiten die armlosen tRNAs zu erkennen. Während das humane Enzym diese tRNAs noch schwach erkennt und teilweise Nukleotide einbaut, nimmt das bakterielle Enzym die beiden armlosen tRNAs als Substrat nicht an. Das CCA-addierenden Enzym aus *R. culicivorax,* hat demzufolge ein großes Substratspektrum. Im Gegensatz dazu toleriert das bakterielle Enzym keine strukturellen Varianten. Anscheinend begünstigte eher eine „leichte adaptive" Evolution das Enzym aus *R. culicivorax* diese große Substratvarianz zu akzeptieren und nicht unbedingt eine komplette und uneingeschränkte Anpassung nur an armlose tRNAs.

Die mitochondrialen Arginyl-tRNA-Synthetase (ArgRS) aus *R. culicivorax*

Die Gensequenz der mt ArgRS aus *R. culicivorax* wurde durch reverse Transkriptions-PCR identifiziert und konnte durch eine eigene Annotation von originalen RNA-seq Daten bestätigt werden. Die Proteinsequenz wurde mittels bioinformatischer Methoden mit ArgRS Sequenzen aus verschiedenen Organismen verglichen. Die Familie der ArgRSs hat eine komplexe Evolutionsgeschichte ohne eindeutig erkennbare Cluster. Die identifizierte ArgRS Sequenz aus *R. culicivorax* ist von einer bakteriellen Untergruppe weit entfernt, kann aber zu den zytosolischen und mitochondrialen Sequenzen von eukaryotischen Organismen eingeordnet werden. Durch diesen Vergleich haben wir eine interessante Eigenschaft für das Protein feststellen können. Üblicherweise besteht die Proteinstruktur einer ArgRS aus einer katalytischen Domäne, einer Bindungsdomäne und einer N-terminalen Domäne, die die Ellenbogenregion in der L-Struktur einer herkömmlichen tRNA erkennt, welche durch die Wechselwirkung der D- und T-Schleifen gebildet wird.

Diese N-terminale Domäne ist nicht länger in der Struktur des Enzyms aus *R. culicivorax* vorhanden und fehlt teilweise oder ganz auch in der ArgRS Proteinsequenz von anderen Nematoden. Dieser Verlust könnte auf eine mögliche Anpassung auf armlose tRNAs (für die die Ellbogenregion nicht existiert) hindeuten und könnte auch ein Hinweis auf ein ko-evolutionäres Ereignis zwischen RNA und Proteinpartner darstellen.

Proteine, welche im Zytosol translatiert, aber zu den Mitochondrien transportiert werden, tragen in der Regel am N-Terminus eine "mitochondriale Import-Sequenz" (MTS). Die MTS wird während des Importprozesses abgespalten, wodurch ein „reifes" Protein resultiert. Oftmals ist es schwierig, die spezifische Spaltungsstelle zu identifizieren, da die MTS in ihrer Aminosäurezusammensetzung und -länge variiert. Um ein funktionelles rekombinantes Protein zu erhalten, wurden 8 ArgRS-Varianten, die sich in der Länge ihrer N-terminalen Sequenz unterscheiden, kloniert und ihre Eigenschaften bezüglich Expression, Reinigung und Aktivität getestet. Wir stellten fest, dass nur einige Varianten während der Expression nicht aggregieren. Die Variante, die sich am besten reinigen und konzentrieren ließ war S29 und wurde für nachfolgende Experimente verwendet.

Aminoacylierungstests wurden mit dem gereinigten Enzym und der armlosen tRNA^{Arg} durchgeführt. Um die Funktionalität des Versuchs zu kontrollieren, wurde ein Vergleichstest mit der ArgRS aus *E. coli* und Hefe und deren homologe tRNAs, sowie der amlosen tRNA^{Arg} aus *R. culicivorax* durchgeführt. Die ArgRS aus *E. coli* und Hefe haben optimale Aktivitäten in unterschiedlichen Puffern, die sich hauptsächlich im $[Mg^{2+}]/[ATP]$ Verhältnis unterscheiden. Wir konnten zeigen, dass beide Enzyme ihre eigenen tRNAs, aber nicht diese von *R. culicivorax* aminoacylieren. Das *R. culicivorax* Enzym hat weder die armlosen tRNAs noch die klassischen tRNAs als Substrat erkannt. Dafür können mehrere Ursachen in Frage kommen. Zum Einem ist es möglich, dass die Enzymkonzentration oder Qualität nicht ausreichend waren oder dass es, wie das *E. coli* Enzym empfindlich gegenüber Reaktionsbedingungen ist. Wir führten daher eine Reihe von Tests mit verschiedenen Pufferzusammensetzungen durch. Bisher konnte aber in keinem der getesteten Reaktionsbedingungen Enzymaktivität nachgewiesen werden.

Fazit und Ausblick

Wir konnten zeigen, dass die kleinsten tRNA der Welt eine funktionelle Rolle haben, zumindest was die Prozessierung mit CCA-addierenden Enzymen betrifft und sie somit wahrscheinlich eine echte biologische Bedeutung haben.

Mit Hilfe der erzielten Ergebnisse können wir nun ihre strukturellen Eigenschaften besser charakterisieren. Dank der in dieser Studie verwendeten Methoden können wir nun genaue Angaben über die Größe und Form der armlosen mt tRNAs machen. Wir sind in der Lage eine detaillierte Sekundärstruktur Vorhersage zu konstruieren. Dies ermöglicht einen Vergleich mit den klassischen tRNAs und die kleinst-möglichen Strukturelemente einer tRNA zu identifizieren, die mit dem Leben kompatibel sind. Darüber hinaus sind weitere Untersuchungen notwendig, um die 3D-Struktur mehr im Detail aufzuklären, was dazu beitragen wird, die Funktionalität von armlosen tRNA besser zu verstehen. Da bisher noch keine vollständig aufgelöste Kristallstruktur einer mt tRNA existiert, stellt dieses Vorhaben eine schwierige, aber sehr spannende Herausforderung dar.

In dieser Studie wurden zum ersten Mal rekombinante Proteine aus *R. culicivorax,* nämlich das CCA-addierenden Enzymen und die mt ArgRS, exprimiert und gereinigt. Sequenz und Struktur beide Proteine ähneln mehr ihren eukaryotischen als bakteriellen Homologen, insbesondere denen aus anderen Nematoden. Allerdings konnten wir auch strukturelle Veränderungen für beide Enzyme feststellen, welche eine Anpassung an die armlosen tRNAs darstellen könnte. Es muss noch überprüft werden, ob das nicht-konservierten C-terminale Ende des CCA-addierenden Enzyms tatsächlich eine Bedeutung für die Akzeptanz von armlosen tRNAs als Substrat hat, oder ob andere Faktoren eine Rolle spielen. Was die mt ArgRS betrifft, so scheint es, dass der Verlust der N-terminalen Domäne eine evolutionäre Antwort auf den Verlust der beiden Arme dieser seltsamen tRNA ist. Der Nachweis von enzymatischer Aktivität für die ArgRS aus *R. culicivorax* würde diese Hypothese endgültig unterstützen.

Während dieser Arbeit wurde die Interaktion zwischen den in der Translation beteiligten tRNAs und zwei ihrer Partnerproteinen untersucht. Die Analyse des CCA-addierenden Enzyms und der Arginyl-tRNA Synthetase bietet interessante Einblicke in Bezug auf die Koevolution von Proteinen. So konnten wir feststellen, dass der Nukleotideneinbau bei armlosen tRNAs am besten mit verwandten CCA-addierenden Enzym aus *R. culicivorax* funktioniert, welches sich offenbar erfolgreich auf die reduzierte Größe der armlosen mitochondrialen tRNA im Laufe der Evolution angepasst.

Während der Aminoacylierungstests zeigte die ArgRS aus *R. culicivorax* bisher keine Aktivität unter den getesteten Bedingungen. Wir schließen daraus, dass wir die Testbedingungen, sowie die Menge und Qualität des Enzyms optimieren müssen.

Letztendlich, spielen kleine nicht-kodierende RNAs eine immer größere Rolle in unserem Leben, da sie mit einer Vielzahl an unterschiedlichen Funktionen an wichtigen Stoffwechselprozessen beteiligt sind. Kleine mt armlose tRNAs kann man auch zu den Mitgliedern dieser Familie von Molekülen zählen. Neben ihrer zentralen Rolle in der Proteinsynthese, haben einige tRNAs auch alternative Funktionen. Ihnen wurde z.B. der Einfluss auf Replikation, Transkription oder Proteinexpression nachgewiesen. Man kann deshalb vermuten, dass die armlosen tRNAs aus *R. culicivorax* eventuell auch noch alternative Funktionen ausführen. Ihre strukturelle und funktionelle Charakterisierung führt sicherlich zum besseren Verständnis diese spezifischen Moleküle.

List of Figures

List of Tables

References

Abelson, J., Trotta, C.R. and Li, H. (1998), "tRNA splicing", *J. Biol. Chem.*, Vol. 273 No. 21, pp. 12685–12688.

Adrion, J.R., White, P.S. and Montooth, K.L. (2016), "The Roles of Compensatory Evolution and Constraint in Aminoacyl tRNA Synthetase Evolution", *Molecular biology and evolution*, Vol. 33 No. 1, pp. 152–161.

Alberts B, Johnson A, Lewis J, et al. (Ed.) (2002), *The RNA World and the Origins of Life*.

Aldinger, C.A., Leisinger, A.-K. and Igloi, G.L. (2012), "The influence of identity elements on the aminoacylation of tRNA(Arg) by plant and Escherichia coli arginyl-tRNA synthetases", *The FEBS journal*, Vol. 279 No. 19, pp. 3622–3638.

Alexandrov, A., Chernyakov, I., Gu, W., Hiley, S.L., Hughes, T.R., Grayhack, E.J. and Phizicky, E.M. (2006), "Rapid tRNA decay can result from lack of nonessential modifications", *Molecular cell*, Vol. 21 No. 1, pp. 87–96.

Altman, S. (2000), "The road to RNase P", *Nat. Struct. Biol.*, Vol. 7 No. 10, pp. 827–828.

Aravind, L. and Koonin, E.V. (1999), "DNA polymerase beta-like nucleotidyltransferase superfamily: identification of three new families, classification and evolutionary history", *Nucleic acids research*, Vol. 27 No. 7, pp. 1609–1618.

Arcari, P. and Brownlee, G.G. (1980), "The nucleotide sequence of a small (3S) seryl-tRNA (anticodon GCU) from beef heart mitochondria", *Nucleic acids research*, Vol. 8 No. 22, pp. 5207–5212.

Arita, M., Suematsu, T., Osanai, A., Inaba, T., Kamiya, H., Kita, K., Sisido, M., Watanabe, Y.-I. and Ohtsuki, T. (2006), "An evolutionary 'intermediate state' of mitochondrial translation systems found in Trichinella species of parasitic nematodes: co-evolution of tRNA and EF-Tu", *Nucleic acids research*, Vol. 34 No. 18, pp. 5291–5299.

Asin-Cayuela, J. and Gustafsson, C.M. (2007), "Mitochondrial transcription and its regulation in mammalian cells", *Trends in biochemical sciences*, Vol. 32 No. 3, pp. 111–117.

Augustin, M.A., Reichert, A.S., Betat, H., Huber, R., Mörl, M. and Steegborn, C. (2003), "Crystal structure of the human CCA-adding enzyme: insights into template-independent polymerization", *Journal of molecular biology*, Vol. 328 No. 5, pp. 985–994.

Azevedo, J.L. and Hyman, B.C. (1993), "Molecular characterization of lengthy mitochondrial DNA duplications from the parasitic nematode Romanomermis culicivorax", *Genetics*, Vol. 133 No. 4, pp. 933–942.

Ban, N., Nissen, P., Hansen, J., Moore, P.B. and Steitz, T.A. (2000), "The complete atomic structure of the large ribosomal subunit at 2.4 A resolution", *Science*, Vol. 289 No. 5481, pp. 905–920.

Barker, D.G. and Winter, G. (1982), "Conserved cysteine and histidine residues in the structures of the tyrosyl and methionyl-tRNA synthetases", *FEBS Lett*, Vol. 145 No. 2, pp. 191–193.

Belval, L., Marquette, A., Mestre, P., Piron, M.-C., Demangeat, G., Merdinoglu, D. and Chich, J.-F. (2015), "A fast and simple method to eliminate Cpn60 from functional recombinant proteins produced by E. coli Arctic Express", *Protein expression and purification*, Vol. 109, pp. 29–34.

Berglund, A.-K., Spanning, E., Biverstahl, H., Maddalo, G., Tellgren-Roth, C., Maler, L. and Glaser, E. (2009), "Dual targeting to mitochondria and chloroplasts: characterization of Thr-tRNA synthetase targeting peptide", *Molecular plant*, Vol. 2 No. 6, pp. 1298–1309.

Betat, H., Rammelt, C., Martin, G. and Mörl, M. (2004), "Exchange of regions between bacterial poly(A) polymerase and the CCA-adding enzyme generates altered specificities", *Molecular cell*, Vol. 15 No. 3, pp. 389–398.

Betat, H., Rammelt, C. and Morl, M. (2010), "tRNA nucleotidyltransferases: ancient catalysts with an unusual mechanism of polymerization", *Cellular and molecular life sciences CMLS*, Vol. 67 No. 9, pp. 1447–1463.

Beuning, P.J. and Musier-Forsyth, K. (1999), "Transfer RNA recognition by aminoacyl-tRNA synthetases", *Biopolymers*, Vol. 52 No. 1, pp. 1–28.

Bhaskaran, H., Rodriguez-Hernandez, A. and Perona, J.J. (2012), "Kinetics of tRNA folding monitored by aminoacylation", *RNA (New York, N.Y.)*, Vol. 18 No. 3, pp. 569–580.

Bi, K., Zheng, Y., Gao, F., Dong, J., Wang, J., Wang, Y. and Gong, W. (2014), "Crystal structure of E. coli arginyl-tRNA synthetase and ligand binding studies revealed key residues in arginine recognition", *Protein & cell*, Vol. 5 No. 2, pp. 151–159.

Bjork, G.R. and Hagervall, T.G. (2014), "Transfer RNA Modification: Presence, Synthesis, and Function", *EcoSal Plus*, Vol. 6 No. 1.

Bonnefond, L., Fender, A., Rudinger-Thirion, J., Giegé, R., Florentz, C. and Sissler, M. (2005), "Toward the full set of human mitochondrial aminoacyl-tRNA synthetases: characterization of AspRS and TyrRS", *Biochemistry*, Vol. 44 No. 12, pp. 4805–4816.

Bonnefond, L., Florentz, C., Giegé, R. and Rudinger-Thirion, J. (2008), "Decreased aminoacylation in pathology-related mutants of mitochondrial tRNATyr is associated with structural perturbations in tRNA architecture", *RNA (New York, N.Y.)*, Vol. 14 No. 4, pp. 641–648.

Bonnefond, L., Frugier, M., Touze, E., Lorber, B., Florentz, C., Giegé, R., Sauter, C. and Rudinger-Thirion, J. (2007), "Crystal structure of human mitochondrial tyrosyl-tRNA synthetase reveals common and idiosyncratic features", *Structure (London, England 1993)*, Vol. 15 No. 11, pp. 1505–1516.

Bralley, P., Chang, S.A. and Jones, G.H. (2005), "A phylogeny of bacterial RNA nucleotidyltransferases: Bacillus halodurans contains two tRNA nucleotidyltransferases", *Journal of bacteriology*, Vol. 187 No. 17, pp. 5927–5936.

Brindefalk, B., Viklund, J., Larsson, D., Thollesson, M. and Andersson, S.G.E. (2007), "Origin and evolution of the mitochondrial aminoacyl-tRNA synthetases", *Molecular biology and evolution*, Vol. 24 No. 3, pp. 743–756.

Brown, A., Amunts, A., Bai, X.-c., Sugimoto, Y., Edwards, P.C., Murshudov, G., Scheres, S.H.W. and Ramakrishnan, V. (2014), "Structure of the large ribosomal subunit from human mitochondria", *Science (New York, N.Y.)*, Vol. 346 No. 6210, pp. 718–722.

Brown, W.M., George, M., JR and Wilson, A.C. (1979), "Rapid evolution of animal mitochondrial DNA", *Proceedings of the National Academy of Sciences of the United States of America*, Vol. 76 No. 4, pp. 1967–1971.

Bruijn, M.H. de and Klug, A. (1983), "A model for the tertiary structure of mammalian mitochondrial transfer RNAs lacking the entire 'dihydrouridine' loop and stem", *The EMBO journal*, Vol. 2 No. 8, pp. 1309–1321.

Bruijn, M.H. de, Schreier, P.H., Eperon, I.C., Barrell, B.G., Chen, E.Y., Armstrong, P.W., Wong, J.F. and Roe, B.A. (1980), "A mammalian mitochondrial serine transfer RNA lacking the "dihydrouridine" loop and stem", *Nucleic acids research*, Vol. 8 No. 22, pp. 5213–5222.

Buck, C.A. and Nass, M.M. (1969), "Studies on mitochondrial tRNA from animal cells", *Journal of molecular biology*, Vol. 41 No. 1, pp. 67–82.

Bullard, J.M., Cai, Y.C., Demeler, B. and Spremulli, L.L. (1999), "Expression and characterization of a human mitochondrial phenylalanyl-tRNA synthetase", *Journal of molecular biology*, Vol. 288 No. 4, pp. 567–577.

Bullard, J.M., Cai, Y.C. and Spremulli, L.L. (2000), "Expression and characterization of the human mitochondrial leucyl-tRNA synthetase", *Biochimica et biophysica acta*, Vol. 1490 No. 3, pp. 245–258.

Bullwinkle, T.J. and Ibba, M. (2014), "Emergence and evolution", *Topics in current chemistry*, Vol. 344, pp. 43–87.

Cannell, I.G., Kong, Y.W. and Bushell, M. (2008), "How do microRNAs regulate gene expression?", *Biochemical Society transactions*, Vol. 36 Pt 6, pp. 1224–1231.

Cao, J. (2014), "The functional role of long non-coding RNAs and epigenetics", *Biological procedures online*, Vol. 16, p. 11.

Cavarelli, J., Delagoutte, B., Eriani, G., Gangloff, J. and Moras, D. (1998), "L-arginine recognition by yeast arginyl-tRNA synthetase", *The EMBO journal*, Vol. 17 No. 18, pp. 5438–5448.

Ceballos, M. and Vioque, A. (2007), "tRNase Z", *Protein Pept. Lett.*, Vol. 14 No. 2, 137 - 145 % 2424025.

Cech, T.R. (1986), "A model for the RNA-catalyzed replication of RNA", *Proc. Natl. Acad. Sci. U.S.A.*, Vol. 83 No. 12, pp. 4360–4363.

Cech, T.R. (2012), "The RNA worlds in context", *Cold Spring Harb Perspect Biol*, Vol. 4 No. 7, a006742.

Chacinska, A., Koehler, C.M., Milenkovic, D., Lithgow, T. and Pfanner, N. (2009), "Importing mitochondrial proteins: machineries and mechanisms", *Cell*, Vol. 138 No. 4, pp. 628–644.

Chihade, J.W., Hayashibara, K., Shiba, K. and Schimmel, P. (1998), "Strong selective pressure to use G:U to mark an RNA acceptor stem for alanine", *Biochemistry*, Vol. 37 No. 25, pp. 9193–9202.

Chimnaronk, S., Gravers Jeppesen, M., Suzuki, T., Nyborg, J. and Watanabe, K. (2005), "Dual-mode recognition of noncanonical tRNAs(Ser) by seryl-tRNA synthetase in mammalian mitochondria", *The EMBO journal*, Vol. 24 No. 19, pp. 3369–3379.

Cho, H.D., Tomita, K., Suzuki, T. and Weiner, A.M. (2002), "U2 small nuclear RNA is a substrate for the CCA-adding enzyme (tRNA nucleotidyltransferase)", *The Journal of biological chemistry*, Vol. 277 No. 5, pp. 3447–3455.

Chomczynski, P. and Sacchi, N. (1987), "Single-step method of RNA isolation by acid guanidinium thiocyanate-phenol-chloroform extraction", *Analytical biochemistry*, Vol. 162 No. 1, pp. 156–159.

Clark, B.F. and Nyborg, J. (1997), "The ternary complex of EF-Tu and its role in protein biosynthesis", *Current opinion in structural biology*, Vol. 7 No. 1, pp. 110–116.

Claros, M.G. and Vincens, P. (1996), "Computational method to predict mitochondrially imported proteins and their targeting sequences", *European journal of biochemistry / FEBS*, Vol. 241 No. 3, pp. 779–786.

Cole, C., Sobala, A., Lu, C., Thatcher, S.R., Bowman, A., Brown, J.W.S., Green, P.J., Barton, G.J. and Hutvagner, G. (2009), "Filtering of deep sequencing data reveals the existence of abundant Dicer-dependent small RNAs derived from tRNAs", *RNA (New York, N.Y.)*, Vol. 15 No. 12, pp. 2147–2160.

Crick, F. (1970), "Central Dogma of Molecular Biology", *Nature*, Vol. 227 No. 5258, pp. 561–563.

Crick, F.H. (1955), "From DNA to protein on degenerate templates and the adapter hypothesis: a note for the RNA Tie Club", *RNA Tie Club,* 1955.

Crick, F.H. (1968), "The origin of the genetic code", *J. Mol. Biol.*, Vol. 38 No. 3, pp. 367–379.

Delagoutte, B., Moras, D. and Cavarelli, J. (2000), "tRNA aminoacylation by arginyl-tRNA synthetase: induced conformations during substrates binding", *The EMBO journal*, Vol. 19 No. 21, pp. 5599–5610.

Derks, K.W.J., Hoeijmakers, J.H.J. and Pothof, J. (2014), "The DNA damage response: the omics era and its impact", *DNA repair*, Vol. 19, pp. 214–220.

Derrick, W.B. and Horowitz, J. (1993), "Probing structural differences between native and in vitro transcribed Escherichia coli valine transfer RNA: evidence for stable base modification-dependent conformers", *Nucleic acids research*, Vol. 21 No. 21, pp. 4948–4953.

Di Giulio, M. (1995), "Was it an ancient gene codifying for a hairpin RNA that, by means of direct duplication, gave rise to the primitive tRNA molecule?", *Journal of theoretical biology*, Vol. 177 No. 1, pp. 95–101.

Di Giulio, M. (2012), "The 'recently' split transfer RNA genes may be close to merging the two halves of the tRNA rather than having just separated them", *Journal of theoretical biology*, Vol. 310, pp. 1–2.

Diebel, K.W., Zhou, K., Clarke, A.B. and Bemis, L.T. (2016), "Beyond the Ribosome: Extra-translational Functions of tRNA Fragments", *Biomarker insights*, Vol. 11 Suppl 1, pp. 1–8.

Divan, A. (Ed.) (2013), *Tools and techniques in biomolecular science,* Impr.: 1, Oxford Univ. Press, Oxford.

Doherty, E.A. and Doudna, J.A. (2001), "Ribozyme structures and mechanisms", *Annual review of biophysics and biomolecular structure*, Vol. 30, pp. 457–475.

Doublie, S., Tabor, S., Long, A.M., Richardson, C.C. and Ellenberger, T. (1998), "Crystal structure of a bacteriophage T7 DNA replication complex at 2.2 A resolution", *Nature*, Vol. 391 No. 6664, pp. 251–258.

Draper, D.E. (2004), "A guide to ions and RNA structure", *RNA*, Vol. 10 No. 3, pp. 335–343.

Du, X. (2003), "Tertiary structure base pairs between D- and TpsiC-loops of Escherichia coli tRNALeu play important roles in both aminoacylation and editing", *Nucleic acids research*, Vol. 31 No. 11, pp. 2865–2872.

Duechler, M., Leszczynska, G., Sochacka, E. and Nawrot, B. (2016), "Nucleoside modifications in the regulation of gene expression: focus on tRNA", *Cellular and molecular life sciences CMLS*, Vol. 73 No. 16, pp. 3075–3095.

Dupasquier, M., Kim, S., Halkidis, K., Gamper, H. and Hou, Y.-M. (2008), "tRNA integrity is a prerequisite for rapid CCA addition: implication for quality control", *Journal of molecular biology*, Vol. 379 No. 3, pp. 579–588.

Eddy, S.R. (2001), "Non-coding RNA genes and the modern RNA world", *Nature reviews. Genetics*, Vol. 2 No. 12, pp. 919–929.

El Yacoubi, B., Bailly, M. and Crecy-Lagard, V. de (2012), "Biosynthesis and function of posttranscriptional modifications of transfer RNAs", *Annual review of genetics*, Vol. 46, pp. 69–95.

Emanuelsson, O., Nielsen, H., Brunak, S. and Heijne, G. von (2000), "Predicting subcellular localization of proteins based on their N-terminal amino acid sequence", *Journal of molecular biology*, Vol. 300 No. 4, pp. 1005–1016.

Emara, M.M., Ivanov, P., Hickman, T., Dawra, N., Tisdale, S., Kedersha, N., Hu, G.-F. and Anderson, P. (2010), "Angiogenin-induced tRNA-derived stress-induced RNAs promote stress-induced stress granule assembly", *The Journal of biological chemistry*, Vol. 285 No. 14, pp. 10959–10968.

Eriani, G., Delarue, M., Poch, O., Gangloff, J. and Moras, D. (1990), "Partition of tRNA synthetases into two classes based on mutually exclusive sets of sequence motifs", *Nature*, Vol. 347 No. 6289, pp. 203–206.

Ernst, F.G.M., Rickert, C., Bluschke, A., Betat, H., Steinhoff, H.-J. and Mörl, M. (2015), "Domain movements during CCA-addition: a new function for motif C in the catalytic core of the human tRNA nucleotidyltransferases", *RNA biology*, Vol. 12 No. 4, pp. 435–446.

Evans, D., Marquez, S.M. and Pace, N.R. (2006), "RNase P: interface of the RNA and protein worlds", *Trends Biochem. Sci.*, Vol. 31 No. 6, pp. 333–341.

Fenton, W.A. and Horwich, A.L. (2003), "Chaperonin-mediated protein folding. Fate of substrate polypeptide", *Quarterly Reviews of Biophysics*, Vol. 36 No. 2, pp. 229–256.

Fernandez-Vizarra, E., Berardinelli, A., Valente, L., Tiranti, V. and Zeviani, M. (2007), "Nonsense mutation in pseudouridylate synthase 1 (PUS1) in two brothers affected by myopathy, lactic acidosis and sideroblastic anaemia (MLASA)", *Journal of medical genetics*, Vol. 44 No. 3, pp. 173–180.

Ferrer, M., Chernikova, T.N., Yakimov, M.M., Golyshin, P.N. and Timmis, K.N. (2003), "Chaperonins govern growth of Escherichia coli at low temperatures", *Nature biotechnology*, Vol. 21 No. 11, pp. 1266–1267.

Florentz, C., Pütz, J., Jühling, F., Schwenzer, H., Stadler, P.F., Lorber, B., Sauter, C. and Sissler, M. (2013), "Translation in Mammalian Mitochondria: Order and Disorder Linked to tRNAs and Aminoacyl-tRNA Synthetases", in Duchêne, A.-M. (Ed.), *Translation in Mitochondria and Other Organelles*, Springer Berlin Heidelberg, Berlin, Heidelberg, pp. 55–83.

Franke, D. and Svergun, D.I. (2009), "DAMMIF, a program for rapid ab-initio shape determination in small-angle scattering", *Journal of applied crystallography*, Vol. 42 Pt 2, pp. 342–346.

Frechin, M., Duchene, A.-M. and Becker, H.D. (2009), "Translating organellar glutamine codons: a case by case scenario?", *RNA biology*, Vol. 6 No. 1, pp. 31–34.

Friederich, M.W., Vacano, E. and Hagerman, P.J. (1998), "Global flexibility of tertiary structure in RNA: yeast tRNAPhe as a model system", *Proceedings of the National Academy of Sciences of the United States of America*, Vol. 95 No. 7, pp. 3572–3577.

Fujishima, K. and Kanai, A. (2014), "tRNA gene diversity in the three domains of life", *Frontiers in genetics*, Vol. 5, p. 142.

Fukai, S., Nureki, O., Sekine, S., Shimada, A., Tao, J., Vassylyev, D.G. and Yokoyama, S. (2000), "Structural basis for double-sieve discrimination of L-valine from L-isoleucine and L-threonine by the complex of tRNA(Val) and valyl-tRNA synthetase", *Cell*, Vol. 103 No. 5, pp. 793–803.

Fukasawa, Y., Tsuji, J., Fu, S.-C., Tomii, K., Horton, P. and Imai, K. (2015), "MitoFates: improved prediction of mitochondrial targeting sequences and their cleavage sites", *Molecular & cellular proteomics MCP*, Vol. 14 No. 4, pp. 1113–1126.

Gakh, O., Cavadini, P. and Isaya, G. (2002), "Mitochondrial processing peptidases", *Biochimica et Biophysica Acta (BBA) - Molecular Cell Research*, Vol. 1592 No. 1, pp. 63–77.

Galloway, C.A., Sowden, M.P. and Smith, H.C. (2003), "Increasing the yield of soluble recombinant protein expressed in E. coli by induction during late log phase", *BioTechniques*, Vol. 34 No. 3, 524-6, 528, 530.

Gaudry, A., Lorber, B., Neuenfeldt, A., Sauter, C., Florentz, C. and Sissler, M. (2012), "Re-designed N-terminus enhances expression, solubility and crystallizability of mitochondrial protein", *Protein engineering, design & selection PEDS*, Vol. 25 No. 9, pp. 473–481.

Gavel, Y. and Heijne, G. von (1990), "Cleavage-site motifs in mitochondrial targeting peptides", *Protein engineering*, Vol. 4 No. 1, pp. 33–37.

Gebetsberger, J. and Polacek, N. (2013), "Slicing tRNAs to boost functional ncRNA diversity", *RNA biology*, Vol. 10 No. 12, pp. 1798–1806.

Giegé, R. (2008), "Toward a more complete view of tRNA biology", *Nature structural & molecular biology*, Vol. 15 No. 10, pp. 1007–1014.

Giegé, R. and Eriani, G. (2001), "Transfer RNA Recognition and Aminoacylation by Synthetases", in Ltd, J.W.&S. (Ed.), *eLS*, John Wiley & Sons, Ltd, Chichester, UK.

Giegé, R., Jühling, F., Pütz, J., Stadler, P., Sauter, C. and Florentz, C. (2012), "Structure of transfer RNAs: similarity and variability", *Wiley interdisciplinary reviews. RNA*, Vol. 3 No. 1, pp. 37–61.

Giegé, R. and Lapointe, J. (2009), *Transfer RNA Aminoacylation and Modified Nucleosides*, DNA and RNA Modification Enzymes:Structure, Mechanism, Function and Evolution, *Molecular Biology Intelligence Unit*, Landes Bioscience, Austin.

Giegé, R., Sissler, M. and Florentz, C. (1998), "Universal rules and idiosyncratic features in tRNA identity", *Nucleic acids research*, Vol. 26 No. 22, pp. 5017–5035.

Gilbert, W. (1986), "Origin of life: The RNA world", *Nature*, Vol. 319 No. 6055, 618 % 20473316.

Gobert, A., Gutmann, B., Taschner, A., Gossringer, M., Holzmann, J., Hartmann, R.K., Rossmanith, W. and Giege, P. (2010), "A single Arabidopsis organellar protein has RNase P activity", *Nat. Struct. Mol. Biol.*, Vol. 17 No. 6, pp. 740–744.

Goodarzi, H., Liu, X., Nguyen, H.C.B., Zhang, S., Fish, L. and Tavazoie, S.F. (2015), "Endogenous tRNA-Derived Fragments Suppress Breast Cancer Progression via YBX1 Displacement", *Cell*, Vol. 161 No. 4, pp. 790–802.

Gopal, G.J. and Kumar, A. (2013), "Strategies for the production of recombinant protein in Escherichia coli", *The protein journal*, Vol. 32 No. 6, pp. 419–425.

Graslund, S., Nordlund, P., Weigelt, J., Hallberg, B.M., Bray, J., Gileadi, O., Knapp, S., Oppermann, U., Arrowsmith, C., Hui, R., Ming, J., dhe-Paganon, S., Park, H.-w., Savchenko, A., Yee, A., Edwards, A., Vincentelli, R., Cambillau, C., Kim, R., Kim, S.-H., Rao, Z., Shi, Y., Terwilliger, T.C., Kim, C.-Y., Hung, L.-W., Waldo, G.S., Peleg, Y., Albeck, S., Unger, T., Dym, O., Prilusky, J., Sussman, J.L., Stevens, R.C., Lesley, S.A., Wilson, I.A., Joachimiak, A., Collart, F., Dementieva, I., Donnelly, M.I., Eschenfeldt, W.H., Kim, Y., Stols, L., Wu, R., Zhou, M., Burley, S.K., Emtage, J.S., Sauder, J.M., Thompson, D., Bain, K., Luz, J., Gheyi, T., Zhang, F., Atwell, S., Almo, S.C., Bonanno, J.B., Fiser, A., Swaminathan, S., Studier, F.W., Chance, M.R., Sali, A., Acton, T.B., Xiao, R., Zhao, L., Ma, L.C., Hunt, J.F., Tong, L., Cunningham, K., Inouye, M., Anderson, S., Janjua, H., Shastry, R., Ho, C.K., Wang, D., Wang, H., Jiang, M., Montelione, G.T., Stuart, D.I., Owens, R.J., Daenke, S., Schutz, A., Heinemann, U., Yokoyama, S., Bussow, K. and Gunsalus, K.C. (2008), "Protein production and purification", *Nature methods*, Vol. 5 No. 2, pp. 135–146.

Gray, M.W. (2012), "Mitochondrial evolution", *Cold Spring Harbor perspectives in biology*, Vol. 4 No. 9, a011403.

Greber, B.J. and Ban, N. (2016), "Structure and Function of the Mitochondrial Ribosome", *Annual review of biochemistry*, Vol. 85, pp. 103–132.

Greber, B.J., Bieri, P., Leibundgut, M., Leitner, A., Aebersold, R., Boehringer, D. and Ban, N. (2015), "Ribosome. The complete structure of the 55S mammalian mitochondrial ribosome", *Science (New York, N.Y.)*, Vol. 348 No. 6232, pp. 303–308.

Grosjean, H. (2015), "RNA modification: the Golden Period 1995-2015", *RNA (New York, N.Y.)*, Vol. 21 No. 4, pp. 625–626.

Grosjean, H., Sprinzl, M. and Steinberg, S. (1995), "Posttranscriptionally modified nucleosides in transfer RNA. Their locations and frequencies", *Biochimie*, Vol. 77 1-2, pp. 139–141.

Guerrier-Takada, C., Gardiner, K., Marsh, T., Pace, N. and Altman, S. (1983), "The RNA moiety of ribonuclease P is the catalytic subunit of the enzyme", *Cell*, Vol. 35 3 Pt 2, pp. 849–857.

Gustilo, E.M., Vendeix, F.A. and Agris, P.F. (2008), "tRNA's modifications bring order to gene expression", *Current opinion in microbiology*, Vol. 11 No. 2, pp. 134–140.

Haacke, A., Fendrich, G., Ramage, P. and Geiser, M. (2009), "Chaperone over-expression in Escherichia coli: apparent increased yields of soluble recombinant protein kinases are due mainly to soluble aggregates", *Protein expression and purification*, Vol. 64 No. 2, pp. 185–193.

Haiser, H.J., Karginov, F.V., Hannon, G.J. and Elliot, M.A. (2008), "Developmentally regulated cleavage of tRNAs in the bacterium Streptomyces coelicolor", *Nucleic acids research*, Vol. 36 No. 3, pp. 732–741.

Hartinger, D., Heinl, S., Schwartz, H.E., Grabherr, R., Schatzmayr, G., Haltrich, D. and Moll, W.-D. (2010), "Enhancement of solubility in Escherichia coli and purification of an aminotransferase from Sphingopyxis sp. MTA144 for deamination of hydrolyzed fumonisin B(1)", *Microbial cell factories*, Vol. 9, p. 62.

He, L. and Hannon, G.J. (2004), "MicroRNAs: small RNAs with a big role in gene regulation", *Nature reviews. Genetics*, Vol. 5 No. 7, pp. 522–531.

Hegg, L.A., Kou, M. and Thurlow, D.L. (1990), "Recognition of the tRNA-like structure in tobacco mosaic viral RNA by ATP/CTP:tRNA nucleotidyltransferases from Escherichia coli and Saccharomyces cerevisiae", *The Journal of biological chemistry*, Vol. 265 No. 29, pp. 17441–17445.

Helm, M. (2006), "Post-transcriptional nucleotide modification and alternative folding of RNA", *Nucleic acids research*, Vol. 34 No. 2, pp. 721–733.

Helm, M. and Attardi, G. (2004), "Nuclear control of cloverleaf structure of human mitochondrial tRNA(Lys)", *Journal of molecular biology*, Vol. 337 No. 3, pp. 545–560.

Holm, L. and Sander, C. (1995), "DNA polymerase beta belongs to an ancient nucleotidyltransferase superfamily", *Trends in biochemical sciences*, Vol. 20 No. 9, pp. 345–347.

Holman, K.M., Wu, J., Ling, J. and Simonovic, M. (2016), "The crystal structure of yeast mitochondrial ThrRS in complex with the canonical threonine tRNA", *Nucleic acids research*, Vol. 44 No. 3, pp. 1428–1439.

Holzmann, J., Frank, P., Loffler, E., Bennett, K.L., Gerner, C. and Rossmanith, W. (2008), "RNase P without RNA: identification and functional reconstitution of the human mitochondrial tRNA processing enzyme", *Cell*, Vol. 135 No. 3, pp. 462–474.

Honda, S., Loher, P., Shigematsu, M., Palazzo, J.P., Suzuki, R., Imoto, I., Rigoutsos, I. and Kirino, Y. (2015), "Sex hormone-dependent tRNA halves enhance cell proliferation in breast and prostate cancers", *Proceedings of the National Academy of Sciences of the United States of America*, Vol. 112 No. 29, E3816-25.

Hopper, A.K., Pai, D.A. and Engelke, D.R. (2010), "Cellular dynamics of tRNAs and their genes", *FEBS letters*, Vol. 584 No. 2, pp. 310–317.

Hopper, A.K. and Phizicky, E.M. (2003), "tRNA transfers to the limelight", *Genes & development*, Vol. 17 No. 2, pp. 162–180.

Hou, Y.-M. and Yang, X. (2013), "Regulation of cell death by transfer RNA", *Antioxidants & redox signaling*, Vol. 19 No. 6, pp. 583–594.

Hyman, B.C. (1988), "Nematode Mitochondrial DNA: Anomalies and Applications", *Journal of nematology*, Vol. 20 No. 4, pp. 523–531.

Hyman, B.C., Beck, J.L. and Weiss, K.C. (1988), "Sequence amplification and gene rearrangement in parasitic nematode mitochondrial DNA", *Genetics*, Vol. 120 No. 3, pp. 707–712.

Ibba, M., Francklyn, C. and Cusack, S. (2009), *The Aminoacyl-tRNA Synthetases, Molecular Biology Intelligence Unit*, Landes Bioscience, Austin.

Ibba, M. and Soll, D. (2000), "Aminoacyl-tRNA synthesis", *Annual review of biochemistry*, Vol. 69, pp. 617–650.

Igloi, G.L. and Leisinger, A.-K. (2014), "Identity elements for the aminoacylation of metazoan mitochondrial tRNA(Arg) have been widely conserved throughout evolution and ensure the fidelity of the AGR codon reassignment", *RNA biology*, Vol. 11 No. 10, pp. 1313–1323.

Igloi, G.L. and Schiefermayr, E. (2009), "Amino acid discrimination by arginyl-tRNA synthetases as revealed by an examination of natural specificity variants", *The FEBS journal*, Vol. 276 No. 5, pp. 1307–1318.

Ivanov, P., Emara, M.M., Villen, J., Gygi, S.P. and Anderson, P. (2011), "Angiogenin-induced tRNA fragments inhibit translation initiation", *Molecular cell*, Vol. 43 No. 4, pp. 613–623.

Jackman, J.E. and Alfonzo, J.D. (2013), "Transfer RNA modifications: nature's combinatorial chemistry playground", *Wiley interdisciplinary reviews. RNA*, Vol. 4 No. 1, pp. 35–48.

Jager, M., Nir, E. and Weiss, S. (2006), "Site-specific labeling of proteins for single-molecule FRET by combining chemical and enzymatic modification", *Protein science a publication of the Protein Society*, Vol. 15 No. 3, pp. 640–646.

Jahn, D., Verkamp, E. and Soll, D. (1992), "Glutamyl-transfer RNA: a precursor of heme and chlorophyll biosynthesis", *Trends in biochemical sciences*, Vol. 17 No. 6, pp. 215–218.

Jochl, C., Rederstorff, M., Hertel, J., Stadler, P.F., Hofacker, I.L., Schrettl, M., Haas, H. and Huttenhofer, A. (2008), "Small ncRNA transcriptome analysis from Aspergillus fumigatus suggests a novel mechanism for regulation of protein synthesis", *Nucleic acids research*, Vol. 36 No. 8, pp. 2677–2689.

Joseph, R.E. and Andreotti, A.H. (2008), "Bacterial expression and purification of interleukin-2 tyrosine kinase: single step separation of the chaperonin impurity", *Protein expression and purification*, Vol. 60 No. 2, pp. 194–197.

Joyce, G.F. (1996), "Building the RNA world. Ribozymes", *Current biology CB*, Vol. 6 No. 8, pp. 965–967.

Jühling, F., Mörl, M., Hartmann, R.K., Sprinzl, M., Stadler, P.F. and Pütz, J. (2009), "tRNAdb 2009: compilation of tRNA sequences and tRNA genes", *Nucleic acids research*, Vol. 37 Database issue, D159-62.

Jühling, F., Pütz, J., Bernt, M., Donath, A., Middendorf, M., Florentz, C. and Stadler, P.F. (2012a), "Improved systematic tRNA gene annotation allows new insights into the evolution of mitochondrial tRNA structures and into the mechanisms of mitochondrial genome rearrangements", *Nucleic acids research*, Vol. 40 No. 7, pp. 2833–2845.

Jühling, F., Pütz, J., Florentz, C. and Stadler, P.F. (2012b), "Armless mitochondrial tRNAs in Enoplea (Nematoda)", *RNA biology*, Vol. 9 No. 9, pp. 1161–1166.

Kamareddine, L. (2012), "The biological control of the malaria vector", *Toxins*, Vol. 4 No. 9, pp. 748–767.

Karakozova, M., Kozak, M., Wong, C.C.L., Bailey, A.O., Yates, J.R.3., Mogilner, A., Zebroski, H. and Kashina, A. (2006), "Arginylation of beta-actin regulates actin cytoskeleton and cell motility", *Science (New York, N.Y.)*, Vol. 313 No. 5784, pp. 192–196.

Kaukinen, U., Lyytikainen, S., Mikkola, S. and Lonnberg, H. (2002), "The reactivity of phosphodiester bonds within linear single-stranded oligoribonucleotides is strongly dependent on the base sequence", *Nucleic acids research*, Vol. 30 No. 2, pp. 468–474.

Kern, D. and Lapointe, J. (1980), "Catalytic mechanism of glutamyl-tRNA synthetase from Escherichia coli. Reaction pathway in the aminoacylation of tRNAGlu", *Biochemistry*, Vol. 19 No. 13, pp. 3060–3068.

Khow, O. and Suntrarachun, S. (2012), "Strategies for production of active eukaryotic proteins in bacterial expression system", *Asian Pacific Journal of Tropical Biomedicine*, Vol. 2 No. 2, pp. 159–162.

Kim, H.S., Cha, S.Y., Jo, C.H., Han, A. and Hwang, K.Y. (2014), "The crystal structure of arginyl-tRNA synthetase from Homo sapiens", *FEBS letters*, Vol. 588 No. 14, pp. 2328–2334.

Kim, S.H., Suddath, F.L., Quigley, G.J., McPherson, A., Sussman, J.L., Wang, A.H., Seeman, N.C. and Rich, A. (1974), "Three-dimensional tertiary structure of yeast phenylalanine transfer RNA", *Science (New York, N.Y.)*, Vol. 185 No. 4149, pp. 435–440.

Kinouchi, M. and Kurokawa, K. (2006), "tRNAfinder: A Software System To Find All tRNA Genes in the DNA Sequence Based on the Cloverleaf Secondary Structure", *Journal of Computer Aided Chemistry*, Vol. 7, pp. 116–124.

Kirchner, S. and Ignatova, Z. (2015), "Emerging roles of tRNA in adaptive translation, signalling dynamics and disease", *Nature reviews. Genetics*, Vol. 16 No. 2, pp. 98–112.

Kirino, Y. and Suzuki, T. (2005), "Human mitochondrial diseases associated with tRNA wobble modification deficiency", *RNA biology*, Vol. 2 No. 2, pp. 41–44.

Kiss, T. (2002), "Small nucleolar RNAs: an abundant group of noncoding RNAs with diverse cellular functions", *Cell*, Vol. 109 No. 2, pp. 145–148.

Klimov, P.B. and Oconnor, B.M. (2009), "Improved tRNA prediction in the American house dust mite reveals widespread occurrence of extremely short minimal tRNAs in acariform mites", *BMC genomics*, Vol. 10, p. 598.

Klipcan, L., Levin, I., Kessler, N., Moor, N., Finarov, I. and Safro, M. (2008), "The tRNA-induced conformational activation of human mitochondrial phenylalanyl-tRNA synthetase", *Structure (London, England 1993)*, Vol. 16 No. 7, pp. 1095–1104.

Klipcan, L., Moor, N., Finarov, I., Kessler, N., Sukhanova, M. and Safro, M.G. (2012), "Crystal structure of human mitochondrial PheRS complexed with tRNA(Phe) in the active "open" state", *Journal of molecular biology*, Vol. 415 No. 3, pp. 527–537.

Kobylinski, K.C., Sylla, M., Black, W., 4th. and Foy, B.D. (2012), "Mermithid nematodes found in adult Anopheles from southeastern Senegal", *Parasites & vectors*, Vol. 5, p. 131.

Konarev, P.V., Volkov, V.V., Sokolova, A.V., Koch, M.H.J. and Svergun, D.I. (2003), "PRIMUS. A Windows PC-based system for small-angle scattering data analysis", *Journal of Applied Crystallography*, Vol. 36 No. 5, pp. 1277–1282.

Konarska, M.M. and Query, C.C. (2005), "Insights into the mechanisms of splicing: more lessons from the ribosome", *Genes & development*, Vol. 19 No. 19, pp. 2255–2260.

Kumar, P., Mudunuri, S.B., Anaya, J. and Dutta, A. (2015), "tRFdb: a database for transfer RNA fragments", *Nucleic Acids Res*, Vol. 43 Database issue, D141 - 145.

Kumazawa, Y., Himeno, H., Miura, K. and Watanabe, K. (1991), "Unilateral aminoacylation specificity between bovine mitochondria and eubacteria", *Journal of biochemistry*, Vol. 109 No. 3, pp. 421–427.

LaRue, B., Newhouse, N., Nicoghosian, K. and Cedergren, R.J. (1981), "The evolution of multi-isoacceptor tRNA families. Sequence of tRNA Leu CAA and tRNA Leu CAG from Anacystis nidulans", *The Journal of biological chemistry*, Vol. 256 No. 4, pp. 1539–1543.

Laslett, D. and Canback, B. (2004), "ARAGORN, a program to detect tRNA genes and tmRNA genes in nucleotide sequences", *Nucleic acids research*, Vol. 32 No. 1, pp. 11–16.

Lee, C., Kramer, G., Graham, D.E. and Appling, D.R. (2007), "Yeast mitochondrial initiator tRNA is methylated at guanosine 37 by the Trm5-encoded tRNA (guanine-N1-)-methyltransferase", *The Journal of biological chemistry*, Vol. 282 No. 38, pp. 27744–27753.

Lee, T. and Feig, A.L. (2008), "The RNA binding protein Hfq interacts specifically with tRNAs", *RNA (New York, N.Y.)*, Vol. 14 No. 3, pp. 514–523.

Lee, Y.S., Shibata, Y., Malhotra, A. and Dutta, A. (2009), "A novel class of small RNAs: tRNA-derived RNA fragments (tRFs)", *Genes & development*, Vol. 23 No. 22, pp. 2639–2649.

Lehman, N. (2010), "RNA in evolution", *Wiley Interdiscip Rev RNA*, Vol. 1 No. 2, 202 - 213 % 4339100.

Levin, L., Blumberg, A., Barshad, G. and Mishmar, D. (2014), "Mito-nuclear co-evolution: the positive and negative sides of functional ancient mutations", *Frontiers in genetics*, Vol. 5, p. 448.

Levitt, M.H. (2013), *Spin Dynamics: Basics of Nuclear Magnetic Resonance,* 2., Auflage, John Wiley & Sons, New York, NY.

Levy R, Hertlein BC, Petersen JJ, Doggett DW and Miller TW (1979), "Aerial application of Romanomermis culicivorax (Mermithidae: Nematoda) to control Anopheles and Culex mosuqitoes in southwest Florida", *Mosquito News No.* 39, pp. 20–25.

Li, F., Xiong, Y., Wang, J., Cho, H.D., Tomita, K., Weiner, A.M. and Steitz, T.A. (2002), "Crystal structures of the Bacillus stearothermophilus CCA-adding enzyme and its complexes with ATP or CTP", *Cell*, Vol. 111 No. 6, pp. 815–824.

Li, Z., Gillis, K.A., Hegg, L.A., Zhang, J. and Thurlow, D.L. (1996), "Effects of nucleotide substitutions within the T-loop of precursor tRNAs on interaction with ATP/CTP:tRNA nucleotidyltransferases from Escherichia coli and yeast", *The Biochemical journal*, 314 (Pt 1), pp. 49–53.

Li, Z., Sun, Y. and Thurlow, D.L. (1997), "RNA minihelices as model substrates for ATP/CTP:tRNA nucleotidyltransferase", *The Biochemical journal*, 327 (Pt 3), pp. 847–851.

Lipfert, J. and Doniach, S. (2007), "Small-angle X-ray scattering from RNA, proteins, and protein complexes", *Annual review of biophysics and biomolecular structure*, Vol. 36, pp. 307–327.

Lizano, E., Scheibe, M., Rammelt, C., Betat, H. and Mörl, M. (2008), "A comparative analysis of CCA-adding enzymes from human and E. coli: differences in CCA addition and tRNA 3'-end repair", *Biochimie*, Vol. 90 No. 5, pp. 762–772.

Lodish H, Berk A, Zipursky SL, et al. (2000), *The Three Roles of RNA in Protein Synthesis*.

Lowe, T.M. and Eddy, S.R. (1997), "tRNAscan-SE: a program for improved detection of transfer RNA genes in genomic sequence", *Nucleic acids research*, Vol. 25 No. 5, pp. 955–964.

Lynch, D.C. and Attardi, G. (1976), "Amino acid specificity of the transfer RNA species coded for by HeLa cell mitochondrial DNA", *Journal of molecular biology*, Vol. 102 No. 1, pp. 125–141.

Machnicka, M.A., Milanowska, K., Osman Oglou, O., Purta, E., Kurkowska, M., Olchowik, A., Januszewski, W., Kalinowski, S., Dunin-Horkawicz, S., Rother, K.M., Helm, M., Bujnicki, J.M. and Grosjean, H. (2013), "MODOMICS: a database of RNA modification pathways--2013 update", *Nucleic acids research*, Vol. 41 Database issue, D262-7.

Martin, G. and Keller, W. (1996), "Mutational analysis of mammalian poly(A) polymerase identifies a region for primer binding and catalytic domain, homologous to the family X polymerases, and to other nucleotidyltransferases", *The EMBO journal*, Vol. 15 No. 10, pp. 2593–2603.

Martin, G. and Keller, W. (2004), "Sequence motifs that distinguish ATP(CTP):tRNA nucleotidyl transferases from eubacterial poly(A) polymerases", *RNA (New York, N.Y.)*, Vol. 10 No. 6, pp. 899–906.

Martin, G. and Keller, W. (2007), "RNA-specific ribonucleotidyl transferases", *RNA (New York, N.Y.)*, Vol. 13 No. 11, pp. 1834–1849.

Masta, S.E. (2000), "Mitochondrial sequence evolution in spiders: intraspecific variation in tRNAs lacking the TPsiC Arm", *Molecular biology and evolution*, Vol. 17 No. 7, pp. 1091–1100.

Mattick, J.S. and Makunin, I.V. (2005), "Small regulatory RNAs in mammals", *Human molecular genetics*, 14 Spec No 1, R121-32.

Mattick, J.S. and Makunin, I.V. (2006), "Non-coding RNA", *Human molecular genetics*, 15 Spec No 1, R17-29.

McClain, W.H. (1993), "Rules that govern tRNA identity in protein synthesis", *Journal of molecular biology*, Vol. 234 No. 2, pp. 257–280.

McManus, M.T. and Sharp, P.A. (2002), "Gene silencing in mammals by small interfering RNAs", *Nature reviews. Genetics*, Vol. 3 No. 10, pp. 737–747.

McShane, A., Hok, E., Tomberlin, J., Eriani, G. and Geslain, R. (2016), "The Enzymatic Paradox of Yeast Arginyl-tRNA Synthetase: Exclusive Arginine Transfer Controlled by a Flexible Mechanism of tRNA Recognition", *PLoS ONE*, Vol. 11 No. 2, e0148460.

Mears, J.A., Cannone, J.J., Stagg, S.M., Gutell, R.R., Agrawal, R.K. and Harvey, S.C. (2002), "Modeling a Minimal Ribosome Based on Comparative Sequence Analysis", *Journal of molecular biology*, Vol. 321 No. 2, pp. 215–234.

Mears, J.A., Sharma, M.R., Gutell, R.R., McCook, A.S., Richardson, P.E., Caulfield, T.R., Agrawal, R.K. and Harvey, S.C. (2006), "A structural model for the large subunit of the mammalian mitochondrial ribosome", *Journal of molecular biology*, Vol. 358 No. 1, pp. 193–212.

Mehler, A.H. and Mitra, S.K. (1967), "The activation of arginyl transfer ribonucleic acid synthetase by transfer ribonucleic acid", *The Journal of biological chemistry*, Vol. 242 No. 23, pp. 5495–5499.

Mertens, H.D.T. and Svergun, D.I. (2010), "Structural characterization of proteins and complexes using small-angle X-ray solution scattering", *Journal of structural biology*, Vol. 172 No. 1, pp. 128–141.

Messmer, M., Pütz, J., Suzuki, T., Suzuki, T., Sauter, C., Sissler, M. and Catherine, F. (2009), "Tertiary network in mammalian mitochondrial tRNAAsp revealed by solution probing and phylogeny", *Nucleic acids research*, Vol. 37 No. 20, pp. 6881–6895.

Miller, S.B., Yildiz, F.Z., Lo, J.A., Wang, B. and D'Souza, V.M. (2014), "A structure-based mechanism for tRNA and retroviral RNA remodelling during primer annealing", *Nature*, Vol. 515 No. 7528, pp. 591–595.

Moras, D., Comarmond, M.B., Fischer, J., Weiss, R., Thierry, J.C., Ebel, J.P. and Giege, R. (1980), "Crystal structure of yeast tRNAAsp", *Nature*, Vol. 288 No. 5792, pp. 669–674.

Morozova, O. and Marra, M.A. (2008), "Applications of next-generation sequencing technologies in functional genomics", *Genomics*, Vol. 92 No. 5, pp. 255–264.

Motorin, Y. and Helm, M. (2010), "tRNA stabilization by modified nucleotides", *Biochemistry*, Vol. 49 No. 24, pp. 4934–4944.

Mudge, S.J., Williams, J.H., Eyre, H.J., Sutherland, G.R., Cowan, P.J. and Power, D.A. (1998), "Complex organisation of the 5'-end of the human glycine tRNA synthetase gene", *Gene*, Vol. 209 1-2, pp. 45–50.

Nagaike, T., Suzuki, T., Tomari, Y., Takemoto-Hori, C., Negayama, F., Watanabe, K. and Ueda, T. (2001), "Identification and characterization of mammalian mitochondrial tRNA nucleotidyltransferases", *The Journal of biological chemistry*, Vol. 276 No. 43, pp. 40041–40049.

Nagao, A., Suzuki, T., Katoh, T., Sakaguchi, Y. and Suzuki, T. (2009), "Biogenesis of glutaminyl-mt tRNAGln in human mitochondria", *Proceedings of the National Academy of Sciences of the United States of America*, Vol. 106 No. 38, pp. 16209–16214.

Navarre, W.W. and Schneewind, O. (1999), "Surface proteins of gram-positive bacteria and mechanisms of their targeting to the cell wall envelope", *Microbiology and molecular biology reviews MMBR*, Vol. 63 No. 1, pp. 174–229.

Neuenfeldt, A., Just, A., Betat, H. and Mörl, M. (2008), "Evolution of tRNA nucleotidyltransferases: a small deletion generated CC-adding enzymes", *Proceedings of the National Academy of Sciences of the United States of America*, Vol. 105 No. 23, pp. 7953–7958.

Neuenfeldt, A., Lorber, B., Ennifar, E., Gaudry, A., Sauter, C., Sissler, M. and Florentz, C. (2013), "Thermodynamic properties distinguish human mitochondrial aspartyl-tRNA synthetase from bacterial homolog with same 3D architecture", *Nucleic acids research*, Vol. 41 No. 4, pp. 2698–2708.

Nevo-Dinur, K., Govindarajan, S. and Amster-Choder, O. (2012), "Subcellular localization of RNA and proteins in prokaryotes", *Trends in genetics TIG*, Vol. 28 No. 7, pp. 314–322.

Nissen, P., Kjeldgaard, M., Thirup, S.r., Polekhina, G., Reshetnikova, L., Clark, B.F.C. and Nyborg, J. (1995), "Crystal Structure of the Ternary Complex of Phe-tRNAPhe, EF-Tu, and a GTP Analog", *Science*, Vol. 270 No. 5241, pp. 1464–1472.

Noller, H.F. (2012), "Evolution of protein synthesis from an RNA world", *Cold Spring Harbor perspectives in biology*, Vol. 4 No. 4, a003681.

Nolte-'t Hoen, E., Buermans, H.P.J., Waasdorp, M., Stoorvogel, W., Wauben, M.H.M. and 't Hoen, Peter A C (2012), "Deep sequencing of RNA from immune cell-derived vesicles uncovers the selective incorporation of small non-coding RNA biotypes with potential regulatory functions", *Nucleic acids research*, Vol. 40 No. 18, pp. 9272–9285.

O'Brien, T.W. (1971), "The general occurrence of 55 S ribosomes in mammalian liver mitochondria", *The Journal of biological chemistry*, Vol. 246 No. 10, pp. 3409–3417.

O'Brien, T.W. (2002), "Evolution of a protein-rich mitochondrial ribosome: implications for human genetic disease", *Gene*, Vol. 286 No. 1, pp. 73–79.

Oguiza, J.A., Malumbres, M., Eriani, G., Pisabarro, A., Mateos, L.M., Martin, F. and Martin, J.F. (1993), "A gene encoding arginyl-tRNA synthetase is located in the upstream region of the lysA gene in Brevibacterium lactofermentum: regulation of argS-lysA cluster expression by arginine", *Journal of bacteriology*, Vol. 175 No. 22, pp. 7356–7362.

Ohtsuki, T., Kawai, G. and Watanabe, K. (2002a), "The minimal tRNA. Unique structure of Ascaris suum mitochondrial tRNA SerUCU having a short T arm and lacking the entire D arm", *FEBS letters*, Vol. 514 No. 1, pp. 37–43.

Ohtsuki, T., Sato, A., Watanabe, Y.-I. and Watanabe, K. (2002b), "A unique serine-specific elongation factor Tu found in nematode mitochondria", *Nature structural biology*, Vol. 9 No. 9, pp. 669–673.

Ohtsuki, T., Watanabe, Y., Takemoto, C., Kawai, G., Ueda, T., Kita, K., Kojima, S., Kaziro, Y., Nyborg, J. and Watanabe, K. (2001), "An "elongated" translation elongation factor Tu for truncated tRNAs in nematode mitochondria", *The Journal of biological chemistry*, Vol. 276 No. 24, pp. 21571–21577.

Ohtsuki, T. and Watanabe, Y.-I. (2007), "T-armless tRNAs and elongated elongation factor Tu", *IUBMB life*, Vol. 59 No. 2, pp. 68–75.

Ojala, D., Montoya, J. and Attardi, G. (1981), "tRNA punctuation model of RNA processing in human mitochondria", *Nature*, Vol. 290 No. 5806, pp. 470–474.

Okabe, M., Tomita, K., Ishitani, R., Ishii, R., Takeuchi, N., Arisaka, F., Nureki, O. and Yokoyama, S. (2003), "Divergent evolutions of trinucleotide polymerization revealed by an archaeal CCA-adding enzyme structure", *The EMBO journal*, Vol. 22 No. 21, pp. 5918–5927.

Okimoto, R., Macfarlane, J.L., Clary, D.O. and Wolstenholme, D.R. (1992), "The mitochondrial genomes of two nematodes, Caenorhabditis elegans and Ascaris suum", *Genetics*, Vol. 130 No. 3, pp. 471–498.

Okimoto, R., Macfarlane, J.L. and Wolstenholme, D.R. (1994), "The mitochondrial ribosomal RNA genes of the nematodes Caenorhabditis elegans and Ascaris suum: consensus secondary-structure models and conserved nucleotide sets for phylogenetic analysis", *Journal of molecular evolution*, Vol. 39 No. 6, pp. 598–613.

Okimoto, R. and Wolstenholme, D.R. (1990), "A set of tRNAs that lack either the T psi C arm or the dihydrouridine arm: towards a minimal tRNA adaptor", *The EMBO journal*, Vol. 9 No. 10, pp. 3405–3411.

Orgel, L.E. (1968), "Evolution of the genetic apparatus", *J. Mol. Biol.*, Vol. 38 No. 3, pp. 381–393.

Palade, G.E. (1955), "A small particulate component of the cytoplasm", *The Journal of biophysical and biochemical cytology*, Vol. 1 No. 1, pp. 59–68.

Petersen, J.J. and Chapman, H.C. (1979), "Checklist of mosquito species tested against the nematode parasite Romanomermis culicivorax", *Journal of medical entomology*, Vol. 15 5-6, pp. 468–471.

Petersen, J.J. and Cupello, J.M. (1981), "Commercial development and future prospects for entomogenous nematodes", *Journal of nematology*, Vol. 13 No. 3, pp. 280–284.

Petoukhov, M.V., Franke, D., Shkumatov, A.V., Tria, G., Kikhney, A.G., Gajda, M., Gorba, C., Mertens, H.D.T., Konarev, P.V. and Svergun, D.I. (2012), "New developments in the ATSAS program package for small-angle scattering data analysis", *Journal of applied crystallography*, Vol. 45 Pt 2, pp. 342–350.

Phizicky, E.M. and Hopper, A.K. (2015), "tRNA processing, modification, and subcellular dynamics: past, present, and future", *RNA*, Vol. 21 No. 4, pp. 483–485.

Platzer, E.G. (2007), "Mermithid nematodes", *Journal of the American Mosquito Control Association*, Vol. 23 2 Suppl, pp. 58–64.

Pliatsika, V., Loher, P., Telonis, A.G. and Rigoutsos, I. (2016), "MINTbase: a framework for the interactive exploration of mitochondrial and nuclear tRNA fragments", *Bioinformatics*, Vol. 32 No. 16, pp. 2481–2489.

Powers, T.O., Platzer, E.G. and Hyman, B.C. (1986), "Large mitochondrial genome and mitochondrial DNA size polymorphism in the mosquito parasite, Romanomermis culicivorax", *Current genetics*, Vol. 11 No. 1, pp. 71–77.

Puglisi, E.V. and Puglisi, J.D. (2007), "Probing the conformation of human tRNA(3)(Lys) in solution by NMR", *FEBS letters*, Vol. 581 No. 27, pp. 5307–5314.

Putnam, C.D., Hammel, M., Hura, G.L. and Tainer, J.A. (2007), "X-ray solution scattering (SAXS) combined with crystallography and computation: defining accurate macromolecular structures, conformations and assemblies in solution", *Quarterly reviews of biophysics*, Vol. 40 No. 3, pp. 191–285.

Pütz, J., Giegé, R. and Florentz, C. (2010), "Diversity and similarity in the tRNA world: overall view and case study on malaria-related tRNAs", *FEBS letters*, Vol. 584 No. 2, pp. 350–358.

Pütz, J., Puglisi, J.D., Florentz, C. and Giege, R. (1991), "Identity elements for specific aminoacylation of yeast tRNA(Asp) by cognate aspartyl-tRNA synthetase", *Science (New York, N.Y.)*, Vol. 252 No. 5013, pp. 1696–1699.

Raina, M. and Ibba, M. (2014), "tRNAs as regulators of biological processes", *Frontiers in genetics*, Vol. 5, p. 171.

Randau, L. and Soll, D. (2008), "Transfer RNA genes in pieces", *EMBO reports*, Vol. 9 No. 7, pp. 623–628.

Rath, V.L., Silvian, L.F., Beijer, B., Sproat, B.S. and Steitz, T.A. (1998), "How glutaminyl-tRNA synthetase selects glutamine", *Structure (London, England 1993)*, Vol. 6 No. 4, pp. 439–449.

Regulski, E.E. and Breaker, R.R. (2008), "In-line probing analysis of riboswitches", *Methods in molecular biology (Clifton, N.J.)*, Vol. 419, pp. 53–67.

Reiter, N.J., Osterman, A., Torres-Larios, A., Swinger, K.K., Pan, T. and Mondragon, A. (2010), "Structure of a bacterial ribonuclease P holoenzyme in complex with tRNA", *Nature*, Vol. 468 No. 7325, pp. 784–789.

Reuven, N.B., Zhou, Z. and Deutscher, M.P. (1997), "Functional Overlap of tRNA Nucleotidyltransferase, Poly(A) Polymerase I, and Polynucleotide Phosphorylase", *Journal of Biological Chemistry*, Vol. 272 No. 52, pp. 33255–33259.

Reznik, E., Miller, M.L., Senbabaoglu, Y., Riaz, N., Sarungbam, J., Tickoo, S.K., Al-Ahmadie, H.A., Lee, W., Seshan, V.E., Hakimi, A.A. and Sander, C. (2016), "Mitochondrial DNA copy number variation across human cancers", *eLife*, Vol. 5.

Rial, D.V. and Ceccarelli, E.A. (2002), "Removal of DnaK contamination during fusion protein purifications", *Protein expression and purification*, Vol. 25 No. 3, pp. 503–507.

Ribas de Pouplana, L. and Schimmel, P. (2001), "Aminoacyl-tRNA synthetases. Potential markers of genetic code development", *Trends in biochemical sciences*, Vol. 26 No. 10, pp. 591–596.

Rich, A. and Schimmel, P.R. (1977), "Structural organization of complexes of transfer RNAs with aminoacyl transfer RNA synthetases", *Nucleic acids research*, Vol. 4 No. 5, pp. 1649–1665.

Robertson, M.P. and Joyce, G.F. (2012), "The origins of the RNA world", *Cold Spring Harbor perspectives in biology*, Vol. 4 No. 5.

Robertus, J.D., Ladner, J.E., Finch, J.T., Rhodes, D., Brown, R.S., Clark, B.F. and Klug, A. (1974), "Structure of yeast phenylalanine tRNA at 3 A resolution", *Nature*, Vol. 250 No. 467, pp. 546–551.

Roeder, R.G. and Rutter, W.J. (1969), "Multiple forms of DNA-dependent RNA polymerase in eukaryotic organisms", *Nature*, Vol. 224 No. 5216, pp. 234–237.

Romer, R. and Hach, R. (1975), "tRNA conformation and magnesium binding. A study of a yeast phenylalanine-specific tRNA by a fluorescent indicator and differential melting curves", *European journal of biochemistry / FEBS*, Vol. 55 No. 1, pp. 271–284.

Rossmanith, W. (2011), "Localization of human RNase Z isoforms: dual nuclear/mitochondrial targeting of the ELAC2 gene product by alternative translation initiation", *PLoS ONE*, Vol. 6 No. 4, e19152.

Roy, H. and Ibba, M. (2008), "RNA-dependent lipid remodeling by bacterial multiple peptide resistance factors", *Proceedings of the National Academy of Sciences of the United States of America*, Vol. 105 No. 12, pp. 4667–4672.

Rudinger, J., Blechschmidt, B., Ribeiro, S. and Sprinzl, M. (1994), "Minimalist aminoacylated RNAs as efficient substrates for elongation factor Tu", *Biochemistry*, Vol. 33 No. 19, pp. 5682–5688.

Sahdev, S., Khattar, S.K. and Saini, K.S. (2008), "Production of active eukaryotic proteins through bacterial expression systems: a review of the existing biotechnology strategies", *Molecular and cellular biochemistry*, Vol. 307 1-2, pp. 249–264.

Sakurai, M., Ohtsuki, T. and Watanabe, K. (2005), "Modification at position 9 with 1-methyladenosine is crucial for structure and function of nematode mitochondrial tRNAs lacking the entire T-arm", *Nucleic acids research*, Vol. 33 No. 5, pp. 1653–1661.

Salinas-Giegé, T., Giegé, R. and Giege, P. (2015), "tRNA biology in mitochondria", *International journal of molecular sciences*, Vol. 16 No. 3, pp. 4518–4559.

Sambrook, J., Fritsch, E.F. and Maniatis, T. (1989), *Molecular cloning: A laboratory manual,* 2. ed., 5. print, Cold Spring Harbor Laboratory Press, Plainview, NY.

Sampson, J.R. and Uhlenbeck, O.C. (1988), "Biochemical and physical characterization of an unmodified yeast phenylalanine transfer RNA transcribed in vitro", *Proceedings of the National Academy of Sciences of the United States of America*, Vol. 85 No. 4, pp. 1033–1037.

Sanger, F., Nicklen, S. and Coulson, A.R. (1977), "DNA sequencing with chain-terminating inhibitors", *Proceedings of the National Academy of Sciences of the United States of America*, Vol. 74 No. 12, pp. 5463–5467.

Sato, A., Watanabe, Y.-I., Suzuki, T., Komiyama, M., Watanabe, K. and Ohtsuki, T. (2006), "Identification of the residues involved in the unique serine specificity of Caenorhabditis elegans mitochondrial EF-Tu2", *Biochemistry*, Vol. 45 No. 36, pp. 10920–10927.

Savojardo, C., Martelli, P.L., Fariselli, P. and Casadio, R. (2014), "TPpred2: improving the prediction of mitochondrial targeting peptide cleavage sites by exploiting sequence motifs", *Bioinformatics (Oxford, England)*, Vol. 30 No. 20, pp. 2973–2974.

Schein, C.H. (1989), "Production of soluble recombinant proteins in bacteria", *BioTechnology No. 7*, pp. 1141–1148.

Schiffer, P.H., Kroiher, M., Kraus, C., Koutsovoulos, G.D., Kumar, S., Camps, J.I.R., Nsah, N.A., Stappert, D., Morris, K., Heger, P., Altmuller, J., Frommolt, P., Nurnberg, P., Thomas, W.K., Blaxter, M.L. and Schierenberg, E. (2013), "The genome of Romanomermis culicivorax: revealing fundamental changes in the core developmental genetic toolkit in Nematoda", *BMC genomics*, Vol. 14, p. 923.

Schimmel, P. (1987), "Aminoacyl tRNA synthetases: general scheme of structure-function relationships in the polypeptides and recognition of transfer RNAs", *Annual review of biochemistry*, Vol. 56, pp. 125–158.

Schluenzen, F., Tocilj, A., Zarivach, R., Harms, J., Gluehmann, M., Janell, D., Bashan, A., Bartels, H., Agmon, I., Franceschi, F. and Yonath, A. (2000), "Structure of functionally activated small ribosomal subunit at 3.3 angstroms resolution", *Cell*, Vol. 102 No. 5, pp. 615–623.

Schmidt, O., Pfanner, N. and Meisinger, C. (2010), "Mitochondrial protein import: from proteomics to functional mechanisms", *Nature reviews. Molecular cell biology*, Vol. 11 No. 9, pp. 655–667.

Schürer, H., Lang, K., Schuster, J. and Mörl, M. (2002), "A universal method to produce in vitro transcripts with homogeneous 3' ends", *Nucleic acids research*, Vol. 30 No. 12, e56.

Schuwirth, B.S., Borovinskaya, M.A., Hau, C.W., Zhang, W., Vila-Sanjurjo, A., Holton, J.M. and Cate, J.H.D. (2005), "Structures of the bacterial ribosome at 3.5 A resolution", *Science (New York, N.Y.)*, Vol. 310 No. 5749, pp. 827–834.

Schwartzbach, C.J. and Spremulli, L.L. (1991), "Interaction of animal mitochondrial EF-Tu.EF-Ts with aminoacyl-tRNA, guanine nucleotides, and ribosomes", *The Journal of biological chemistry*, Vol. 266 No. 25, pp. 16324–16330.

Serganov, A. and Patel, D.J. (2007), "Ribozymes, riboswitches and beyond: regulation of gene expression without proteins", *Nature reviews. Genetics*, Vol. 8 No. 10, pp. 776–790.

Shamseldean, M.M. and Platzer, E.G. (1989), "Romanomermis culicivorax: penetration of larval mosquitoes", *Journal of invertebrate pathology*, Vol. 54 No. 2, pp. 191–199.

Sharma, M.R., Koc, E.C., Datta, P.P., Booth, T.M., Spremulli, L.L. and Agrawal, R.K. (2003), "Structure of the Mammalian Mitochondrial Ribosome Reveals an Expanded Functional Role for Its Component Proteins", *Cell*, Vol. 115 No. 1, pp. 97–108.

Sheppard, K., Yuan, J., Hohn, M.J., Jester, B., Devine, K.M. and Soll, D. (2008), "From one amino acid to another: tRNA-dependent amino acid biosynthesis", *Nucleic acids research*, Vol. 36 No. 6, pp. 1813–1825.

Shi, H. and Moore, P.B. (2000), "The crystal structure of yeast phenylalanine tRNA at 1.93 A resolution: a classic structure revisited", *RNA (New York, N.Y.)*, Vol. 6 No. 8, pp. 1091–1105.

Shi, P.Y., Maizels, N. and Weiner, A.M. (1998), "CCA addition by tRNA nucleotidyltransferase: polymerization without translocation?", *The EMBO journal*, Vol. 17 No. 11, pp. 3197–3206.

Shigematsu, M., Honda, S. and Kirino, Y. (2014), "Transfer RNA as a source of small functional RNA", *J Mol Biol Mol Imaging*, Vol. 1 No. 2, % 26117139.

Shimada, A., Nureki, O., Goto, M., Takahashi, S. and Yokoyama, S. (2001a), "Structural and mutational studies of the recognition of the arginine tRNA-specific major identity element, A20, by arginyl-tRNA synthetase", *Proceedings of the National Academy of Sciences of the United States of America*, Vol. 98 No. 24, pp. 13537–13542.

Shimada, A., Nureki, O., Goto, M., Takahashi, S. and Yokoyama, S. (2001b), *THERMUS THERMOPHILUS ARGINYL-TRNA SYNTHETASE*.

Sissler, M., Giege, R. and Florentz, C. (1996), "Arginine aminoacylation identity is context-dependent and ensured by alternate recognition sets in the anticodon loop of accepting tRNA transcripts", *The EMBO journal*, Vol. 15 No. 18, pp. 5069–5076.

Sissler, M., Giege, R. and Florentz, C. (1998), "The RNA sequence context defines the mechanistic routes by which yeast arginyl-tRNA synthetase charges tRNA", *RNA (New York, N.Y.)*, Vol. 4 No. 6, pp. 647–657.

Sissler, M., Lorber, B., Messmer, M., Schaller, A., Putz, J. and Florentz, C. (2008), "Handling mammalian mitochondrial tRNAs and aminoacyl-tRNA synthetases for functional and structural characterization", *Methods (San Diego, Calif.)*, Vol. 44 No. 2, pp. 176–189.

Small, I., Peeters, N., Legeai, F. and Lurin, C. (2004), "Predotar: A tool for rapidly screening proteomes for N-terminal targeting sequences", *Proteomics*, Vol. 4 No. 6, pp. 1581–1590.

Smith, D.R. (2016), "The past, present and future of mitochondrial genomics: have we sequenced enough mtDNAs?", *Brief Funct Genomics*, Vol. 15 No. 1, pp. 47–54.

Sobala, A. and Hutvagner, G. (2011), "Transfer RNA-derived fragments: origins, processing, and functions", *Wiley interdisciplinary reviews. RNA*, Vol. 2 No. 6, pp. 853–862.

Sobala, A. and Hutvagner, G. (2013), "Small RNAs derived from the 5' end of tRNA can inhibit protein translation in human cells", *RNA biology*, Vol. 10 No. 4, pp. 553–563.

Sprinzl, M. (1998), "Compilation of tRNA sequences and sequences of tRNA genes", *Nucleic acids research*, Vol. 26 No. 1, pp. 148–153.

Sprinzl, M. and Cramer, F. (1979), "The -C-C-A end of tRNA and its role in protein biosynthesis", *Progress in nucleic acid research and molecular biology*, Vol. 22, pp. 1–69.

Stein, A. and Crothers, D.M. (1976), "Conformational changes of transfer RNA. The role of magnesium(II)", *Biochemistry*, Vol. 15 No. 1, pp. 160–168.

Steitz, T.A. (1998), "A mechanism for all polymerases", *Nature*, Vol. 391 No. 6664, pp. 231–232.

Steitz, T.A., Smerdon, S.J., Jager, J. and Joyce, C.M. (1994), "A unified polymerase mechanism for nonhomologous DNA and RNA polymerases", *Science (New York, N.Y.)*, Vol. 266 No. 5193, pp. 2022–2025.

Sugiura, I., Nureki, O., Ugaji-Yoshikawa, Y., Kuwabara, S., Shimada, A., Tateno, M., Lorber, B., Giege, R., Moras, D., Yokoyama, S. and Konno, M. (2000), "The 2.0 A crystal structure of Thermus thermophilus methionyl-tRNA synthetase reveals two RNA-binding modules", *Structure*, Vol. 8 No. 2, pp. 197–208.

Sun, F.-J. and Caetano-Anolles, G. (2008), "The origin and evolution of tRNA inferred from phylogenetic analysis of structure", *Journal of molecular evolution*, Vol. 66 No. 1, pp. 21–35.

Suzuki, T., Nagao, A. and Suzuki, T. (2011), "Human mitochondrial tRNAs: biogenesis, function, structural aspects, and diseases", *Annual review of genetics*, Vol. 45, pp. 299–329.

Suzuki, T. and Suzuki, T. (2014), "A complete landscape of post-transcriptional modifications in mammalian mitochondrial tRNAs", *Nucleic acids research*, Vol. 42 No. 11, pp. 7346–7357.

Suzuki, T., Terasaki, M., Takemoto-Hori, C., Hanada, T., Ueda, T., Wada, A. and Watanabe, K. (2001), "Structural compensation for the deficit of rRNA with proteins in the mammalian mitochondrial ribosome. Systematic analysis of protein components of the large ribosomal subunit from mammalian mitochondria", *The Journal of biological chemistry*, Vol. 276 No. 24, pp. 21724–21736.

Svergun, D., Barberato, C. and Koch, M.H.J. (1995), "CRYSOL – a Program to Evaluate X-ray Solution Scattering of Biological Macromolecules from Atomic Coordinates", *Journal of Applied Crystallography*, Vol. 28 No. 6, pp. 768–773.

Svergun, D.I. (1992), "Determination of the regularization parameter in indirect-transform methods using perceptual criteria", *Journal of Applied Crystallography*, Vol. 25 No. 4, pp. 495–503.

Svergun, D.I. and Koch, M.H.J. (2003), "Small-angle scattering studies of biological macromolecules in solution", *Rep. Prog. Phys No.* 66, pp. 1735–1782.

Sylvester, J.E., Fischel-Ghodsian, N., Mougey, E.B. and O'brien, T.W. (2004), "Mitochondrial ribosomal proteins. Candidate genes for mitochondrial disease", *Genetics in Medicine*, Vol. 6 No. 2, pp. 73–80.

Tamura, K., Himeno, H., Asahara, H., Hasegawa, T. and Shimizu, M. (1992), "In vitro study of E.coli tRNA Arg and tRNA Lys identity elements", *Nucleic Acids Research*, Vol. 20 No. 9, pp. 2335–2339.

Tang, S.-N. and Huang, J.-F. (2005), "Evolution of different oligomeric glycyl-tRNA synthetases", *FEBS letters*, Vol. 579 No. 6, pp. 1441–1445.

The ENDCODE project consortium (2012), "An integrated encyclopedia of DNA elements in the human genome", *Nature*, Vol. 489 No. 7414, pp. 57–74.

Thompson, D.M. and Parker, R. (2009), "The RNase Rny1p cleaves tRNAs and promotes cell death during oxidative stress in Saccharomyces cerevisiae", *The Journal of cell biology*, Vol. 185 No. 1, pp. 43–50.

Tocchini-Valentini, G.D., Fruscoloni, P. and Tocchini-Valentini, G.P. (2009), "Processing of multiple-intron-containing pretRNA", *Proc. Natl. Acad. Sci. U.S.A.*, Vol. 106 No. 48, pp. 20246–20251.

Toh, Y., Takeshita, D., Numata, T., Fukai, S., Nureki, O. and Tomita, K. (2009), "Mechanism for the definition of elongation and termination by the class II CCA-adding enzyme", *The EMBO journal*, Vol. 28 No. 21, pp. 3353–3365.

Tolkunova, E., Park, H., Xia, J., King, M.P. and Davidson, E. (2000), "The human lysyl-tRNA synthetase gene encodes both the cytoplasmic and mitochondrial enzymes by means of an unusual alternative splicing of the primary transcript", *The Journal of biological chemistry*, Vol. 275 No. 45, pp. 35063–35069.

Tomari, Y., Suzuki, T. and Ueda, T. (2002), "tRNA recognition by CCA-adding enzyme", *Nucleic acids research. Supplement (2001) No.* 2, pp. 77–78.

Tomita, K., Fukai, S., Ishitani, R., Ueda, T., Takeuchi, N., Vassylyev, D.G. and Nureki, O. (2004), "Structural basis for template-independent RNA polymerization", *Nature*, Vol. 430 No. 7000, pp. 700–704.

Toseland, C.P. (2013), "Fluorescent labeling and modification of proteins", *Journal of chemical biology*, Vol. 6 No. 3, pp. 85–95.

Tretbar, S., Neuenfeldt, A., Betat, H. and Mörl, M. (2011), "An inhibitory C-terminal region dictates the specificity of A-adding enzymes", *Proceedings of the National Academy of Sciences of the United States of America*, Vol. 108 No. 52, pp. 21040–21045.

Tyagi, N.K., Fenton, W.A. and Horwich, A.L. (2009), "GroEL/GroES cycling: ATP binds to an open ring before substrate protein favoring protein binding and production of the native state", *Proceedings of the National Academy of Sciences of the United States of America*, Vol. 106 No. 48, pp. 20264–20269.

Tzameli, I. (2012), "The evolving role of mitochondria in metabolism", *Trends in endocrinology and metabolism: TEM*, Vol. 23 No. 9, pp. 417–419.

Valadkhan, S. and Gunawardane, L.S. (2013), "Role of small nuclear RNAs in eukaryotic gene expression", *Essays in biochemistry*, Vol. 54, pp. 79–90.

Varani, G., Chen, Y. and Leeper, T.C. (2004), "NMR studies of protein-nucleic acid interactions", *Methods in molecular biology (Clifton, N.J.)*, Vol. 278, pp. 289–312.

Vasil'eva, I.A. and Moor, N.A. (2007), "Interaction of aminoacyl-tRNA synthetases with tRNA. General principles and distinguishing characteristics of the high-molecular-weight substrate recognition", *Biochemistry (Moscow)*, Vol. 72 No. 3, pp. 247–263.

Vörtler, S. and Mörl, M. (2010), "tRNA-nucleotidyltransferases: highly unusual RNA polymerases with vital functions", *FEBS letters*, Vol. 584 No. 2, pp. 297–302.

Watanabe, K. (2010), "Unique features of animal mitochondrial translation systems", *Proceedings of the Japan Academy, Series B*, Vol. 86 No. 1, pp. 11–39.

Watanabe, Y.-i., Tsurui, H., Ueda, T., Furusihima-Shimogawara, R., Takamiya, S., Kita, K., Nishikawa, K. and Watanabe, K. (1997), "Primary sequence of mitochondrial tRNAArg of a nematode Ascaris suum. Occurrence of unmodified adenosine at the first position of the anticodon", *Biochimica et Biophysica Acta (BBA) - Gene Structure and Expression*, Vol. 1350 No. 2, pp. 119–122.

Watanabe, Y.-I., Suematsu, T. and Ohtsuki, T. (2014), "Losing the stem-loop structure from metazoan mitochondrial tRNAs and co-evolution of interacting factors", *Frontiers in genetics*, Vol. 5, p. 109.

Watson, J.D. and Crick, F.H. (1953), "Molecular structure of nucleic acids; a structure for deoxyribose nucleic acid", *Nature*, Vol. 171 No. 4356, pp. 737–738.

Webster, T., Tsai, H., Kula, M., Mackie, G.A. and Schimmel, P. (1984), "Specific sequence homology and three-dimensional structure of an aminoacyl transfer RNA synthetase", *Science*, Vol. 226 No. 4680, pp. 1315–1317.

Weiner, A.M. and Maizels, N. (1999), "The Genomic Tag Hypothesis. Modern Viruses as Molecular Fossils of Ancient Strategies for Genomic Replication, and Clues regarding the Origin of Protein Synthesis", *Biological Bulletin*, Vol. 196 No. 3, p. 327.

Wende, S., Bonin, S., Gotze, O., Betat, H. and Morl, M. (2015), "The identity of the discriminator base has an impact on CCA addition", *Nucleic acids research*, Vol. 43 No. 11, pp. 5617–5629.

Wende, S., Platzer, E.G., Jühling, F., Pütz, J., Florentz, C., Stadler, P.F. and Mörl, M. (2014), "Biological evidence for the world's smallest tRNAs", *Biochimie*, Vol. 100, pp. 151–158.

Westhof, E. and Auffinger, P. (2001), "Transfer RNA Structure", in *eLS*, John Wiley & Sons, Ltd, Chichester, UK.

White, R.J. (2011), "Transcription by RNA polymerase III: more complex than we thought", *Nature reviews. Genetics*, Vol. 12 No. 7, pp. 459–463.

Widmann, J., Di Giulio, M., Yarus, M. and Knight, R. (2005), "tRNA creation by hairpin duplication", *Journal of molecular evolution*, Vol. 61 No. 4, pp. 524–530.

Williams, M.A., Johzuka, Y. and Mulligan, R.M. (2000), "Addition of non-genomically encoded nucleotides to the 3'-terminus of maize mitochondrial mRNAs: truncated rps12 mRNAs frequently terminate with CCA", *Nucleic acids research*, Vol. 28 No. 22, pp. 4444–4451.

Wilson, D.N. and Doudna Cate, J.H. (2012), "The structure and function of the eukaryotic ribosome", *Cold Spring Harbor perspectives in biology*, Vol. 4 No. 5.

Wilusz, J.E., Sunwoo, H. and Spector, D.L. (2009), "Long noncoding RNAs: functional surprises from the RNA world", *Genes & development*, Vol. 23 No. 13, pp. 1494–1504.

Wilusz, J.E., Whipple, J.M., Phizicky, E.M. and Sharp, P.A. (2011), "tRNAs marked with CCACCA are targeted for degradation", *Science (New York, N.Y.)*, Vol. 334 No. 6057, pp. 817–821.

Wolstenholme, D.R., Macfarlane, J.L., Okimoto, R., Clary, D.O. and Wahleithner, J.A. (1987), "Bizarre tRNAs inferred from DNA sequences of mitochondrial genomes of nematode worms", *Proceedings of the National Academy of Sciences of the United States of America*, Vol. 84 No. 5, pp. 1324–1328.

Wolstenholme, D.R., Okimoto, R. and Macfarlane, J.L. (1994), "Nucleotide correlations that suggest tertiary interactions in the TV-replacement loop-containing mitochondrial tRNAs of the nematodes, Caenorhabditis elegans and Ascaris suum", *Nucleic acids research*, Vol. 22 No. 20, pp. 4300–4306.

Woodson, S.A. and Koculi, E. (2009), "Analysis of RNA Folding by Native Polyacrylamide Gel Electrophoresis", in *Biophysical, Chemical, and Functional Probes of RNA Structure, Interactions and Folding: Part B*, *Methods in Enzymology*, Vol. 469, Elsevier, pp. 189–208.

Xiong, Y., Li, F., Wang, J., Weiner, A.M. and Steitz, T.A. (2003), "Crystal structures of an archaeal class I CCA-adding enzyme and its nucleotide complexes", *Molecular cell*, Vol. 12 No. 5, pp. 1165–1172.

Xiong, Y. and Steitz, T.A. (2006), "A story with a good ending: tRNA 3'-end maturation by CCA-adding enzymes", *Current opinion in structural biology*, Vol. 16 No. 1, pp. 12–17.

Yamasaki, S., Ivanov, P., Hu, G.-F. and Anderson, P. (2009), "Angiogenin cleaves tRNA and promotes stress-induced translational repression", *The Journal of cell biology*, Vol. 185 No. 1, pp. 35–42.

Yamazaki, N., Ueshima, R., Terrett, J.A., Yokobori, S., Kaifu, M., Segawa, R., Kobayashi, T., Numachi, K., Ueda, T., Nishikawa, K., Watanabe, K. and Thomas, R.H. (1997), "Evolution of pulmonate gastropod mitochondrial genomes: comparisons of gene organizations of Euhadra, Cepaea and Albinaria and implications of unusual tRNA secondary structures", *Genetics*, Vol. 145 No. 3, pp. 749–758.

Yao, Y.-N., Wang, L., Wu, X.-F. and Wang, E.-D. (2003), "Human mitochondrial leucyl-tRNA synthetase with high activity produced from Escherichia coli", *Protein expression and purification*, Vol. 30 No. 1, pp. 112–116.

Yarus, M. (2011), "Getting past the RNA world: the initial Darwinian ancestor", *Cold Spring Harb Perspect Biol*, Vol. 3 No. 4.

Yokogawa, T., Kitamura, Y., Nakamura, D., Ohno, S. and Nishikawa, K. (2010), "Optimization of the hybridization-based method for purification of thermostable tRNAs in the presence of tetraalkylammonium salts", *Nucleic acids research*, Vol. 38 No. 6, e89.

Yue, D., Maizels, N. and Weiner, A.M. (1996), "CCA-adding enzymes and poly(A) polymerases are all members of the same nucleotidyltransferase superfamily: characterization of the CCA-adding enzyme from the archaeal hyperthermophile Sulfolobus shibatae", *RNA (New York, N.Y.)*, Vol. 2 No. 9, pp. 895–908.

Yusupov, M.M., Yusupova, G.Z., Baucom, A., Lieberman, K., Earnest, T.N., Cate, J.H. and Noller, H.F. (2001), "Crystal structure of the ribosome at 5.5 A resolution", *Science*, Vol. 292 No. 5518, pp. 883–896.

Zamecnik, P.C., Keller, E.B., Littlefield, J.W., Hoagland, M.B. and Loftfield, R.B. (1956), "Mechanism of incorporation of labeled amino acids into protein", *Journal of cellular physiology. Supplement*, Vol. 47 Suppl 1, pp. 81–101.

Zhang, S., Sun, L. and Kragler, F. (2009), "The phloem-delivered RNA pool contains small noncoding RNAs and interferes with translation", *Plant physiology*, Vol. 150 No. 1, pp. 378–387.

Zhang, Y. (2008), "I-TASSER server for protein 3D structure prediction", *BMC bioinformatics*, Vol. 9, p. 40.

Zhao, F., Ohtsuki, T., Yamada, K., Yoshinari, S., Kita, K., Watanabe, Y.-I. and Watanabe, K. (2005), "Isolation and physiochemical properties of protein-rich nematode mitochondrial ribosomes", *Biochemistry*, Vol. 44 No. 25, pp. 9232–9237.

Zhu, L. and Deutscher, M.P. (1987), "tRNA nucleotidyltransferase is not essential for Escherichia coli viability", *The EMBO journal*, Vol. 6 No. 8, pp. 2473–2477.

Curriculum vitae

Personal information

Name:	Tina Jühling (née Müller)
Adresse:	Kahllachweg 5, D-77694 Kehl
Email:	tina.mueller@uni-leipzig;de
	t.muller@ibmc-cnrs.unistra.fr
Date of birth:	25.07.1988
Place of birth:	Haldensleben

School education

1995 – 1999	Grundschule Bruno-Beye-Ring, Magdeburg
1999 – 2001	Sekundarschule Freiherr-vom-Stein, Magdeburg
2001 – 2007	Gymnasium Otto-von-Guericke, Magdeburg
2007	Abitur

Academic education

2008 – 2011	French/German studies in Human- and Molecular Biology, (Universität des Saarlandes)/ and in Molecular and cellular biology (Université de Strasbourg)
2011 – 2013	Master studies in Molecular and Cellular Biology, Philipps-Universität Marburg
2013 – 2015	International PhD program in Cotutelle de Thèse, Universität Leipzig (group of Prof. Dr. Mario Mörl, Institut für Biochemie)
2015 – 2016	PhD program continued at Université de Strasbourg (group of Prof. Dr. Catherine Florentz, IBMC/CNRS UPR 9002)

Eigenständigkeitserklärung

Hiermit erkläre ich, dass ich diese Arbeit selbstständig verfasst und keine anderen als die angegebenen Quellen und Hilfsmittel verwendet habe.

Strasbourg, 5. November 2016

Transfer RNAs (tRNAs) are important adapter molecules linking the genetic information of messenger RNAs (mRNA) with the primary amino acid sequence of proteins. In all kingdoms of life, these small RNA transcripts have a typical cloverleaf-like secondary structure, consisting of an acceptor stem, a D-arm, an anticodon arm, a variable loop, and a T-arm. The 3′ terminus ends with the CCA sequence, which is often post-transcriptionally added by CCA-adding enzymes. The CCA-tail is an important prerequisite for the attachment of the correct amino acid by aminoacyl-tRNA synthetases (aaRS). Mitochondrial (mt) tRNAs show a high derivation from this canonical tRNA structure with reduced D- or T-arms, or even completely lack one of these elements. An extreme case of structural truncations can be observed in mitochondria of Enoplea. Here, mitochondrial tRNAs of half of the size of their cytosolic counterparts are present, representing the smallest tRNAs identified so far. It could already be shown that several of these miniaturized armless tRNAs are indeed functional in the nematode worm *Romanomermis culicivorax*. This situation raises several questions concerning the molecular mechanisms of co-evolution of tRNAs and their partner proteins, which ensure the maintenance of a functional protein synthesis.

This study aims the biofunctional characterization of such "bizarre" tRNAs in defining their structural properties, and in studying different aspects of their functionality, especially their interactions with CCA-adding enzymes and aaRSs from different organisms. For this purpose, *in vitro* transcripts were used for structure probing approaches, such as enzymatic and chemical probing, nuclear magnetic resonance (NMR) spectroscopy, and small-angle X-ray scattering (SAXS). We show that armless tRNAs form a hairpin-shaped secondary structure, including an internal double bulge that replaces D- and T-arms of the secondary cloverleaf structure of classical tRNAs. 3D structures are characterized by a high intrinsic flexibility, which probably allows to compensate structural reduction.

The *Rcu* CCA-adding enzyme and mt ArgRS coding sequences have been identified, and were cloned for the first time. Recombinant proteins have been studied for their interaction with armless and cytosolic tRNAs in CCA-incorporations assays, and aminoacylation assays. We demonstrate that armless mt tRNAs represent functional molecules for CCA-incorporation, indicating adaptations of CCA-adding enzymes to armless tRNAs without losing their ability to recognize cytosolic tRNAs. Initial tests could not demonstrate aminoacylation activity of the *Rcu* mt ArgRS. However, the mt ArgRS from *R. culicivorax* exhibits a structural particularity because it lacks an important domain that normally recognizes the elbow region of tRNAs that is no longer present in armless tRNAs due to the missing D-and T-arm. This suggests a co-evolution event of both partner molecules.